



Microclimatic response to urban morphology

The case of Turin

Master's Thesis by Melis Özalp
M.Sc. in Architecture for Sustainable Design
Politecnico di Torino



**Politecnico
di Torino**

**Microclimatic response to urban morphology:
The case of Turin**

Politecnico di Torino

M.Sc. Program in Architecture for Sustainable Design
Year 2021/2022

Master's Thesis

Student
Supervisor
Co-supervisor

Melis Özalp
Riccardo Pollo
Matteo Trane

I would like to express my gratitude to my thesis supervisor Riccardo Pollo and co-supervisor Matteo Trane for their valuable guidance throughout this thesis.

My special thanks are extended to SDG11 Lab for the technical support.

Finally, I wish to thank my family, my friends and my colleagues for providing me with continuous support and encouragement.

contents

Glossary

Abstract

Research Questions

chapter 1 **Introduction & Background**

1.0. Introduction

1.1. Methodology

1.2. Sustainable Development Goals

1.3. Adaptation & Mitigation

1.4. Urban Morphology & Microclimate

1.5. Urban Heat Island

chapter 2 **Best Practices**

2.1. The Case of Thessaloniki, Greece

2.2. The North Desert Village, USA

2.3. EuropaCity, France

chapter 3 **The Case of Turin**

- 3.1.** Historical Evolution of Turin's Urban Form
- 3.2.** Climatic Context
- 3.3.** Green Areas
- 3.4.** Air Quality
- 3.5.** Water Infrastructure
- 3.6.** Mapping Turin: Classification of Urban Fabric

chapter 4 **Pilots**

- 4.1.** San Donato
- 4.2.** Le Vallette
- 4.3.** Mirafiori Nord
- 4.4.** Mirafiori Sud
- 4.5.** Ex-Mercati Generali
- 4.6.** Lingotto

chapter 5 **Results & Discussion**

- 5.1.** ENVI-met Process
- 5.2.** Discussion

chapter 6 **Conclusion**

Bibliography



Glossary

Urban morphology – the study of urban form that examines the formation and transformation of cities, towns and villages (Chen, 2014).

Microclimate – the suite of climatic conditions of a particular location or a relatively small area, that differ from the one of its surroundings (consisting of environmental variables such as potential air temperature, surface temperature, wind speed and outdoor comfort indicators) (Martin & Hine, 2008).

Urban fabric – the physical texture of an urban area which is shaped by the streetscapes, buildings, landscaping, roads and other infrastructure (Salat, 2011).

Urban heat island (UHI) – an urban or metropolitan area where the temperature is significantly higher compared to that of its surroundings, commonly associated with intense human activities (Taha, 2004).

Emissivity – the ability of the material to emit or absorb radiation (Dryden, 1982), $E+R=1$ where E refers to emissivity and R refers to reflectivity (Musikant, 2003).

Albedo – the ability of a surface that allows it to reflect solar radiation, measured between 0 and 1 (0 being full absorption and 1 being full reflectivity) (Lopez-Cabeza et. al, 2022).

Evapotranspiration – the total loss of water to the atmosphere from land surface, through evaporation from the soil and through transpiration from plants (Allaby, 2008).

PET (Physiological Equivalent Temperature) – a thermal comfort index which is equivalent to the air temperature where the heat balance of the human body is maintained with core and skin temperatures equal to those of the evaluated conditions (Höppe, 1999).

Adaptation – adjustments in natural or built environments in response to the expected or actual outcomes of climate change (Intergovernmental Panel on Climate Change, 2001).

Mitigation – interventions that deal with the causes of climate change, such as to reduce the emission sources (Locatelli, 2011).

Urban canyon – a three-dimensional space between the buildings limited by two boards (building walls) and a bottom (road) (Nunez & Oke, 1977), where the main parameters are height (H), width (W) and the orientation (Boeters et. al, 2012).

Aspect ratio – the ratio between the mean height of an urban canyon and its width (Emmanuel, 2021).



Abstract

The human contribution to the climate crisis has long been a topic of interest to the scientific community. The motivation of this thesis is to investigate the impact of human settlement on the course of climate change, by analyzing the role of the urban morphology of the cities on the urban microclimate. The methodology that has been followed can be broken down into following key phases: scientific background, mapping, site analysis, simulation, discussion, conclusion. Following this structure, the first part of the thesis seeks to illuminate the main concepts of the study and presents a selection of practices prior to this thesis, with a similar scope to the one of its own. The city of Turin was considered as an initial macro scale case study, which was subjected to a classification through mapping, to determine different types of urban fabric. These categories served as a pool of micro scale case studies, from which a representative plot for each category has been selected to be examined both through site analysis and microclimatic simulations carried out through ENVI-met software. Paying specific attention to supporting the reliability of the research, this comparison was carried out by setting common parameters within the urban

characteristics (built/unbuilt ratio, horizontal greenery ratio and asphalt ratio) of the selected plots. The outputs of the simulation made it possible to distinguish between the microclimatic responses to each type of urban fabric, through an evaluation of the key environmental values, such as air temperature, surface temperature, PET (physical equivalent temperature) and wind speed. In light of the above-mentioned methodology and mentality, the core focus of the thesis is to deal with the significance of studying the form of the cities as a method of investigating climate change related vulnerabilities and adaptation responses. The findings prompt rethinking of the way to approach the challenge of climate crisis and encourage generating urban scale visions regarding adaptation and mitigation strategies.

Key words: *urban morphology, urban fabric, microclimate, outdoor comfort, adaptation, mitigation, ENVI-met*



Research Questions

The main research question that this thesis addresses is:

How does the urban form affect the microclimate in the city of Turin?

The sub-research questions that this thesis seeks to illuminate are:

What are the most significant parameters of Turin's urban environment that influence the microclimate in Turin?

How can Turin's urban fabric be classified?

How is the outdoor comfort related to other environmental variables (surface temperature and potential air temperature)?

What could the possible adaptation and mitigation strategies be, to help reduce the negative impacts of climate change?

1

Introduction & Background

1.0. Introduction

1.1. Methodology

1.2. Sustainable Development Goals

1.3. Adaptation & Mitigation

1.4. Urban Morphology & Microclimate

1.5. Urban Heat Island

With the rise of the human dominance on our planet, the shifts in temperature and weather patterns have become more evident. These occasions are referred to as **climate change**. Although these shifts might be due to natural causes (such as solar cycle variations) on occasion, the **intensity of human activities** is considered as the main factor that accelerates the process. These activities include burning fossil fuels, which results in **greenhouse gas emissions** that trap the sun heat and thus, increase the temperature (United Nations, 2022).

It is significant to understand that climate change is not only an issue that the next generations would need to cope with, but an already existing phenomena that requires **immediate action**. The strategies that would help tackling this challenge should focus on **the sake of the whole planet**, besides the benefit of humankind alone.

1.0

Introduction

According to the European Council, the amount of people that live in urban areas is approximately three quarters of the European population, which equals to around 325 million people, 40% of these having been settled in the cities alone. The urbanization rate of the world's population is expected to reach 60% by 2030 (United Nations Department of Economic and Social Affairs, 2022). The demand to have an active life in cities has increased over time, following the quality of life that the cities offer. The opportunities that a city can provide cover a remarkable amount of essential needs, including job opportunities, education and social life.

As the interest in living in urban areas has increased, the climatic consequences have followed. The anthropogenic activities resulted in serious damage to the planet, mainly driven by rapid population growth, exploitation of natural sources and fossil fuel reserves, waste production and reduction in the quality of water, soil and air (Gauzin-Müller & Favet, 2002). This damage has been quantified by the Intergovernmental Panel on Climate Change (IPCC) as they have estimated that the earth has warmed up by 0.3 and 0.6°C with a sea level rise of 15 to 25 cm

on average in the past century (Intergovernmental Panel on Climate Change, 1995).

To support well-being in cities and to avoid the negative outcomes of the increasing population and the energy demand in cities, the UN encourages people to take action to be able to prosper all together as humankind. The organization emphasizes the need for an intelligent urban planning vision for safe, affordable and resilient cities, supported by a green and culturally inspiring environment (United Nations, n.d.). According to this approach, the function of a city is considered as an interactive environment where human and non-human are taken into account equally, rather than a hub of human survival alone.

Taking into account the above-mentioned mentality, the topic of human influence on climate change has been examined through different perspectives among the scientific community. A part of these studies focuses particularly on the interconnections between human settlements and the climate change. For this approach, urban morphology, being the “study of urban form” (Lilley, 2009), plays a critical role as it studies the spatial configurations of the cities. These configurations have a significant impact on the microclimate, and thus, the well-being of humans and the environment.

In this thesis, the city of Turin and its neighborhoods have been chosen as case studies to study these interactions between the microclimatic variables and how they are influenced by the urban fabric. The interactions between the urban elements (such as surfaces, plants and atmosphere) in an environment

are complex, as they tend to show evidence of diversity in means of temperature and flow patterns, which are defined through diverse physical principals such as reflection, absorption and evapotranspiration (Esch, 2015). To be able to analyze these complex interactions and to evaluate the different outcomes of urban decision-making processes, the need for computer-based tools and numerical simulations is undeniable (Bruse & Fleer, 1998). Therefore, ENVI-met software has been used for the simulations that have been carried out during the research.

When not studied and organized well, urban morphology can lead to unfavorable conditions such as uncomfortable wind occurrences and heat anomalies. To be able to understand how to obtain optimal conditions and to achieve a more sustainable future, both for the humankind and the surrounding ecosystems, it is important to understand these interconnections and use them as a guide to design for adaptation and mitigation strategies.

1.1

Methodology

The methodology that has been followed during this thesis can be divided into following steps:

Scientific background: It was important to carry out a literature review as the first step of the thesis, to be able to get more familiar with the key concepts and to get to know the prior studies that have been conducted with a similar scope.

Studying the best practices: The literature review was useful to select several best practices throughout the world, with a focus on the adaptation and mitigation strategies for more resilient cities as well as the interconnections between the urban morphology and the microclimate.

Studying the city: Following the literature review and the best practices, the city of Turin has been studied through its history as well as its geographical and climatic conditions. In this stage, it was important to understand the current applications in Turin concerning the environmental quality.

Mapping the city: Having studied the city in detail, the next step was to understand the typologies of urban fabric that are present in the city. To achieve this, a classification that includes four categories and ten typologies has been developed and represented through mapping. During the mapping process, 26 sheets of 1/5000 scale *carta tecnica** (Geoportale Comune di Torino, n.d.) have been used and each carta tecnica has been mapped in detail, to be merged together at the end of the individual mapping processes. The mapping exercise has been carried out through Adobe Photoshop with the aim of providing a clear representation of such a detailed process. Each typology of urban fabric has been represented by a different color/hatch combination.

Selection of case studies (pilots): The map that was created in the previous step served as a pool of micro scale case studies. A case study for each type of urban fabric (except for the ones that do not represent a solid tissue formation) was chosen to evaluate the microclimatic response to their individual urban form. The case study areas consist of different neighborhoods in Turin, namely San Donato, Le Vallette, Mirafiori Nord, Mirafiori Sud, Ex-Mercati Generali and Lingotto. It is significant to underline here that the intention was to follow a comparative approach. Therefore, the areas have been chosen to share common parameters. These common parameters (built density, horizontal greenery ratio, asphalt ratio) were determined through the calculation of relevant areas (both from Google Earth and the CAD version of Turin's masterplan provided by Geoportale Torino) and they helped creating a common ground where it is possible to observe the impact of the built environment and vertical greenery variables. The case studies that share the same common parameters were

* **Carta tecnica:** The maps provided by Comune di Torino in different urban scales that represent the territory (building heights, greenery, mobility network etc.), dividing the city into plots.

put in the same group: Group 1 - San Donato (this area has been evaluated alone, as it already consists of four types of urban fabric), Group 2 - Le Vallette, Mirafiori Nord and Mirafiori Sud, Group 3 - Ex-Mercati Generali, Lingotto. In addition to this systematic comparison process, a broader evaluation including all sites has been performed as well.

Modelling & Simulation: Each case study has been modelled and simulated through ENVI-met software. ENVI-met is a software that evaluates the interactions of surface, plant and air in an urban environment, and thus, microclimatic outcomes of these variables (ENVI-met, 2021). The outputs of several environmental variables (potential air temperature, surface temperature, PET, wind speed) and views from the 3D models have been exported to be evaluated in the discussion step. A detailed overview of the software, modelling, simulation, outputs and post-processing is presented in Chapter 5 where the discussion of the results takes place as well.

Discussion & Conclusion: As mentioned above, the discussion follows a comparative approach. It is divided into three sections, the first part evaluates the microclimatic responses to individual parameters of urban environment: urban structure, vegetation and materials. The second part demonstrates the lowest and highest recorded values of the environmental variables for each case study area at 12:00 and 15:00, as a preparation for the third part. The third part of the discussion seeks to evaluate the trends of the environmental variables for the points that have the least favorable outdoor comfort conditions (thus, PET values), which have been chosen from each case study area. This

evaluation was done through the graphs exported from ENVI-met for three selected points from each site. These three points are selected from three different locations from each site: the first point was chosen from residential public spaces, the second point was chosen from urban canyons with an orientation of NW-SE and the third point was chosen from urban canyons with an orientation of NE-SW. The data collected from ENVI-met for all points have been divided into three tables with respect to their locations.

Finally, the conclusion chapter of the thesis aims to summarizing the key findings of the research. Following these findings, several adaptation and mitigation strategies have been proposed. The limitations of this research and the recommendations for further studies can also be found in this chapter.

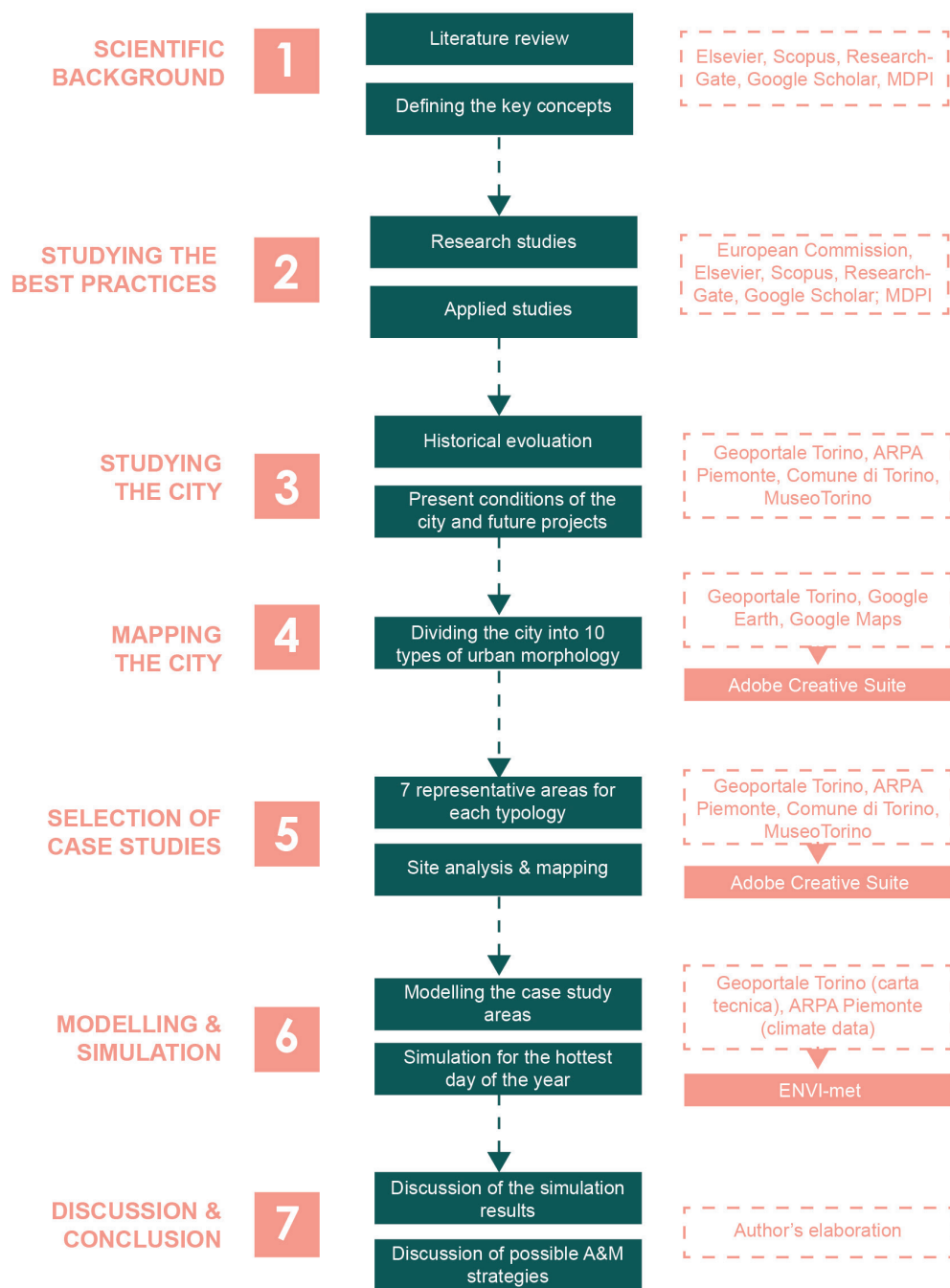


Figure 1. Methodology scheme of the thesis.

1.2

Sustainable Development Goals

Sustainable Development Goals (SDGs), having been introduced by the United Nations in 2015, is a universal call that aims at achieving better conditions as a planet and sustaining the needs of today without compromising the abilities of the future. SDGs have been put forward as a part of 2030 Agenda for Sustainable Development that defines a 15-year plan during which the goals are planned to be achieved (United Nations, 2018). The seventeen goals are interconnected, as the actions in a specific field would have impacts on the outcome of the others and thus, to achieve sustainable development, a balance between social, environmental and economical aspects should be reached (United Nations Development Programme, 2015).

1.1.1. SDG 11: Sustainable Cities and Communities

An indispensable component of the global response to climate change is considered to be the urban centers (UN-Habitat, 2011; World Bank, 2010). The 11th of Sustainable Development Goals (SDG11), namely “Sustainable Cities and Communities”, has been brought forward to

examine and improve urban life while balancing human comfort with environmental consciousness. While doing that, it suggests an inclusive approach, inviting people to take part in achieving resilient cities by collaborating with their local government. In this manner, main topics that SDG11 focus on could be listed as environmental impact reduction, sustainable mobility, safe and affordable housing, inclusive green public spaces and resource efficiency (United Nations, n.d.).

The year 2030 has been set as a milestone to gain ground on the targets of SDG11 (United Nations, n.d.).

1.1.2. SDG 13: Climate Action

2019 was not only recorded as the second warmest year, but also it was the year where carbon dioxide levels and other greenhouse gas emissions reached to new records (United Nations, 2021). In 2020, the emissions regarding travel have dropped significantly due to COVID-19 related pandemic measurement, however, UN underlines that this improvement is temporarily and “climate change is



Figure 2. Icon of SDG11: Sustainable Cities and Communities. (United Nations, n.d.)



Figure 3. Icon of SDG13: Climate Action. (United Nations, 2022)

not on pause” (United Nations, 2021). Therefore, urgent action is required for the benefit of the whole planet.

The Paris Agreement, agreed in 2015, aims at limiting the increase in global temperature well below two degrees Celsius in this century (United Nations, 2021). By doing this, the agreement seeks to strengthen the international response to the issue of climate change. Taking into account the above-mentioned target and understanding the negative impacts of climate change, SDG13 encourages actions that would help safeguarding the planet, through education, innovation and adherence (United Nations, 2022).

1.3

Adaptation & Mitigation

As the consciousness for climate change developed, it brought along adaptation and mitigation strategies with itself. Adaptation can be defined as foreseeing the possible outcomes of the climate problem and taking precautions to limit the negative impacts that might occur, or benefiting from the opportunities that it might create, where possible. Embracing a different perspective, mitigation strategies seek for the cure to this challenge at the core of the problem rather than dealing directly with the results: they aim at reducing the greenhouse gas emission into the atmosphere achieved either by the reduction of the sources of these gases or by reinforcing the sources where they can be stored. All in all, the focal point for mitigation is the source of climate change, while adaptation deals with the results (Schipper, 2006).

The diverse definitions of these policies have lead them to be treated unequally through their history. Local authorities tend to treat these strategies separately (Göpfert et al., 2019b; Grafakos et al. 2020; Reckien et al. 2018), rather than searching for ways to integrate them. In her research, Schipper (2006) examines the early 1990s' approach to these strategies and refers to "adaptation" as "the overlooked

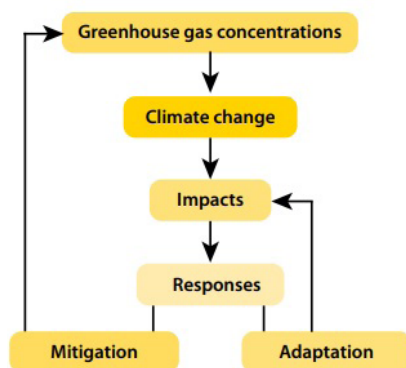


Figure 4. *The relationship between adaptation, mitigation and climate change. (Locatelli, 2014)*

cousin of greenhouse gas mitigation”. In other words, among a part of the scientific community and among those who address climate change, it was believed that taking care of the core of the climate issue by paying particular attention to mitigation strategies would be more beneficial, which put the result-focused adaptation strategies under shadow. According to the literature, only in the last few years, a shift from separation to integration while addressing adaptation and mitigation strategies have been observed (Göpfert et al. 2019a). Cities should put forth a concerted effort to understanding the reasonings of both policy objectives while including them cohesively in decision-making and urban planning processes (Göpfert et al. 2019b). In this manner, it is not possible to neglect the importance of adaptation strategies as mitigation policies would not be sufficient alone, mainly due to the emissions that have already been committed in the past (Ayers & Huq, 2008).

EEA Report No 12/2016 examines several case studies that prompt an understanding of how these two policies could be combined (European Environment Agency, 2016). One of these case

studies focus on an old office building in Rotterdam, dating back to 1940s. Jounz (the company that is the main tenant of the building) realized the potential of transforming the building in a way that it would match the sustainable business goals of the company and started taking action. The adaptation process included key decisions such as preserving the parts of the building that are still functional, while applying triple glazing and high insulation to the newly added floors. The implementations on the new floors helped keeping the air inside the building cool through summer time, preventing the impact of high temperature. Additionally, an aquifer thermal energy storage system (ATES) has been proposed to absorb the heat during the summer, to reuse it in winter. Furthermore, a rooftop garden has been designed with an aim of delaying storm water run-off due to heavy rain sessions that the climate change triggers. The garden also serves as a ground for peaceful coexistence of flora and fauna. As a result, the building consumes 63% less energy than an average office building in the Netherlands would.

Another case that includes actions against climate change takes place in Barcelona, Spain. Compared to the above-mentioned case study in Rotterdam, this case study, namely Barcelona Green Infrastructure and Biodiversity Plan 2020, covers a larger scale as its focus is not only a building and its surroundings, but is considering the urban context (European Commission & European Environment Agency, 2016). Taking the challenge of climate change seriously, Barcelona has been applying inspiring policies that concentrate on well-defined green infrastructure and its proven positive impact on the urban microclimate (Ajuntament de Barcelona, n.d.). The local government aims at

achieving this infrastructure through urban farming and gardening as well as green spaces and corridors in urban areas. A good instance of the synergy between mitigation and adaptation policies is the plant selection approach. While choosing plant species for Barcelona Trees Master Plan, plants with low water requirements were preferred and automatic irrigation systems are used for the watering of the trees, for which controlling takes place to prevent any sort of leak (European Commission & European Environment Agency, 2016).



Figure 5. Presence of greenery among the urban fabric of Barcelona. (Ajuntament de Barcelona, 2013)

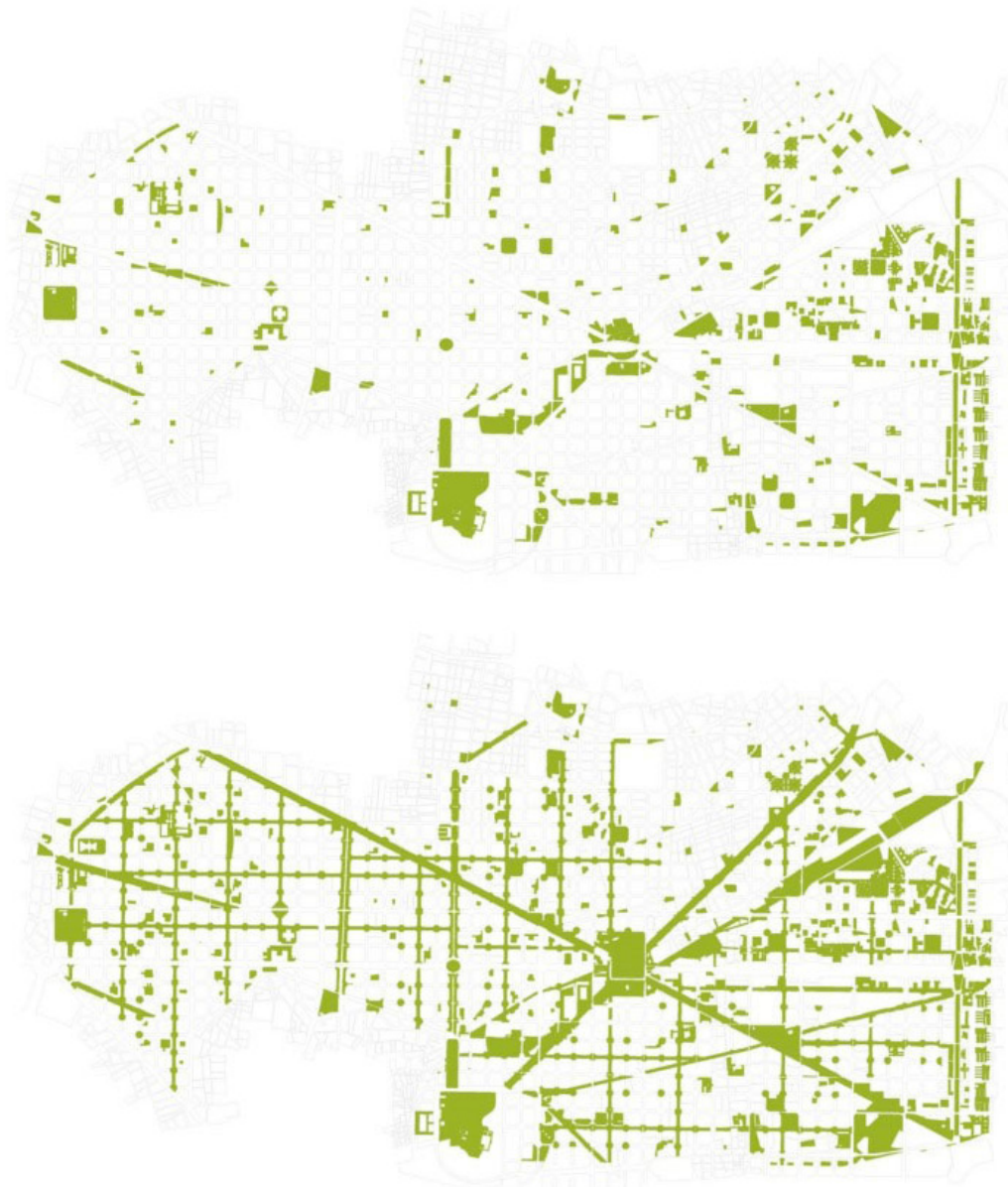


Figure 6. Green space density before and after the Superilles implementation. (Postaria, 2021)

Figure 7. A collage representing a futuristic image of the city in the light of the objectives of Barcelona Green Infrastructure and Biodiversity Plan 2020. (Ajuntament de Barcelona, 2013)





1.4

Urban Morphology & Microclimate

While discussing the impact of climate change on the cities, one must examine how the components of the city act together. The term “city” defines diverse domains, such as diverse economical conditions, lifestyles, demographics and land uses (Taubenböck et al., 2020). Built-up morphologies are one of the most perceivable domains among these, as how we observe a city in the initial phase would be by its physical form (Taubenböck et al., 2020).

Climate change inarguably has a strong interconnection with the urban texture, the urban form components, and thus, the macroform. The branch of science that studies the causes of these changes, transformations and correlated legal aspects is termed urban morphology. In the International Encyclopedia of Human Geography, urban morphology is defined briefly as the “study of urban form” (Lilley, 2009). Having emerged towards the end of 19th century, urban morphology could be referred to as a multidisciplinary practice where geography, architecture and urban studies intersect.

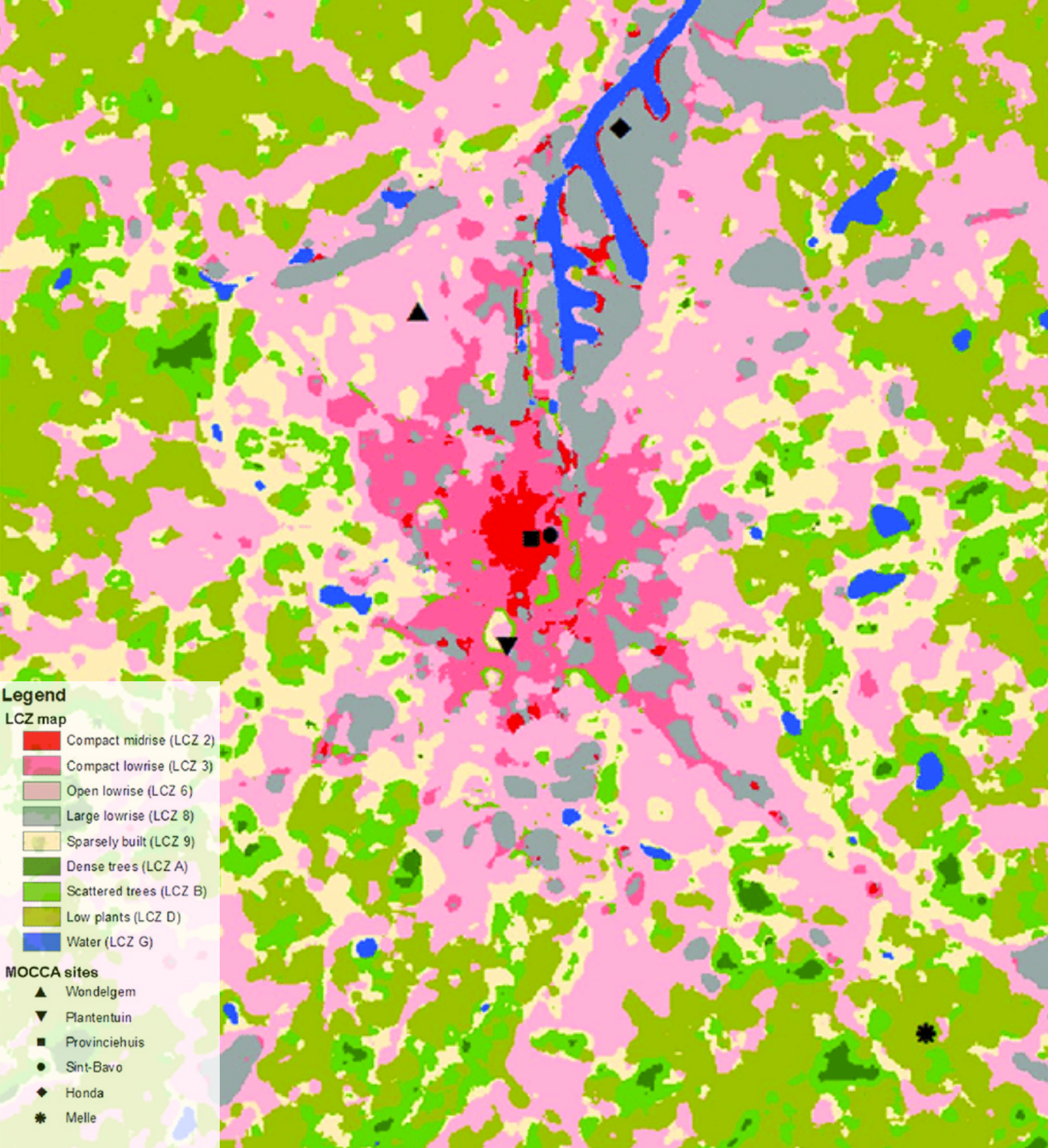
Oke et al. (2017) have listed the key parameters of urban form that affect the atmosphere as fabric, surface cover and urban structure. The term fabric refers to the materials (both natural and construction) that shape the elements (such as vegetation, buildings and roads) in urban spaces. The thermal, radiative and moisture characteristics of the surfaces are decided by the fabric. These characteristics define the material's ability to reflect, absorb and emit the radiation as well as its behaviour when it faces water and heat (acceptance, transference, reflectance). Surface cover refers to the configurations of different fabrics (such built-up, vegetated, paved, water). The partition of heat is associated with surface cover. And finally, the three-dimensional organization of the elements that shape urban environments could be described as urban structure. This term is mostly associated with the dimensions of the buildings and streets. As for the urban scale, the structure is significant for its assistance while determining the aerodynamic roughness and albedo of an urban environment. Within the buildings scale, it is useful as it rules the patterns of airflow and radiative exchange.

As Salat (2011) confirms, urban morphology has a strong impact on ventilation and radiation exchange. Therefore, it is possible to say that urban form factors are useful while evaluating the current situation of the cities as well as future urban scale proposals. Through the use of these factors, one can extract many outputs such as the bioclimatic potential of urban sites or indications regarding how to design comfortable public spaces in terms of wind and sun.

Classification of urban fabric: The scientific community has long been performing urban morphology related studies to classify and organize the distribution of urban functions, to solve the disorder of these functions and to help identifying urban environments issues in the cities (Le Thanh Hoa, 2013). These studies are carried out through several different methods and approaches.

One of the studies that examine this topic could serve as a clear instance to generate a better understanding of the methodology of this thesis and the application field of urban morphology. A study that prompts rethinking of the conventional way of urban fabric classification among the scientific community has been carried out by Stewart and Oke (2012), where they introduce a new classification system to help the scientific community have a common ground while comparing diverse spatial formations. In their own words, they have presented the so-called Local Climate Zones (LCZ) as a “comprehensive climate-based classification of urban and rural sites for temperature studies” and they aim at “improving consistency and accuracy” within the scientific community while reporting urban climate (Stewart & Oke, 2012). With this system, Stewart and Oke embrace a more detailed approach of categorizing, in contrast to the simple and conventional way of defining an area as “urban” or “rural”. Nevertheless, the researchers also note that the proposed system is generic and the output would not be suitable to depict thorough site-specific oddities, despite its flexibility to be applied globally, to any geographical location (Stewart & Oke, 2012).

Figure 8. Overview of the MOCCA network on a local climate zone map of the study area. (Caluwaerts et al., 2016)



Legend

LCZ map

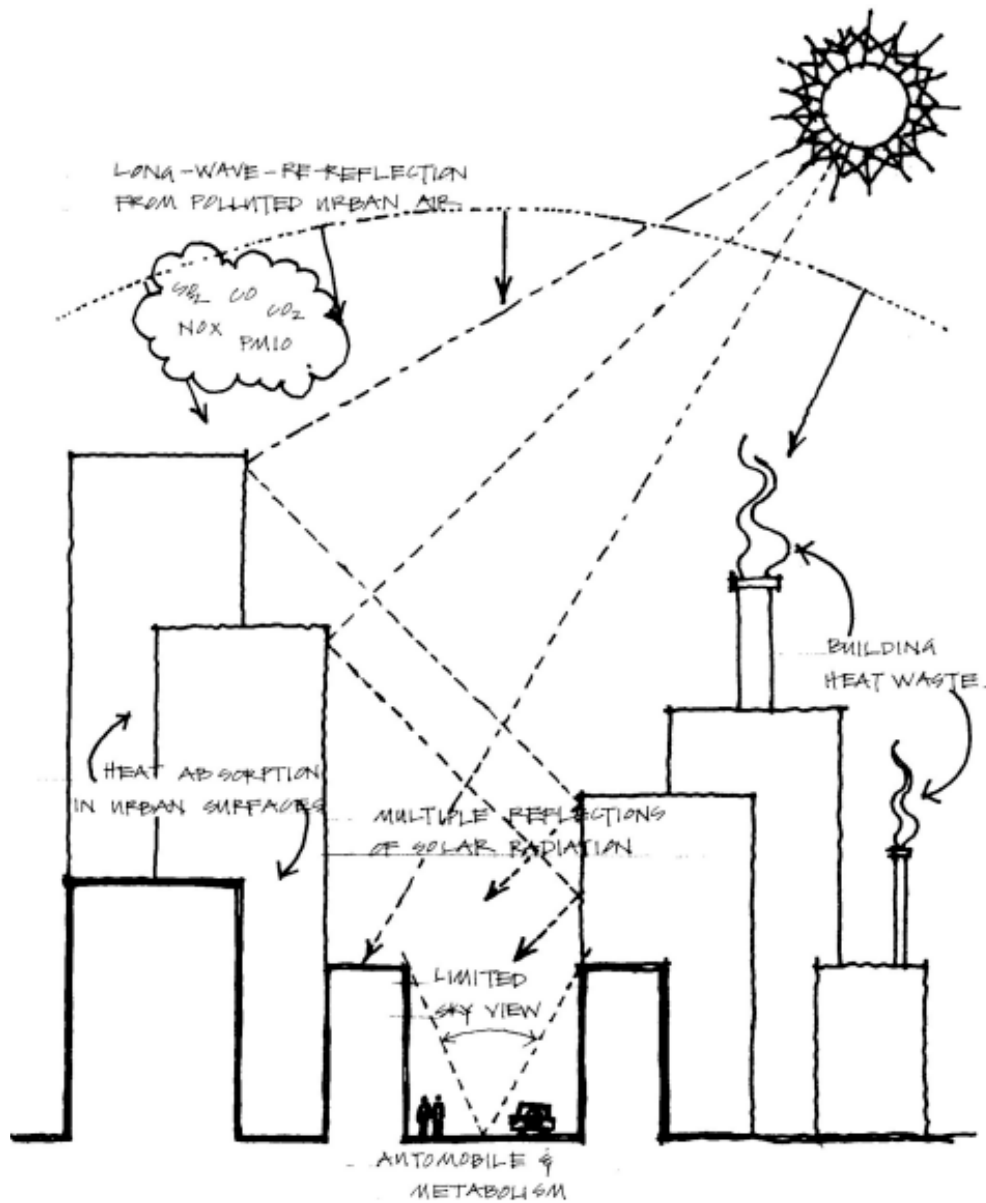
- Compact midrise (LCZ 2)
- Compact lowrise (LCZ 3)
- Open lowrise (LCZ 6)
- Large lowrise (LCZ 8)
- Sparsely built (LCZ 9)
- Dense trees (LCZ A)
- Scattered trees (LCZ B)
- Low plants (LCZ D)
- Water (LCZ G)

MOCCA sites

- ▲ Wondelgem
- ▼ Plantentuin
- Provinciehuis
- Sint-Bavo
- ◆ Honda
- * Melle

interconnections

Figure 9. Summary view of the factors affecting the urban microclimate. (Emmanuel, 2005)



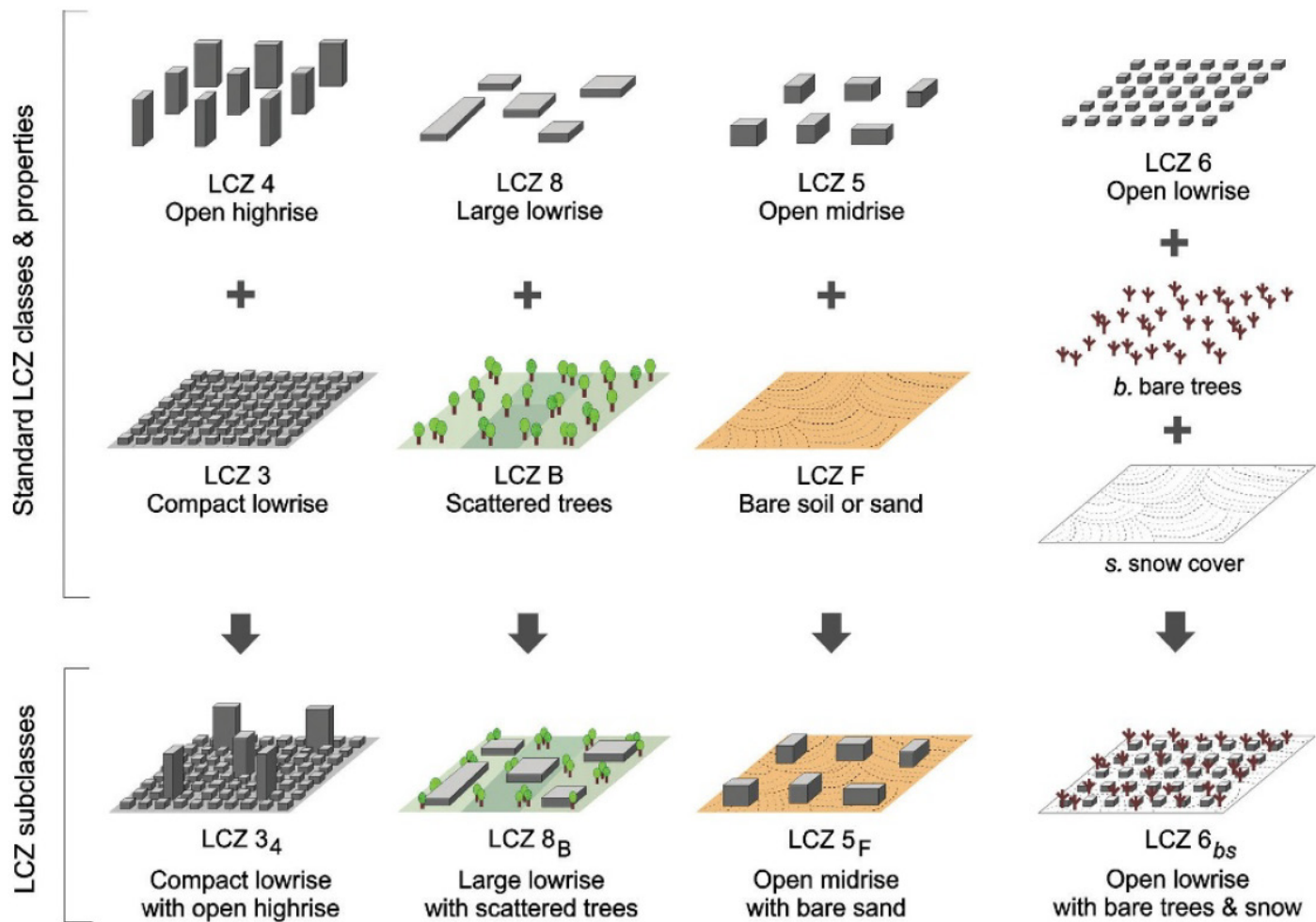


Figure 10. LCZ subclasses to represent combinations of “built” and “land cover” types. (Stewart & Oke, 2012)

classification

Several studies have been performed based on the above-mentioned classification system by Stewart and Oke (2012). One of these has been carried out by Taubenböck et al. (2020), and it aims to classifying 110 cities into 7 types, depending on the spatial urban configuration differences. In conclusion, the findings raise two main discussions: The first result demonstrates that similar cultural, demographical and socio-economic conditions result in similar configurations, whereas the second proves that different geographies and climates can share significantly common characteristics when it comes to urban spatial configuration (Taubenböck et al., 2020).

Thermal comfort: Thermal comfort is defined as “the condition of mind that expresses satisfaction with the thermal environment and is assessed by subjective evaluation” (American Society of Heating, Refrigerating and Air-Conditioning Engineers, 2021). In other words, it is how the human body perceives an environment and thus, it is affected by two main components of an urban environment: meteorological factors (such as air temperature, relative humidity, wind speed and direction, solar radiation) and personal factors (such as gender, age, length of stay) (Lobaccaro et al., 2021). The outdoor thermal comfort can be measured through different comfort indexes, such as PMV, UTCI and PET (Matzarakis et al., 1999). In this thesis PET (physiological equivalent temperature) has been used to evaluate the outdoor thermal comfort of different urban forms in Turin. Höpfe (1999) defines PET as a thermal comfort index which is equivalent to the air temperature where the heat balance of the human body is maintained with core and skin temperatures equal to those of the evaluated conditions.

1.5

Urban Heat Island (UHI)

Urban morphology defines and represents the main character of the city. Microclimate, thermal comfort, vegetation, density and urban quality are the main components that shape urban morphology. These components could be considered as variables that evolve over time as cities grow, and this growing process results in different states of balance between these urban components. The process might cause additional variables to emerge, such as the Urban Heat Island (UHI) effect. UHI, having been coined in the 1940s (Stewart & Oke, 2012), could be defined as an urban or metropolitan area where temperature is recorded to be higher than that of its surroundings (Taha, 2004).

This effect is mainly associated with intense human activity, lack of vegetation and/or water bodies, low surface reflectance or albedo, unorganized built density and lack of ventilation (Hulley, 2012). UHI does not only create uncomfortably warm environments, but also brings additional problems into the scene, such as the need for cooling solutions, and thus, energy consumption and additional costs for construction and infrastructure maintenance (Coffel, 2018).

2

Best Practices

2.1. The case of Thessaloniki, Greece

2.2. The North Desert Village, USA

2.3. EuropaCity, France

During the process of gathering a scientific background for this thesis, many researches and projects focusing on the interconnections between urban morphology, microclimate and A&M (adaptation and mitigation) strategies have been examined. Some of these researches have been presented as examples in the previous chapter, to be able to support the scientific background and to create a better understanding of the scope of this thesis. In this chapter, a selection of prior studies that share a similar scope or mentality to the one of this thesis will be presented. The first two studies are research oriented and they aim at understanding the interconnections between the urban elements and microclimate. The third one is a competition project, which was significant to include in this chapter as it portrays applicable sustainability strategies.

2.1

The Case of Thessaloniki, Greece

type	research
title	“The Contribution of Urban Morphology to the Formation of the Microclimate in Compact Urban Cores: A Study in the City Center of Thessaloniki”
year	2021
location	thessaloniki, greece
authors	g. koukli, a. yiannakou

The first in depth example to be presented is relevant for the aim of this thesis, not only due to its theme, but also due to the methodology that has been followed while carrying out the research. The research has been performed for two adjacent areas in Thessaloniki, Greece. The first step was to carry out an analysis in detail, considering the urban characteristics of the site. The initial differences (regarding the spatial organization) between the sites were determined in this phase. These differences were recognized through a site analysis which

focused on land uses, built and unbuilt area ratios, the amount of green cultivation and the orientation of urban canyons.

Within the second step, the researchers recorded a typology of the built areas, building heights and the width of urban canyon, serving as crucial calculations regarding the main geometric characteristics of both sites. The researchers then used this data to classify urban canyons, which were divided into categories according to airflow regime. The approach of categorizing different variations of an urban element (in this case, the urban canyons) is a useful method to be able to recognize patterns within a city as well as to be able to associate these patterns with microclimatic outcomes.

The final step of the research consists of the modelling and simulation process through ENVI-met© software (version 4.4.3). These simulations helped the researchers understand the microclimatic conditions prevailing in both sites of their study area.

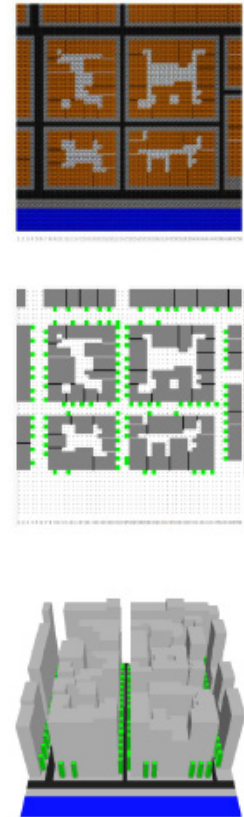


Figure 11. Plans and 3D view exported from ENVI-met. (Koukli & Yiannakou, 2021)



Figure 12. Site plan of the evaluated building blocks. (Koukli & Yiannakou, 2021)

BUILDING BLOCK	BUILDING BLOCK AREA (m ²)	2D FORM OF BUILDING BLOCK	3D FORM OF BUILDING BLOCK	GROUND COVER (m ²)	BUILT-UP AREA (m ²)	AVERAGE ROAD WIDTH (m)	AVERAGE HEIGHT (m)	AVERAGE NUMBER OF FLOORS	COVERAGE RATIO	BUILDING RATIO	H/W OF URBAN CANYON	AIR FLOW REGIME
1A	4242			2839	20,833	13	32	7	0.67	4.91	Str. Chr. Sotiris between B.B. 1A and 2A= 3.5	skimming flow
2A	5246			3515	26,962	13	33	8	0.67	5.13	Str. P. Koromila between B.B. 2A and 4A= 3.4	skimming flow
3A	2879			1812	14,268	13	31	8	0.62	4.95	Str. Chr. Sotiris between B.B. 3A and 4A= 2.9	skimming flow
4A	3647			2402	16,666	13	29	7	0.65	4.56	Str. Mockentaou between B.B. 2A, 4A and 1B, 2B= 3	skimming flow
1B	4610			3058	20,890	17	33	7	0.66	4.53	Str. L. Marganti between B.B. 1B and 2B= 3.5	skimming flow
2B	3402			2046	13,307	17	29	6	0.60	3.91	Str. Stratigou Kallari between B.B. 2B and 3B= 1.6	skimming flow
3B	4643			2799	22,072	17	32	8	0.59	4.75	Str. D. Gounari between B.B. 3B and 4B= 1.4	skimming flow
4B	3575			2316	18,075	17	33	7	0.64	5.05	-	-

Figure 13. Table summarizing the urban form parameters of the building blocks. (Koukli & Yiannakou, 2021)

The outputs regarding air temperature, the average expected thermal index such as the predicted mean vote (PMV) and wind speed allowed them to observe the variations in the microclimatic phenomena as well as why and how these parameters are linked to the urban morphology.

The area, consisting of 8 building blocks and covering an area of 50,573 m², is located on the south eastern edge of the main center of Thessaloniki. The study area is a typical mixed-use area, within the center of an old Mediterranean city (Papagiannakis et al., 2020). The initial site analysis lead the researchers to the conclusion that the main historical and commercial center of the city has limited public, open, and green spaces. The researches also note that the city has a lower percentage of greenery compared to an average European city. The findings of the research underline the strong interconnection between the urban microclimate and the urban morphology:

Compact form: It has been observed that the climatic condition variations are more evident within compact urban areas as the climatic condition changes within the points that have a short distance in between. Focusing particularly on compact building configuration that is common in the city center, the researchers realized that this type of form has a positive impact on the microclimate on occasion, especially during the summer time. This is due to the shading and protection that this form provides, both for the roads and in some cases, for the built environment. Nonetheless, they emphasize that this behaviour would have an opposite impact in the winter time where shaded areas are less desirable and sun exposure is preferred.

Ventilation of urban spaces: According to the wind and temperature simulations performed by the researchers, it was realized that in the cases where urban canyons are perpendicular to the wind flow, the air temperature is improved, compared to the parallel orientation of these two variables (for the summer season). Additionally, the lack of ventilation was observed even in the areas where the urban canyon and wind flow directions were perpendicular. In this case, the reason for insufficient ventilation would be the high H/W ratio and the lack of openings through the building block.

Greenery: The authors underline that the microclimate-friendly effects of trees are significant when they are planted in groups. According to their study, spot-planting does not have a notable positive impact on air temperature whereas sufficiently and generously planted trees on both sides of a road result in an improved microclimate. The lack of groups of dense trees and shading within open areas, prevent the formation of an obstacle against hot wind flow, and thus result in heavy thermal loads and uncomfortable conditions.

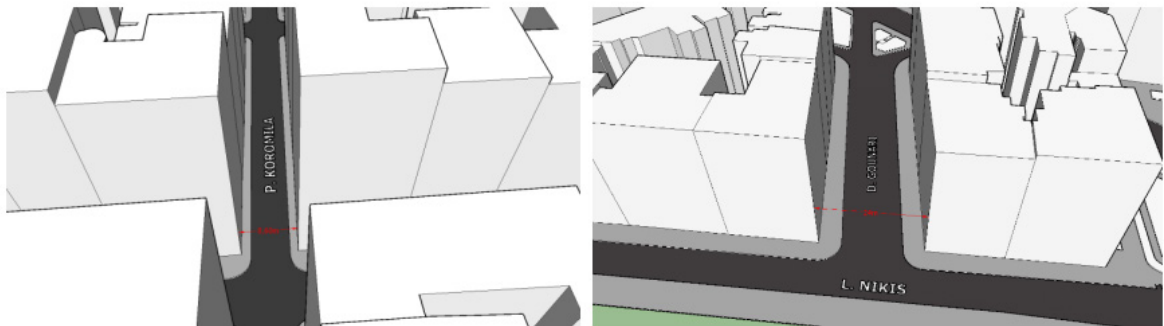


Figure 14. Urban canyon models of the selected areas. (Koukli & Yiannakou, 2021)

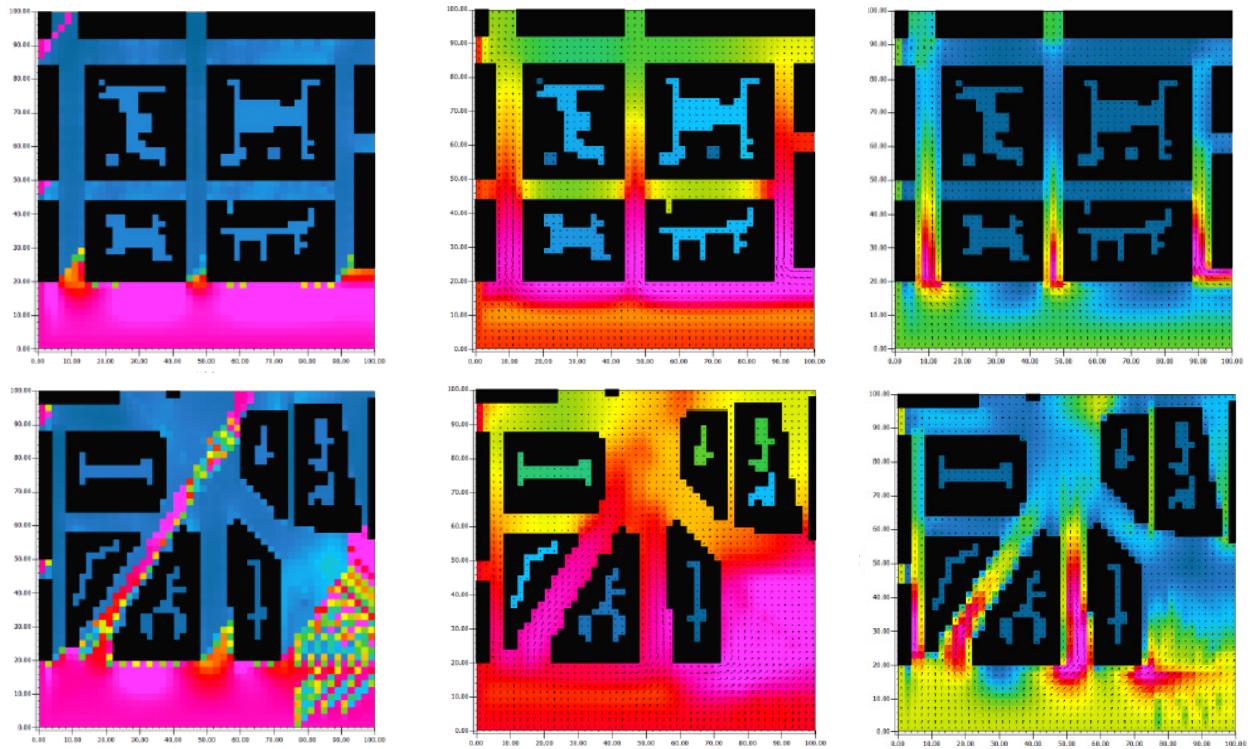


Figure 15. ENVI-met outputs of the research. Left: Predicted Mean Vote results at 15:00 for both areas, Middle: Air Temperature results at 15:00 for both areas, Right: Wind Speed results at 15:00 for both areas. (Koukli & Yiannakou, 2021)

2.2

The North Desert Village, USA

type	research
title	“Impact of urban form and design on mid-afternoon microclimate in Phoenix Local Climate Zones”
year	2014
location	arizona state university, USA
authors	a. middel, k. hän, a.j. brazel, c.a. martin, s. guhathakatura

The study has been conducted by a group of researchers that aimed to understand the influence of diverse types of urban form and landscaping decisions on urban heating and cooling. For this purpose, they have selected the North Desert Village (NDV) residential community (located in Arizona State University's Polytechnic campus) as a study site. The site has been established in 2005 as a “neighbourhood-scale landscape design experiment” (Arizona State University Global Institute of Sustainability and Innovation, n.d.).

The authors of the paper have examined how the urban form and the landscape affect the mid-afternoon microclimate in five representative neighbourhoods within the selected study area. Categorizing the three dominant residential types, being mesic, oasis, and xeric, the research investigates the cooling and warming potential of these forms, related to landscaping and the built environment. It is noted within the abstract of the research that the Local Climate Zones (LCZ) classification scheme of Stewart and Oke (2012) has been followed for the evaluated scenarios.

During the discussion part of the research, the authors confirm the cooling benefits of vegetation presence in an urban area. Nevertheless, they emphasize that the cooling effect is not only the result of vegetation and surface materials, but it is also dependent on the “spatial arrangement of urban features” and thus, the urban form. The findings suggest that the compact urban form is more beneficial for daylight cooling. During daytime, urban form has a larger impact on the temperatures than that of landscaping.

Referring to the prior studies that take the compact urban form as a topic of debate, the authors evaluate both the positive and negative impacts of this specific urban form. Although there are remarkable advantages of compact urban form (such as transportation energy savings), several prior studies criticize this type of urban form as high concentration of built surfaces intensify the UHI effects as well as causing an increase on radiative heating. From another perspective, the authors prompt rethinking of the impact of taller buildings as they are advantageous when it comes to daytime shading, which results in reducing the urban heat.

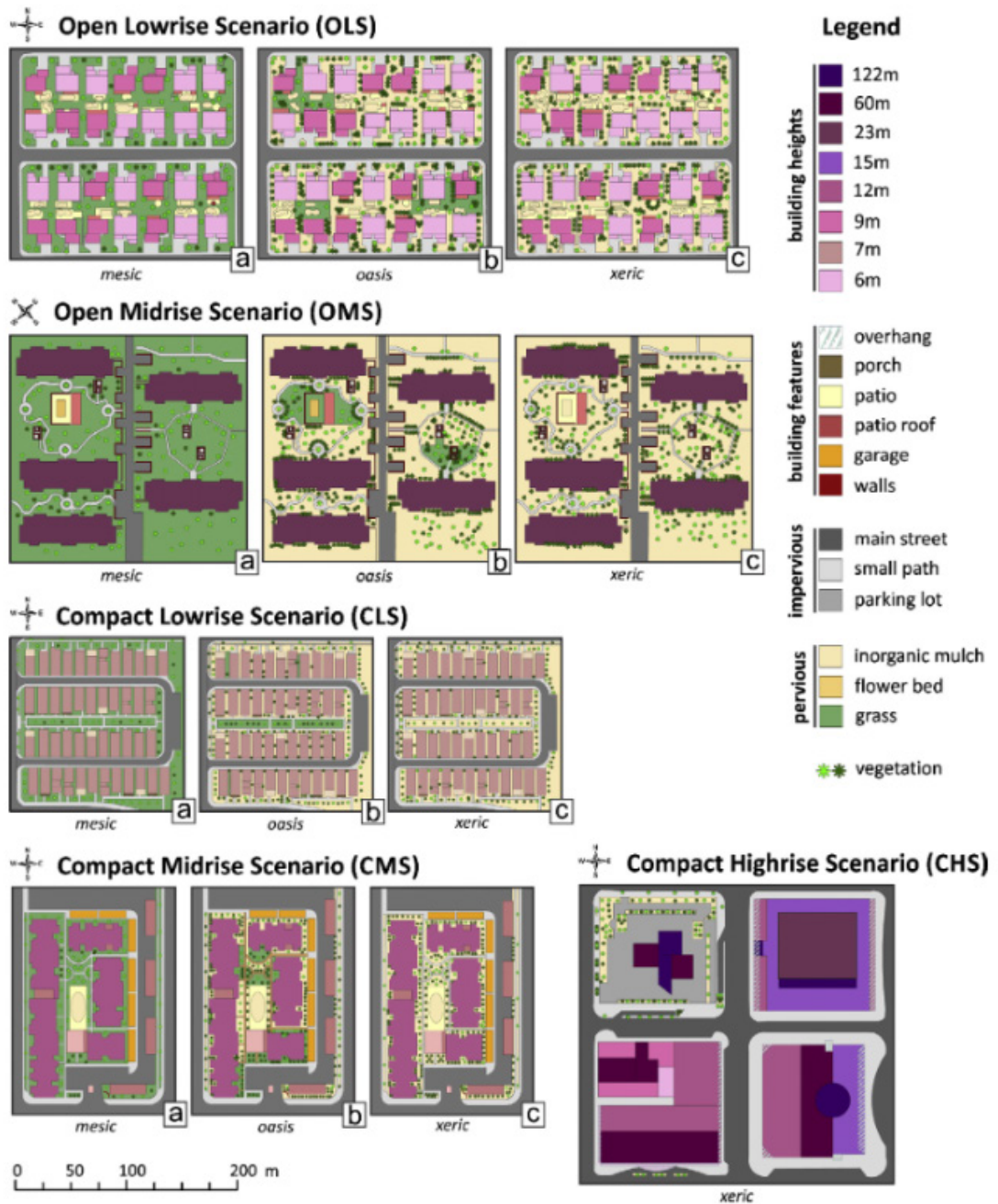


Figure 16. Urban form scenarios classified into Local Climate Zones (LCZ) and combined with four landscaping options: (a) mesic, (b) oasis, (c) xeric. (Middel et al. 2014)

Furthermore, the results emphasize the significance of the orientation of urban canyons that are shaped by mid- or high- rise buildings as when aligned with the direction of the wind flow, they help in decreasing daytime temperature.

Finally, the authors summarize the main findings of their research as follows:

“Cooling is not only a function of vegetation and surface materials, but also dependent on the form and spatial arrangement of urban features. At the microscale, urban form has a larger impact on daytime temperatures than landscaping. In mid-afternoon, dense urban forms can create local cool islands. Spatial differences in cooling are strongly related to solar radiation and local shading patterns. The LCZ classification scheme is a useful concept for integrating local climate knowledge into urban planning and design practices.”
(Middel et al. 2014).

2.3

EuropaCity, France

status	competition winner
architect	Bjarke Ingels Group
completion year	2025
location	paris, france

Following a vision that reads “urban form that combines dense city and open landscapes”, the winning proposal for the EuropaCity competition could be defined as a “massive earthwork” (Vinnitskaya, 2013). Hidden under a landscape-covered roof, forming a sense of topography, the mixed-use functions are organized, including accommodation services, shops, restaurants, leisure facilities, exhibition areas, an artificial ski slope and a water park. Thanks to the landscape roof covering these facilities, the project is in a visible harmony with the urban fabric and the green spaces. Access to the different levels of the project is provided through this roof (Transsolar KlimaEngineering, n.d.).

Moreover, the project stands out with its sustainability concept which covers green tech implementations and energy savings, as well as improved quality for outdoor spaces. The contributors of the project consider the reduction of energy demand as the first step to achieve a net zero carbon balance. Therefore, EuropaCity aims at generating more energy on site than it consumes, putting organic waste back in the cycle through urban farming or producing energy and using renewable energy sources instead of fossil fuels. The energy demand of the whole city is covered by the combination of geothermal energy, biofuels and solar energy. To quote the architects of the project (BIG), *“EuropaCity will be an experimental hybrid between urbanism and landscape design: center and periphery overlapped in the simultaneous co-existence of a recreational open landscape of rolling hills superimposed on an urban neighborhood of walkable streets, plazas and parks”* (Vinnitskaya, 2013).

They envision the project as “a laboratory for sustainable technologies and a showcase for viable green tech implementations that does not only save energy, but also improves the quality of the urban environment” (Butler, 2013). All of these applications would demonstrate an example of how to deal with the challenges of our century and guide towards a future where above mentioned strategies and mentality is widespread (Transsolar KlimaEngineering, n.d.).

Figure 17. Rendering of EuropaCity.
(Transsolar KlimaEngineering, n.d.)





3

The Case of Turin

3.1. Historical Evolution of Turin's Urban Form

3.2. Climatic Context

3.3. Green Areas

3.4. Air Quality

3.5. Water Infrastructure

3.6. Mapping Turin: Classification of Urban Fabric

Following the previous chapters of literature and global practices, this chapter focuses mainly on the city of Turin to develop an understanding of the evolution of the city as well as its sources which could potentially contribute to mitigation and adaptation strategies that could be applied (or in plans to be applied) in the city.

After discussing the current situation and future plans for the city, the city is divided into ten diverse types of urban fabric, achieved through an in-depth analysis, and consequently, a detailed mapping process of each building block in the city. The maps aim to illustrate the distribution of urban tissue in Turin and would serve as a pool for the selection process of case studies that would investigate the microclimatic response to each typology of urban fabric in the next chapters.

3.1

Historical Evolution of Turin's Urban Form

The summary in this section is mainly based on the online exhibition by Museo Torino, namely "Torino: storia di una città" (MuseoTorino et al., 2012). Other sources that have been used for this section have been added as in-text reference, where relevant.

The strategical location of Turin has always been remarkable through its history, being one of the simple access points through the Alps. The River Po intersects the city that is surrounded by hills and the mountains, being the Ligurian Apennines to the south, Monferrato hills to the east and the Alps to the west. The city owes a remarkable amount of its industrial reputation to these geographical and physical conditions, where it used to benefit from the water power sources that were available through the water channels along the river Dora, Stura and Po (MuseoTorino et al., 2012).

It would be useful to investigate the historical evolution of the city, under the light of historical evidences that demonstrate the political, economical and demographical aspects of it. The above-mentioned features of the city created a strong base for the growth of the economic

and demographic resources. The subjugation to the house of Savoia in 1280 marks a remarkable point in the history of the city, where a new chapter for the historical and urban planning of the city began. Following the directions of the Dukes Emanuele Filiberto (1563-1580) and Carlo Emanuele I (1580-1630), the first implementations took place in the form of the expansion of the new city, which was completed by Vittorio Amedeo I (1630-1637). The fortifications of the city were the two main goals of Emanuele Filiberto's urban policy, as he encouraged placing the new castle and the Duke's residence to the opposite sides of the Roman castrum to be able to sustain the city's need to be defended while being besieged (MuseoTorino et al., 2012).

Subsequently, Carlo Emanuele could dedicate himself to generating the project of the new civil city which aimed at integrating the old Roman and medieval city within an almond-shaped wall circuit. This implementation allowed for a tripling in the size of the city. From 1673 onwards, the "well-governed city image" and thus, the fidelity to the project of the dynasty were confirmed through the implementations regarding the second extension of the city of Turin, which was initiated on the axis of the military road of Po. Following the death of Charles Emmanuel II (1675) and the reign of Maria Giovanna Battista of Savoy Nemours (1675-1684), a perceivable strength loss has occurred within the government, which put the growth of the city and the continuity of the project that was being applied to achieve a well-structured city in danger. The palaces that intend to emphasize and become a symbol of the power of the government has started to rise (MuseoTorino et al., 2012).

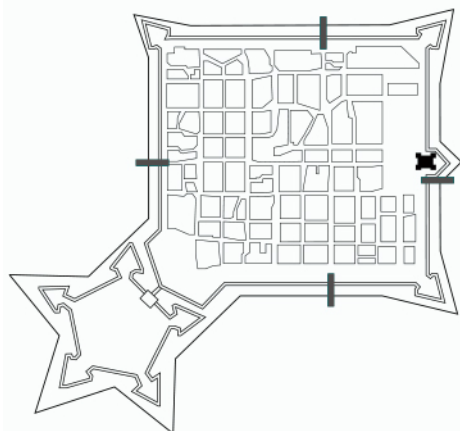
After the Treaty of Utrecht in 1713, the city of Turin gained the title of being the capital of the Kingdom of Sicily as well, soon to be that of Sardinia which allowed the dukes to have the royal title and recognition in Europe. The highlight of this period was the governance of Vittorio Amedeo II, who had decided to renew the architectural image of the city, inspired by the international case studies. To give life to this idea, he contacted Filippo Juvarra (the prominent architect of this era, from Messina) where he gave him the responsibility of carrying the city to a state of being an 18th century world capital (MuseoTorino et al., 2012).

As the first royal architect (1714), Juvarra had an urban renewal approach of “widespread centrality”, which was based on the powerful relationship between the institutional government and the entire territory. He applied his very own reflection regarding the hierarchy of urban and outer space, through which the generic characteristics of the 17th century city has been overcome. The first implementations of Juvarra aimed at extending the city towards the west, at Porta Susina, as well as the design and completion of emblematic buildings of the state, such as the Secretariats of State (Le Segreterie di Stato e i Regi Archivi) and the so-called military quarters barracks (Quartieri Militari), the basilica of Superga, the building of Stupinigi, the unrealized project of the palace at the castle of Rivoli, as well as the facade and the staircase of Palazzo Madama (MuseoTorino et al., 2012).

Another focus of the urban development during this era was the restructuring of the ancient center of the city, with the enlargement of Porta Palazzo (the current Via Milano), shaping the two blocks towards the north gate of the city

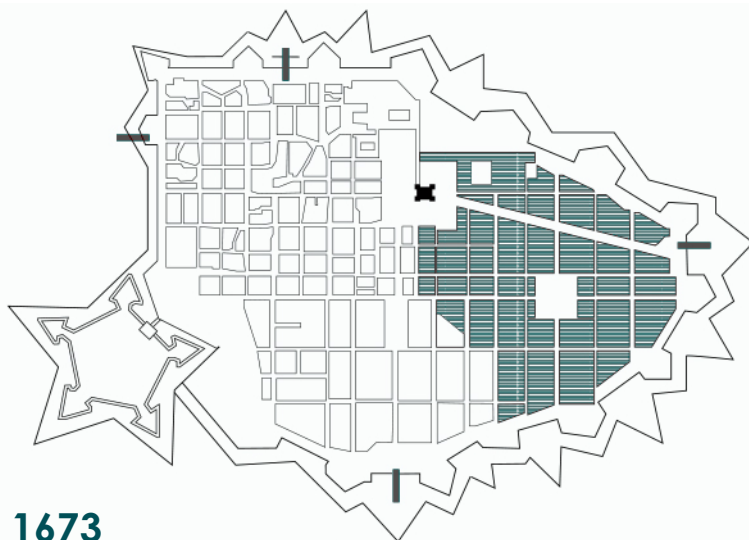
with the rhomboid square nearby. This whole process could be referred to as the third expansion of city, in the course of which the which the proposed layout has continued to follow the orthogonal Roman grid. Followingly, Juvarra moved to Madrid due to the call of Philip V of Bourbon and towards mid-1700s, a new vision for the capital was followed. The scenographic idea of Juvarra was replaced with an approach that considers the urban dimension, meaning that the idea was an entire transformation of the city, instead of partial implementations. Through the legislative instruments, public and private architecture were promoted to configurate a packed and uniform image of the city that combines the aesthetical and functional features. This led to the deliberation regarding the fate of the suburb. The noble population was encouraged to take part in the transformation of the city through entrepreneurship, and by the presence of construction sites opened in the suburban part of the city; which could be referred as a Baroque territorial system (MuseoTorino et al., 2012).

As the French sovereignty had begun and Turin had lost its status of being the Italian capital (1802), the city evolved to be a service center and a commercial hub between Italy and France. The dismantling process of the fortifications around the city has begun, along with the placement of large squares at the end of ancient road outlets, proposing a “promenade” system through the use of vegetation. This system was applied to replace the ramparts that were in the process of being dismantled. As the urban cadastral system begun, the city was divided into four parts regarding the classification of commercial flows and the streets and squares of Turin have been assigned a fixed name,



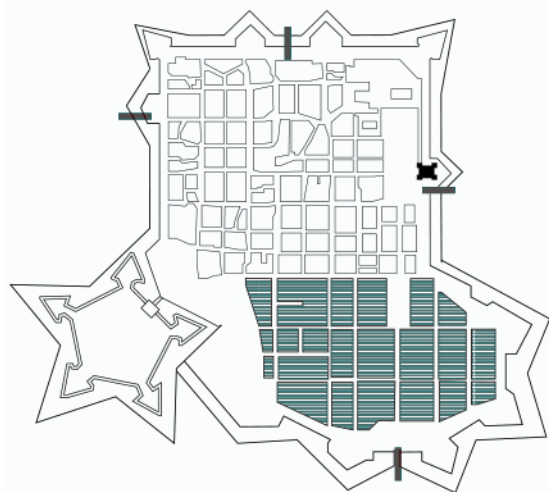
1577

Initial borders



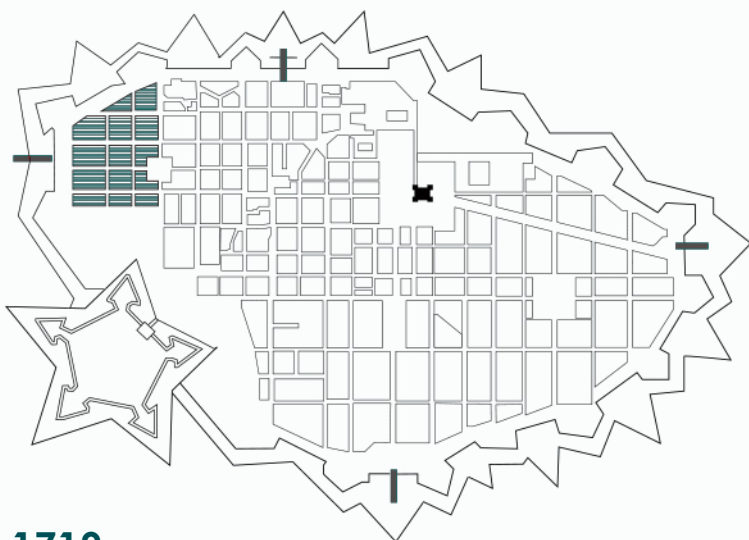
1673

Second enlargement



1620

First enlargement



1719

Third enlargement

Figure 18. Historical evolution of the central part of the city between 1577-1719. (based on: Ricchiardi, 2018)

along with the indications of the house numbers: a system that was firstly introduced in Paris (MuseoTorino et al., 2012).

Turin, regaining its capital title, was under the French urban influence at the time. The land of the demolished city walls was continuing to be sold in the area of Piazza Emanuele Filiberto (now of Piazza della Repubblica) and of Porta Nuova (now being Piazza Carlo Felice). The construction work was also intensely ongoing around these areas, along with Borgo Nuovo between Porta Nuova and the Po. The construction of Piazza di Po (now being Piazza Vittorio Veneto) had begun circa mid-1820s. Followingly, at the beginning of 1840s, the problem of the extension of the urban perimeter outside Porta Nuova, in Vanchiglia and in the land around the citadel arose (MuseoTorino et al., 2012).

During the second half of the 19th century, the new customs barrier route was established. The Citadel was demolished, which prepared a base for an immense extension of land, where Piazza Statuto, Porta Susa and Novara railway station are located. The connection options to Porta Nuova were improved, tracing an orthogonal grid of avenues that have three lines, unlike the large “promenades” that were built under the French influence. The goal was to strengthen the connection of these extensions to the ancient city and porches were used as a key element for this purpose (MuseoTorino et al., 2012).

Although Turin has become a major attraction for political migrancy and financial investments, the situation has changed reversely when the city

lost its status of being the capital of a kingdom. This occasion is followed by an exodus of population and the restructuring of the economic system. However, the city has leisurely grown out of the crisis during the late 19th century, being a center of manufacture and thus, a dichotomy has started to emerge between the bourgeois part of the city and the residential areas (as well as the suburb) where the working class accommodated (MuseoTorino et al., 2012).

The growth of the city continued rapidly with the start of 1900s, both within and outside of the customs barrier: outside of the barrier, the villages of Campidoglio, Regio Parco, Monte Bianco, Monte Rosa, via Giachino, Vittoria and “di Nizza” have been shaped, due to the lack of taxation for construction materials and to not being under the control of the municipality. Whereas, within the barrier, two neighborhoods (Borgo San Paolo and another beyond Dora) have served as a settlement for the working class (MuseoTorino et al., 2012).

During this era, the first traces of the settlements can be observed on the east side of the River Po, where the hill begins. These settlements would look over the first urban park, being Valentino, and would serve as a residential area for the bourgeoisie.

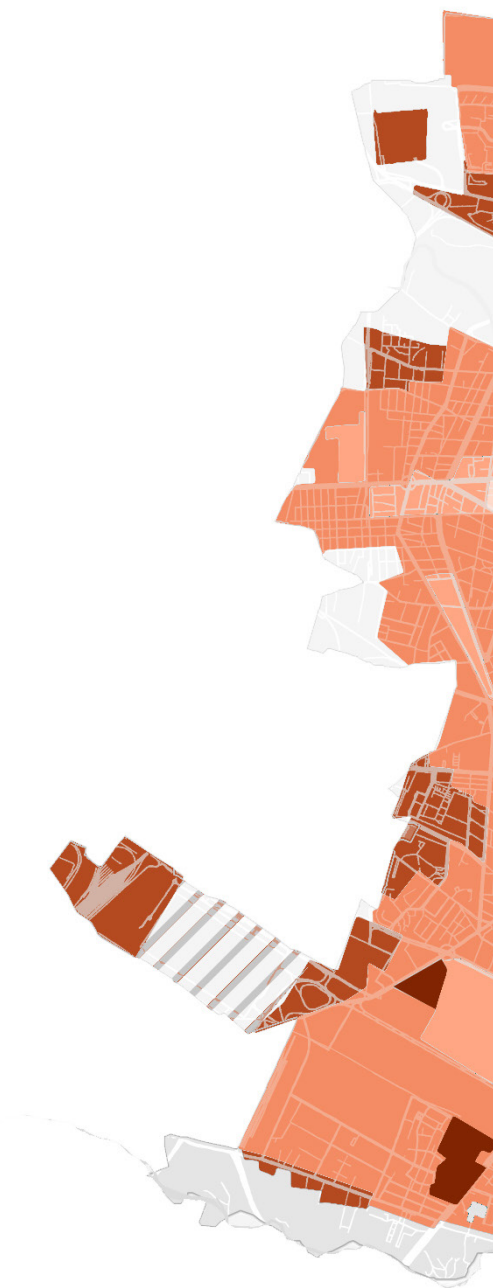
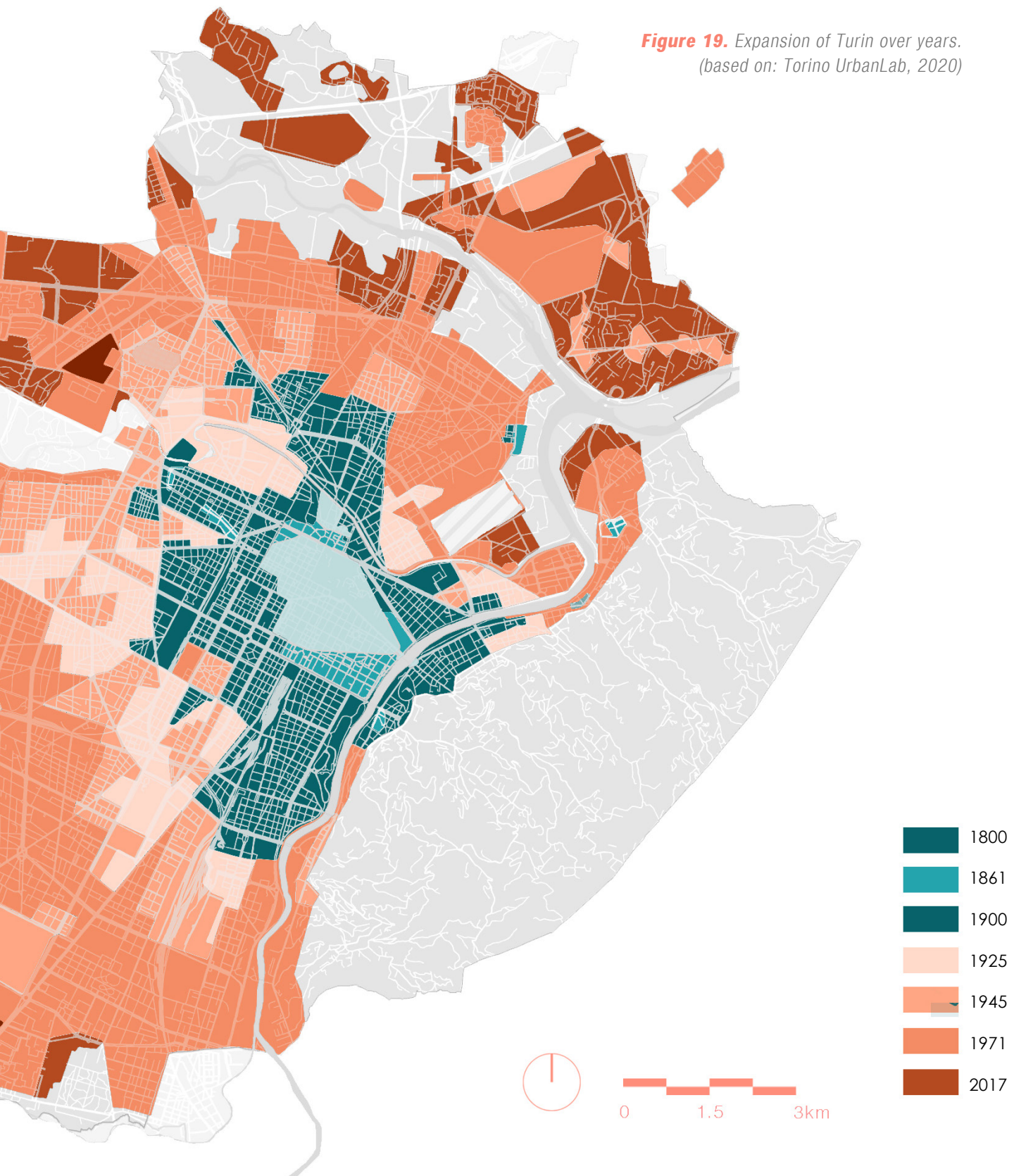


Figure 19. Expansion of Turin over years.
(based on: Torino UrbanLab, 2020)



Thereafter, with the construction of a sewerage system and the diagonal cuts of significant streets, this era could be considered concluded by 1908, as the first drafting of the new masterplan (*il nuovo piano regolatore*) was made. The manufacturing of automobile was newly born, which would inevitably lead to the reorganization of the production fields in the future. The establishment of the FIAT Mirafiori factory in 1939, resulted in a flow of immigrants from other regions of Italy, which has triggered the need of housing. Subsequently, the industrialization process of Turin affected its urban fabric in both ways: quickly designed residential units built for the workers and industrial areas that were later abandoned. Moreover, a second flow of newcomers arrived after the Second World War as the industry recovered after the war and workers from Veneto and other regions in the country started to fill the city (Ricchiardi, 2018).

It can be said that the urban renewal dates back to the late 19th century, in the modern age, when European cities were subjected to sanitary engineering to improve urban health conditions. During that time, the main metropolises, such as Paris, Barcelona, London or Turin, transformed their urban fabric through massive demolitions and reconstructions, while searching for air, light and modernity. In these cases, urban renewal is related to large demolitions or repurposing of former buildings with new ones (Barosio et al., 2016).

With a goal of de-industrialization, the City of Turin approved the General Urban Master Plan in 1995, addressing urban regeneration and urban redevelopment. There were two main elements that would determine the future of Turin's urban transformation: the outcomes of Fordism (leaving more

than six million square meters of abandoned industrial areas behind) and 2006 Olympic Winter Games (for which the city had received a large amount of investments from public and private sectors). Following the guidance of the General Urban Master Plan, many urban regeneration and recovery actions have started, in addition to the launching of the projects concerning urban quality improvement and strengthening the social fabric, such as the cases of Spina 2, San Salvatio and Urban 2 project in Mirafiori Nord (Barosio et al., 2016).

3.2

Climatic Context

3.2.1. The evolution of long-time data series

Before discussing the microclimatic response to the urban form, it is significant to have a better understanding of Turin's climatic conditions with a particular focus on its vulnerabilities. Therefore, a part of the literature review was dedicated to analyze the findings of the scientific community with a focus on this topic.

Garzena et al. (2018) have conducted a research where they analyzed the long-time climate data series, being one of the longest for the whole Italy, dating 260 years prior to their date of analysis. Throughout their research, they have analyzed not only the data regarding temperature, precipitation, tropical nights and the cool days, but also the effect of the city's urban growth on these parameters, and eventually, on the development of UHI. According to the data that was discussed within the research, it is possible to observe the increase in the temperature and the reduction in the number of cool days over years (see Figure 20). Figure 20 illustrates the historical evolution of the air temperature, population and the increasing use of vehicles and cars. Before 1920, the trends of population and air temperature do not show a clear correlation.

However, between 1920 and 1970, both of them exhibit an increasing trend, making it evident that their trends are correlated to each other (Garzena et al., 2018).

After the population has its peak in 1974, as a result of the economic boom and the rapid industrialization of the city, although the population trend seems to decrease, the temperature trend does not follow the same behaviour. Instead, it keeps increasing as another important determinant starts to show a similar trend: the use of vehicles. As for the relationship between the temperature and the number of vehicles, it is clear from the graph that after 1980s, their trends are correlated to one another more strictly than before (Garzena et al., 2018).

3.2.2. Climatic vulnerabilities of the city and the territory

According to the report of the Turin municipality concerning the “Analysis of Climatic Vulnerabilities in Turin”, the temperature increase in the last twenty years has increased up to 5 degrees above the average temperature within the interval of 1971 and 2000. Additionally, this value is close to the warmest summer temperatures which have been recorded during the summers of 2003, 2015 and 2017 (Arpa Piemonte Dipartimento Rischio Naturali e Ambientali & Citta di Torino, 2020).

Within the same report, the number of tropical days and nights have also been addressed. Tropical days refer to the days where the maximum temperature is recorded to be higher than 30 degrees (Arpa Piemonte Dipartimento Rischio Naturali e Ambientali & Citta di Torino, 2020), whereas tropical nights

are described as the night where the temperature is higher than 20 degrees (European Commission & European Environment Agency, n.d.).

In the case of Turin, the number of days characterized by physiological discomfort has been analyzed for the intervals of 1989-2016 and 2001-2016, to be able to determine whether a separate trend within the last 15 years (according to the time of the research) occurred. When this data was put in the same chart as the number of tropical days and tropical nights, it was understood that the number of the days characterized by discomfort have increased within the second interval (2001-2016), except for that of the tropical nights (Arpa Piemonte Dipartimento Rischi Naturali e Ambientali & Citta di Torino, 2020).

The report from Arpa concerning the climate of Piedmont region notes that 2021 has been the 15th warmest year in the past 64 years with an average temperature of about 9.9°C and an average temperature anomaly around +0.8°C compared to the 1971-2000 climatology. For the first time since 2014, a season with below-normal temperatures have been recorded in 2021. Additionally, Spring 2021 has been the first season to break the sequence of the warmest seasons in climatology, which covers the interval from Autumn 2014 to Winter 2021 (Arpa Piemonte Dipartimento Rischi Naturali e Ambientali, 2021).

3.2.3. Urban heat islands in Turin

In the case of Turin, Arpa Piemonte has conducted a climate assessment study for the urban area of the city and presented the results in May 2018. The distribution of the heat island risk through the city has been summarized in the Climate Resilience Plan by the Municipality of Turin (Città di Torino, 2020).

According to the report:

- 27% of the region has been defined to have a low risk of heat island;
- 44% of the region has been defined to have a medium risk of heat island;
- 2% of the region has been defined to have a high risk of heat island;
- the remaining 27% represents the areas that are considered to have no risk of heat island.

The analysis demonstrates that the urban fabric of the city is mostly classified as “moderate-danger area”. As for the high-risk areas, they are not limited to but clearly visible around two large industrial zones, namely the IVECO complex in the north-east and the FIAT complex in the south-west (Citta di Torino, 2020).

After having reached the conclusion where industrial zones are the ones that are subjected to a higher risk of heat island, a deeper analysis was conducted with a focus on the impact of these zones on their surrounding areas. According to this analysis, the average temperatures during the selected extreme heat events are 3°C higher than the city average, in the areas that are in a distance of 50 meters from the industrial buildings. Between 50-100 meters, this value drops down to but still reaches 1°C (Citta di Torino, 2020).

Figure 20. Historical evolution of the air temperature, population, vehicles and cars in Turin. (Garzena et. al, 2018)

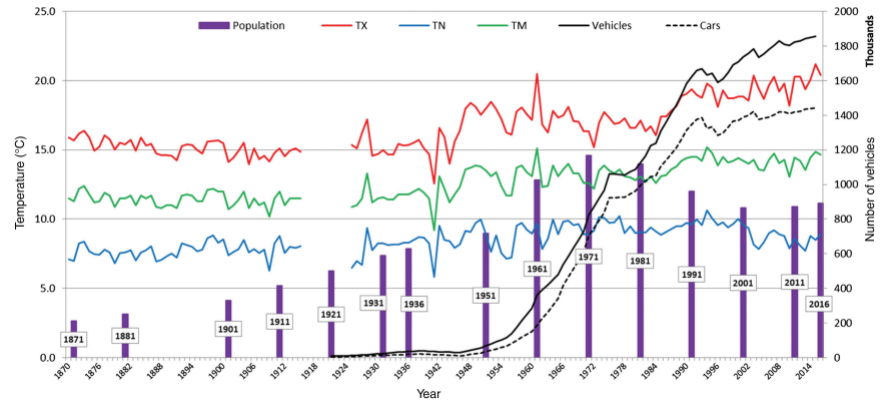
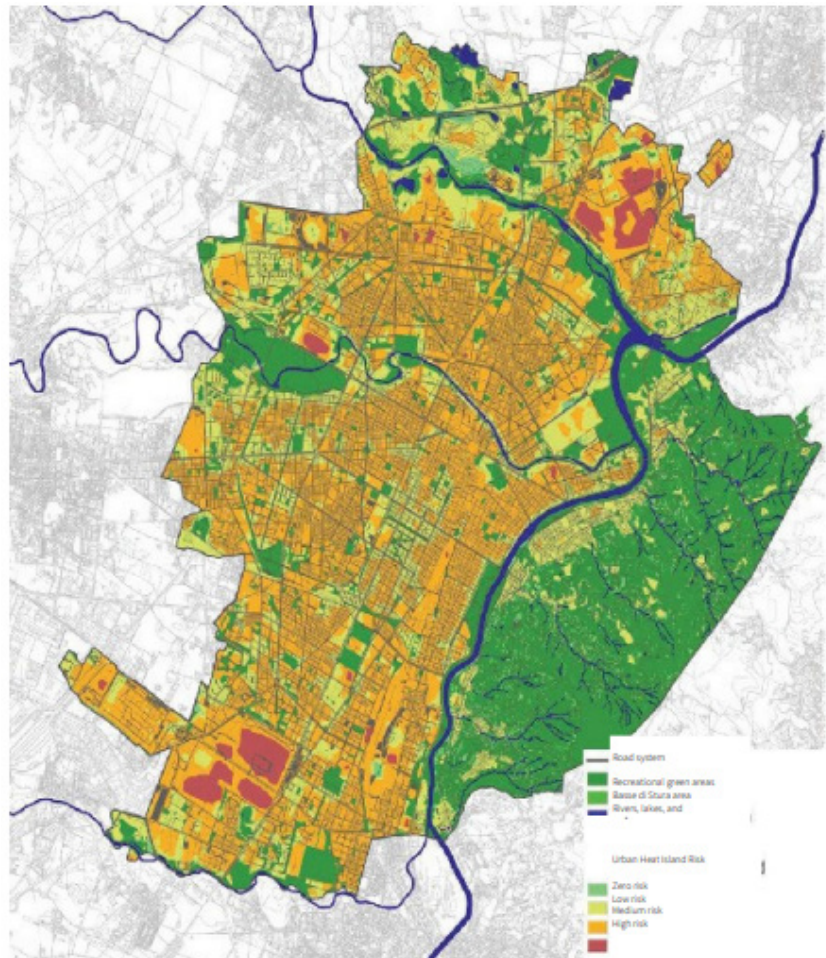


Figure 21. Distribution of Urban Heat Islands in Turin. (Città di Torino, 2020)



3.3

Green Areas

Green areas are considered as important urban elements that contribute to mitigating the UHI effect (Wong & Yu, 2005). In the words of Wong and Yu (2005), “Green areas are actually the ecological measure to combat the problems of the concrete jungle”. Through evaporation and transpiration (evapotranspiration), vegetation cools the environment. Through its shading effect, it cools surfaces and limits their short-wave radiation absorption. As the open fields have a high sky view factor, they provide good conditions where the heat can escape through long-wave radiation (Kleerekoper, 2016).

In the case of Turin, the city is surrounded by large parks such as Valentino, Colletta, Pellerina, Tesoriera, Ruffini and Colonnetti, in addition to the hill that is on the east side of the river Po. These parks are complemented by a system of gardens, playgrounds and plazas along which trees are lined. Particularly after 1960s, the urban planning regulations made it mandatory to include gardens and playgrounds within urbanized areas. Therefore, it is possible to say that these regulations played a significant role in including green areas within urban environments in Turin (Torino Urban Lab, 2018).

Figure 22. Cooling influence comparison between urban environments that have two small parks and one large park. (Kuypers et al., 2018)

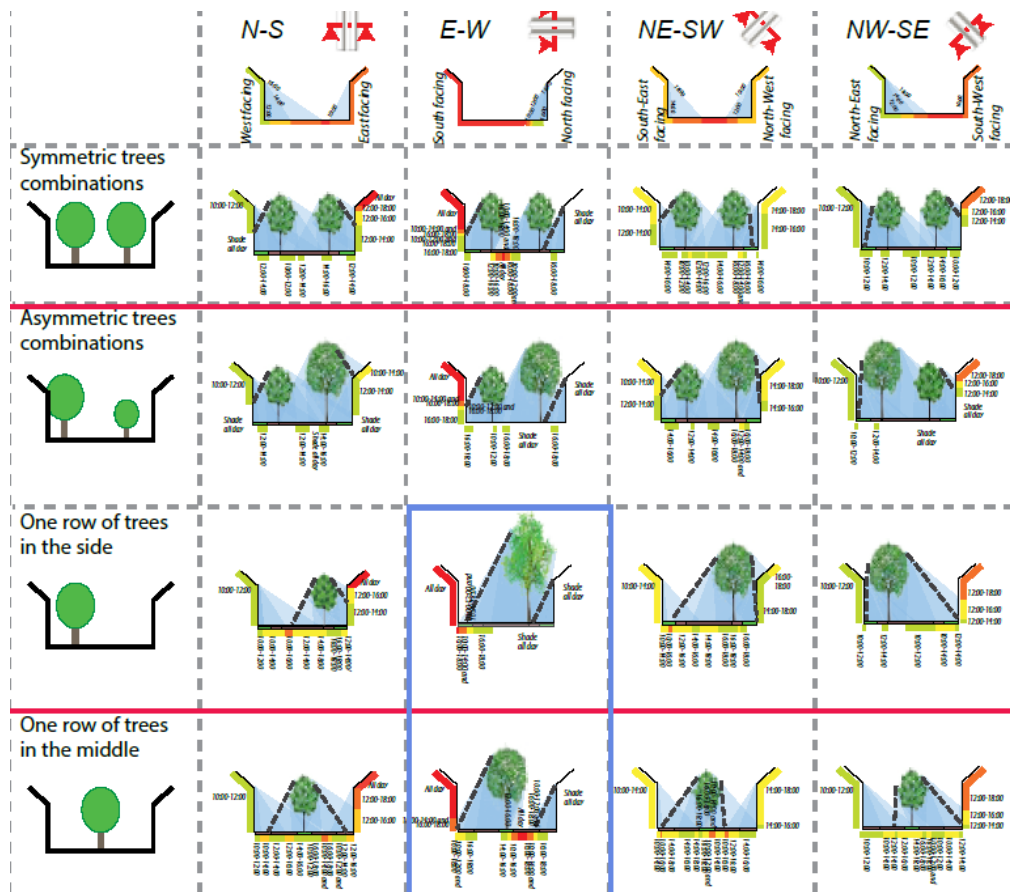
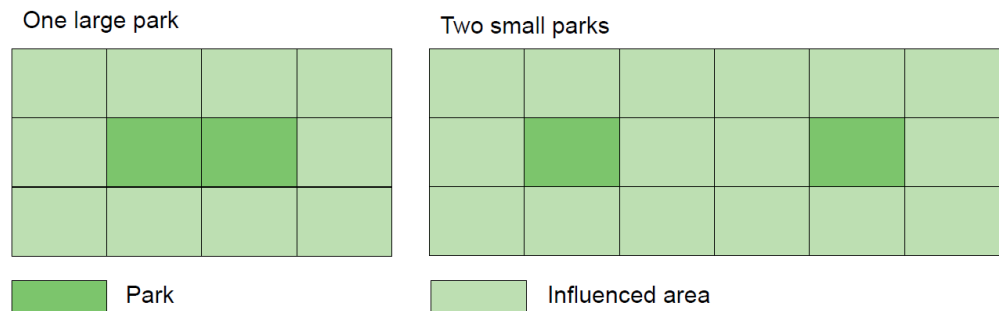


Figure 23. Selection of the most suitable solutions for street shading and keeping the solar access for the walls/windows. (Hotkevica, 2013)

In addition to the open fields, vertical greenery plays a significant role when it comes to the microclimatic conditions of a city. Street trees might seem to have a low impact in this manner, due to their scattered distribution. However, they do not only provide cooling during summer but also they help in breaking the wind, and eventually blocking long-wave radiation, which results in slowing down the heat loss to the atmosphere (Kleerekoper, 2016). As for the case of Turin, many of the main and side roads of the city are followed by tree axes. The number of these road-side trees are more than 82.000: the main roads include more majestic species such as horse-chestnut trees (*aesculus hippocastanum*), plane trees (*platanus*), linden trees (*tilia*) and hackberry trees (*celtis*), whereas the minor roads are followed by the species of *prunus* and *wisteria*, rounding up to 70 species in total (Torino Urban Lab, 2018).

Beyond their role in controlling heat distribution (and thus, in some cases, eliminating the cooling costs), green areas also help reduce air and water pollution. As for air pollution, trees serve as capturers of particulate matter (PM), by attracting the positively charged particles as a result of them being negatively charged (Kleerekoper, 2016). Furthermore, the emissions of the cars that are parked in the shade are recorded to be lower (Scott et al., 1999). Regarding water pollution, the green areas prevent discharge into groundwater or rivers and streams with their ability to bind nutrients and heavy metals in the soil (Kleerekoper, 2016).

The stakeholders, local communities and the government are working hand-in-hand to eliminate the negative impacts of climate change through taking action. To be able to define strategies for the rich nature of Turin, the strategic

plan of green infrastructure was launched in parallel with the preparation of the climate adaptation plan. Examining the greenery of Turin, the strategic plan of the green infrastructure aims at defining strategies not only for the enhancement of greenery as well as increasing the ecological connectivity and biodiversity (Comune di Torino, 2020b).



Figure 24. Greenery data of Turin. (Comune di Torino, n.d.-b)

3.4

Air Quality

The management and controlling of the air quality in a city is one of the most significant issues concerning environmental protection, especially due to its impact on the health and well-being of the inhabitants. In the case of Turin, the air quality is dependent on the pollutants caused by anthropogenic activities and the particular geographical situation of the entire territory of Po Valley (Pianura Padana), as well as the critical climatic and meteorological conditions. Among the Italian cities, Turin is known to be one of those with the highest rate of air pollution (Comune di Torino, 2020a).

3.4.1. Main Pollutants

Particulate matter (PM10 and PM2.5) could be defined as a set of solid or liquid substances in the air, with dimensions ranging from 10 or 2.5 μm (Arpa Piemonte & Città metropolitana di Torino, 2022). The reaction of different pollutants in the atmosphere result in the formation of particulate matter.

Nitrogen dioxide is a pollutant that is an outcome of fuel combustion processes in the air, while ozone is defined as a photochemical pollutant which is the outcome of solar radiation and temperature from the pollutants that are already present in the air (ozone precursors) (Citta di Torino, Arpa Piemonte & Azienda Sanitaria Locale, 2019). Ozone and PM usually coexist during the overheated season.

3.4.2. Current Situation

The PM10 limitations by the Italian law requires not to exceed an annual average of 40 µg/m³ and a daily average of 50 µg/m³, where the daily average is not supposed to be exceeded more than 35 times a year. As for PM2.5, the limit is up to an annual average of 45 µg/m³.

The Annual Air Quality Report for Turin in 2021 (Uno Sguardo All'Aria 2021) demonstrates that nine out of the twelve pollutants that were measured have met the target values. PM10 and nitrogen dioxide have exceeded their limit values. However, the reduction of these pollutants have

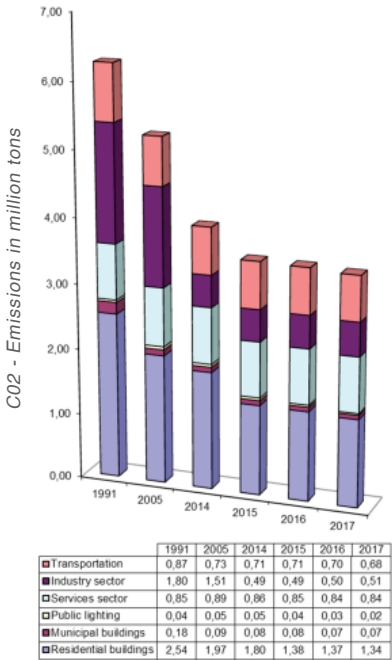


Figure 25. CO2 emissions from diverse sources. (Città di Torino, 2020)

shown significant improvements compared to the measurements of the previous years. This comparison is mainly between 2021 and the years 2018-2019 instead of 2020, as during 2020, non-comparable emission anomalies have been recorded due to the COVID-19 measurements (Arpa Piemonte & Città metropolitana di Torino, 2022).

As for the PM10 particulate matter concentrations, daily limits have been exceeded within the urban area and have been recorded to get close to the daily limit in the suburbs. The concentrations measured by the traffic stations were still high, as in some cases the recorded value was two times more than the permitted one. In contrast to the daily limits, the annual limit value has been met in all zones that were monitored (Arpa Piemonte & Città metropolitana di Torino, 2022).

When the air pollution data regarding nitrogen dioxide measurements were examined, the improvements in reduction compared to years 2018-2019 were realized and the reduction of emissions in 2020 due to pandemic-related measurements were evident. On the other hand, ozone has been recorded to exceed the human health protection target value for all the measurement stations (except for Ceresole Reale) and not to show evidence of concentration reduction (Arpa Piemonte & Città metropolitana di Torino, 2022). The report also notes that, according to the results derived by time series, the emission reduction measurements have not always been enough to reach the target limit within a given time frame. In fact, a delay within the schedule of improvement is evident.

Nevertheless, the data shows that the measures, that have been determined by different levels of decision-making authorities to limit the emissions that are caused by vehicles, have been effective to achieve improvements regarding nitrogen dioxide emissions. Additionally, the report confirms that large-scale measurements concerning the emissions of PM10 are being applied (with a focus on agriculture and biomass burning sources) and the outcomes are expected to emerge in the near future (Arpa Piemonte & Città metropolitana di Torino, 2022).

Despite the city's nature and the attempts of including green through the city, green areas alone are not enough for high air quality. Pollutants including nitrogen dioxide, ozone, and benzopyrene threaten the air quality of the city and in many cases, they exceed the legal limitations with trends varying through different parts of the city (Torino Urban Lab, 2018). Therefore, to be able to achieve reduction of greenhouse gas emissions, it is necessary for one to adapt to a more sustainable way of living in their personal lives, to deal with the causes directly.

3.5

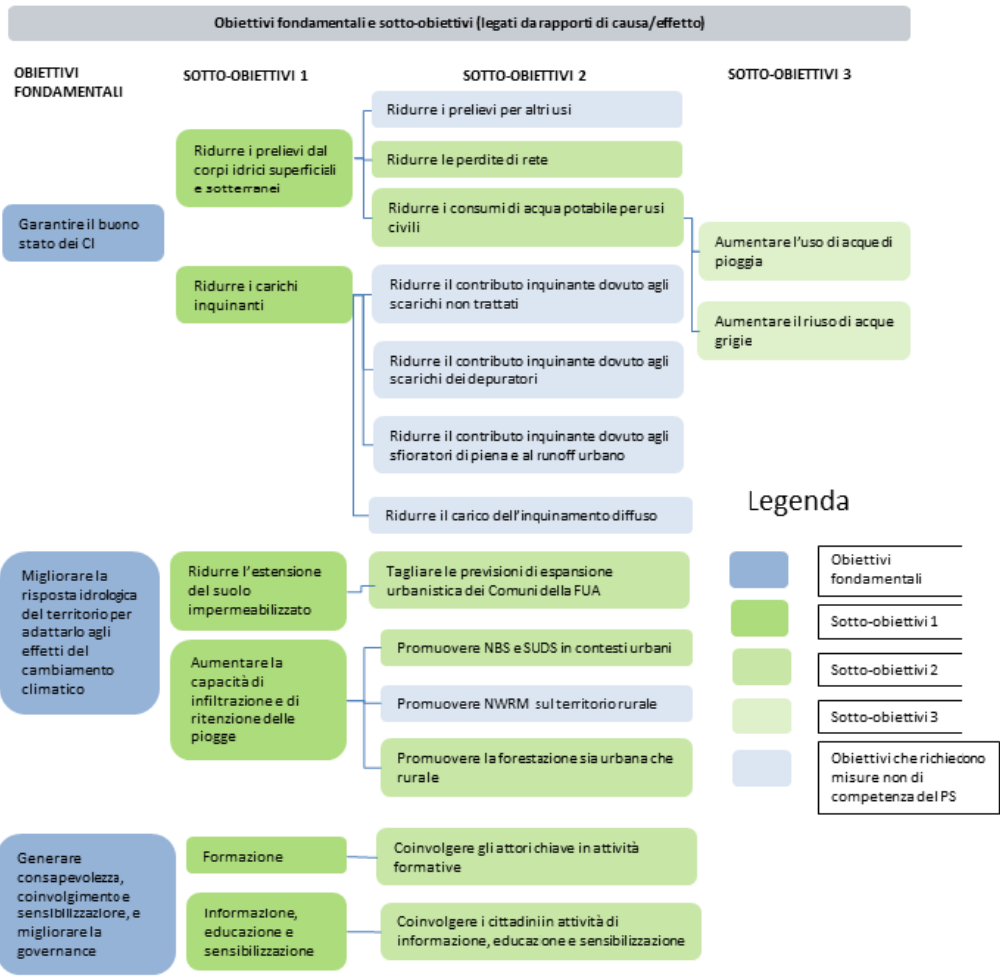
Water Infrastructure

As an element that provides evaporative cooling, water improves the microclimatic conditions of the environment where it is located. To an extent of approximately 30-50 meters, the average cooling effect of water is 1-3°C (Kleerekoper, 2016). Thus, when water management is combined with implementations such as water ponds, rainwater harvesting and floodable squares, it supports adaptation (urban drainage, mitigation of the effects of extreme events) and mitigation (decreasing the energy demand for heating, pumping and distribution systems) strategies (Trane et al., 2021).

While referring to water related implementations for sustainability strategies, it is necessary to underline the significance of water reuse as well. Being aware of the hydrological risks caused by climate change, the city participates in the CWC (City Water Cycles) project which intends to support cities through reformation of obsolete urban water infrastructure while applying the circular economy approach. The following topics are addressed in the project: recycling and reusing waste water, improving efficiency in the distribution and the use of water, ensuring the good quality of water bodies, rainwater

collection and use, promoting sustainable use of water, preserving the natural flow of water bodies. These points are highlighted through the Strategic Plan and Action Plan on Sustainable Water Management in Urban Areas which has been developed with a focus on sustainable water management in an urban setting (Citta di Torino, 2022).

Figure 26. Fundamental objectives and sub-objectives of the Strategic Plan and Action Plan on Sustainable Water Management in Urban Areas. (Città di Torino, 2022)



3.6

Mapping Turin: Classification of Urban Fabric

Mapping has been used in prior studies as a tool to read the urban morphology of a city or a given environment (Caluwaerts et al., 2016). In this section of the thesis, the city of Turin is divided into four urban morphological categories, and in total, ten typologies. The classification is as follows:

Category 1: Continuous

Continuous regular – the building blocks that have a rectangular shape and that do not have significant openings among their borders.

Continuous irregular – the building blocks that have an irregular form and that do not have significant openings among their borders, commonly recognized by their positioning along diagonal mobility axes.

Category 2: Discontinuous

Discontinuous regular – the building blocks that have a rectangular shape and that have openings among their borders.

Discontinuous irregular – the building blocks that have an irregular form, and that have openings among their borders, commonly recognized by their positioning along diagonal mobility axes.

Category 3: Scattered

Order-not dense – the settlements that have a defined order among themselves, commonly scattered in a shared public space where they are not too close to each other.

Order-dense – the settlements that do not have a defined order among themselves, commonly placed densely within a shared public space.

Order-dense – the settlements that do not have a regular planning and that are scattered within parcels.

Category 4: No Tissue

Shaped along slope – the settlements that are placed among the mobility axes that follow the natural valley terrain of Turin, commonly found towards the outskirts where hill formations are present.

Suburb-nature – the parts of the city where there is not a significant evidence

of tissue and that is characterized by agricultural zones, forests and further natural components of the urban form.

Industrial-complex mass – the masses of the factories or multifunctional complexes that commonly cover a large surface of land, commonly recognized by their immense volume when compared to those of their surroundings.

The maps in the following pages of this section illustrate the expansion of the city clearly, especially when compared to the expansion map of the city (see pages 51-52 for the expansion map). It is possible to observe that the central part of the city appears to have a compact form, consisting of the first two categories (continuous and discontinuous building block). The additional settlement beyond the tax borders of the city and the ones that are the outcome of the industrial revolution and the immigrant flow are spread around different parts of the municipal borders and they either have their own order (resulting in gated communities), or are scattered along parcels without a clear order. Moving further towards the outskirts of the city, it is possible to observe the disappearance of the urban fabric due to the geographical parameters (such as the hills), as the positioning of the dwellings along the slopes are mostly characterized by the angle of the slope. Another significant element that affects the urban fabric is composed of the large industrial masses: an outcome of the industrial revolution and the so-called “economic boom”. Industrialization is not only an important part of Turin’s fabric that has characterized the history of the city, but it also remains as an issue as it resulted in acres of abandoned pre-industrial settlements.

category 1 continuous

type 1 continuous-regular

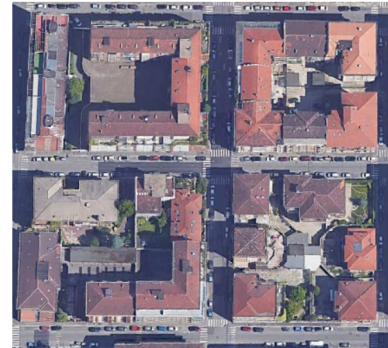


type 2 continuous-irregular



category 2 discontinuous

type 3 discontinuous-regular



type 4 discontinuous-irregular



Figure 27. Representative satellite images for different types of urban fabric in Turin. (Satellite images were exported from Google Earth)

category 3

scattered

type 5

order-not dense



type 6

order-dense



type 7

no order



category 4

no tissue

type 8

shaped along slope



type 9

suburb-nature

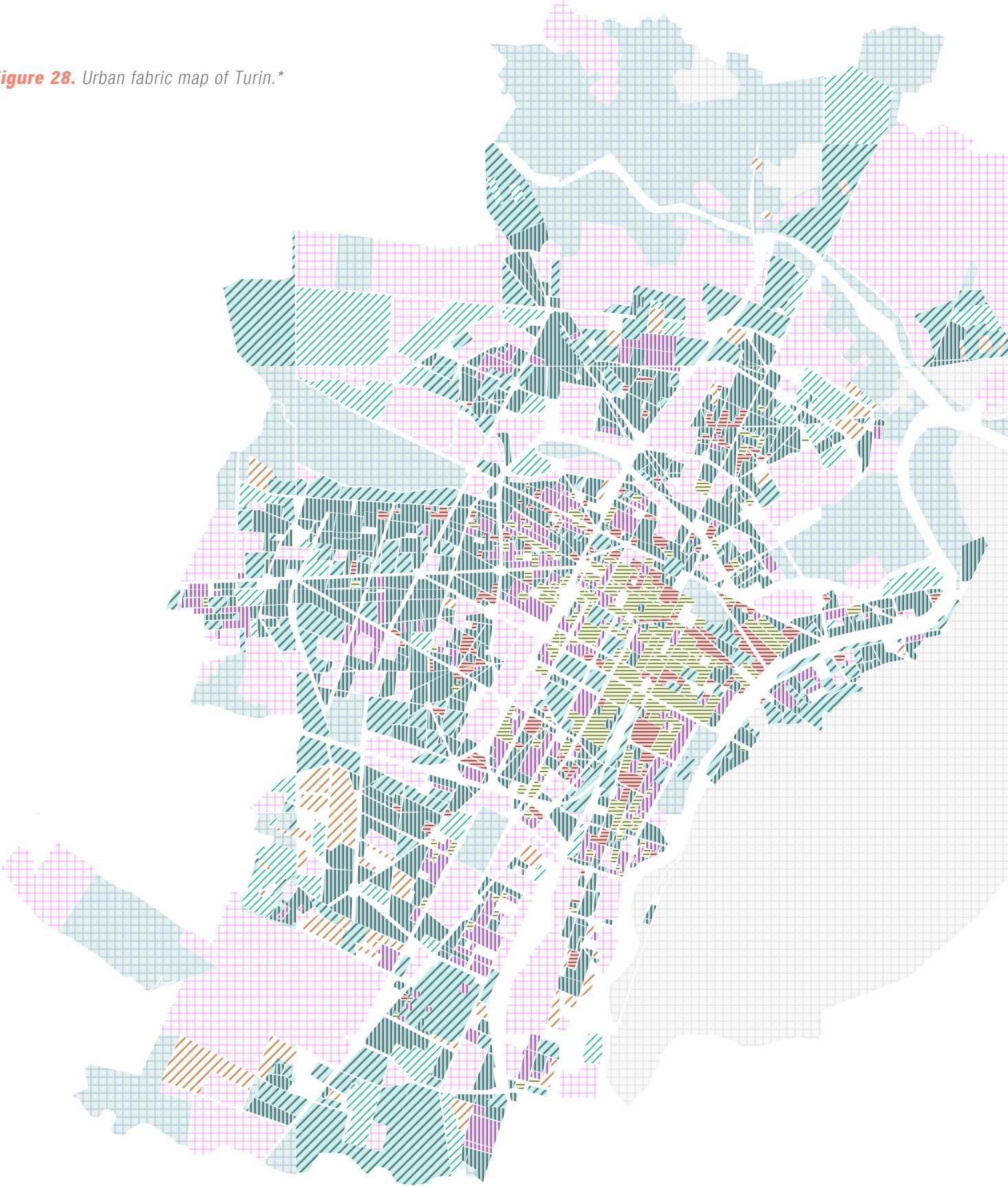


type 10

industrial-complex



Figure 28. Urban fabric map of Turin.*



mapping Turin

10 types of urban fabric

CATEGORY 1

continuous



type 1

continuous regular



type 2

continuous irregular

CATEGORY 2

discontinuous



type 3

discontinuous regular



type 4

discontinuous irregular

CATEGORY 3

scattered



type 5

order-not dense



type 6

order-dense



type 7

no order

CATEGORY 4

no tissue



type 8

shaped along slope



type 9

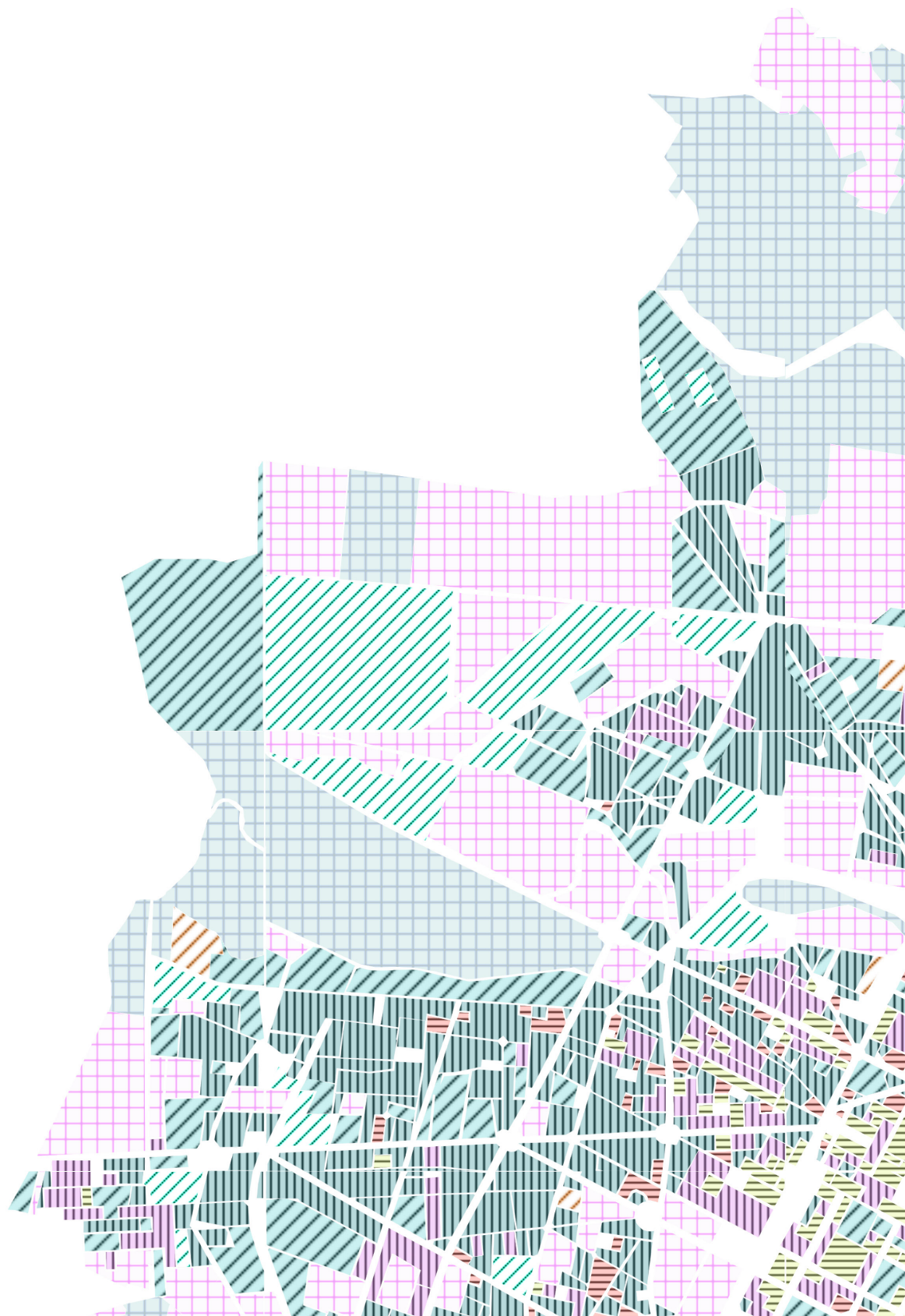
suburb-nature

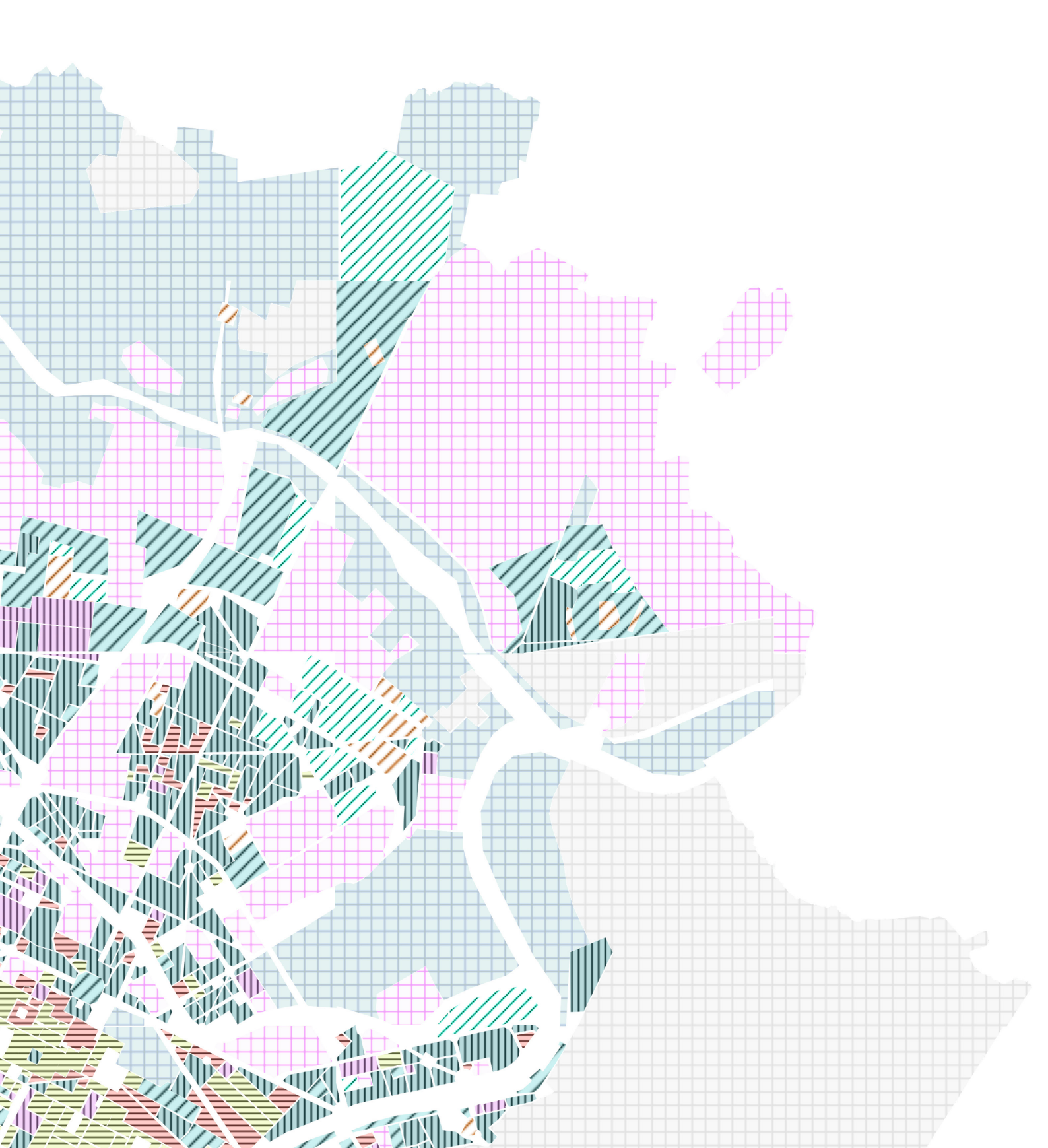


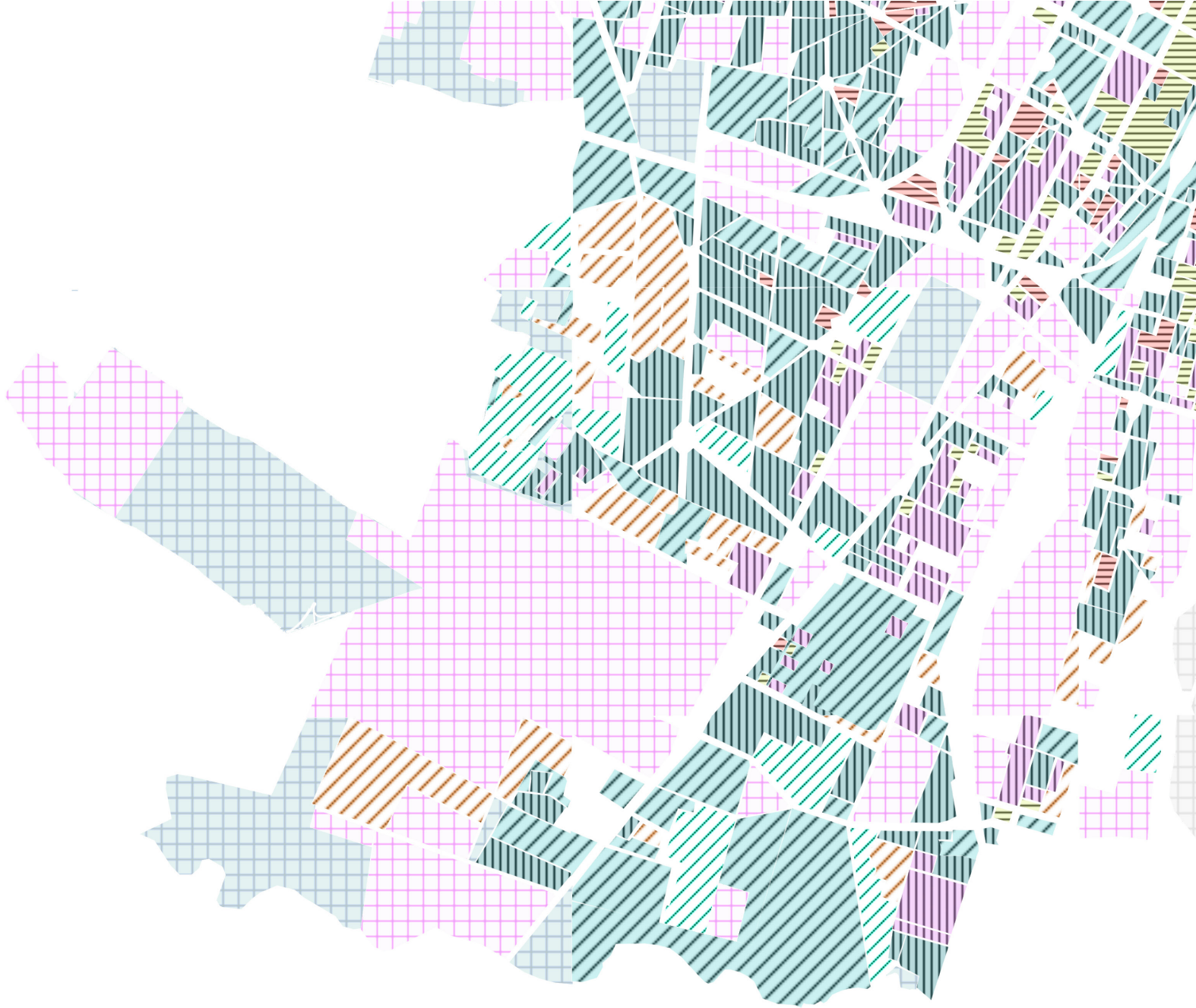
type 10

industrial-complex mass

**The map has been designed by the author, referring to online carta tecnica data provided by the municipality. (Geoportale Comune di Torino, n.d.)*









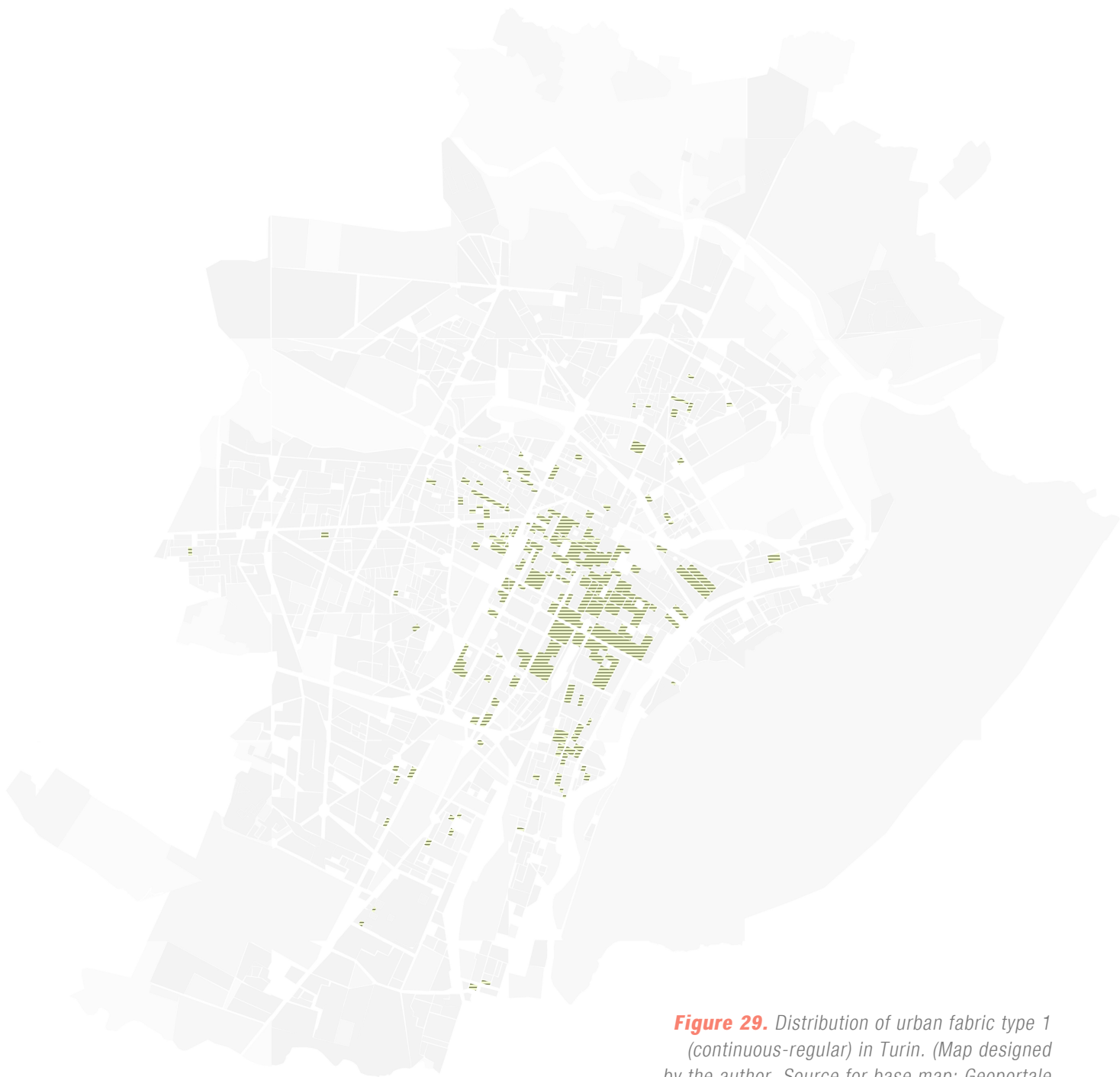


Figure 29. Distribution of urban fabric type 1 (continuous-regular) in Turin. (Map designed by the author. Source for base map: Geoportale Comune di Torino, n.d.)

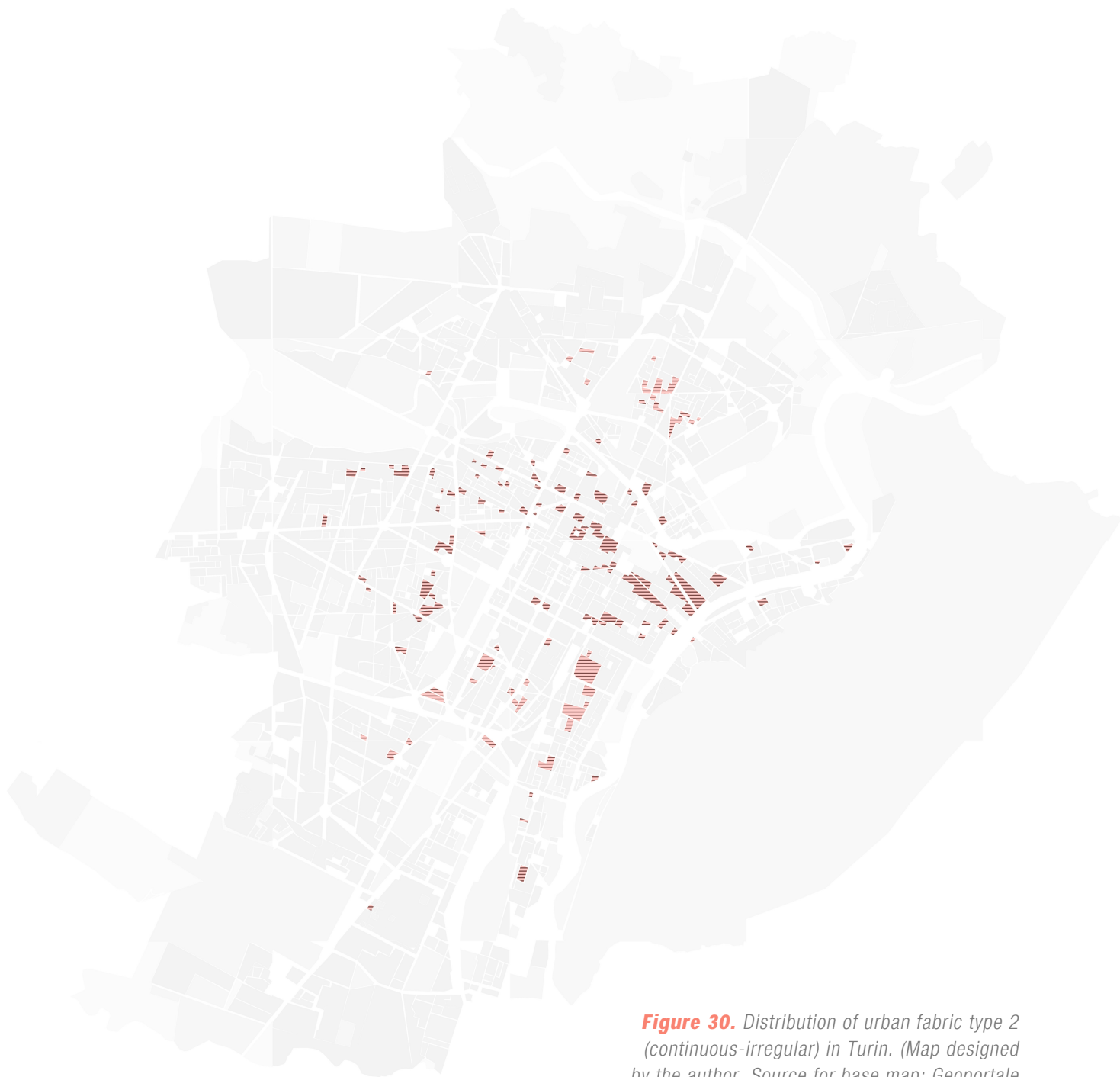


Figure 30. Distribution of urban fabric type 2 (continuous-irregular) in Turin. (Map designed by the author. Source for base map: Geoportale Comune di Torino, n.d.)

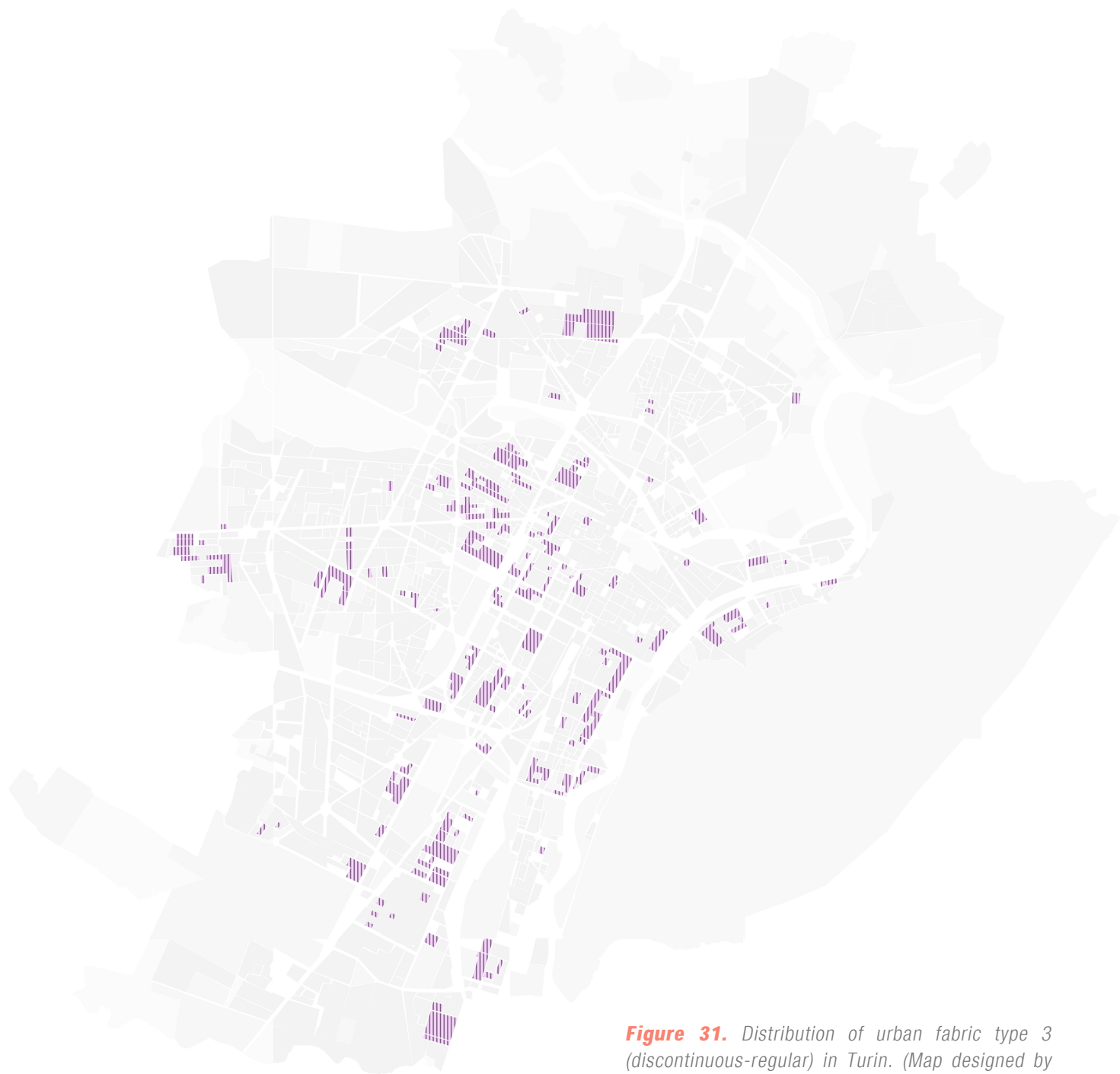


Figure 31. Distribution of urban fabric type 3 (discontinuous-regular) in Turin. (Map designed by the author. Source for base map: Geoportale Comune di Torino, n.d.)

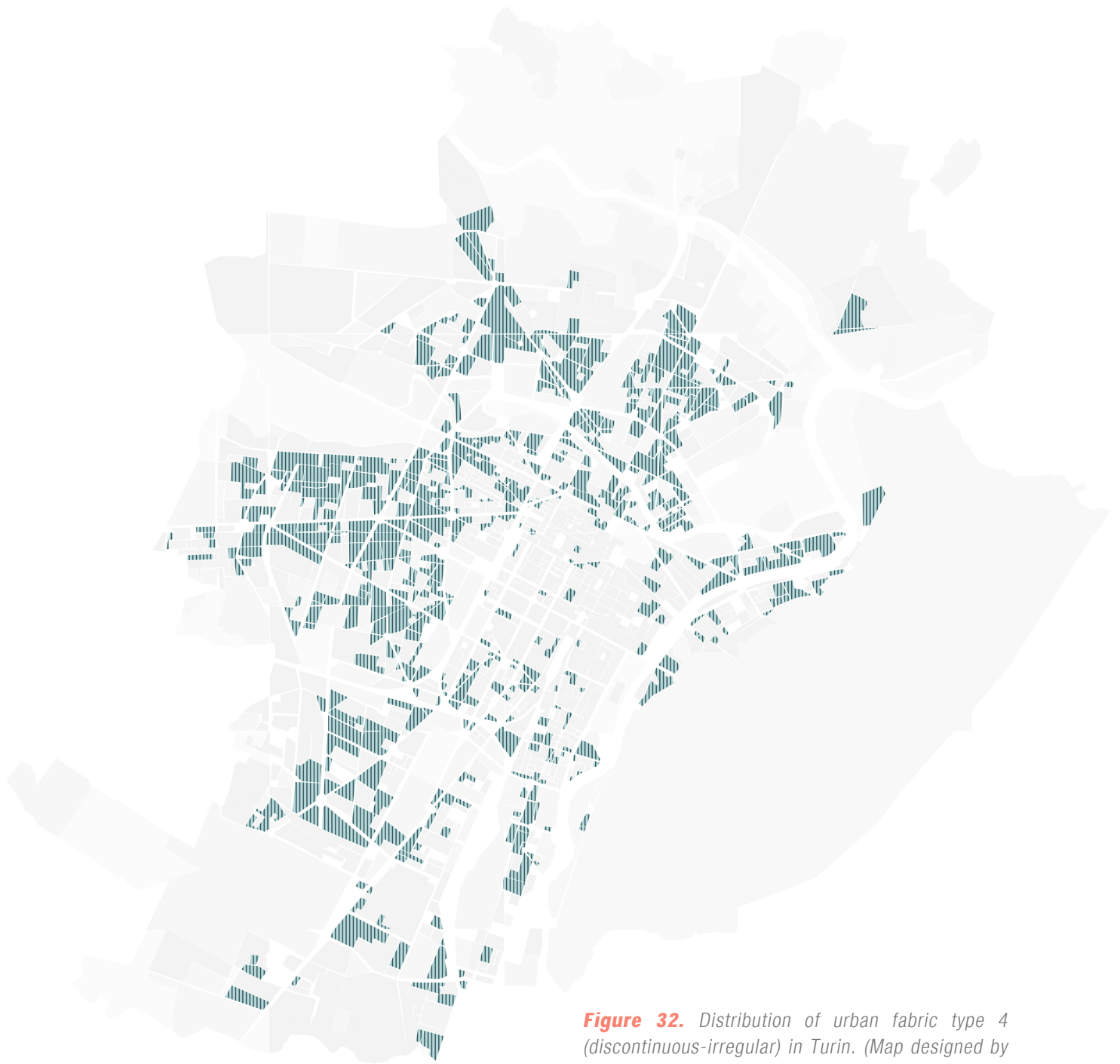


Figure 32. *Distribution of urban fabric type 4 (discontinuous-irregular) in Turin. (Map designed by the author. Source for base map: Geoportale Comune di Torino, n.d.)*

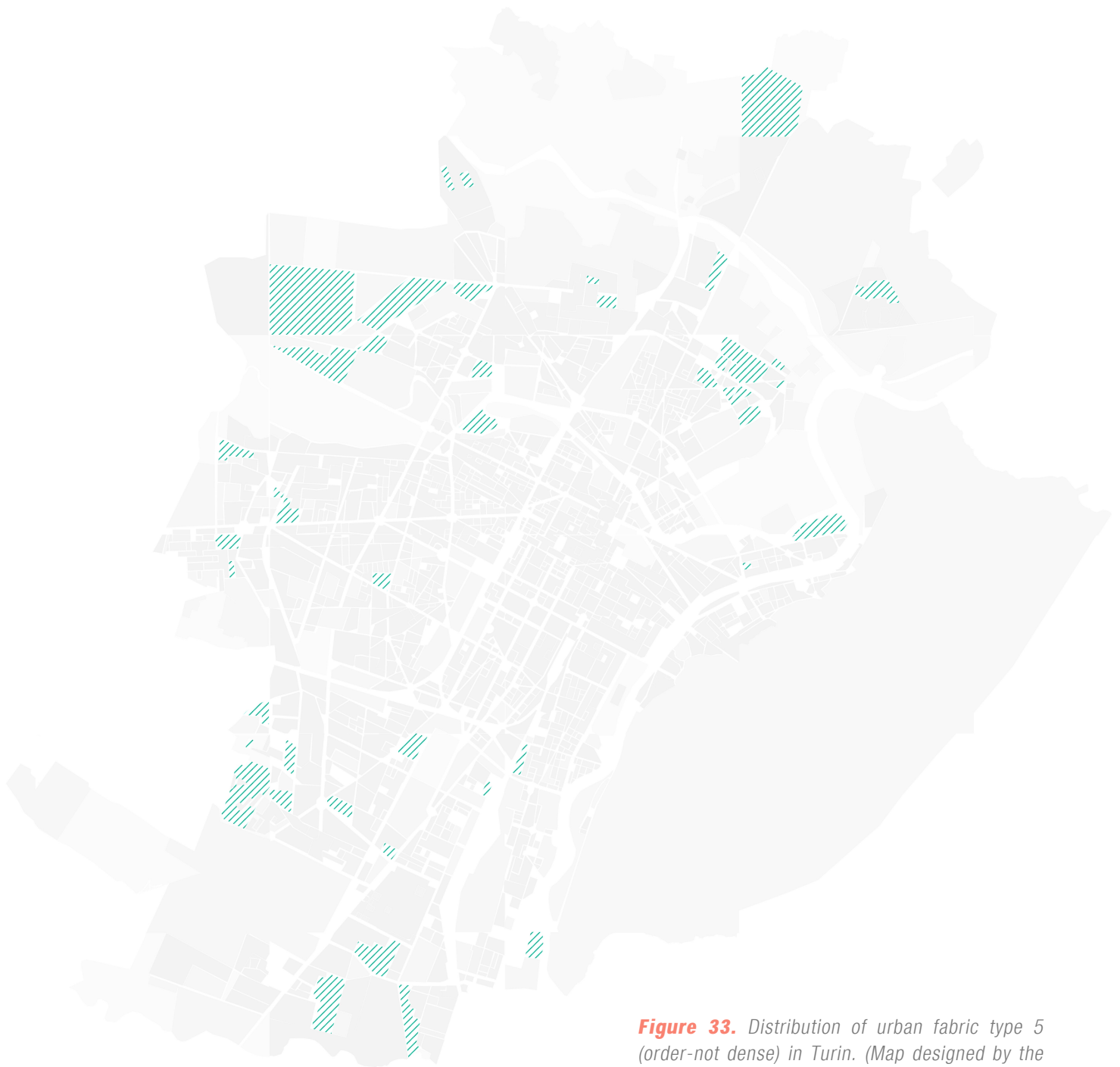


Figure 33. Distribution of urban fabric type 5 (order-not dense) in Turin. (Map designed by the author. Source for base map: Geoportale Comune di Torino, n.d.)

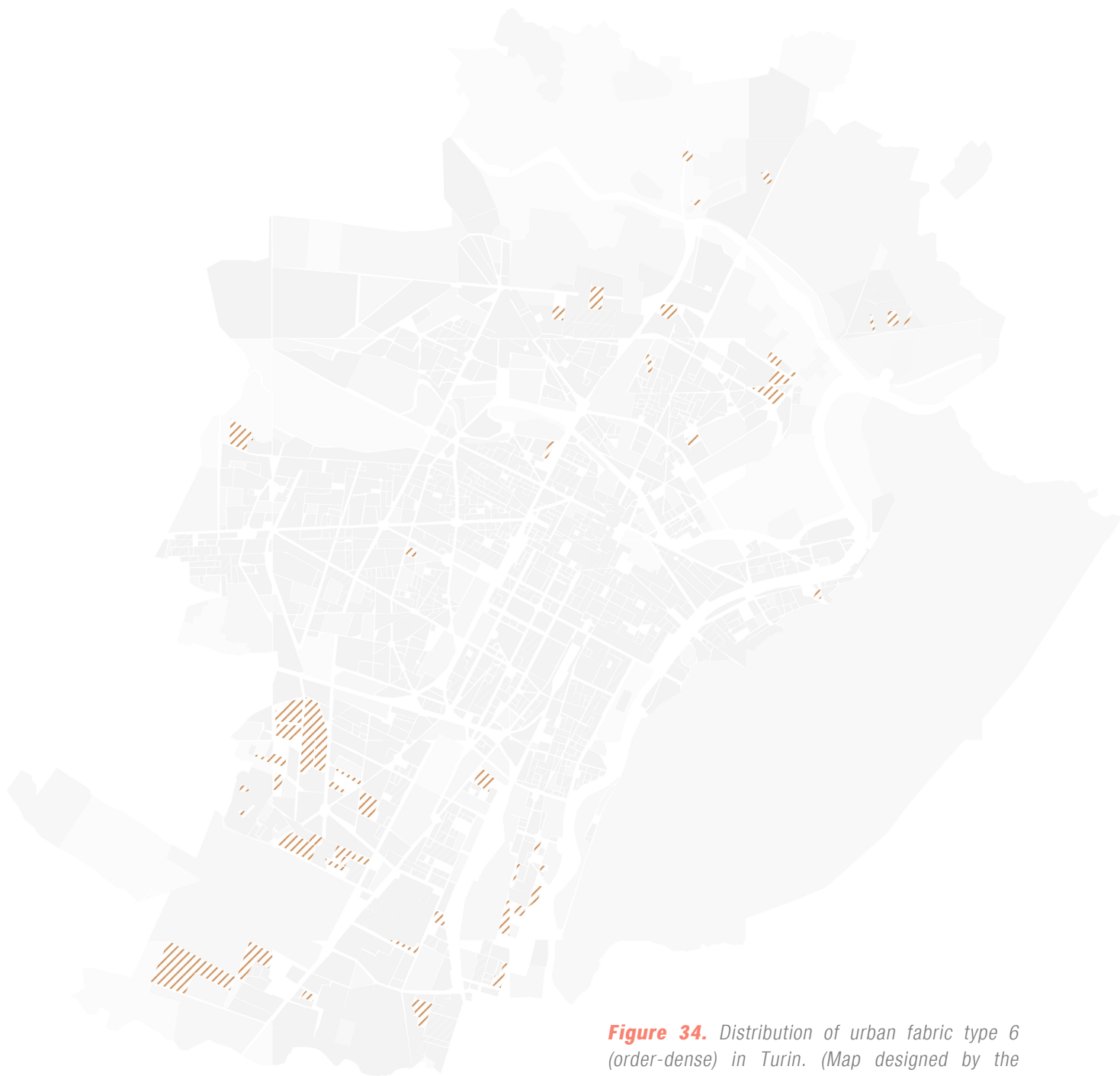


Figure 34. Distribution of urban fabric type 6 (order-dense) in Turin. (Map designed by the author. Source for base map: Geoportale Comune di Torino, n.d.)

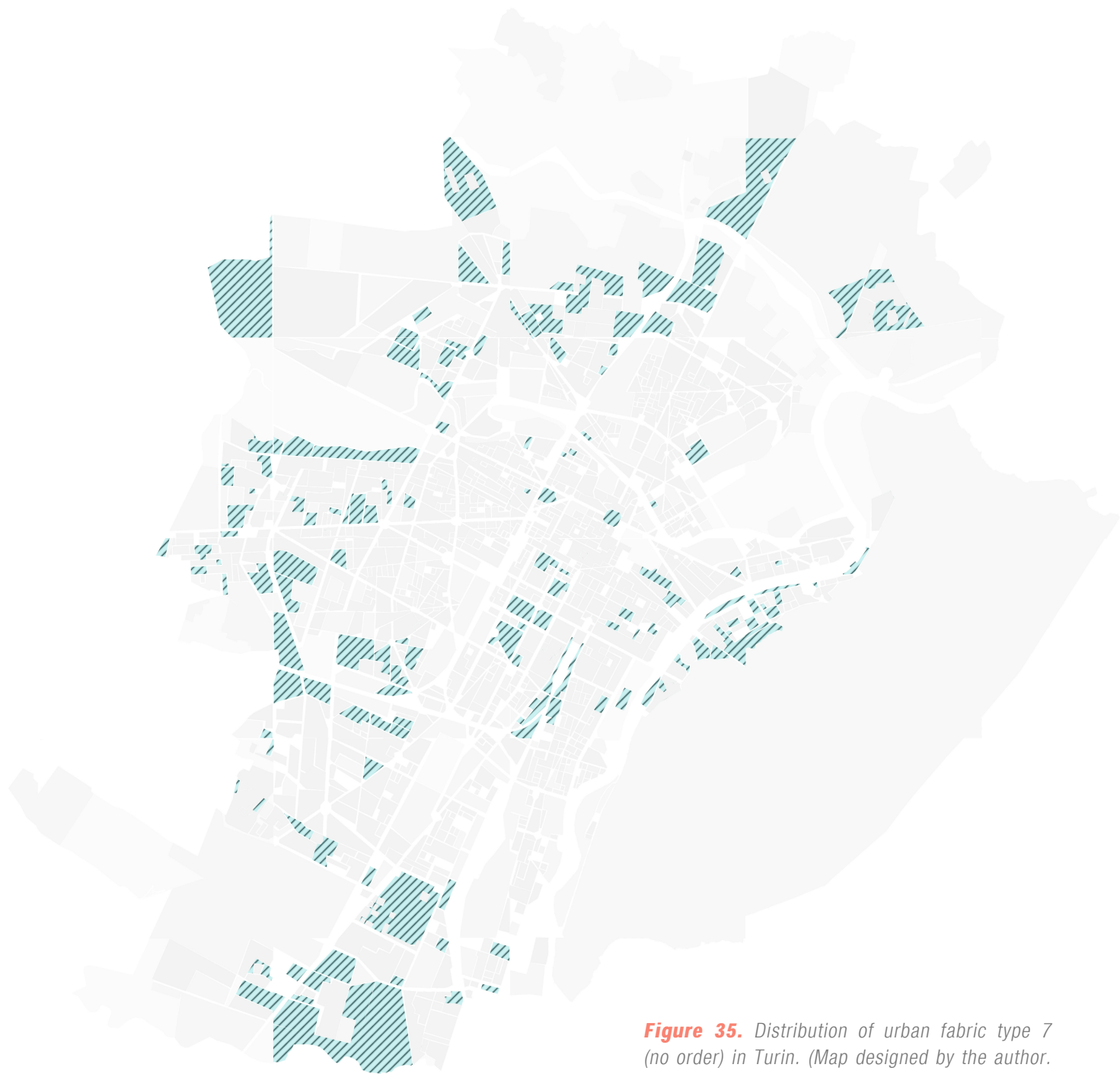


Figure 35. Distribution of urban fabric type 7 (no order) in Turin. (Map designed by the author. Source for base map: Geoportale Comune di Torino, n.d.)

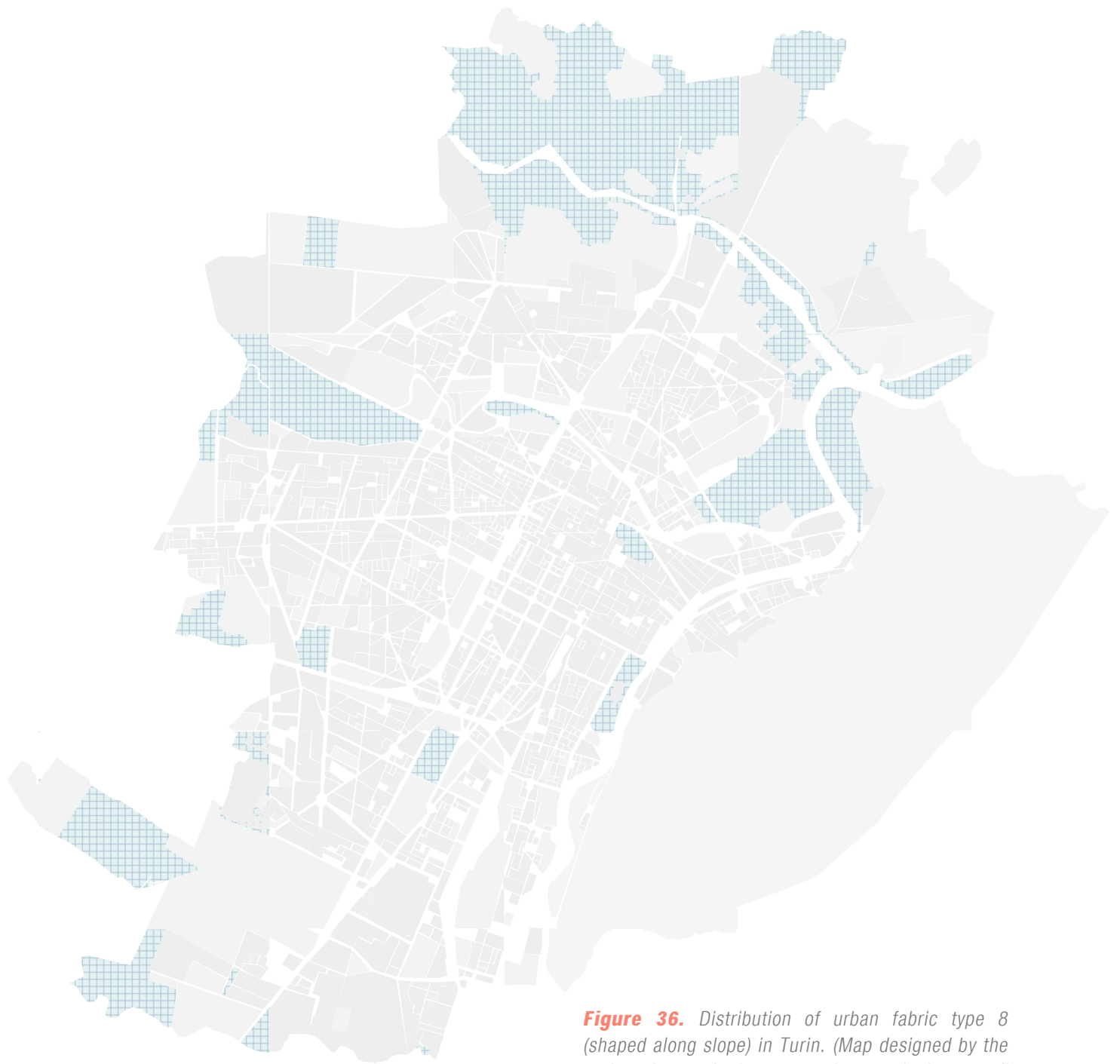


Figure 36. *Distribution of urban fabric type 8 (shaped along slope) in Turin. (Map designed by the author. Source for base map: Geoportale Comune di Torino, n.d.)*



Figure 37. Distribution of urban fabric type 9 (suburb-nature) in Turin. (Map designed by the author. Source for base map: Geoportale Comune di Torino, n.d.)

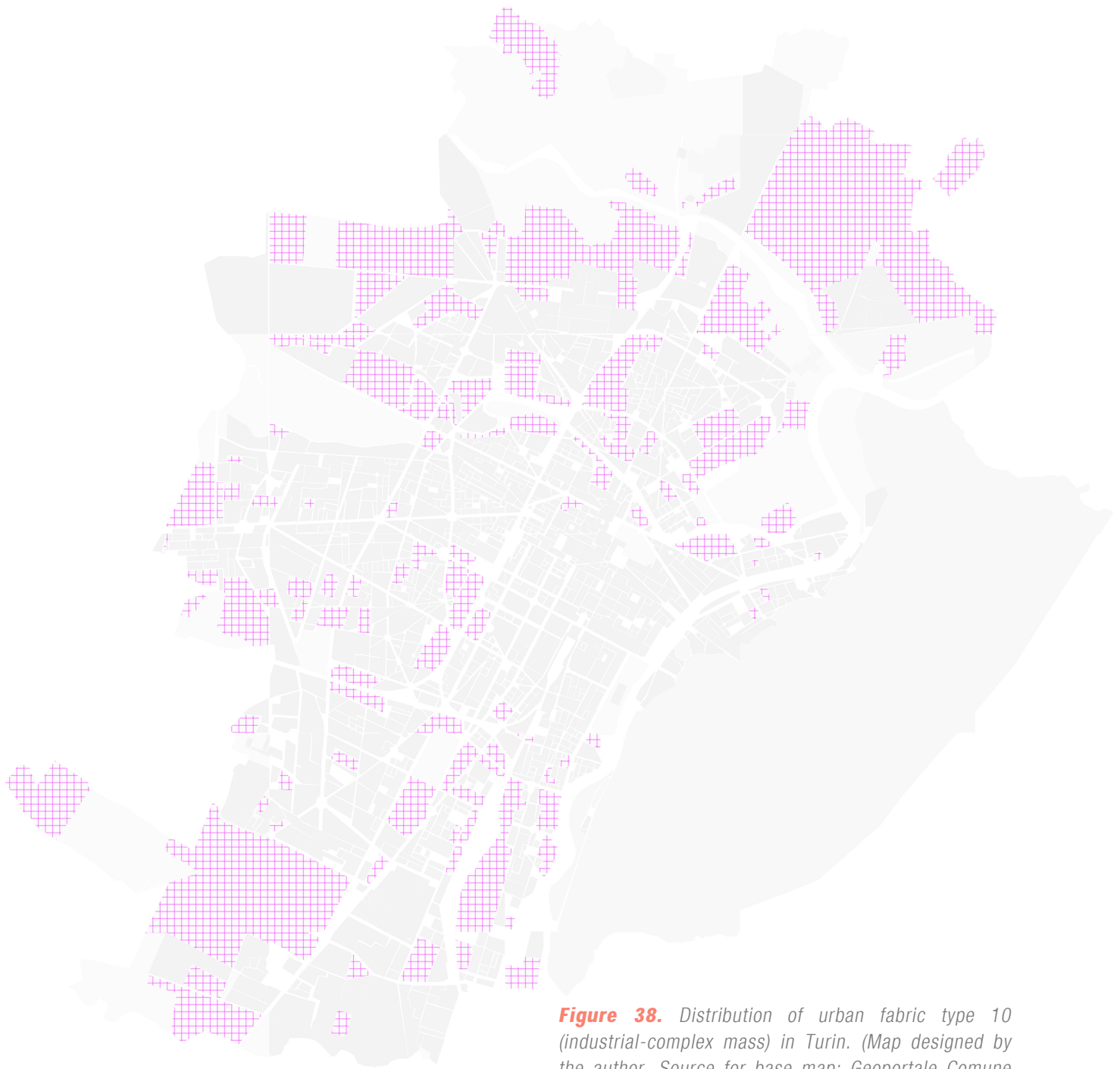


Figure 38. Distribution of urban fabric type 10 (industrial-complex mass) in Turin. (Map designed by the author. Source for base map: Geoportale Comune di Torino, n.d.)



Pilots

4.1. San Donato

4.2. Vallette

4.3. Mirafiori Nord

4.4. Mirafiori Sud

4.5. Ex-Mercati Generali

4.6. Lingotto

In this chapter, the case studies that were chosen from different neighbourhoods in Turin will be presented. These areas have been chosen to represent the different types of urban fabric that have been determined within the previous chapter.

It is significant to underline that during the selection process of the sites, three common parameters have been determined for the sites that would be compared: built density, horizontal greenery ratio and asphalt ratio. The reasoning behind this choice is to be able to provide an equal ground where the case studies would be compared as well as the effects of the built environment and its form could be observed.

Last but not least, all of the chosen sites have a significant value due to their role through the history of the city, as these sites have clearly witnessed the urban transformation of the city due to its expansion.

le vallette

type 5

Parameters for Vallette,
Mirafiori Nord, Mirafiori Sud:

Built: 11-13%

Horizontal greenery: 23-25%

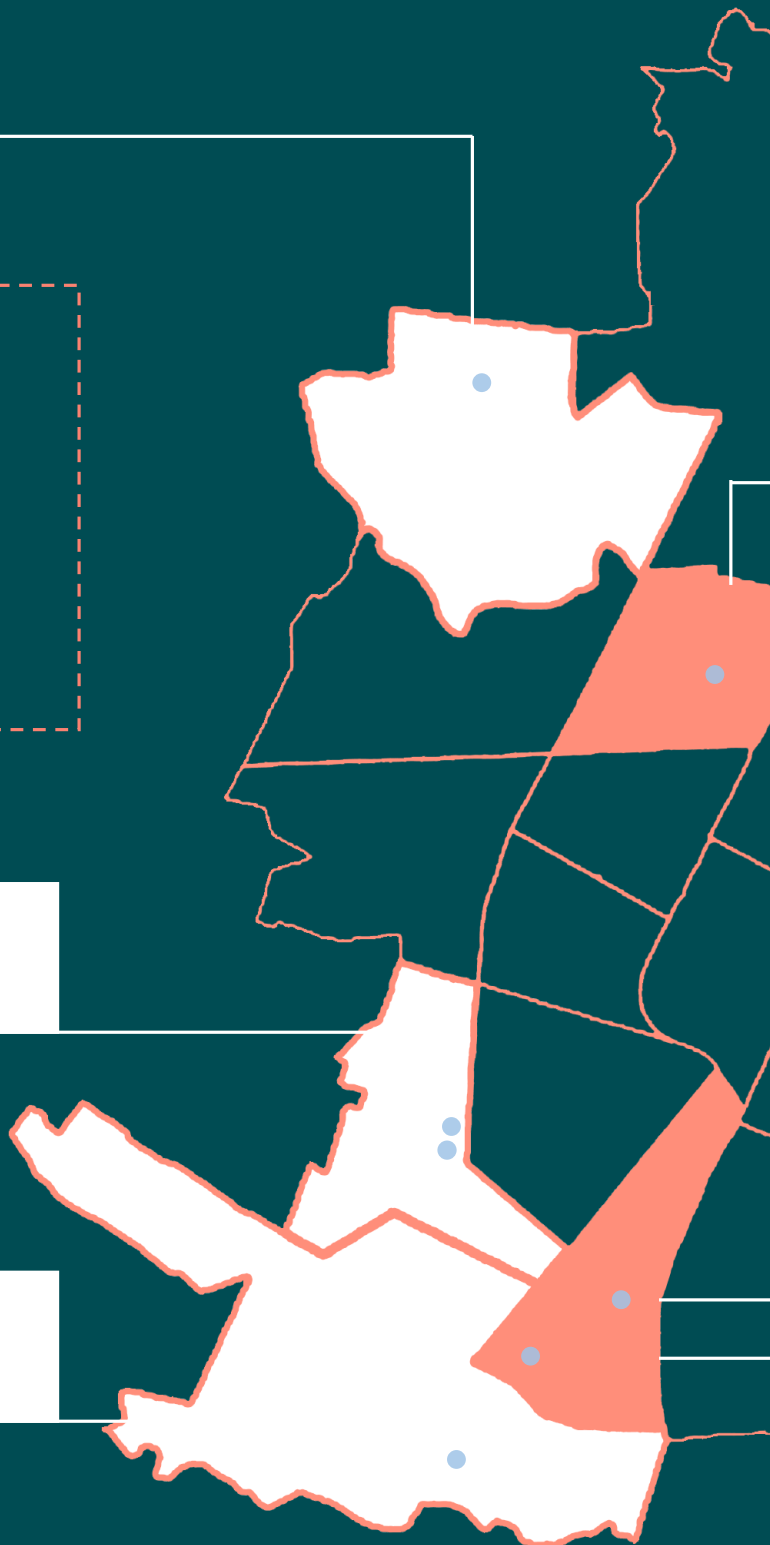
Asphalt: 20.5-23.5%

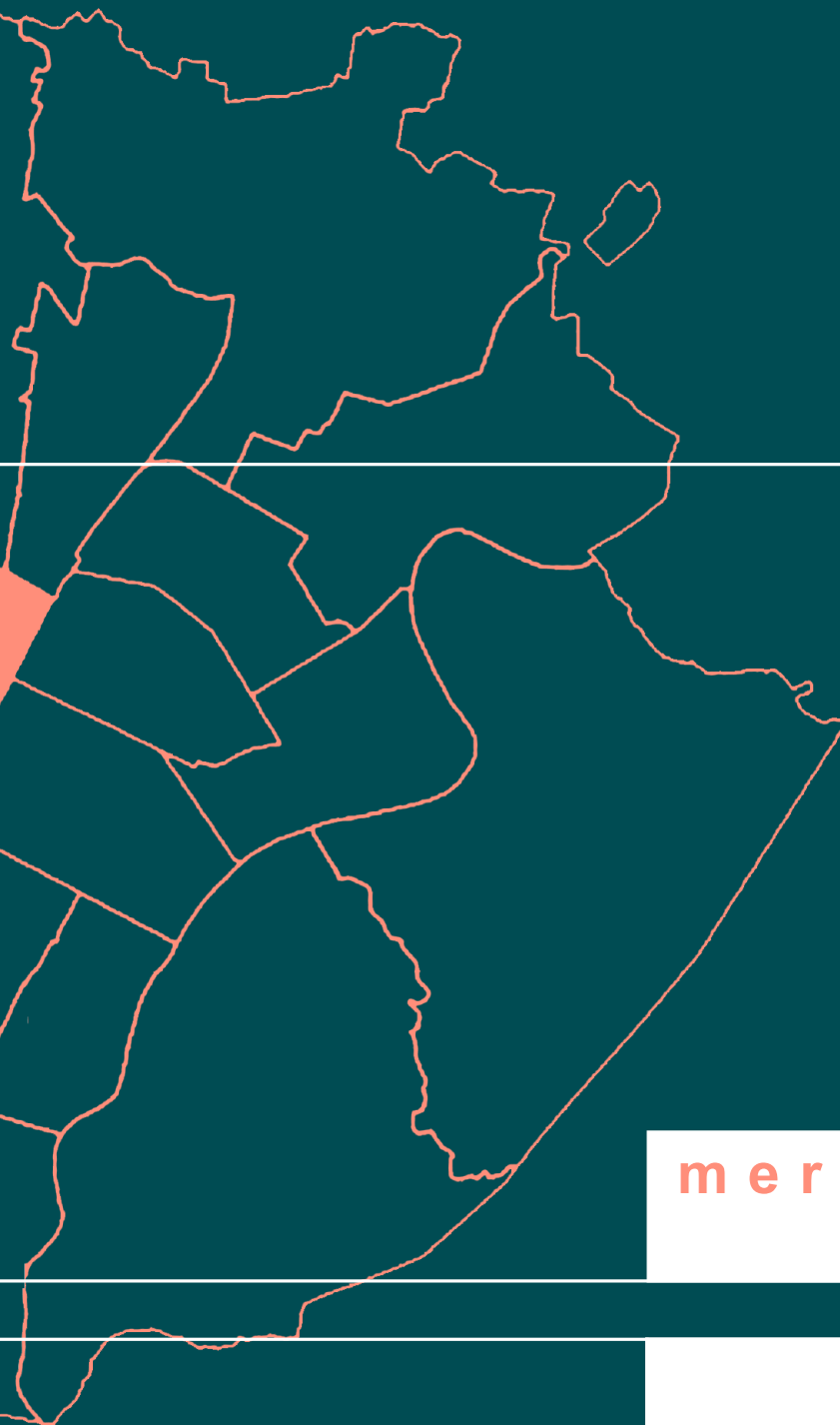
mirafiori nord

type 5, 6

mirafiori sud

type 5





No parameters for
compact city

san donato
type 1, 2, 3, 4

Parameters for Ex-
Mercati Generali,
Lingotto:

Built: 14-17 %
Horizontal greenery:
21-23 %
Asphalt: 13-16 %

mercati generali
type 6

lingotto
type 4

Figure 39. Locations and common parameters of the case studies in Turin.
Source for base map: Geoportale Comune di Torino, n.d.

4.1

Case Study 1: San Donato

location	san donato, turin
neighbourhood area	2.35 km ²
neighbourhood population	49,490
case study area	56,090 m ²
building height range	3-37 m

Located on the north side of Corso Regina Margherita, this site has been chosen since it contains four different types of blocks according to the classification that has been presented in the previous chapter of this thesis. San Donato case study represents the first four types of Turin's urban fabric classification (carried out in the previous chapter), namely "**continuous-regular block**", "**continuous-irregular block**", "**discontinuous-regular block**" and "**discontinuous-irregular block**".

The site is located in San Donato, more specifically around the northwest corner of "Basso San Donato". Basso San Donato originally belongs to the region Valdoccò, where in the earlier times highly industrial activities were taking place (MuseoTorino, n.d.-a).

The definition of the area has evolved as the city grew westward. Following the expansion of the surrounding villages along the canals, the construction of the Turin-Novara railway and the realization of Corso Regina Margherita, have all affected the development of Borgo San Donato. Additionally, in the early 20th century, massive industrial areas (textile, iron and steel factories) were built around the zone, namely Cotonifici, Ferriere and Michelin. These industrial implementations lead the building development of the area in the same direction (MuseoTorino, n.d.-a).

Through the construction of the bridge over Dora river served as a second route (named Corso Umbria today, forming the northern border of the site that has been chosen for the case study) in addition to Via Livorno, “Valdocco barrier” has been overcome which remarkably increased the accessibility to the area. Above all, the construction of the Stimate di San Francesco church in 1927 defined a meeting and interaction area, namely Piazza Umbria (located to the north of the case study area), which has been actively used by the inhabitants since the end of 20th century (MuseoTorino, n.d.-a.).

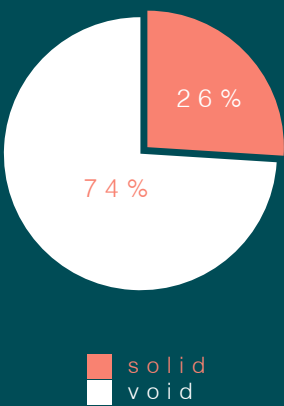


Figure 40.
Built density ratio for San Donato case study.

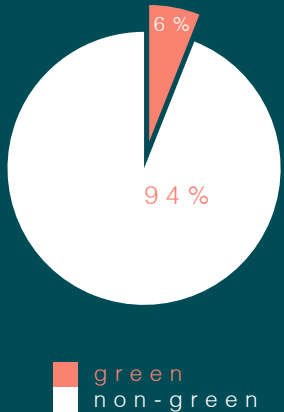


Figure 41.
Horizontal greenery ratio for San Donato case study.

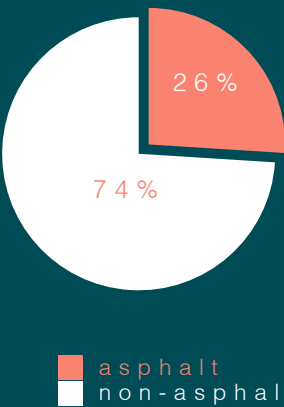


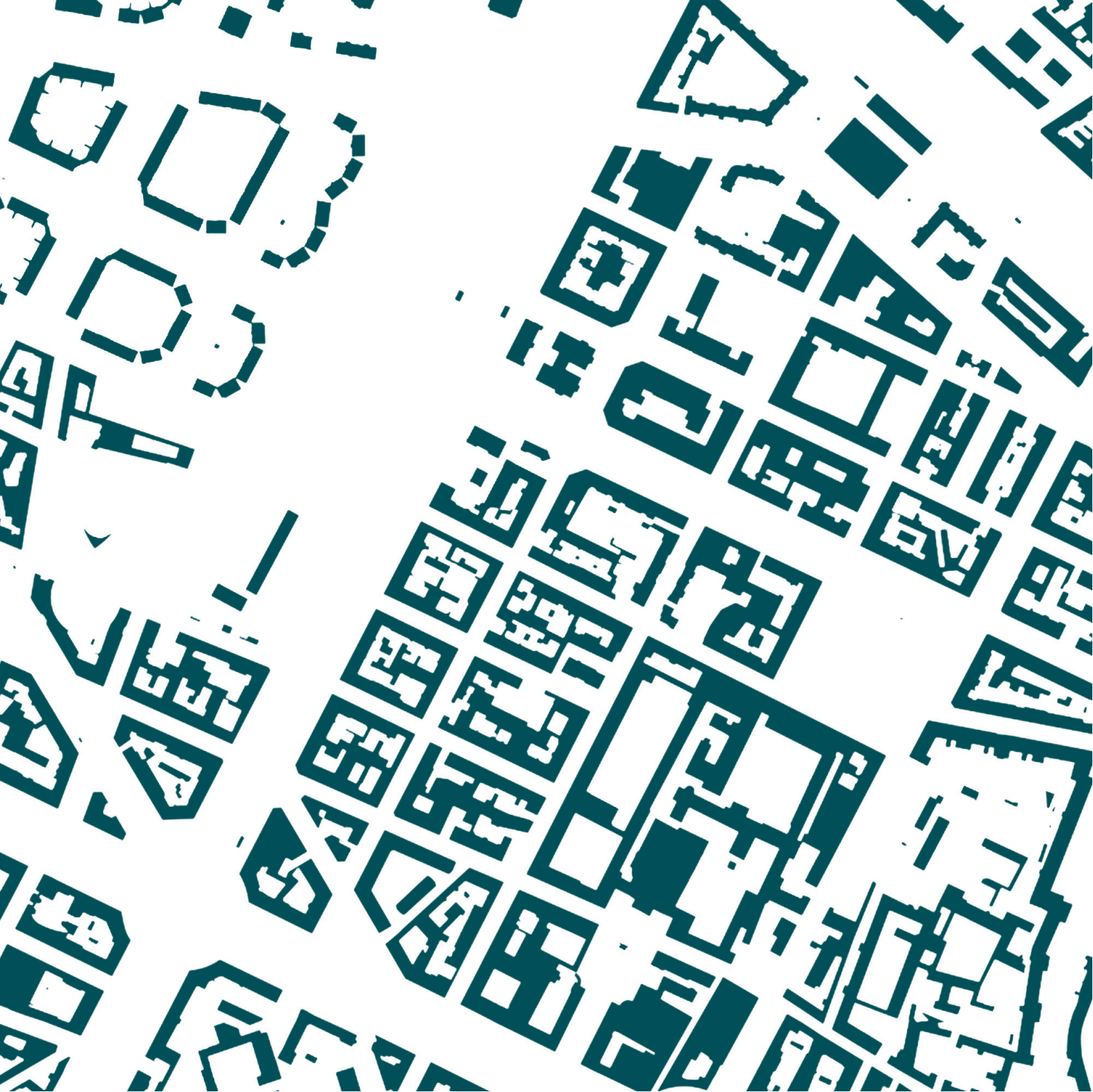
Figure 42.
Asphalt ratio for San Donato case study.



Figure 43.

Solid-void map of San Donato case study area.

Source for base map: Geoportale Comune di Torino, n.d.



0 50 100 150 200 250m





Figure 44.

Road network of San Donato case study area.

Source for base map: Geoportale Comune di Torino, n.d.

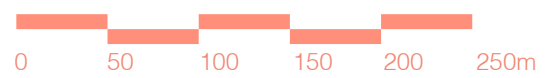
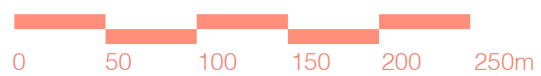




Figure 45.

Built density and greenery in San Donato case study area.

Source for base map: Geoportale Comune di Torino, n.d.



category 2

type 3

- semi-closed block
- discontinuous
- regular shaped

category 1

type 1

- fully closed block
- continuous
- regular shaped

category 1

type 1

- fully closed block
- continuous
- regular shaped

Figure 46.

San Donato case study area divided into different typologies of urban morphology.

Source for base map: Geoportale Comune di Torino, n.d.



category 2

type 4

- semi-closed block
- discontinuous
- irregular shaped

category 1

type 2

- fully closed block
- continuous
- irregular shaped



- 
- 14:54 - 14:59
▪ 26/03/2022

point 2
5 cars

point 1
168 cars

- 14:45 - 14:50
▪ 26/03/2022

Figure 47.

Car traffic in San Donato case study area.

Source for base map: Geoportale Comune di Torino, n.d.



point 3
75 cars

- 15:01-15:06
- 26/03/2022

- 15:10-15:15
- 26/03/2022

point 4
98 cars

0 25 50 75 100 125m





Figure 48.

Ortho image of Le Vallette case study area.
(Exported from Google Earth)



0 50 100 150 200 250m



Figure 49.
View from Via Don
Bosco towards the
building blocks of
San Donato case
study area.
(Photograph taken
by the author)



Figure 50.
View from Corso
Regina Margherita
towards San Donato
case study area.
(Photograph taken
by the author)





Figure 51.
View over Corso
Principe Oddone
towards the building
blocks of San Donato
case study area.
(Photograph taken by
the author)

4.2

Case Study 2: Le Vallette

location	le vallette, turin
neighbourhood area	3.64 km ²
neighbourhood population	10,151
case study area	87,416 m ²
building height range	3-30 m

The case study of Le Vallette represents the fifth typology of Turin's urban fabric classification (carried out in the previous chapter), namely **“order-not dense”**.

The realization of the Vallette neighbourhood could be considered later compared to an average neighbourhood in Turin. The history of the quarter dates to the second half of 20th century, as it has been built between 1957-1978, making it the youngest district in Turin (MuseoTorino, n.d.-b). It has been developed as large scale public housing district on a planned basis.

It is possible to observe a sense of variety among typological and form-related solutions through the neighbourhood. In other words, Vallette hosts a heterogeneous urban form. This is due to the fact that the design team consisted of 45 individuals, separated in 9 groups. For instance, on one hand,

the presence of 6-7 storey houses with terraces could be observed (between Corso Ferrara and Via delle Pervinche) and on the other hand, a building organization that includes wide inner courtyards and sloped roofs takes place (the zone between Via delle Pervinche, Via delle Primule and Viale dei Mughetti). In certain parts of the neighbourhood, the traces of the local traditional building typology are present whereas in others, the solutions are influenced by the Scandinavian and English experiences (MuseoTorino, n.d.-b).

Although the Le Valette neighborhood has a high density of greenery in general, the plot that has been chosen to share a similar density of greenery to those of the Mirafiori Nord and Mirafiori Sud case study areas, to be able to compare them on a common basis.

The main accessibility scheme has been carefully examined during the site trip. The above-mentioned different units are separated with roads that are used for vehicular traffic. Within the units, among different building blocks within the same unit, pedestrian access is provided by paths, which lead to service areas for the inhabitants. Nevertheless, the lack of public services among the neighbourhood cannot be overseen and this deficiency forms a sense of discontinuity from the central part of the city.

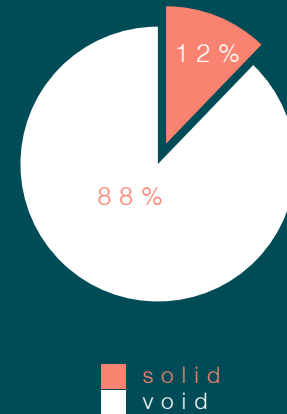


Figure 52.
Built density
ratio for
Le Vallette
case study.

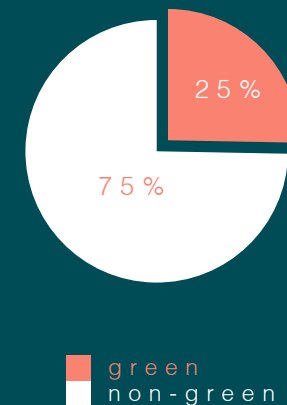


Figure 53.
Horizontal
greenery
ratio for
Le Vallette
case study.

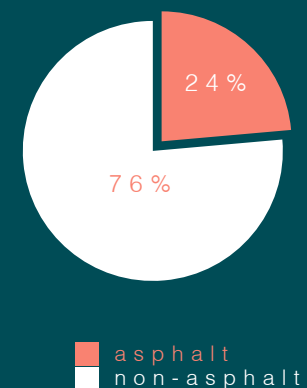


Figure 54.
Asphalt
ratio for
Le Vallette
case study.

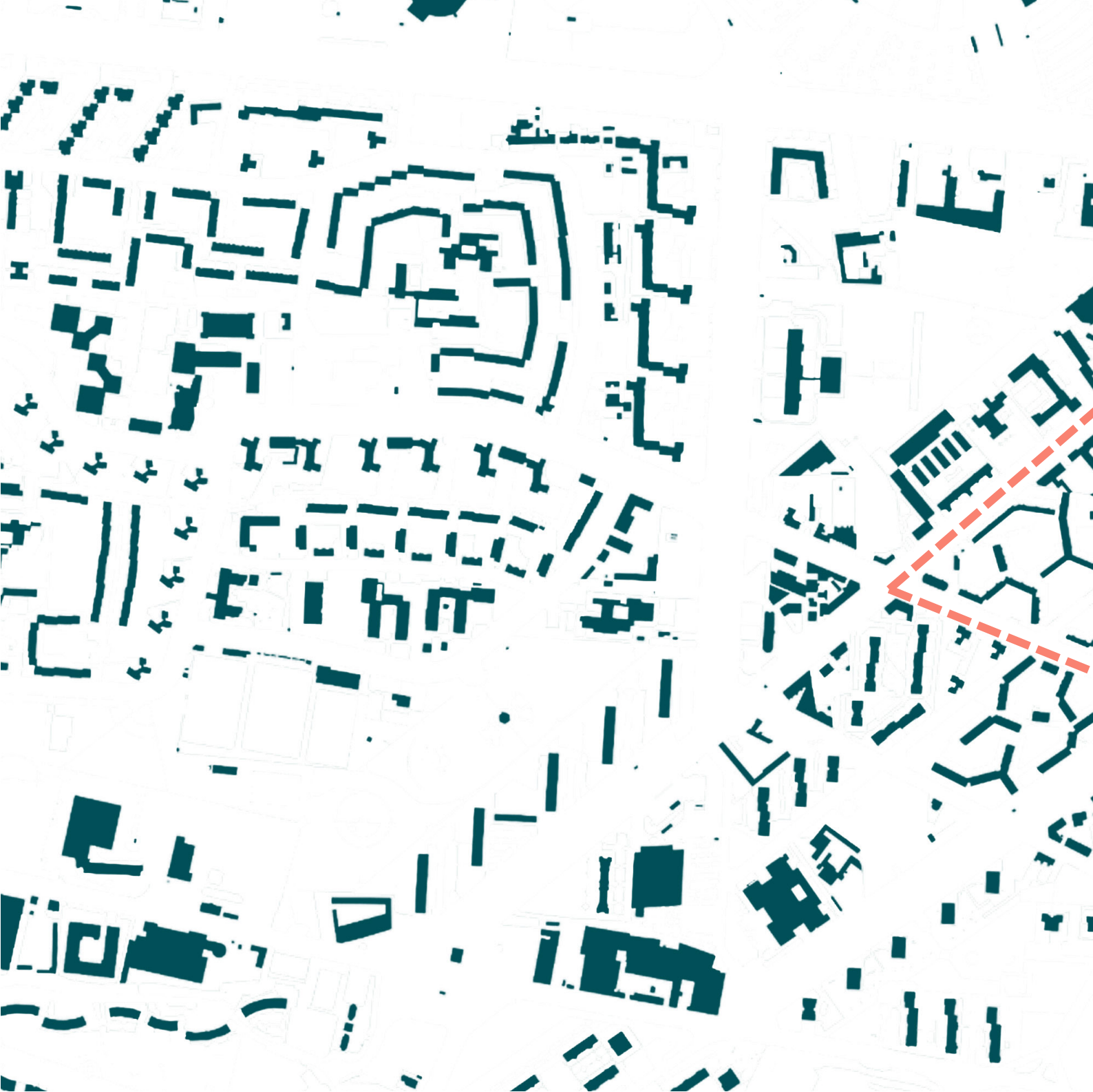


Figure 55.

Solid-void map of Le Vallette case study area.

Source for base map: Geoportale Comune di Torino, n.d.



0 100 200 300 400 500m



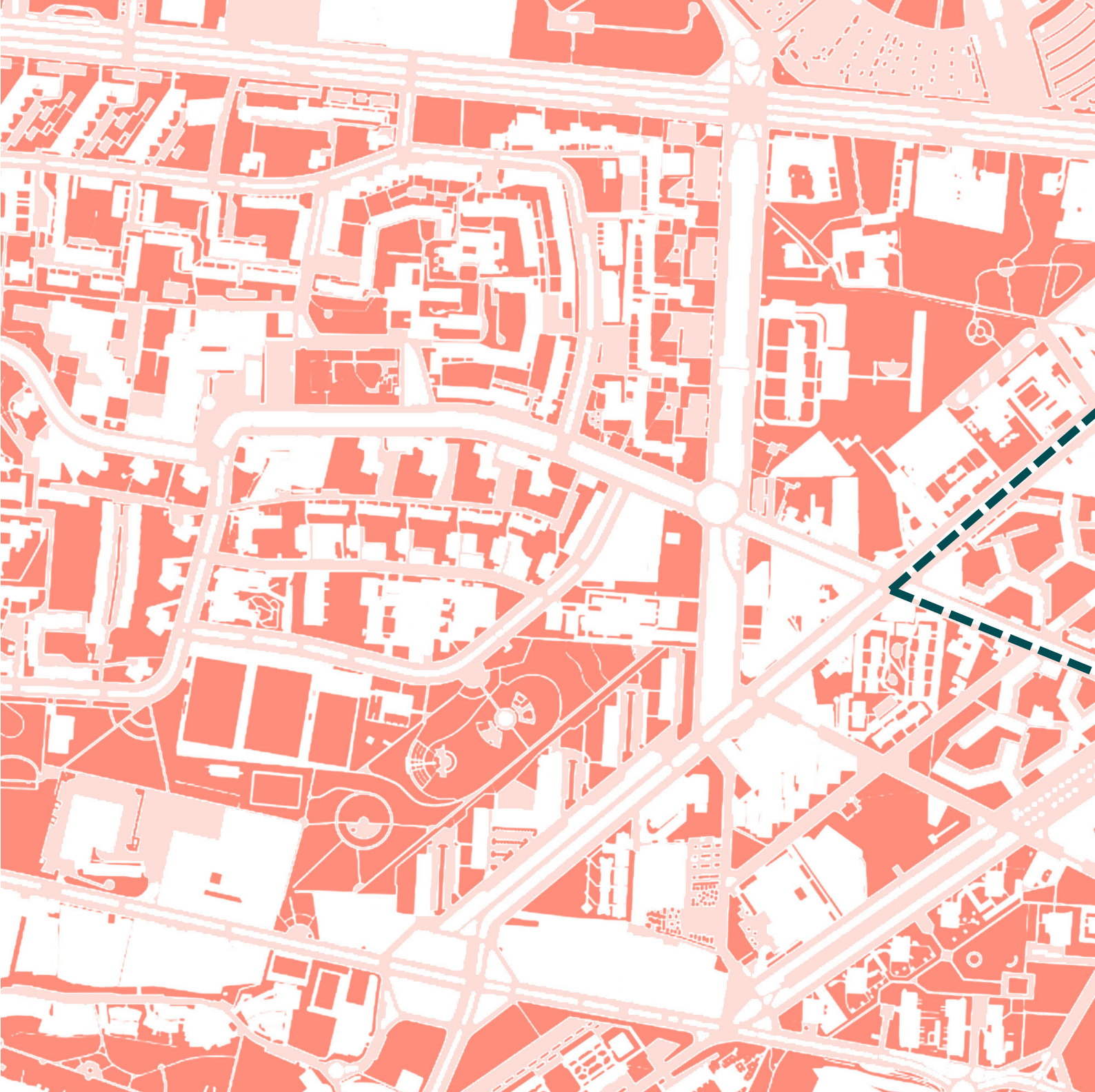
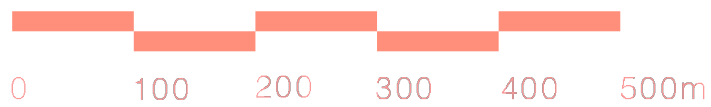
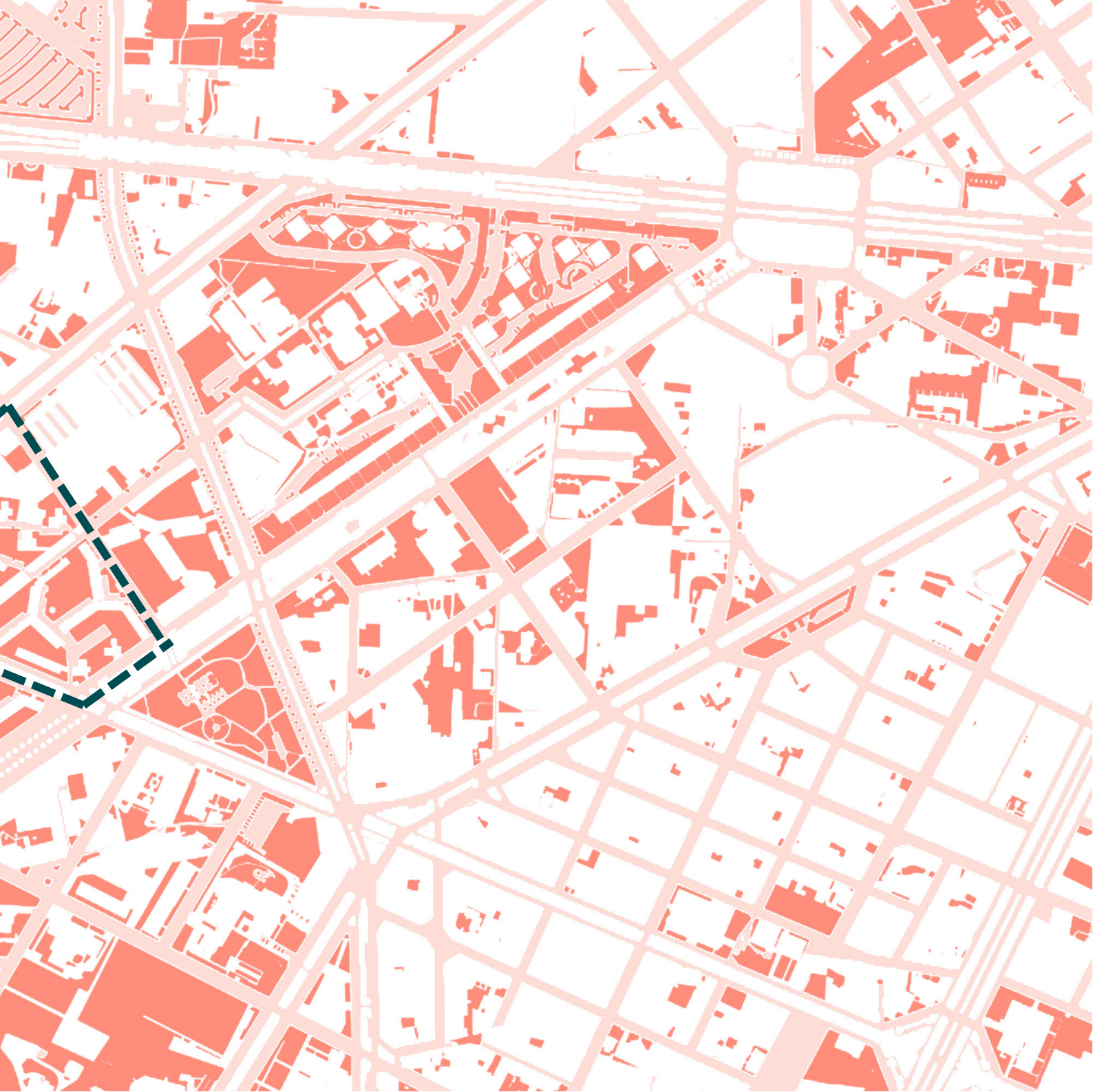
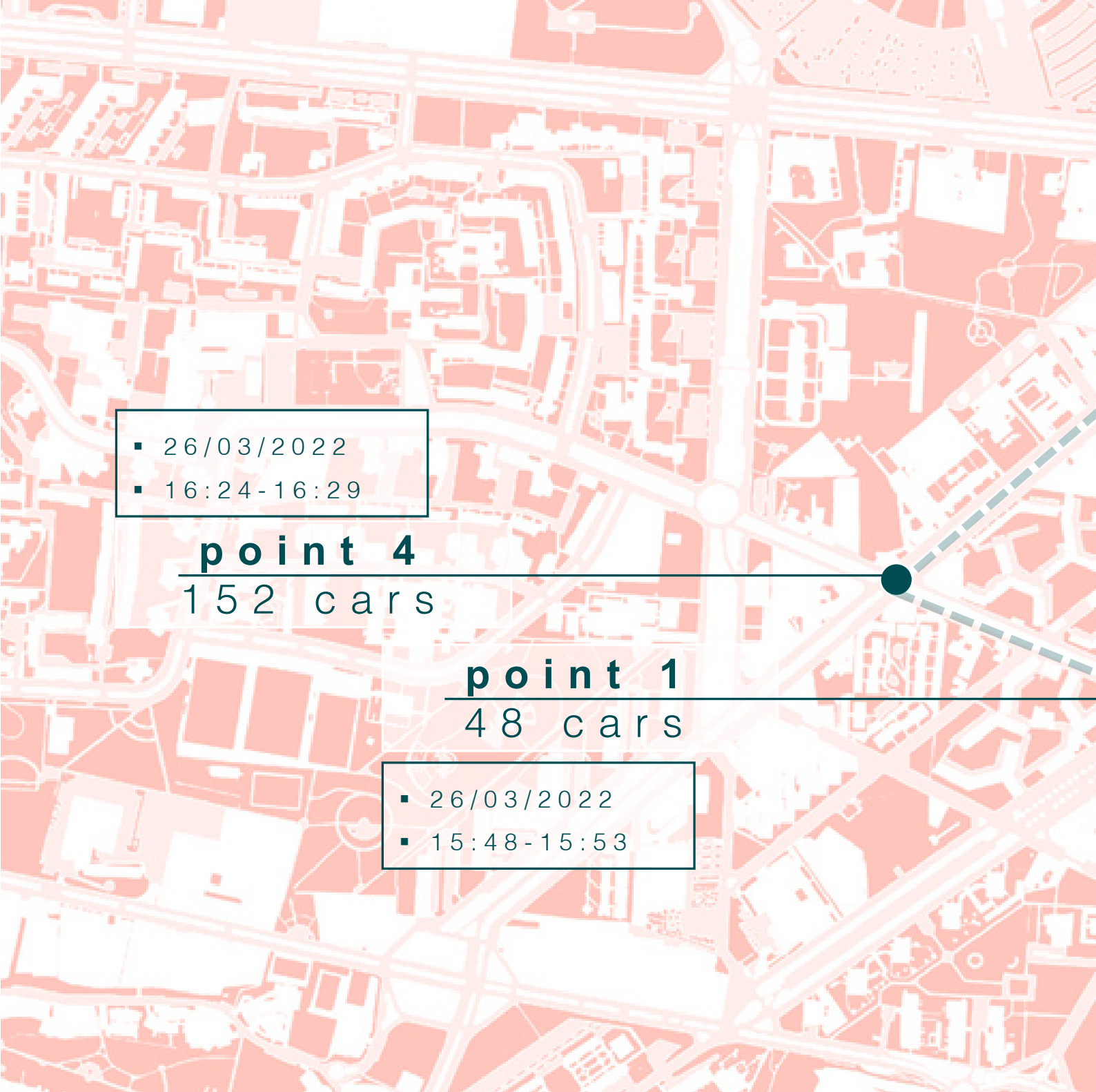


Figure 56.

Road network and greenery in San Donato case study area.

Source for base map: Geoportale Comune di Torino, n.d.





- 26/03/2022
- 16:24 - 16:29

point 4
152 cars

point 1
48 cars

- 26/03/2022
- 15:48 - 15:53

Figure 57.

Car traffic in Le Vallette case study area.

Source for base map: Geoportale Comune di Torino, n.d.



- 26/03/2022
- 16:12-16:17

point 3

126 cars

point 2

23 cars

- 26/03/2022
- 16:02-16:07

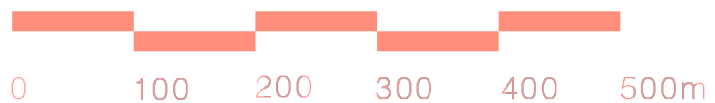




Figure 58.

Ortho image of Le Vallette case study area.
(Exported from Google Earth)



Figure 59.
Close-up view of
residential blocks
in Le Vallette case
study area.
(Photograph taken
by the author)



Figure 60.
View from Corso
Toscana towards Le
Vallette case study
area. (Photograph
taken by the author)





Figure 61.
View from Via
Parenzo towards the
residential blocks
of Le Vallette case
study area.
(Photograph taken by
the author)



Figure 62.
Panoramic view of
the residential units
in Le Vallette case
study.
(Photograph taken by
the author)

4.3

Case Study 3: Mirafiori Nord

location	mirafiori nord, turin
neighbourhood area	3.76 km ²
neighbourhood population	103,258
case study area	85,589 m ² (area 1), 150,014 (area 2)
building height range	3-33 m

The case study of Mirafiori Nord represents the fifth (Area 1) and the sixth (Area 2) typology of Turin's urban fabric classification (carried out in the previous chapter), namely **"order-not dense"** and **"order-dense"**.

The urban fabric of Mirafiori Nord is characterized by the public housing units. A large majority of these has been built for the workers of FIAT Mirafiori, following the establishment of the factory in 1939 (Comune di Torino, n.d.-c). One of the main factors that triggered the need of housing has been the so-called "economic boom", which resulted in a flow of immigrants from other regions of Italy after the Second World War.

Towards the northwest of the modelled area, between Corso Allamano and Via Guido Reni, a densely built urban form is present. The so-called Città Giardino (garden city) is the second application of its kind in Turin, the first having been constructed in Mirafiori Sud in 1920s (Comune di Torino, n.d.-a).

The garden city in Mirafiori Nord has been realized in 1950s, and is significant for its role in the urban development of the neighbourhood, providing the area with a better organization of roads, lighting and drinking water (Comune di Torino, n.d.-a).

Since 2002, local authorities, residents and the European Union are working together on an urban regeneration plan concerning the improvement of quality of life and environment in Mirafiori Nord. Being called Urban 2, the program focuses on three main areas of intervention: a green axis (aiming at environmental sustainability and physical development), a blue axis (aiming at economic and infrastructural development) and a red axis (aiming at social integration and cultural growth) (Comune di Torino, n.d.-c).

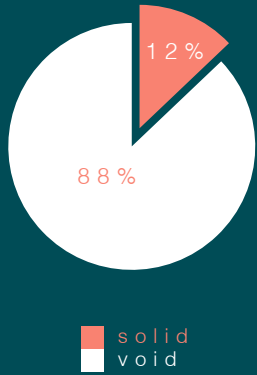


Figure 63.
Built density
ratio for
Mirafiori
Nord case
study
(average of
both areas).

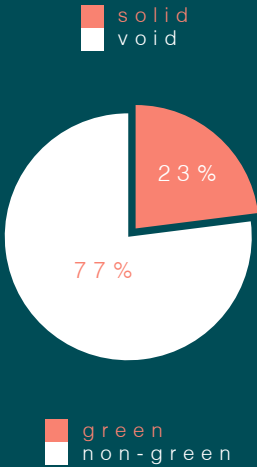


Figure 64.
Horizontal
greenery
ratio for
Mirafiori
Nord case
study
(average of
both areas).

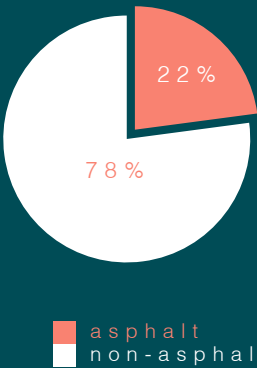


Figure 65.
Asphalt
ratio for
Mirafiori
Nord case
study
(average of
both areas).



Figure 66.

Solid-void map of Mirafiori Nord case study areas.

Source for base map: Geoportale Comune di Torino, n.d.



0 100 200 300 400 500m



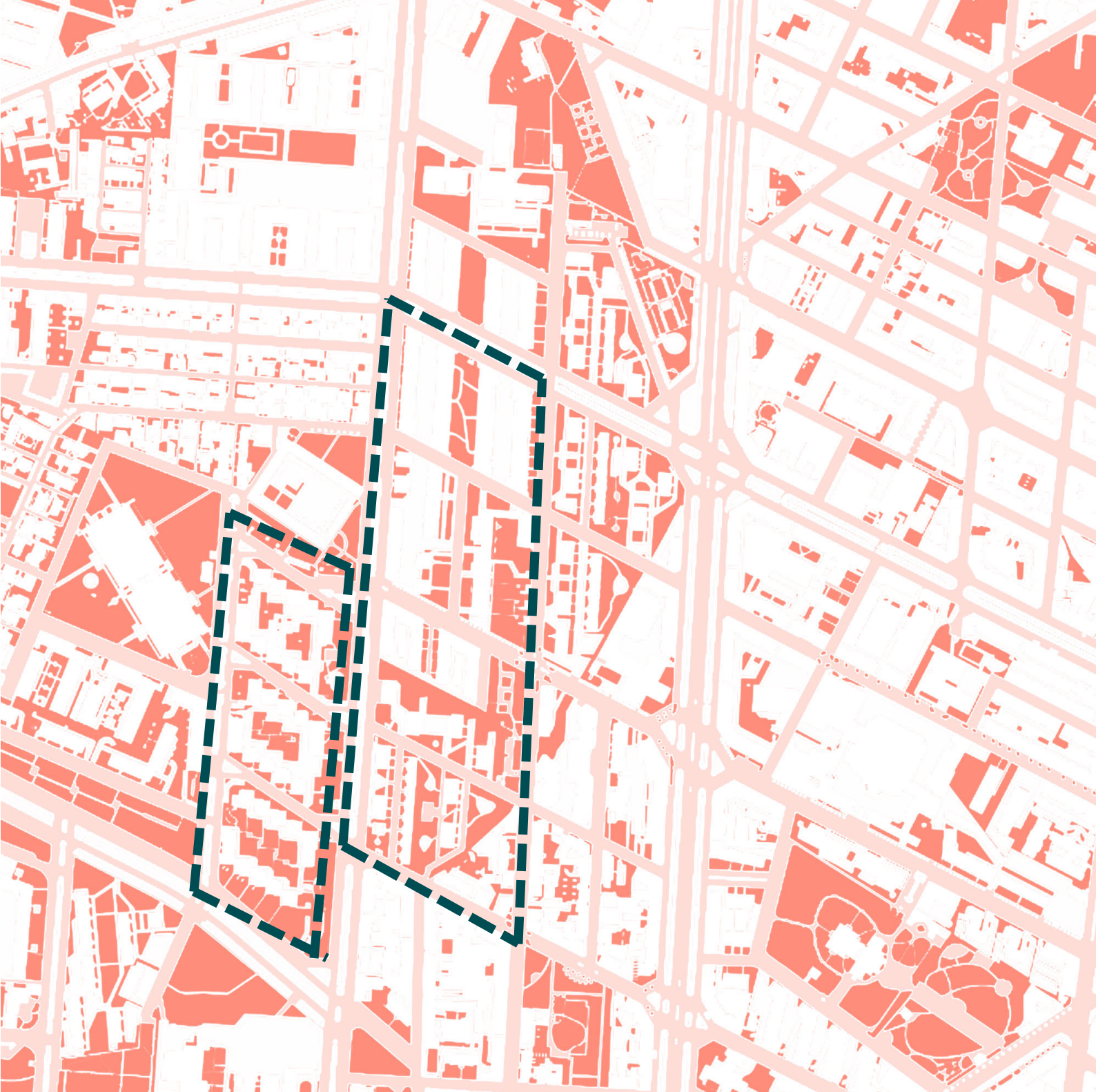


Figure 67.

Road network and greenery in Mirafiori Nord case study areas.

Source for base map: Geoportale Comune di Torino, n.d.

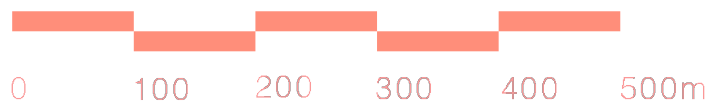




Figure 68.

Car traffic in Mirafiori Nord case study area.

Source for base map: Geoportale Comune di Torino, n.d.

point 1

50 cars

- 04/06/2022
- 10:38-10:43

point 2

31 cars

- 04/06/2022
- 10:50-10:55

point 3

107 cars

- 04/06/2022
- 10:25-10:30

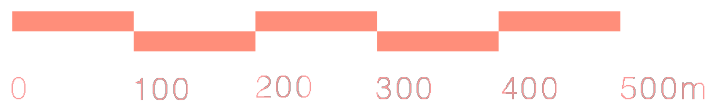




Figure 69.

Ortho image of Mirafiori Nord case study areas.
(Exported from Google Earth)



0 50 100 150 200 250m





Figure 70. Residential blocks of Mirafiori Nord case study area on the west. (Photograph taken by the author)



Figure 71. View of Corso Gaetano Salvemini. (Photograph taken by the author)

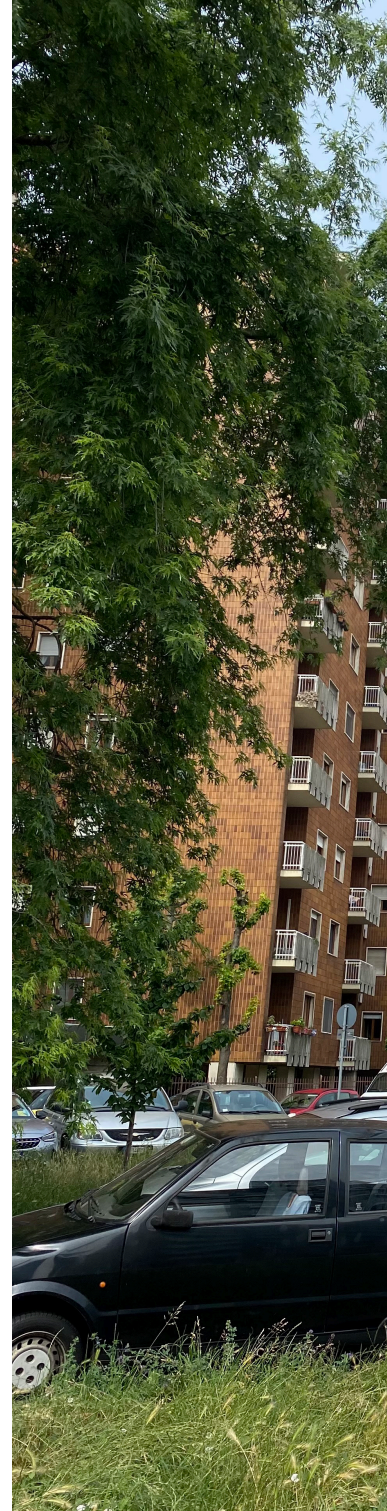




Figure 73. View from Corso Gaetano Salvemini towards the residential blocks of Mirafiori Nord case study area on the west. (Photograph taken by the author)



Figure 72. Close-up view of residential blocks of Mirafiori Nord case study area on the west. (Photograph taken by the author)

Figure 74.
*Residential area of
Mirafiori Nord case
study. (Photograph
taken by the author)*



Figure 75.
*View from Via Boston
towards Mirafiori
Nord case study area.
(Photograph taken by
the author)*





Figure 76.
*Residential block of
Mirafiori Nord case
study area on the
east. (Photograph
taken by the author)*

4.4

Case Study 4: Mirafiori Sud

location	mirafiori sud, turin
neighbourhood area	11.49 km ²
neighbourhood population	33,693
case study area	69,095 m ²
building height range	3-30 m

The case study of Mirafiori Sud represents the fifth typology of Turin's urban fabric classification (carried out in the previous chapter), namely "**order-not dense**".

Mirafiori Sud clearly symbolizes the outcome of the industrialization and the resulting growth that Turin was subjected to. The growth of the neighborhood initiated with the worker flow in 60s and 70s (Fondazione della Comunità di Mirafiori Onlus, n.d.). Several urban redevelopment projects have been applied by the municipality to be able to sustain the needs of the locals and the workers arriving from southern Italy to work in FIAT. Nevertheless, the economic growth of the city had negative impacts on a local scale, not only concerning the urban form but also social integration. The end of the so-called economic boom resulted

in abandoned spaces within the territory. Currently, it is one of the least populated neighborhoods in Turin and the residents are mostly the retired inhabitants that have moved to the city during its industrial expansion period (Fondazione della Comunità di Mirafiori Onlus, n.d.).

The area that has been selected as a case study, has an urban characteristic that is defined by linear and L-shaped building blocks, oriented towards north-south or east-west. Following the site analysis, it has been noticed that these building blocks create shared courtyards in between buildings, where playgrounds and green areas are commonly found. It was observed that the circulation spaces between the buildings are well-shaded, despite the low density of buildings. This effect is the result of generous tree placement and building heights. Additionally, a linear park is situated along the Strada delle Cacce, covered by tall and dense trees, where the inhabitants choose to walk their pets. Towards the north-east end of the site, to the east of the linear park, the National Institute of Meteorological Research (Istituto Nazionale di Ricerca Metrologica) is located. In contrast, a criticality of the site is the concrete square to the west side, with no evidence of shading or vegetation.

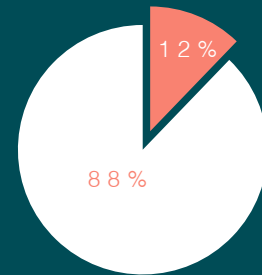


Figure 77.
Built density
ratio for
Mirafiori
Sud case
study.

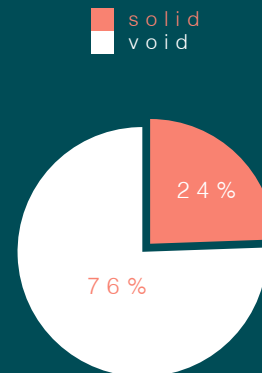


Figure 78.
Horizontal
greenery
ratio for
Mirafiori
Sud case
study.

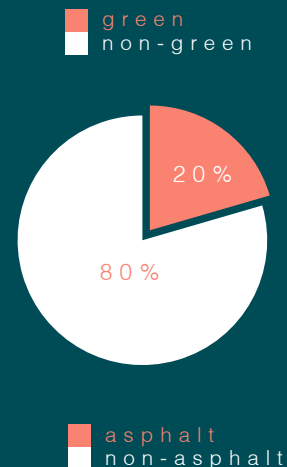


Figure 79.
Asphalt
ratio for
Mirafiori
Sud case
study.

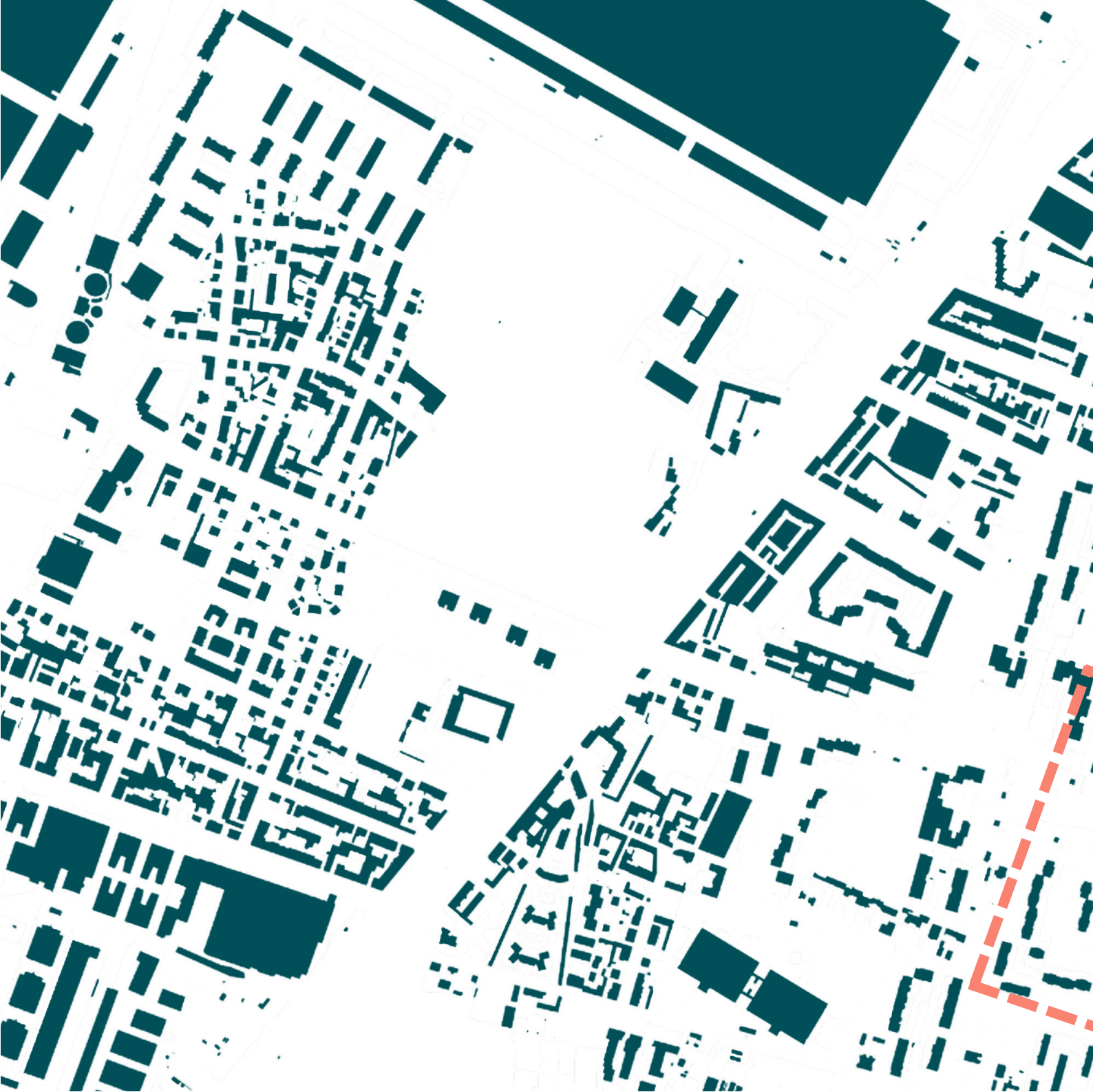
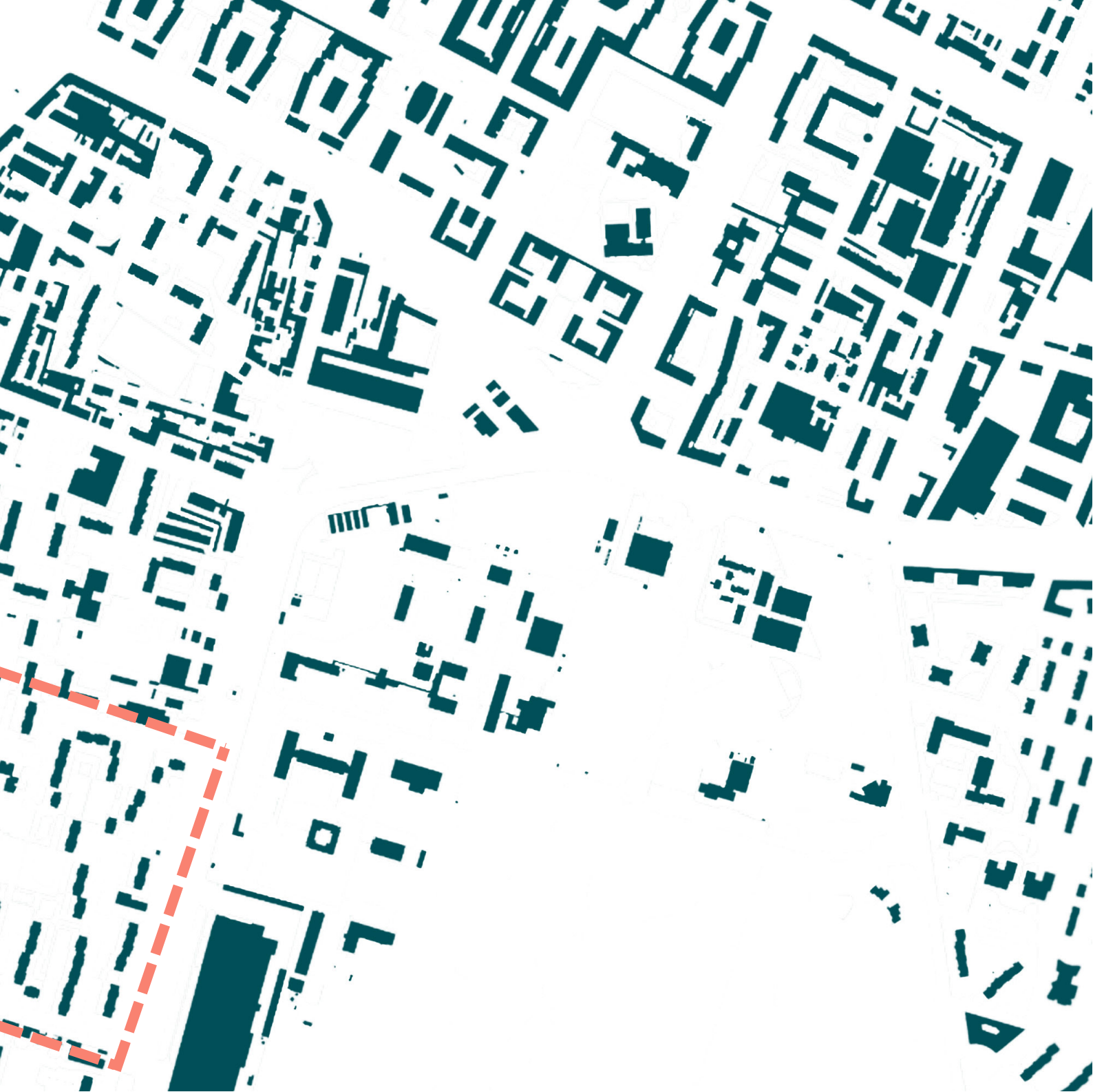


Figure 80.

Solid-void map of Mirafiori Sud case study area.

Source for base map: Geoportale Comune di Torino, n.d.



0 100 200 300 400 500m





Figure 81.

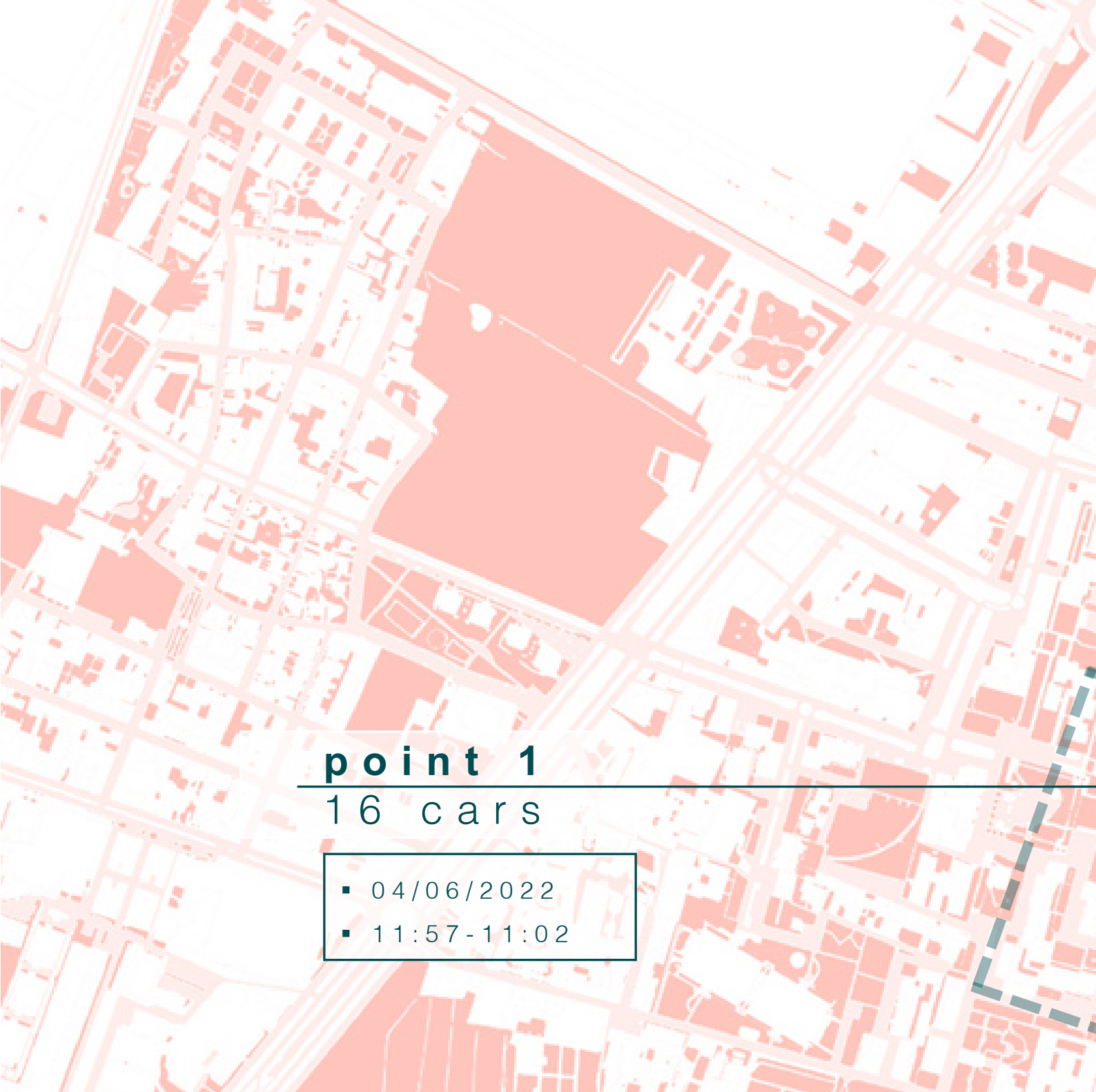
Road network and greenery in Mirafiori Sud case study area.

Source for base map: Geoportale Comune di Torino, n.d.



0 100 200 300 400 500m





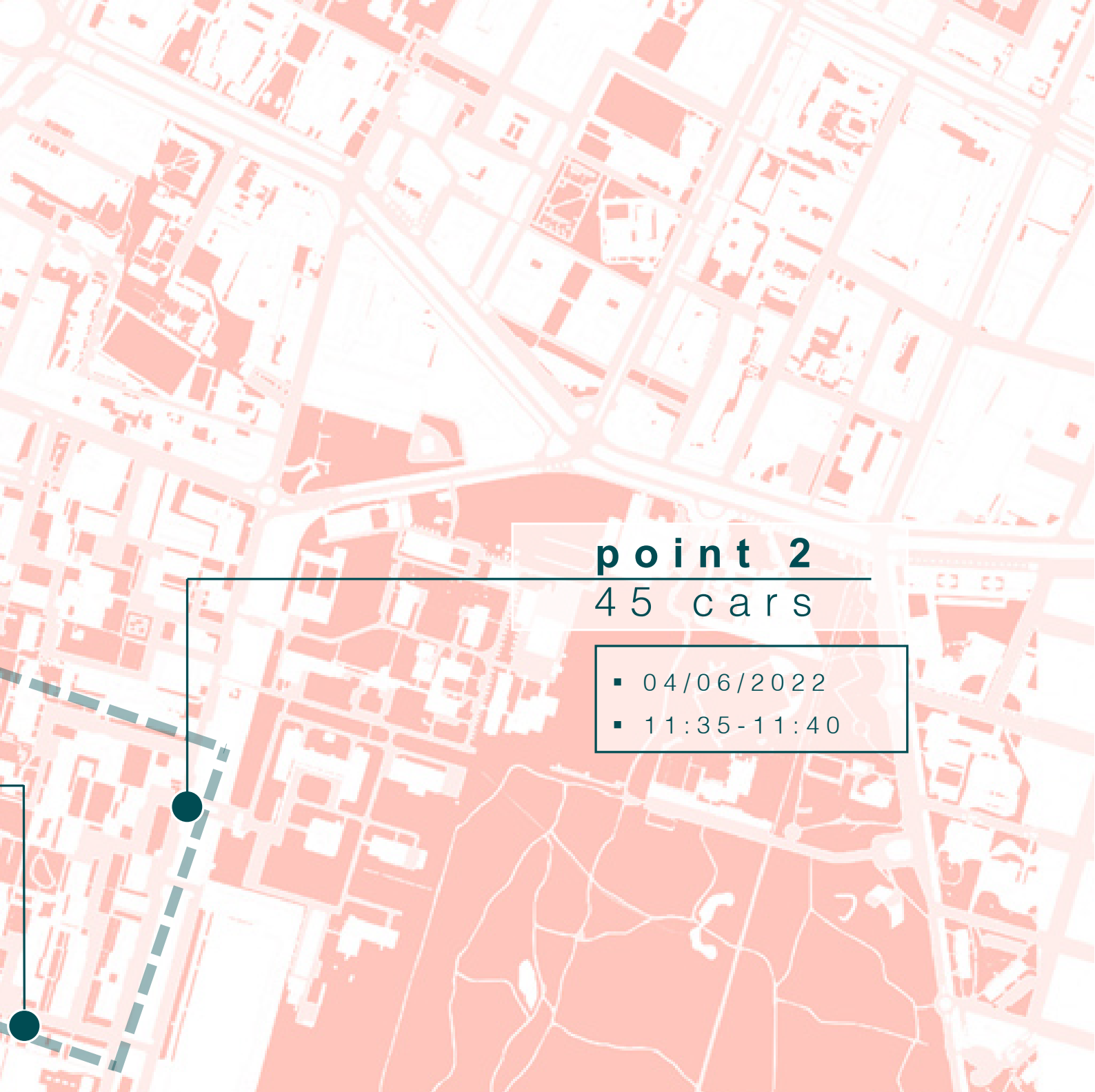
point 1
16 cars

- 04/06/2022
- 11:57-11:02

Figure 82.

Car traffic in Mirafiori Sud case study area.

Source for base map: Geoportale Comune di Torino, n.d.



point 2

45 cars

- 04/06/2022
- 11:35-11:40



0 100 200 300 400 500m





Figure 83.

Ortho image of Mirafiori Sud case study area.
(Exported from Google Earth)



0 50 100 150 200 250m

Figure 84.
*Residential area of
Mirafiori Sud case
study. (Photograph
taken by the author)*





Figure 85.
View from Piazza
Santi Apostoli towards
the residential units
of Mirafiori Sud case
study. (Photograph
taken by the author)



Figure 86.
Presence of greenery
in Mirafiori Sud case
study area.
(Photograph taken by
the author)

Figure 87.
*View from Strada delle
Cacce. (Photograph
taken by the author)*



Figure 88.
*The residential units
of Mirafiori Sud
case study area.
(Photograph taken by
the author)*





Figure 89.
Green area within
Mirafiori Sud case
study. (Photograph
taken by the author)

4.5

Case Study 5: Ex-Mercati Generali

location	lingotto, turin
neighbourhood area	1.8 km ²
neighbourhood population	49,705
case study area	65,000 m ²
building height range	3-30 m

The case study of Ex-Mercati Generali represents the sixth typology of Turin's urban fabric classification (carried out in the previous chapter), namely “**order-dense**”.

Being the legacy of the Winter Olympics that were held in Turin in 2006, the complex has been designed to host athletes. Until 2001, “mercati generali” (the market area) was present in the same zone (MuseoTorino, n.d.-c).

This small neighbourhood consists of buildings that have heights varying between 5 and 8 storeys. The colorful design of the so-called “village” makes it easily recognizable. As of today, the three lots of the area host functions

such as social housing, Arpa offices and student accommodation. The eastern border of the area is shaped by railways, which limits the accessibility of the site from that direction (MuseoTorino, n.d.-c).

The architects (Steidle Architekten) have designed the Villaggio Olimpico complex as cubically rising single building units up to four floors with large terraces and outdoor areas (Steidle Architekten, n.d.).

Towards the north of the site, the remains of the former Mercati Generali fill the lot between Via Giordano Bruno and the railway line. It is considered as one of the most clear instances of rationalist architecture in Turin (MuseoTorino, n.d.-c).

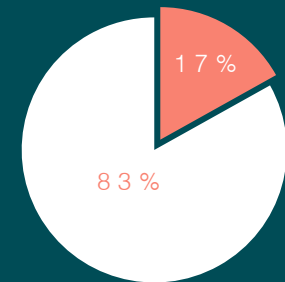


Figure 90.
Built density
ratio for
Ex-Mercati
Generali
case study.

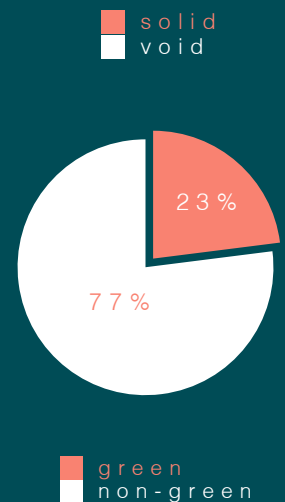


Figure 91.
Horizontal
greenery
ratio for
Ex-Mercati
Generali
case study.

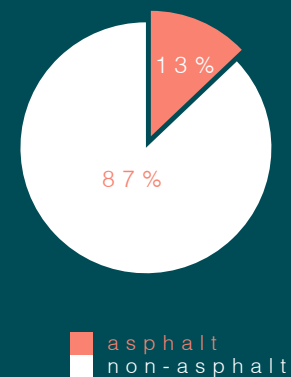


Figure 92.
Asphalt
ratio for
Ex-Mercati
Generali
case study.

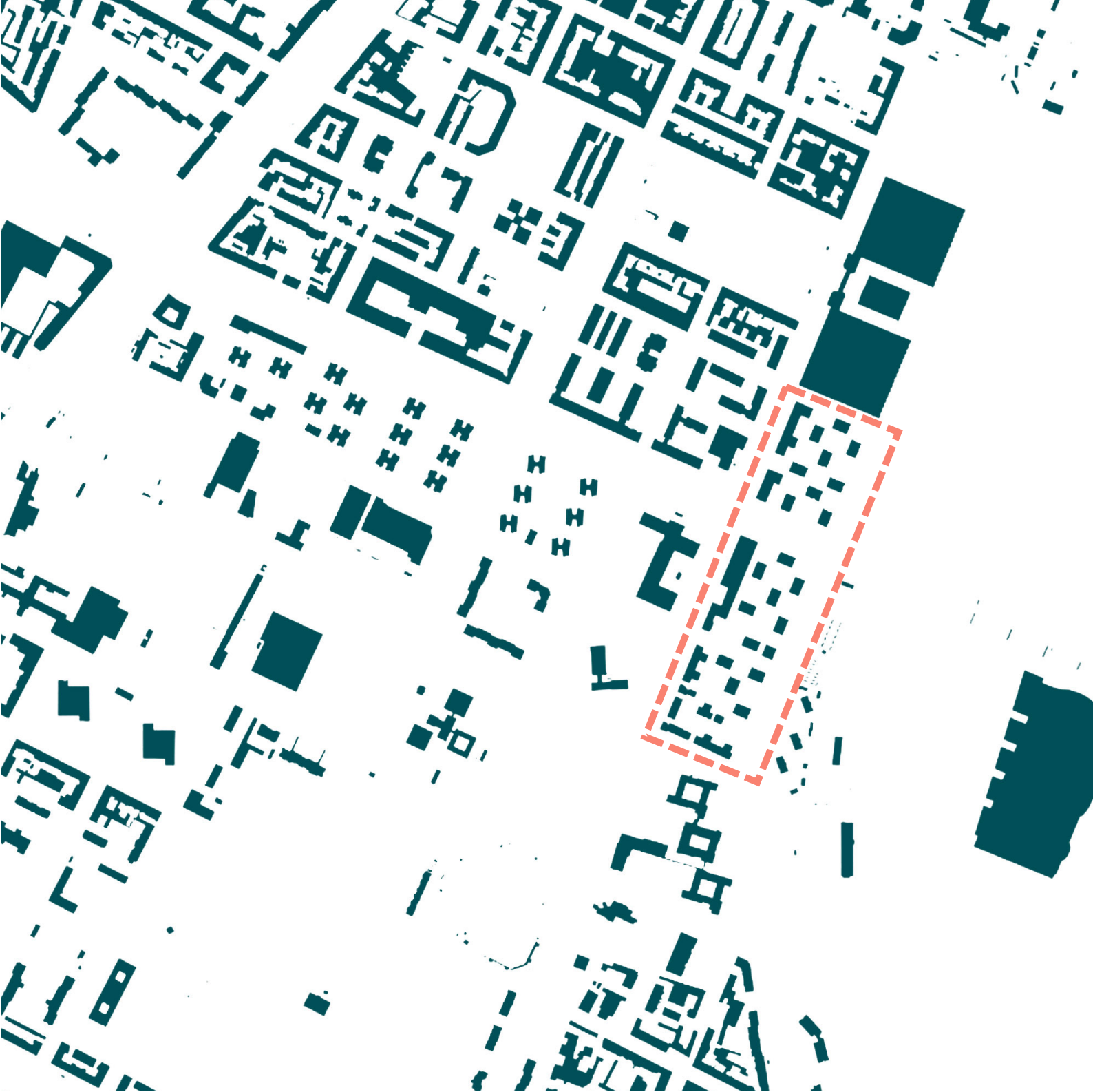
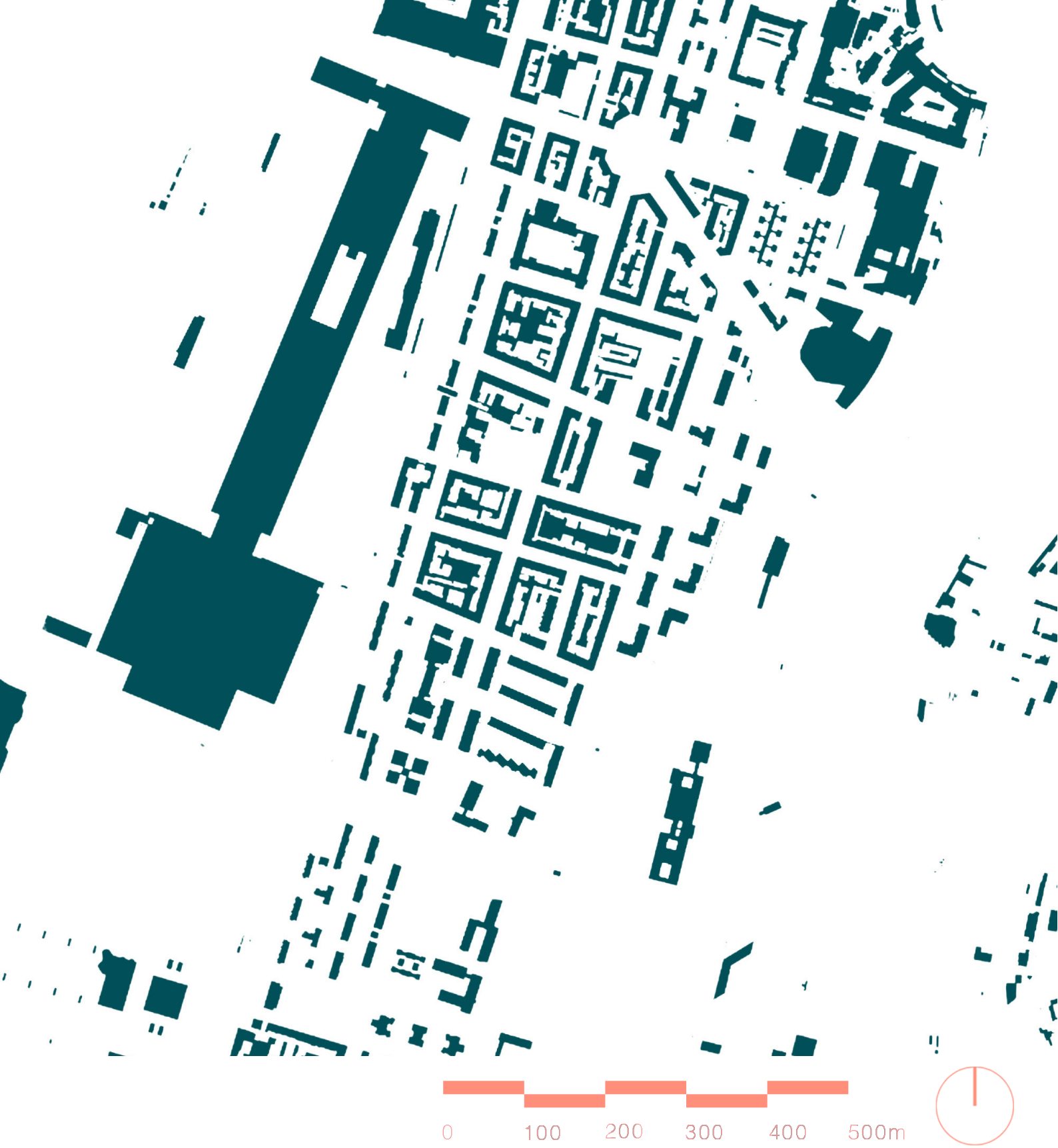


Figure 93.

Solid-void map of Ex-Mercati Generali case study area.

Source for base map: Geoportale Comune di Torino, n.d.



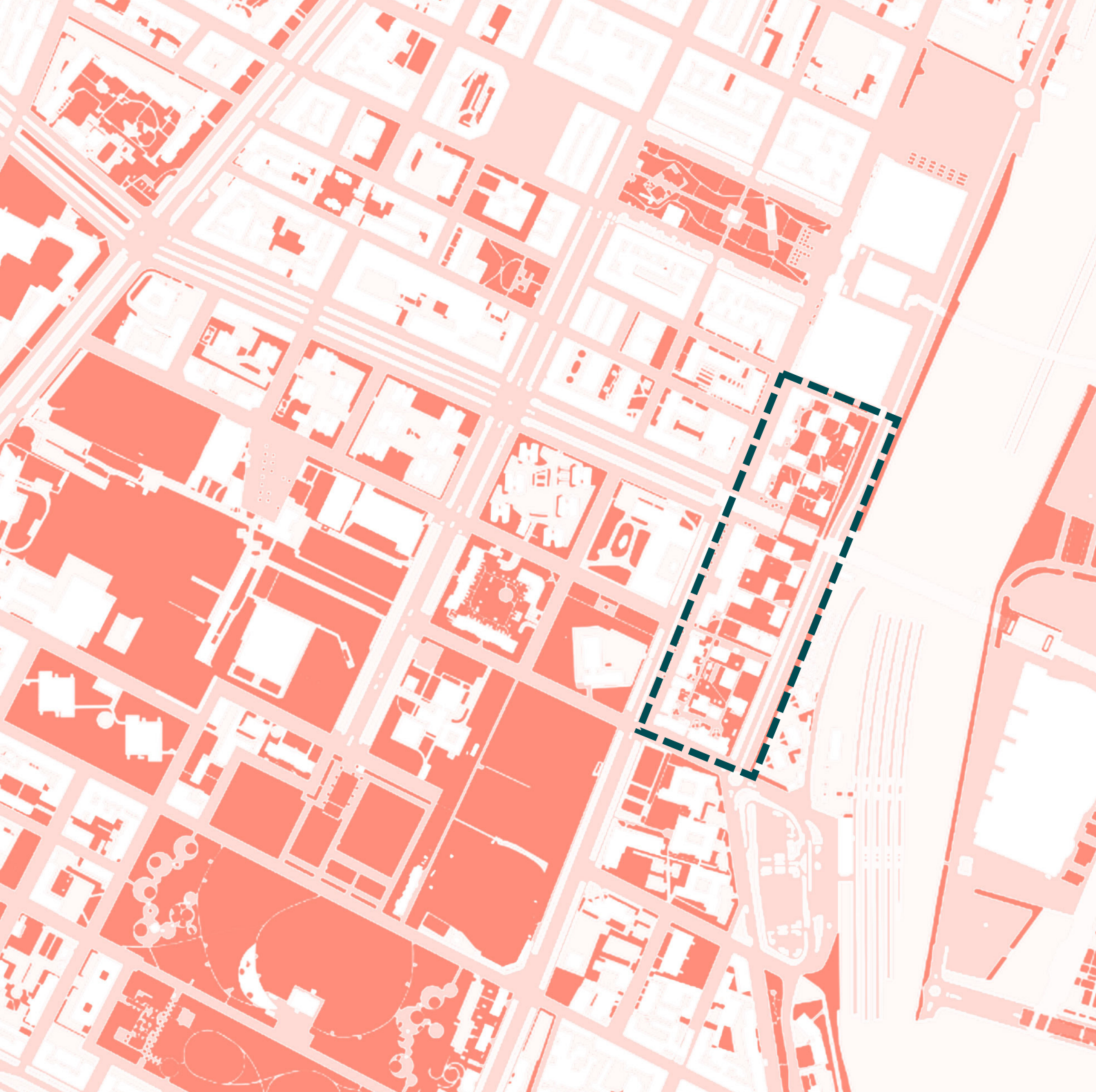


Figure 94.

Road network and greenery in Ex-Mercati Generali case study area.

Source for base map: Geoportale Comune di Torino, n.d.



0 100 200 300 400 500m



- 04/06/2022
- 16:20-16:25

point 1
38 cars

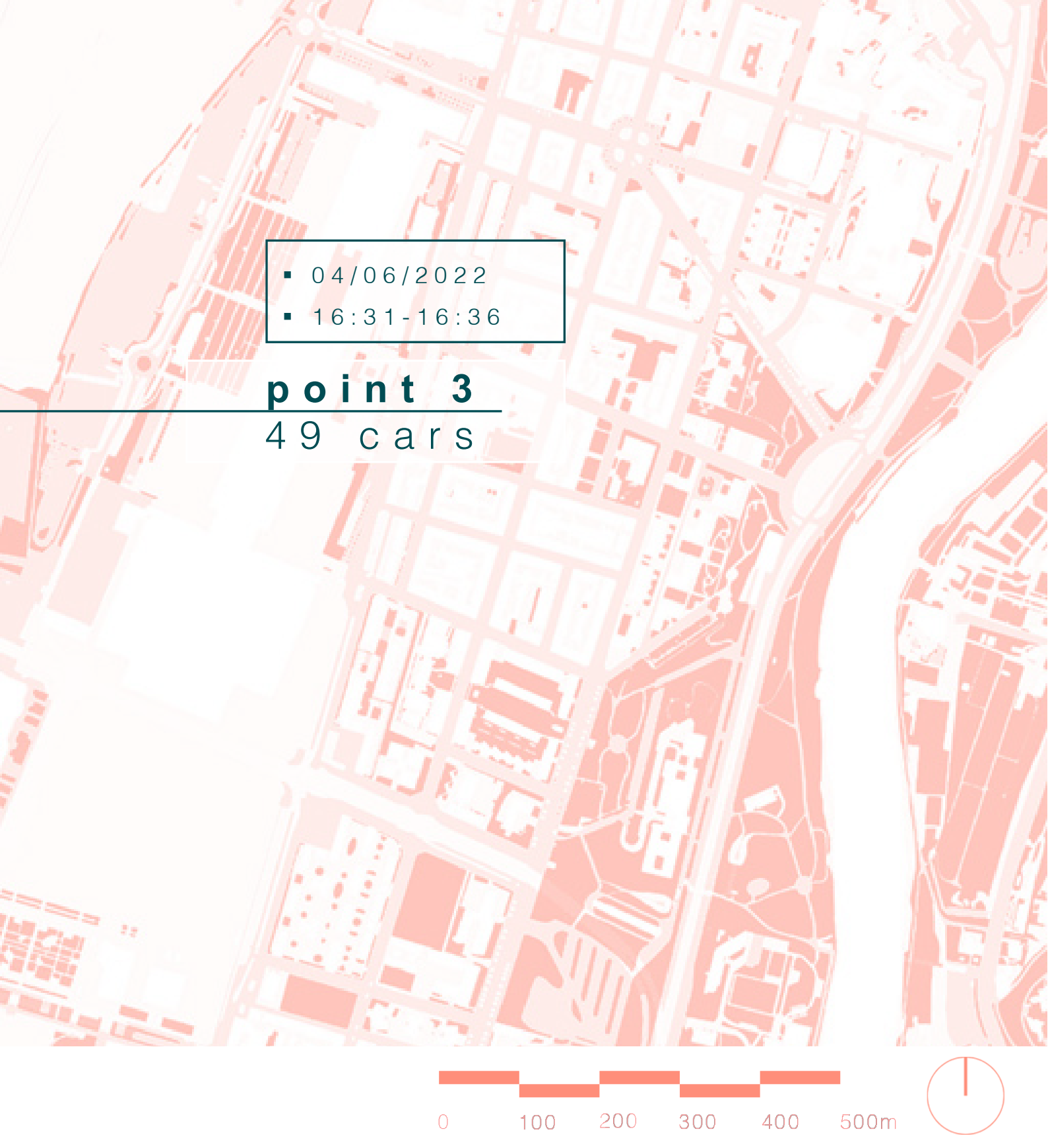
- 04/06/2022
- 16:05-16:10

point 2
62 cars

Figure 95.

Car traffic in Ex-Mercati Generali case study area.

Source for base map: Geoportale Comune di Torino, n.d.

- 
- 04/06/2022
 - 16:31-16:36

point 3
49 cars

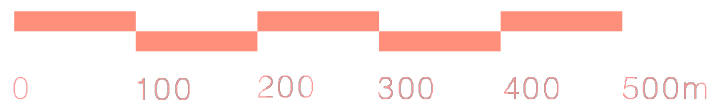




Figure 96.

Ortho image of Ex-Mercati Generali case study area.
(Exported from Google Earth)



Figure 97.
View of Arco Olimpico,
taken from Via Zino Zini.
(Photograph taken by the
author)



Figure 98.
The residential units of
Ex-Villaggio Olimpico
and Arpa building.
(Photograph taken by the
author)





Figure 99.
*The path between
Ex-Villaggio Olimpico
residential area and Via
Zino Zini. (Photograph
taken by the author)*

4.6

Case Study 6: Lingotto

location	lingotto, turin
neighbourhood area	1.8 km ²
neighbourhood population	49,705
case study area	161,670 m ²
building height range	3-45 m

The case study of Lingotto represents the fourth typology of Turin's urban fabric classification (carried out in the previous chapter), namely “**discontinuous-irregular**”.

Lingotto is a district in Turin that is remarkable for the role that it played for the industrial history of the city as it hosted the car factory of FIAT in the early 20th century. Currently, the administrative headquarters of the same automotive company is located in Lingotto. The district is limited by the railways to the east side, which results in an accessibility problem as well as heat flows from the overheated railways. The remains of the former FIAT factory were repurposed as

a multifunctional complex, which helped the district to become revalued.

The case study site is adjacent to a high-traffic road (Corso Unione Sovietica) and a busy roundabout (Piazzale Caio Mario) is located at the south-western end of the site. Across the well-vegetated high-traffic roads (Corso Unione Sovietica and Corso Giovanni Agnelli), the immense mass of the FIAT car factory can be recognized. Between the two above-mentioned roads, a large asphalt/concrete parking lot is present.

The site consists of interrupted building blocks that form individual courtyards through their positioning. Between the buildings, there is no evidence of densely placed vertical greenery, however, scattered trees are present. In the middle of the site a playground and a dog park are located. The decentralized location of the site and the inaccessibility of services is compensated by local shops and markets that residents can benefit from.

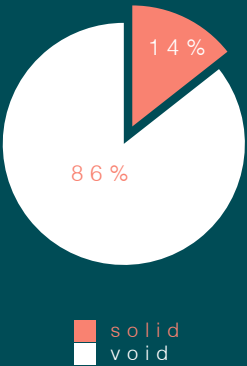


Figure 100.
Built density
ratio for
Lingotto
case study.

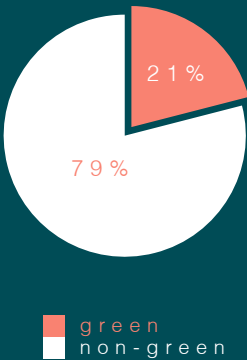


Figure 101.
Horizontal
greenery
ratio for
Lingotto
case study.

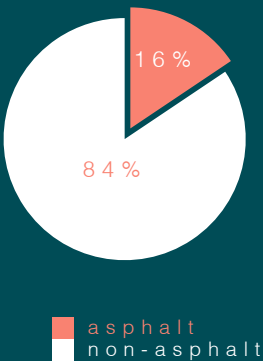


Figure 102.
Asphalt
ratio for
Lingotto
case study.

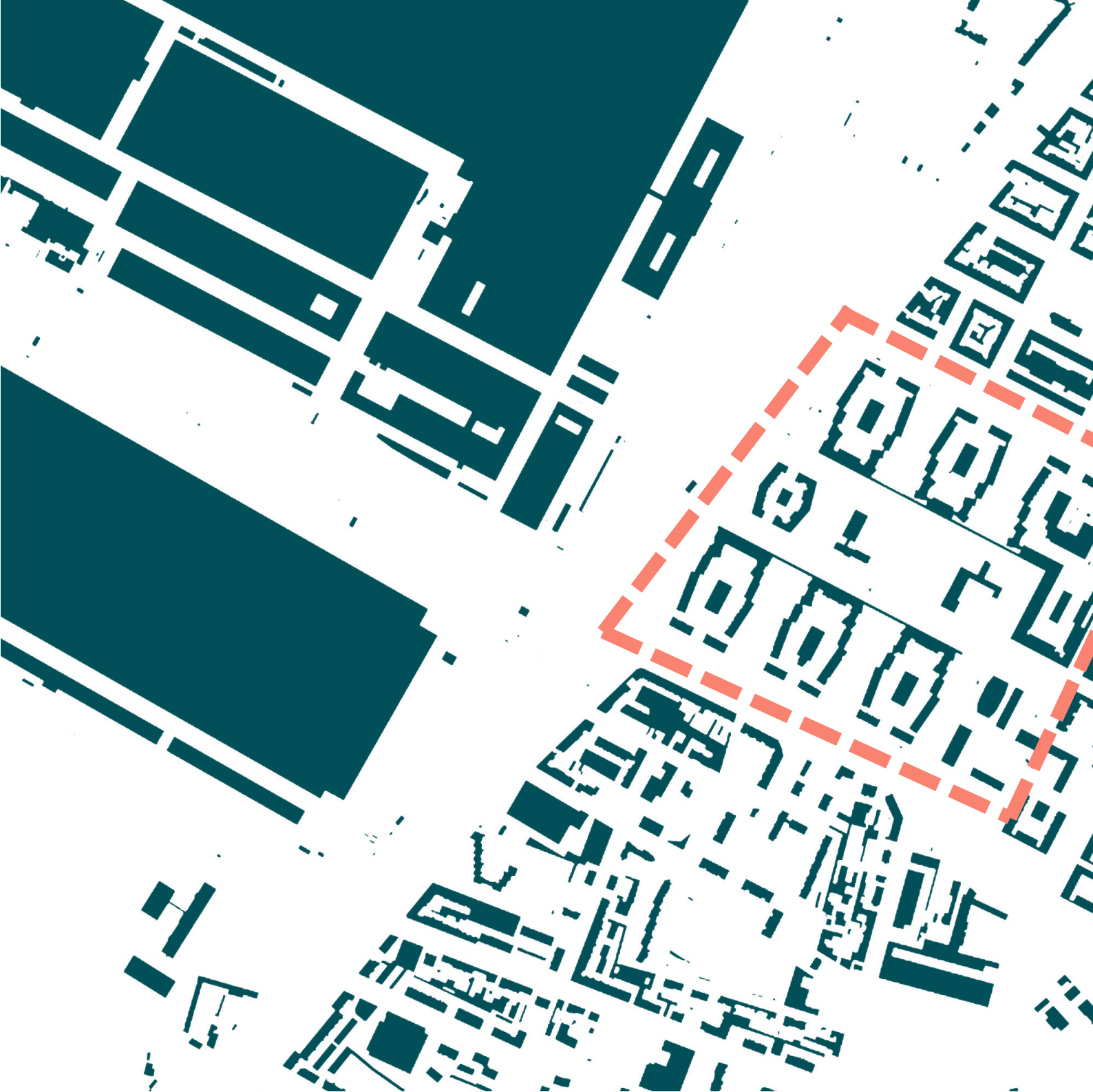
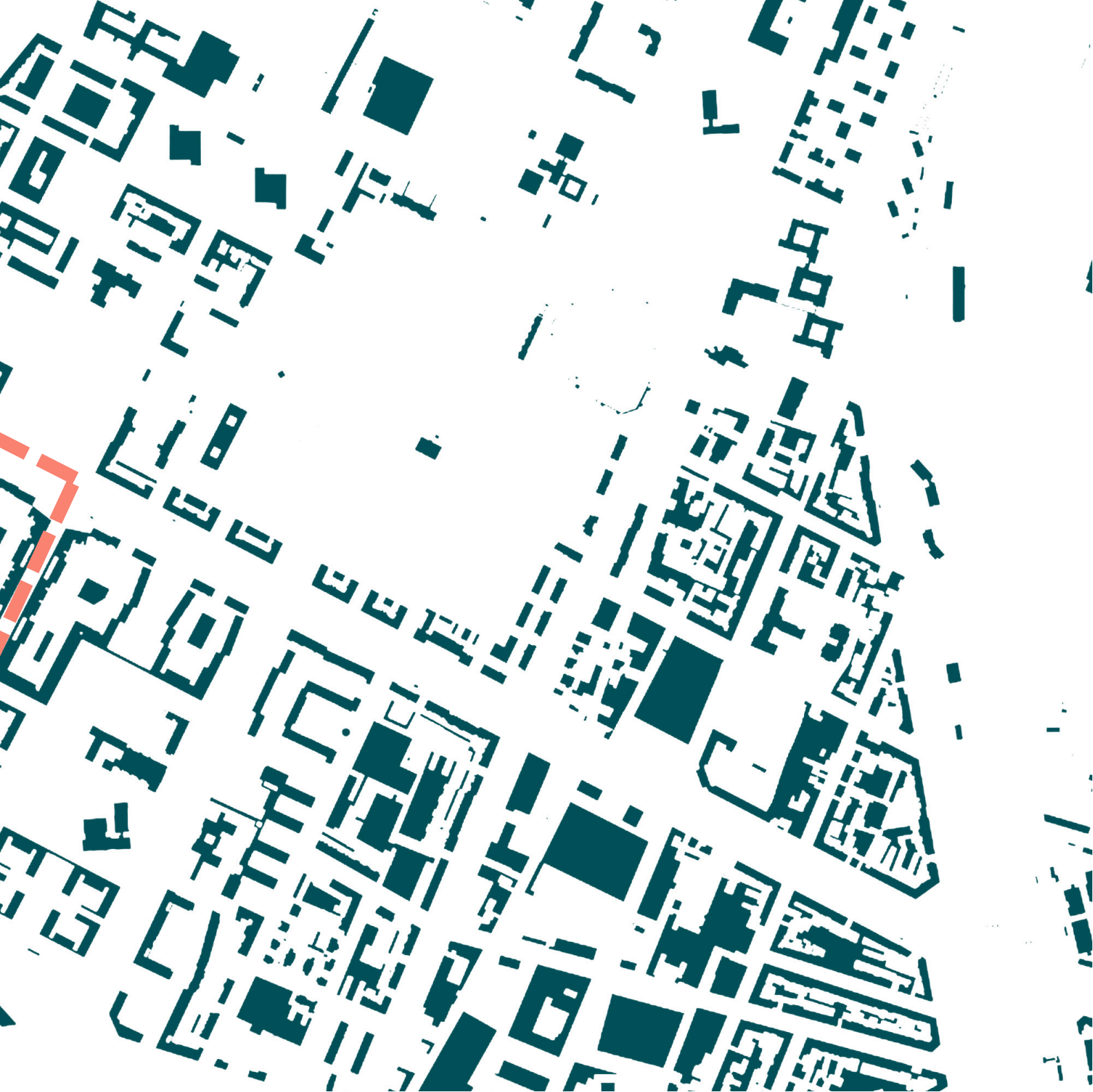


Figure 103.

Solid-void map of Lingotto case study area.

Source for base map: Geoportale Comune di Torino, n.d.



0 100 200 300 400 500m



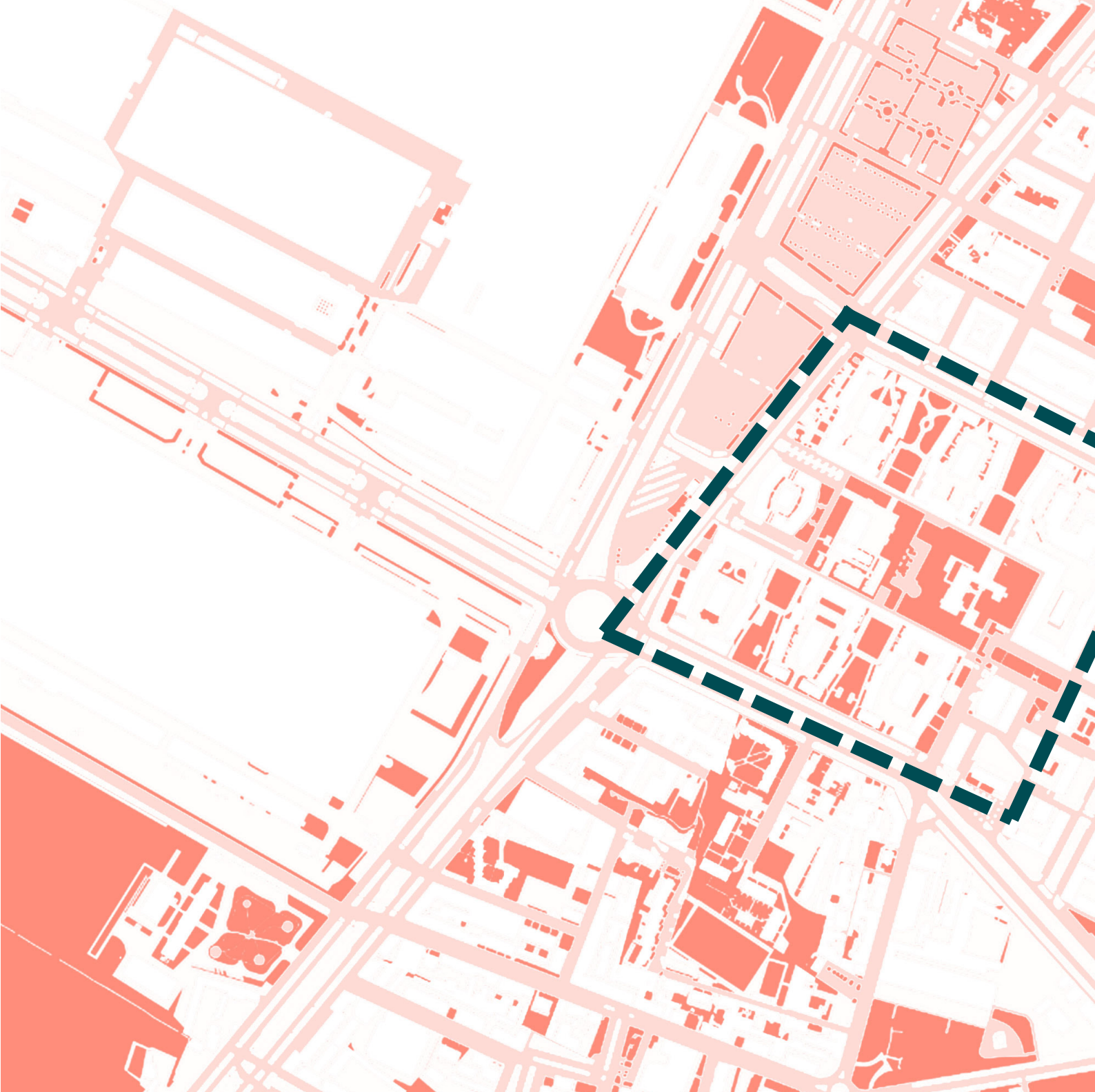


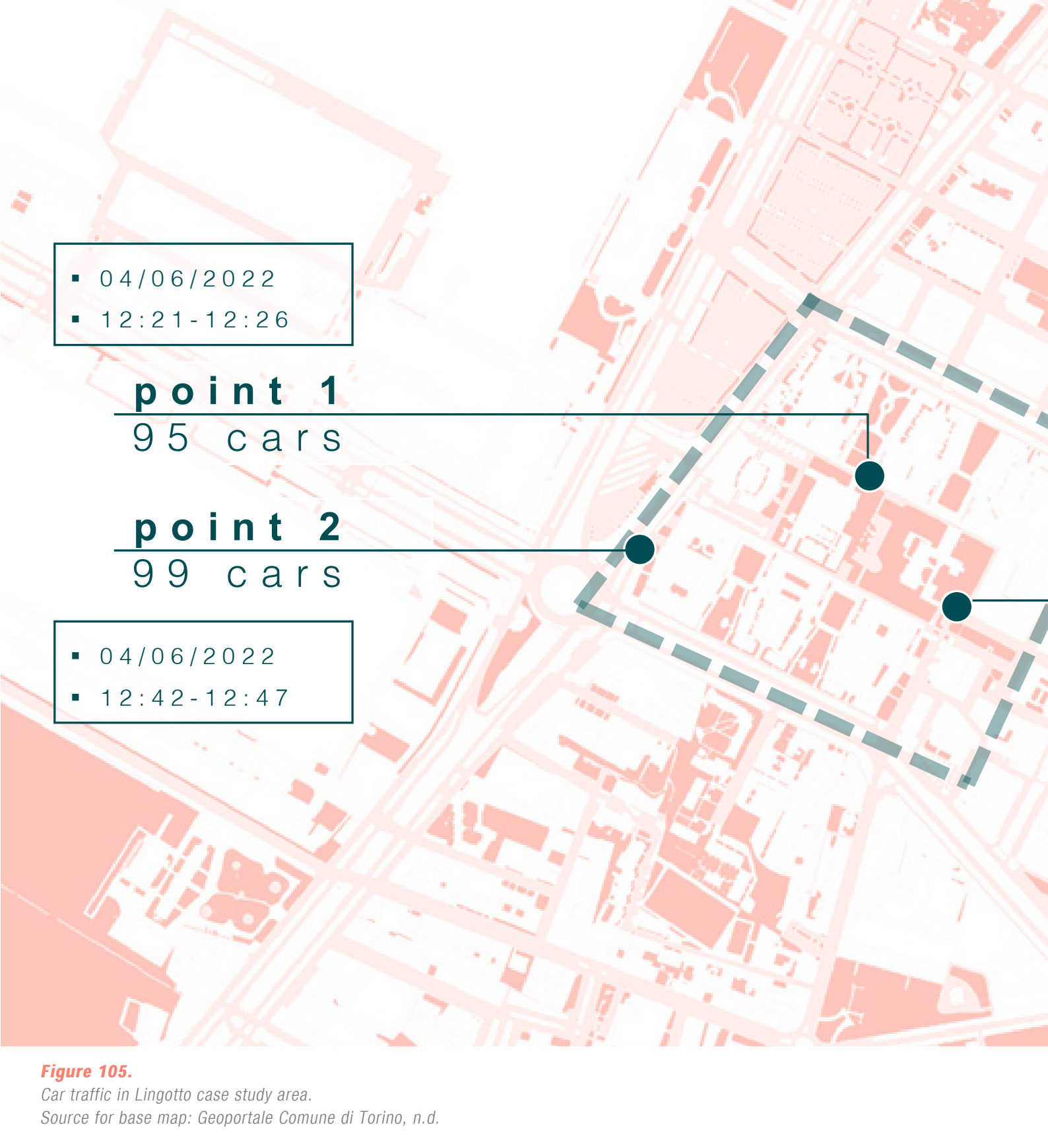
Figure 104.

Road network and greenery in Lingotto case study area.
Source for base map: Geoportale Comune di Torino, n.d.



0 100 200 300 400 500m



- 
- 04/06/2022
 - 12:21-12:26

point 1
95 cars

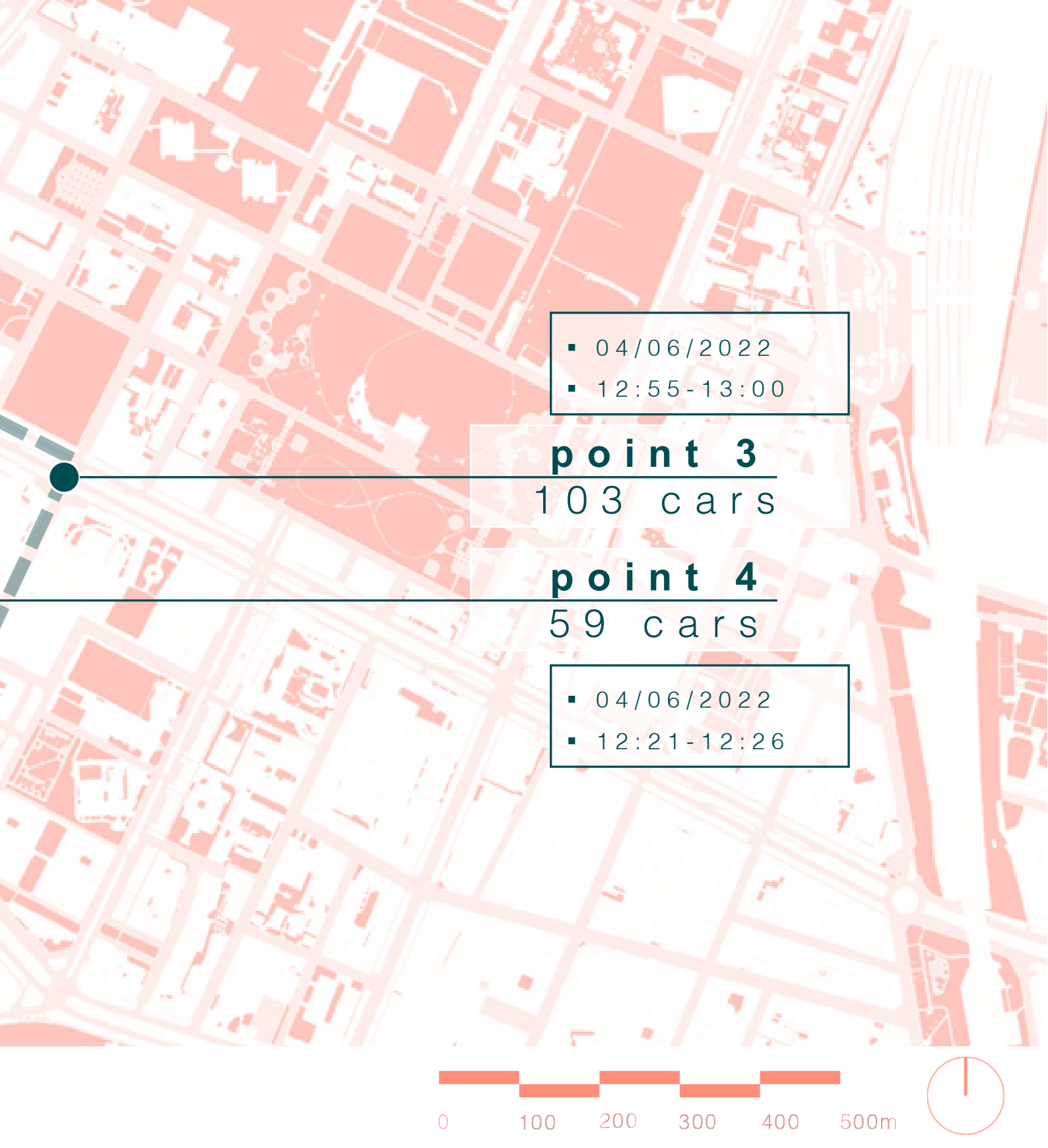
point 2
99 cars

- 04/06/2022
- 12:42-12:47

Figure 105.

Car traffic in Lingotto case study area.

Source for base map: Geoportale Comune di Torino, n.d.

- 
- 04/06/2022
 - 12:55-13:00

point 3
103 cars

point 4
59 cars

- 04/06/2022
- 12:21-12:26

0 100 200 300 400 500m





Figure 106.

Ortho image of Lingotto case study area.
(Exported from Google Earth)



Figure 107.
Residential area in
Lingotto case study.
(Photograph taken
by the author)



Figure 108.
Covered circulation
area and local
services in Lingotto
case study.
(Photograph taken
by the author)





Figure 109.

View of the south east end of Lingotto case study area.
(Photograph taken by the author)



Figure 110.

View from Corso Unione Sovietica.
(Photograph taken by the author)



Results & Discussion

5.1. ENVI-met Process

(Software Information, Modelling, Simulation, Output)

5.2. Discussion

(Urban Structure, Vegetation, Materials, Peak Points,
Behavior of Environmental Variables for Selected Points)

In this chapter, the results of the simulations that have been obtained using ENVI-met software will be discussed. The outputs that were examined within this chapter are air temperature, surface temperature, PET and wind speed. These outputs have been evaluated through analyzing their interconnection with three urban environment elements: urban geometry, vegetation, materials.

The discussion follows a comparative approach where each individual case study has been evaluated both in isolation and in comparison to the others, with those that they share common ratios of built density, horizontal greenery and asphalt ratio. Nevertheless, an overall comparison of all sites have been performed as well. Although the focus is on the hours of 12:00 and 15:00, more results have been attached to the annex. For a simple comparison process, both for the author and for the reader, a fixed legend has been determined for each output in a way that the legend interval for a specific hour would cover the minimum and maximum values of all case studies.

5.1

ENVI-met Process

5.1.1 . Software information

In this thesis, ENVI-met was used as a tool for the simulation of six case studies. ENVI-met is a three-dimensional microclimate model that allows analysing how small scale changes or interventions in urban design could effect the microclimate. It serves as a software to simulate the interactions between surfaces, plants and the atmosphere in an urban environment. Fields such as architecture, landscape architecture, environmental planning and buildings benefit from ENVI-met's capability to demonstrate the interconnection between urban areas and microclimate. Being a prognostic model and taking the essential laws of fluid dynamics and thermodynamics as a base, ENVI-met is capable of simulating the flow around and between buildings, exchange processes at the ground surface and at building walls, building physics, impact of vegetation of the local microclimate, bioclimatology and pollutant dispersion (ENVI-met, 2021).

** **Nesting grids:** Additional grids that are added to the borders of the model with an aim of minimizing the errors that might occur towards the boundaries of the model.*

5.1.2. Modelling

Before the modelling process, it was necessary to download carta tecnica (see “1.1. Methodology” section for the definition) data from Geoportale Torino. For the cases where a site has areas on more than one carta tecnica, the maps were put together. As ENVI-met requires bitmap (.bmp) files as the base of the models, these maps were converted into bitmap format through Adobe Photoshop.

Initial adjustments for modelling: For modelling the case studies, ENVI-met version 5.0.2 was used. The software includes six sections: Monde, Spaces, ENVI-guide, ENVI-core, BIO-met and Leonardo. Projects/Workspaces module has been used to create separate folders and individual settings for each case study. Followingly, Spaces module has been used to create the model. This process has started with adjusting the “Model Info” section, which contains the base information of the model. The input data is as follows:

location	turin
geographic coordinates	lat. 47.07, long. 7.69
number of <i>nesting grids</i> *	4
wall material	default wall - moderate insulation
roof material	roofing: tile

In addition to these parameters, it was necessary to adjust the resolution of the model before starting to model. In this thesis, **a resolution of 4x4x2** was used for each case study. For each model the case study area was multiplied by 4 to define the model area, to evaluate the borders of the case study areas better and to limit the errors that might occur through the model borders. As the modelled sites are large urban areas (ranging between 170,000 m² and 657,000 m²) that include many blocks, this helped accelerating the simulation process which still lasted for days for each site. The relevant dimensions that have been used for each model are listed below:

case study	dimensions	area	number of grids	resolution
san donato	420 x 400 m	170,000 m ²	105 x 100 x 40	4 x 4 x 2
le vallette	600 x 435 m	261,000 m ²	150 x 113 x 40	4 x 4 x 2
mirafiori nord	730 x 900 m	657,000 m ²	183 x 225 x 45	4 x 4 x 2
mirafiori sud	400 x 520 m	208,000 m ²	100 x 130 x 40	4 x 4 x 2
ex-mercati generali	375 x 520 m	195,000 m ²	94 x 130 x 40	4 x 4 x 2
lingotto	700 x 690 m	490,000 m ²	175 x 173 x 48	4 x 4 x 2

Table 1. Dimensions regarding the simulation domains of each case study.

DEM: Following the above-mentioned initial adjustments, a layer of DEM was created for the whole site with a height of three meters. This choice is due to the need of modelling railroad networks where necessary (e.g. the site of Mercati Generali South), as the railroads would be placed below the main pedestrian circulation level. Thus, DEM was not placed on top of the parts of the model which represent railroads.

Buildings and vegetation: Subsequently, buildings and vegetation were added to the models. As for the building heights, the data that was collected from the Geoportale maps were compared to Google Maps. As ENVI-met allows customized materials, “15 cm grass” material was created, to be used in all the sites with one exception: San Donato. The reasoning behind this application is the fact that all the areas having large areas of horizontal greenery, except for San Donato. To be able to observe the impact of limited amount of greenery (compared to the built context), it was necessary to keep the grass height higher in the model for San Donato.

Materials: To proceed after placing the building masses and vegetation, relevant materials were assigned to the soil. All of the materials except for asphalt have been used directly from the database. In the case of asphalt, a customized material was created by adjusting the emissivity of the material to improve the reliability of the output. The materials that were used from the database of ENVI-met are listed below:

material	envi-met code	albedo	emissivity	function in the model
asphalt	[01ASPU]	0.1	0.95	vehicle road, parking lots
concrete pavement gray	[0100PG]	0.5	0.9	pavements
concrete pavement light	[0100PL]	0.8	0.9	bright pavements, playgrounds and courtyards
concrete pavement dark	[0100PD]	0.2	0.9	dark pavements and courtyards, railway tracks, parking lots
brick road (red stones)	[0100KK]	0.3	0.9	playgrounds, public spaces, parking lots
terre batue (smashed brick)	[0100TB]	0.8	0.9	playgrounds, public spaces
loamy soil	[000000]	0	0.98	building and vegetation base
sandy soil	[0100SD]	0	0.9	sites under construction

Table 2. Material choices for ENVI-met models.

Trees: For all sites, the public tree data from Geoportale (Geoportale Comune di Torino, n.d.) has been followed and applied to the model. Since Geoportale provides the species of trees, specific tree species were assigned for each tree. For the trees that are not available on Geoportale but have been detected during the site trip and from Google Maps, default trees from ENVI-met database have been used, with respect to the characteristics of the actual tree (such as height, deciduous, conifer).

tree species	san donato	vallette	mirafiori nord	mirafiori sud	ex-mercati generali	lingotto
london plane tree (middle)						
london plane tree (old)						
acer negundo						
acer platanoides						
acer pseudoplatanus						
thuja (young)						
bird cherry (young)						
tilia						
tilia cordata						
tilia platyphyllos						
pine tree (young)						
pine tree (middle)						
olea europaea						
acer campastre						
spherical, large trunk, dense, small (5m)						
spherical, large trunk, dense, medium (15m)						
spherical, large trunk, dense, large (25m)						
horse chestnut (young)						
horse chestnut (middle)						
horse chestnut (old)						
dutch elm (old)						
little leaf lime "greenspire" (middle)						
pendunculata oak (old)						
picea abies						
tulip tree (middle)						
norway maple "globosum" (middle)						
silver maple (middle)						
cylindric, large trunk, dense, small (10m)						
cylindric, large trunk, dense, medium (15m)						
platanus acerifolia						
carpinus betulus						
fagus sylvatica						
american sweet gum (middle)						
tree hazel (middle)						
populus nigra						
ginkgo/fan leave tree (middle)						
sweet chestnut/maron						
persian walnut						
quercus robur						
wild cherry "plena" (young)						
hornbeam						
ulmus minor						
conic, large trunk, dense, small (5m)						
conic, large trunk, dense, medium (15m)						
conic, large trunk, dense, large (25m)						
tree of heaven (middle)						
heart-shaped, large trunk, dense, medium (15m)						
red oak						
fraxinus excelsior						
populus alba						

Table 3. Plants used from ENVI-met database.

5.1.3. Simulation

ENVI-guide is the module where the simulation settings are adjusted. The simulation period was set as 48 hours, starting from 19.07.2020 (the hottest day of the year) at 00:00. The website of Arpa Piemonte was used as a source for the input parameters concerning air temperature, relative humidity, wind speed and wind direction for each hour of the day (see Table 4). Simple forcing was used to feed the software with the information that it needs regarding the meteorological boundary conditions. The simulation was run through ENVI-core module with each simulation taking approximately 4-7 days, depending on the size of the modelling area.

5.1.4. Output

The outputs of the simulation were imported into “Leonardo” section of ENVI-met, which allows exporting plan and section views from any plane of the simulation domain. For potential air temperature and wind speed results, “atmosphere” file has been used as a source, whereas for surface temperature results, “surface” file has been relevant. To analyze the results of physiological equivalent temperature (PET), “BIO-met” module of the software has been used, which allows not only the calculation of PET but also other comfort indexes such as UTCI and PMV. Once the times of the day and the plane height for which the PET value is intended to be examined are chosen, one can calculate the PET value. The results of this calculation creates a folder named “biomet” in the simulation output folder. This data was imported to the Leonardo module to be able to

hour	T air (°C)	R.H. (%)	wind speed (m/s)	wind direction
12:00:00 AM	22,5	76	1,5	67
1:00:00 AM	21,6	81	1,8	61
2:00:00 AM	20,5	85	1,2	45
3:00:00 AM	19,9	90	1,2	0
4:00:00 AM	19,1	92	1,4	197
5:00:00 AM	19,1	89	1,6	216
6:00:00 AM	21,4	80	1,1	101
7:00:00 AM	23,8	62	1,9	74
8:00:00 AM	25,9	52	1,3	69
9:00:00 AM	27,9	46	1	328
10:00:00 AM	29,9	48	1,2	49
11:00:00 AM	31	39	2,3	93
12:00:00 PM	31,8	38	1,7	72
1:00:00 PM	32,8	34	2,8	53
2:00:00 PM	33,1	38	1,9	48
3:00:00 PM	33	37	2,5	66
4:00:00 PM	32,7	42	2,4	82
5:00:00 PM	30,9	55	1,6	177
6:00:00 PM	27,5	56	1,8	217
7:00:00 PM	25,7	60	2	53
8:00:00 PM	24,1	69	1,6	51
9:00:00 PM	24,6	68	2	223
10:00:00 PM	23,8	72	1,6	190
11:00:00 PM	23,4	72	2,4	207

Table 4. Input values for the simulation. (Arpa Piemonte, n.d.)

visualize the distribution of outdoor comfort levels. The outputs for potential air temperature, surface temperature, PET and wind speed have been extracted for 9:00, 12:00, 15:00 and 18:00. As for the plans, the cutting plane was set to be 2 meters above the ground (except for surface temperature, which was set to 0), representing an estimation of human-eye level. In the models, the total height for the cutting plane was marked as 5 meters, due to 3 meters of underground soil. Additionally, a common legend was set for each time of the day, to achieve a simpler comparison process. Within this chapter, the results for hours of 12:00 and 15:00 will be demonstrated. A. The data concerning the hours 9:00 and 18:00 can be found in the Annex.

In addition to the exported maps, the points that have the worst conditions of PET in each case study area have been selected. This has been done using “explore grid” option, which allows to pick specific points on the map and to export the trends of different environmental variables (in this case, PET, surface temperature and potential air temperature) as graphs. The locations of the picked points in the model are as follows:

case study	point A (residential public space)	point B (NW-SE oriented urban canyon)	point C (NE-SW oriented urban canyon)
san donato	i=52, j=45	i=41, j=57	i=54, j=60
le vallette	i=74, j=87	i=91, j=83	i=123, j=80
mirafiori nord	i=87, j=152	i=98, j=43	i=76, j=137
mirafiori sud	i=67, j=102	i=76, j=107	i=87, j=66
ex-mercati generali	i=24, j=28	i=17, j=20	i=46, j=109
lingotto	i=44, j=82	i=100, j=131	i=150, j=61

Table 5. ENVI-met model coordinates of the points that have the least favorable PET conditions.

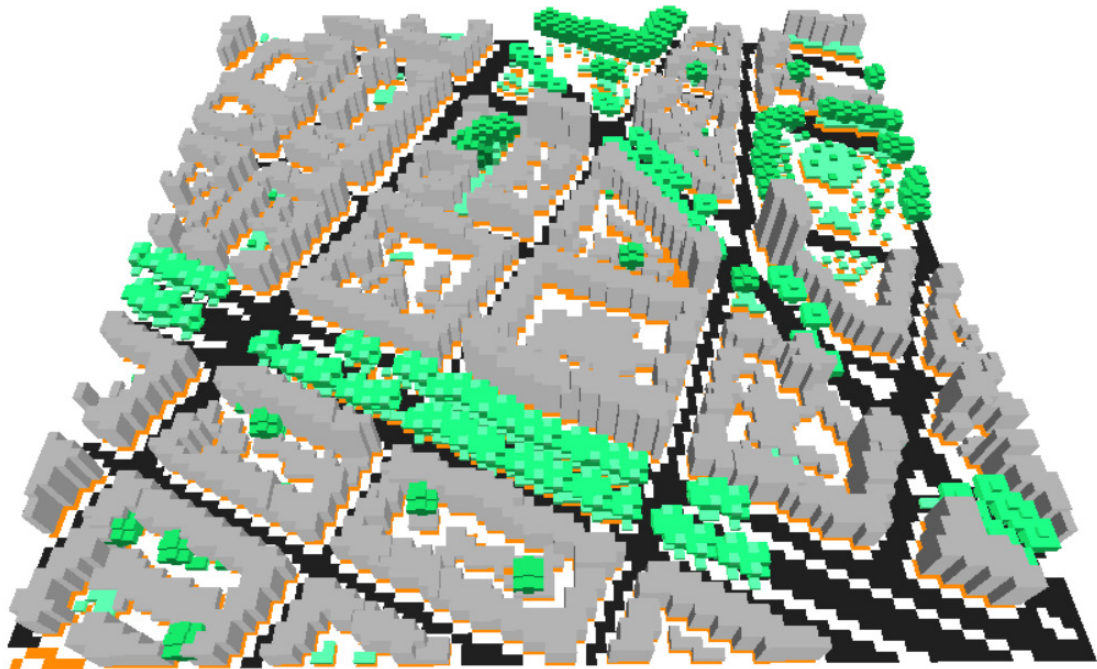


Figure 111. 3D model of San Donato case study. (Exported from ENVI-met)



Figure 112. 2D plan illustrating building and vegetation presence in San Donato case study. (Exported from ENVI-met)

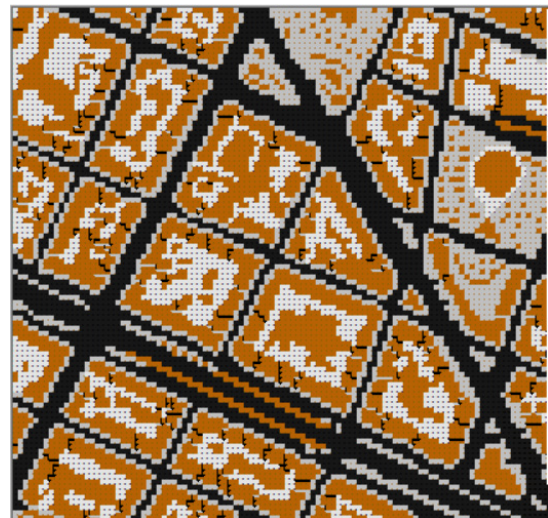


Figure 113. 2D plan illustrating the material distribution in San Donato case study. (Exported from ENVI-met)



Figure 114. 2D plan illustrating building and vegetation presence in Le Vallette case study. (Exported from ENVI-met)

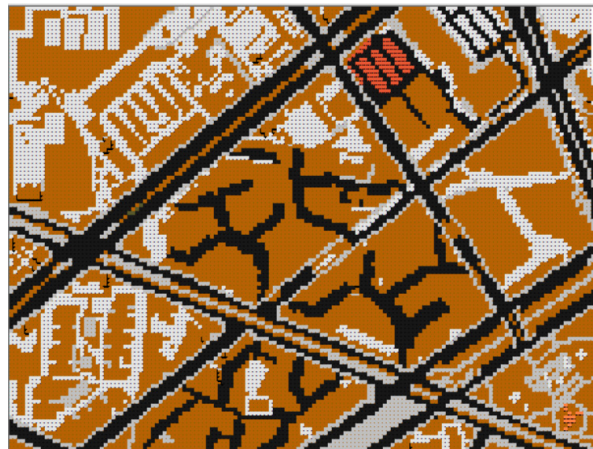


Figure 115. 2D plan illustrating the material distribution in Le Vallette case study. (Exported from ENVI-met)

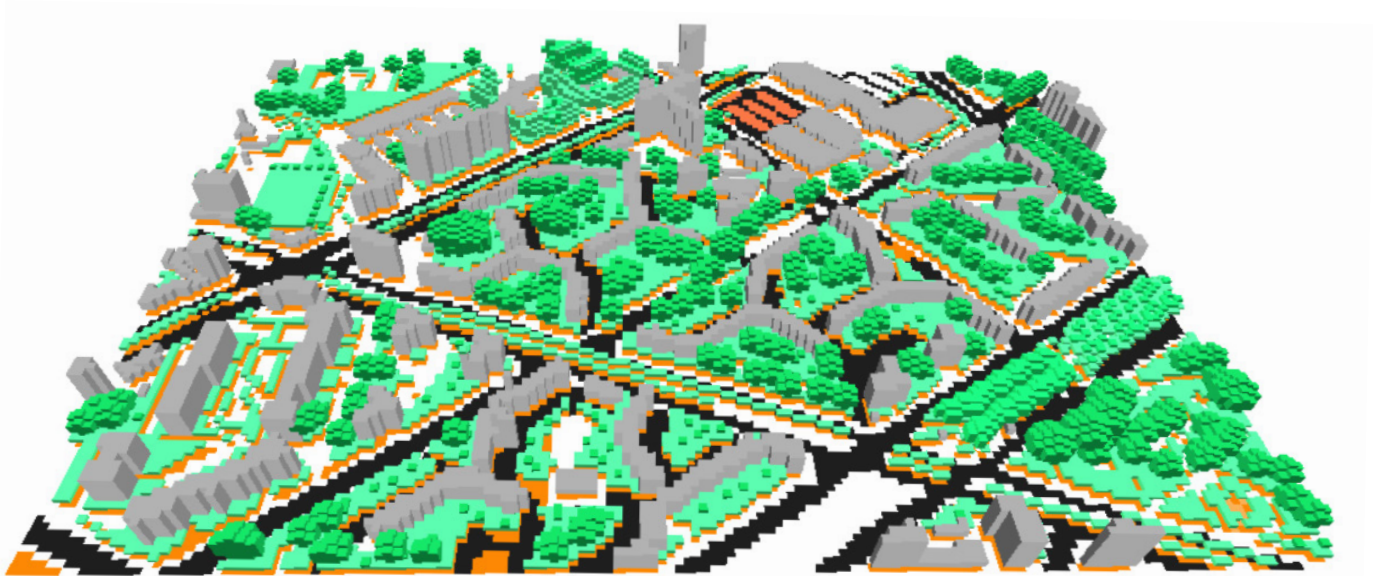


Figure 116. 3D model of Le Vallette case study. (Exported from ENVI-met)

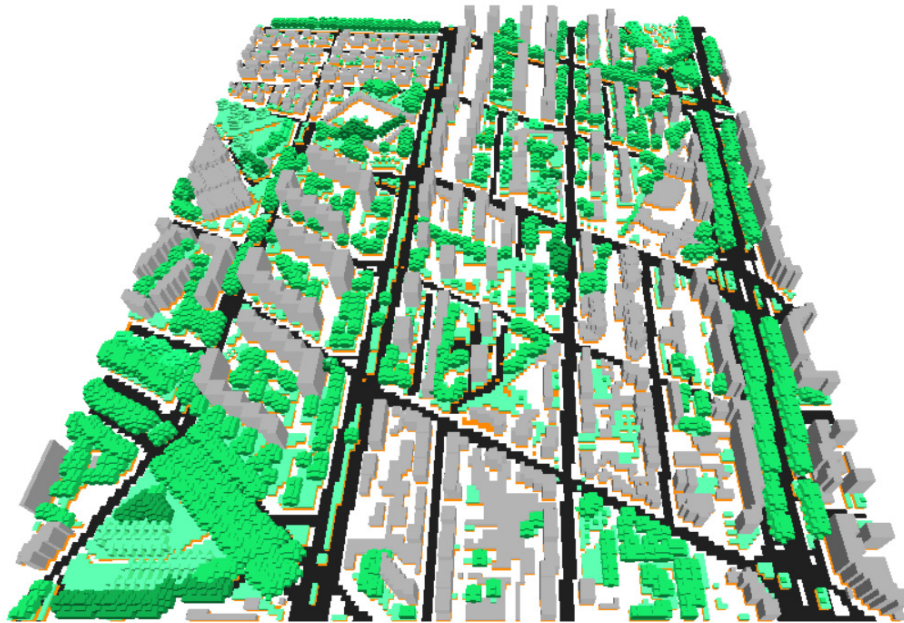


Figure 117. 3D model of Mirafiori Nord case study. (Exported from ENVI-met)



Figure 118. 2D plan illustrating building and vegetation presence in Mirafiori Nord case study. (Exported from ENVI-met)



Figure 119. 2D plan illustrating the material distribution in Mirafiori Nord case study. (Exported from ENVI-met)



Figure 120. 2D plan illustrating building and vegetation presence in Mirafiori Sud case study. (Exported from ENVI-met)

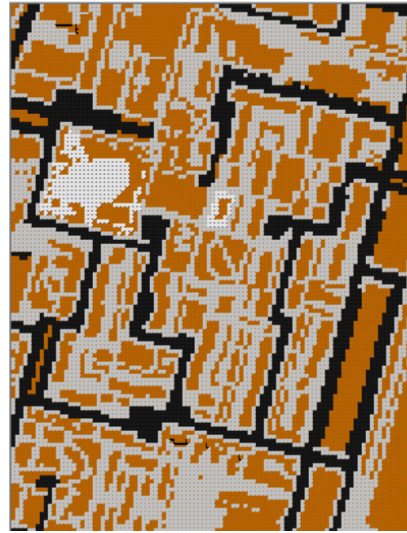


Figure 121. 2D plan illustrating the material distribution in Mirafiori Sud case study. (Exported from ENVI-met)

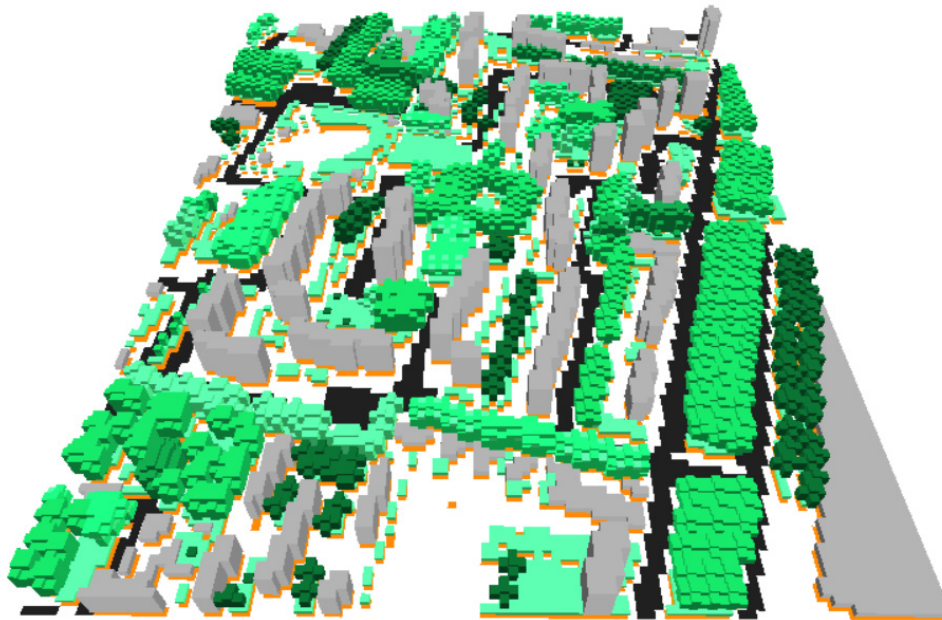


Figure 122. 3D model of Mirafiori Sud case study. (Exported from ENVI-met)

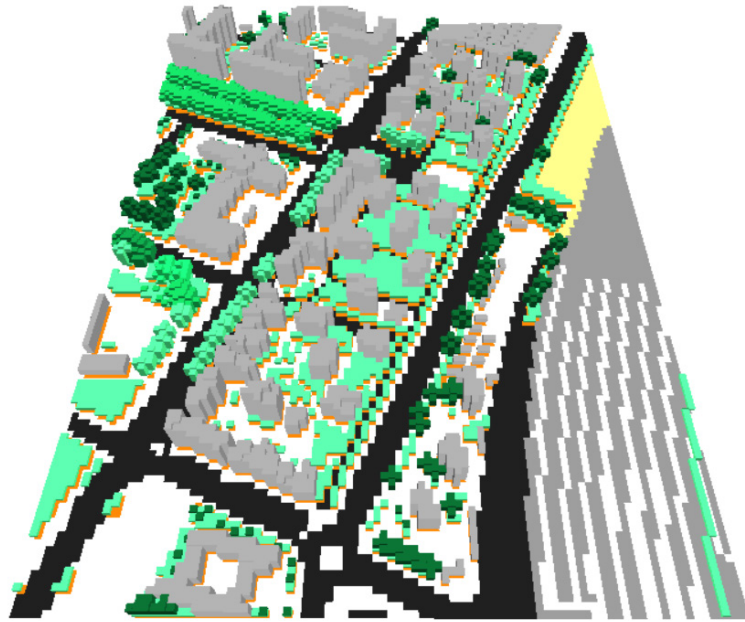


Figure 123. 3D model of Ex-Mercati Generali case study. (Exported from ENVI-met)



Figure 124. 2D plan illustrating building and vegetation presence in Ex-Mercati Generali case study. (Exported from ENVI-met)

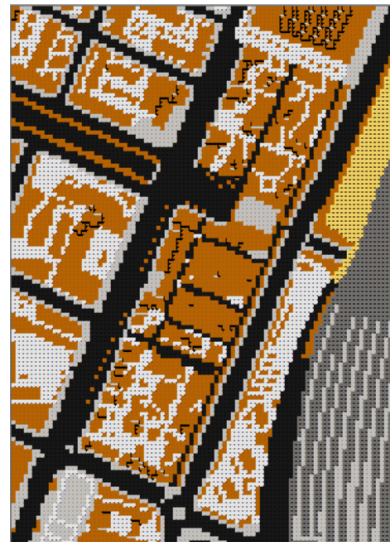


Figure 125. 2D plan illustrating the material distribution in Ex-Mercati Generali case study. (Exported from ENVI-met)

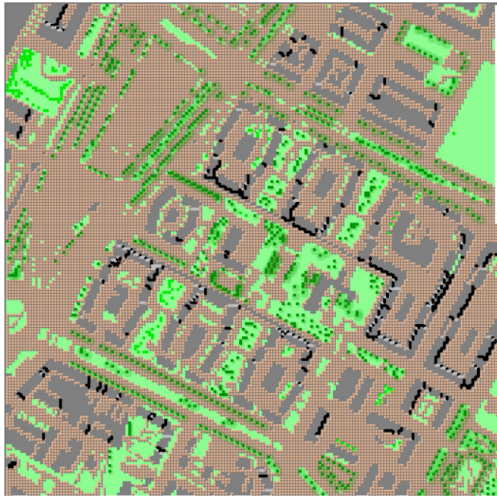


Figure 126. 2D plan illustrating building and vegetation presence in Lingotto case study. (Exported from ENVI-met)

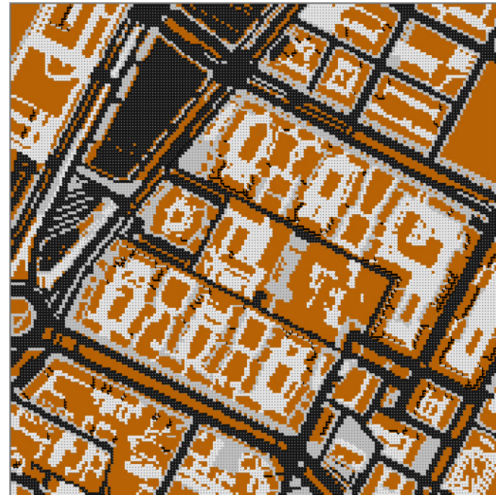


Figure 127. 2D plan illustrating the material distribution in Lingotto case study. (Exported from ENVI-met)

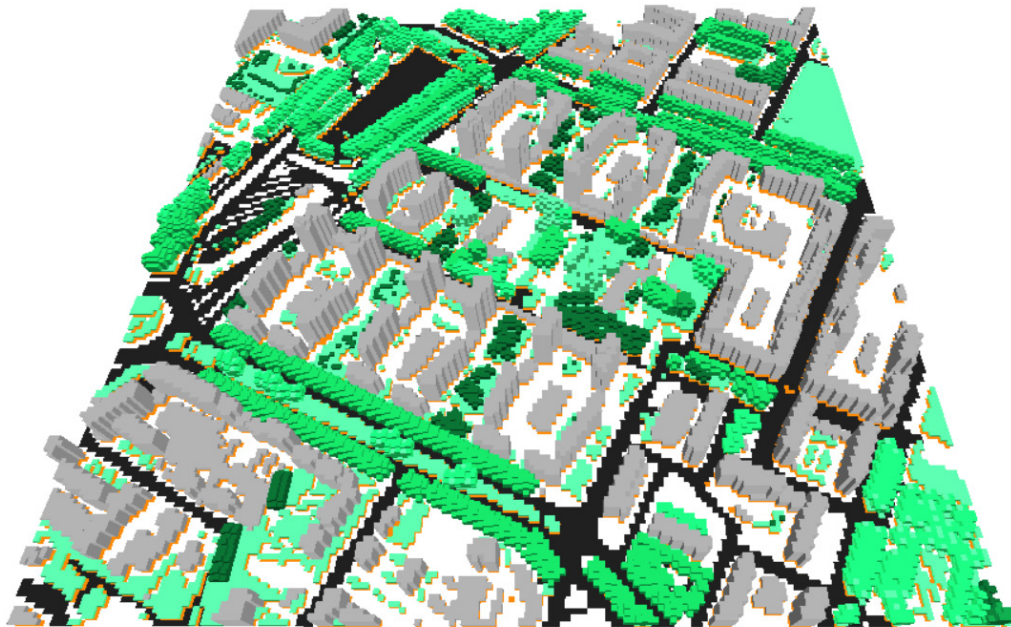
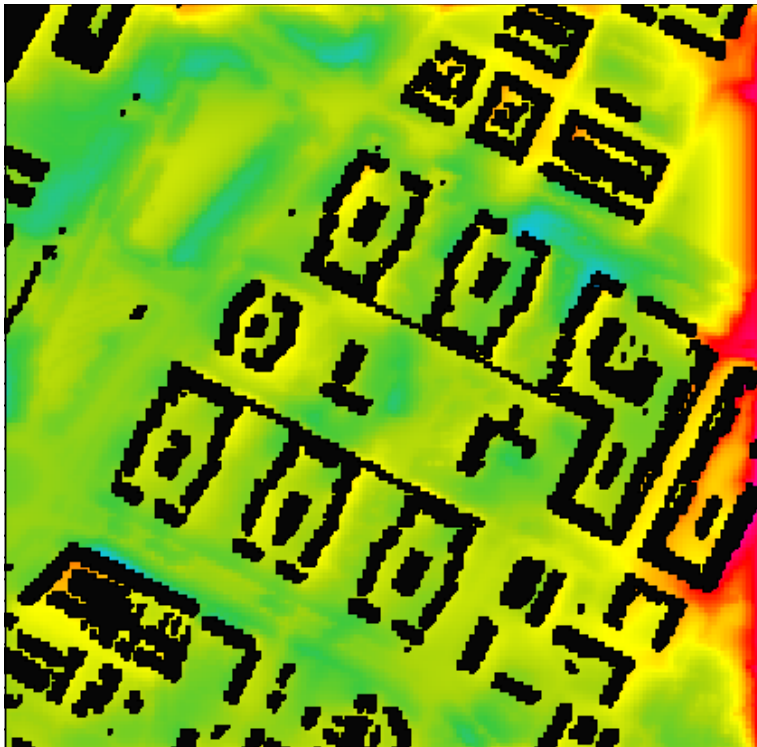
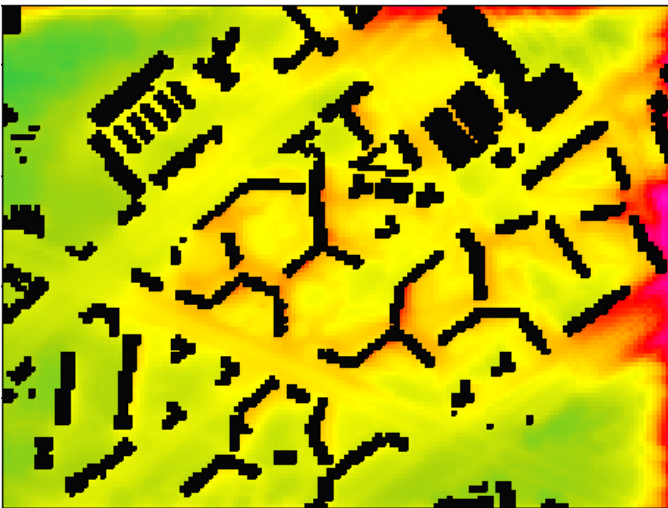


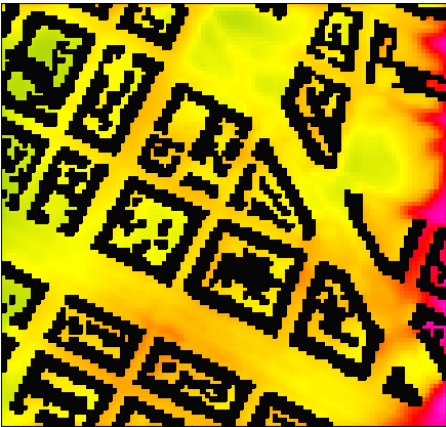
Figure 128. 3D model of Lingotto case study. (Exported from ENVI-met)



lingotto

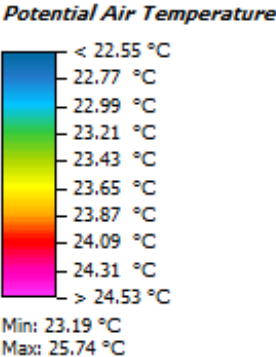


le vallette



san donato

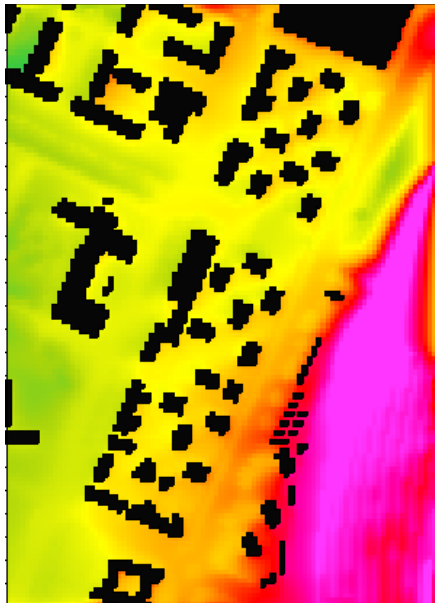
	san donato	vallette	mirafiori nord	mirafiori sud	ex-mercati generali	lingotto
max at 9	22.22	22.15	22.45	22.02	20.42	22.21
min at 9	21.33	21.19	21.2	20.98	19.25	19.09
max at 12	24.42	24.37	24.43	24.29	25.74	24.41
min at 12	23.45	23.22	23.26	22.94	23.19	22.57
max at 15	26.51	26.41	26.52	26.4	27.12	26.45
min at 15	25.05	24.82	24.65	24.45	24.89	24.28
max at 18	25.92	25.92	25.82	25.93	26.46	25.97
min at 18	25.32	25.05	24.96	24.65	25.07	24.24



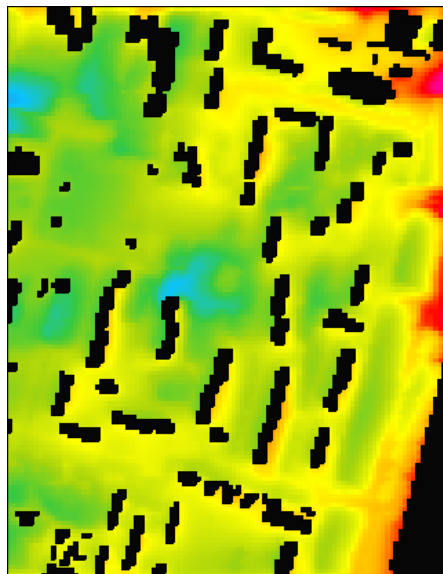
Potential Air Temperature

on 19/07/2020 at 12:00
position of view plane: 5m (k=6)

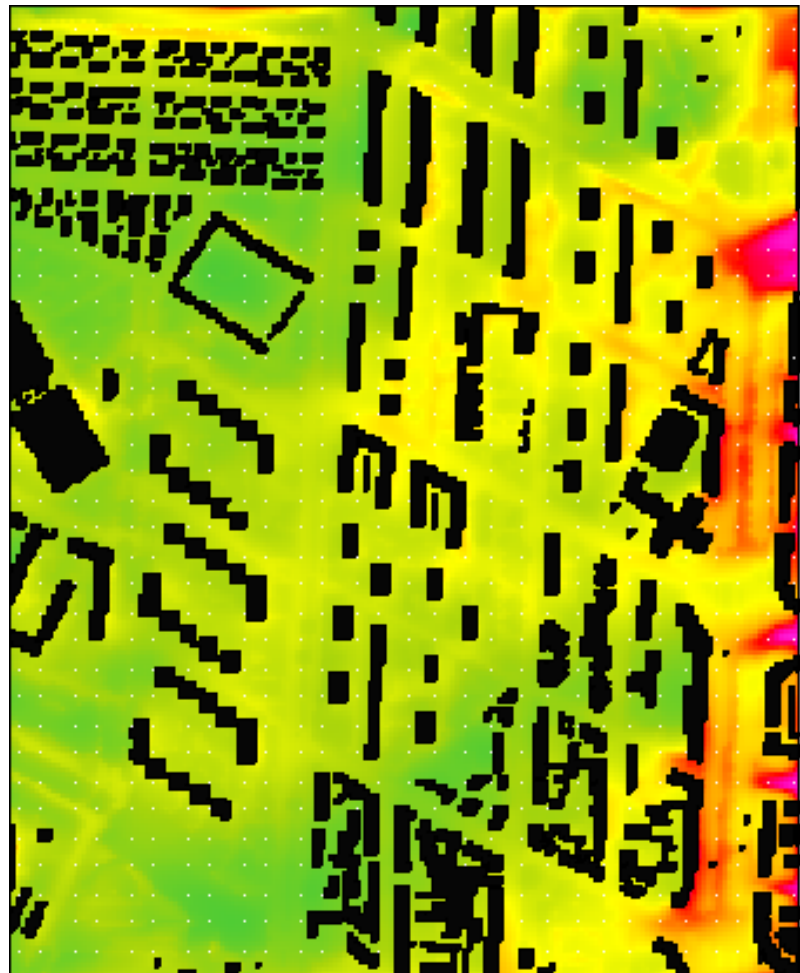
Figure 129. Simulation outputs for potential air temperature
on 19/07/2020 at 12:00. (Exported from ENVI-met)



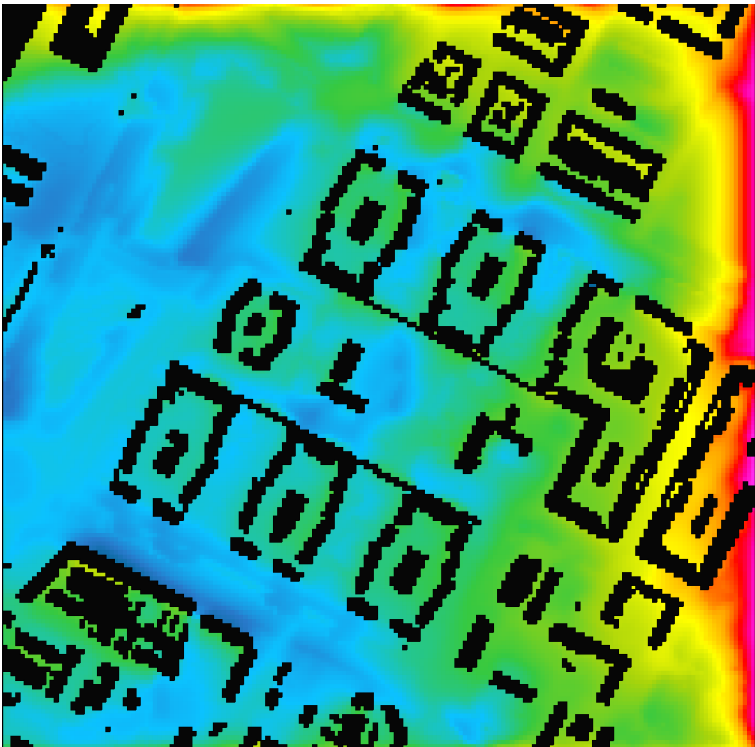
ex-mercati
generali



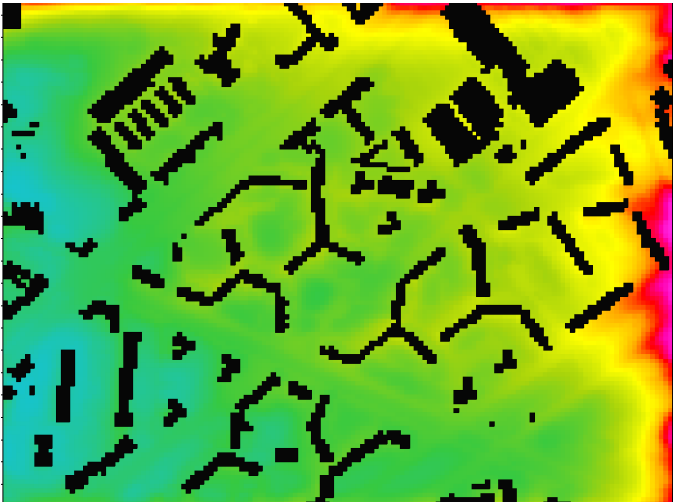
mirafiori sud



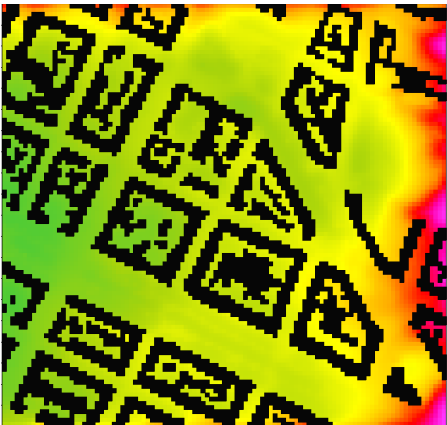
mirafiori nord



lingotto

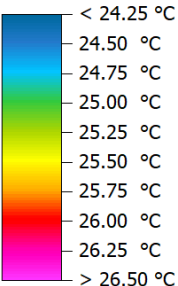


le vallette



san donato

Potential Air Temperature

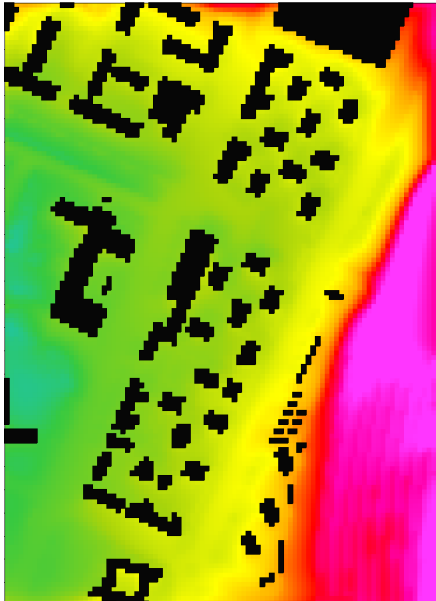


	san donato	vallette	mirafiori nord	mirafiori sud	ex-mercati generali	lingotto
max at 9	22.22	22.15	22.45	22.02	20.42	22.21
min at 9	21.33	21.19	21.2	20.98	19.25	19.09
max at 12	24.42	24.37	24.43	24.29	25.74	24.41
min at 12	23.45	23.22	23.26	22.94	23.19	22.57
max at 15	26.51	26.41	26.52	26.4	27.12	26.45
min at 15	25.05	24.82	24.65	24.45	24.89	24.28
max at 18	25.92	25.92	25.82	25.93	26.46	25.97
min at 18	25.32	25.05	24.96	24.65	25.07	24.24

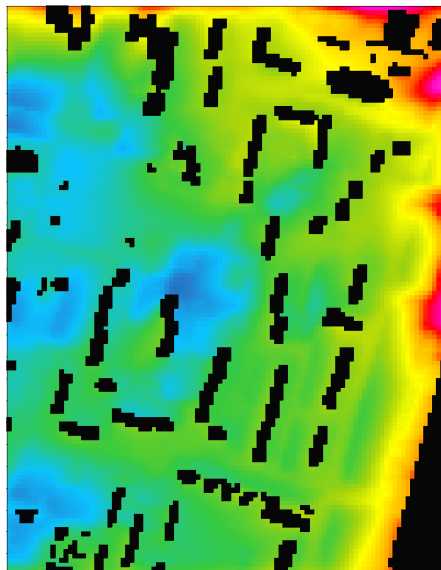
Potential Air Temperature

on 19/07/2020 at 15:00
position of view plane: 5m (k=6)

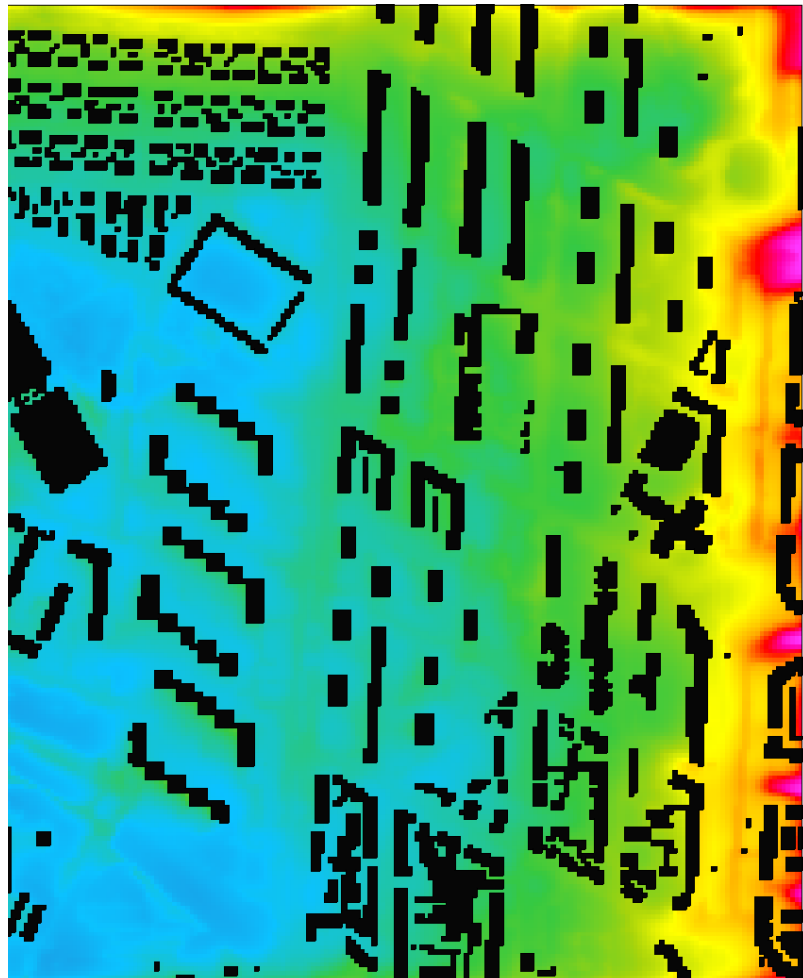
Figure 130. Simulation outputs for potential air temperature
on 19/07/2020 at 15:00. (Exported from ENVI-met)



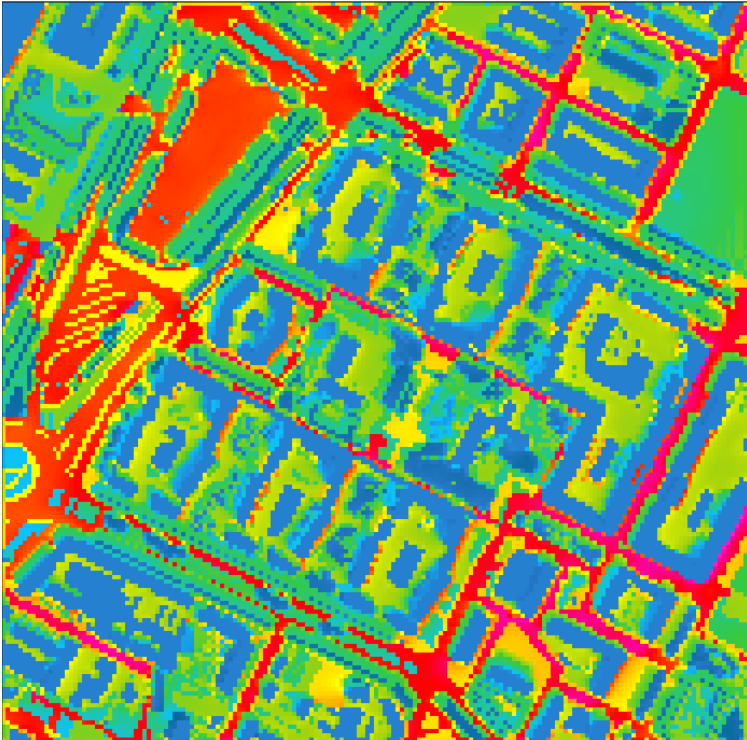
ex-mercati
generali



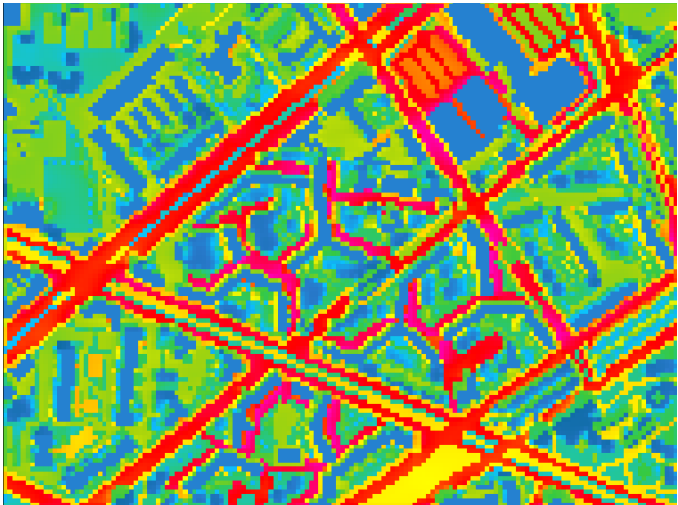
mirafiori sud



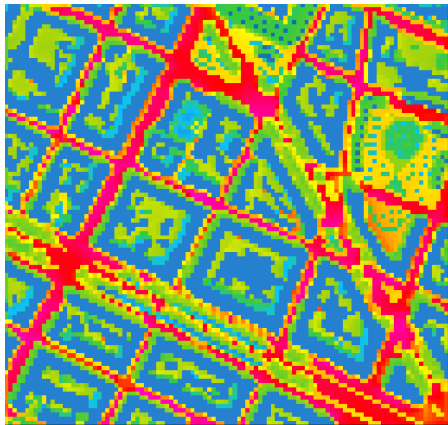
mirafiori nord



lingotto

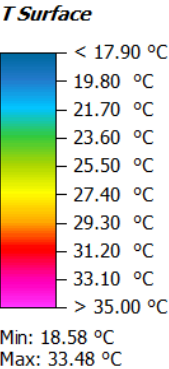


le vallette



san donato

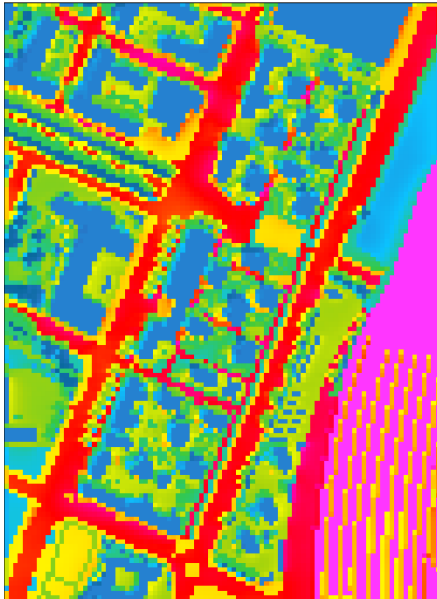
	san donato	vallette	mirafiori nord	mirafiori sud	ex-mercati generali	lingotto
max. at 9h	29.36	29.96	28.42	30.58	32.92	30.84
min. at 9h	17.34	17.34	17.4	16.23	16.36	16.07
max. at 12h	33.48	33.49	33.11	33.52	44.47	34.13
min. at 12h	18.58	18.43	18.38	17.97	18.03	17.98
max. at 15h	34.84	34.18	34.47	33.89	46.61	34.7
min. at 15h	19.57	19.36	19.1	18.88	18.9	18.79
max. at 18h	32.88	31.27	31.54	31.15	38.54	32.91
min. at 18h	19.29	19.26	19.19	18.83	18.99	18.74



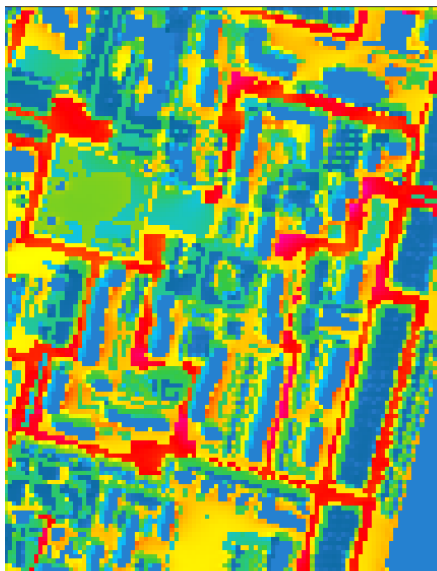
Surface Temperature

on 19/07/2020 at 12:00
position of view plane: 5m (k=0)

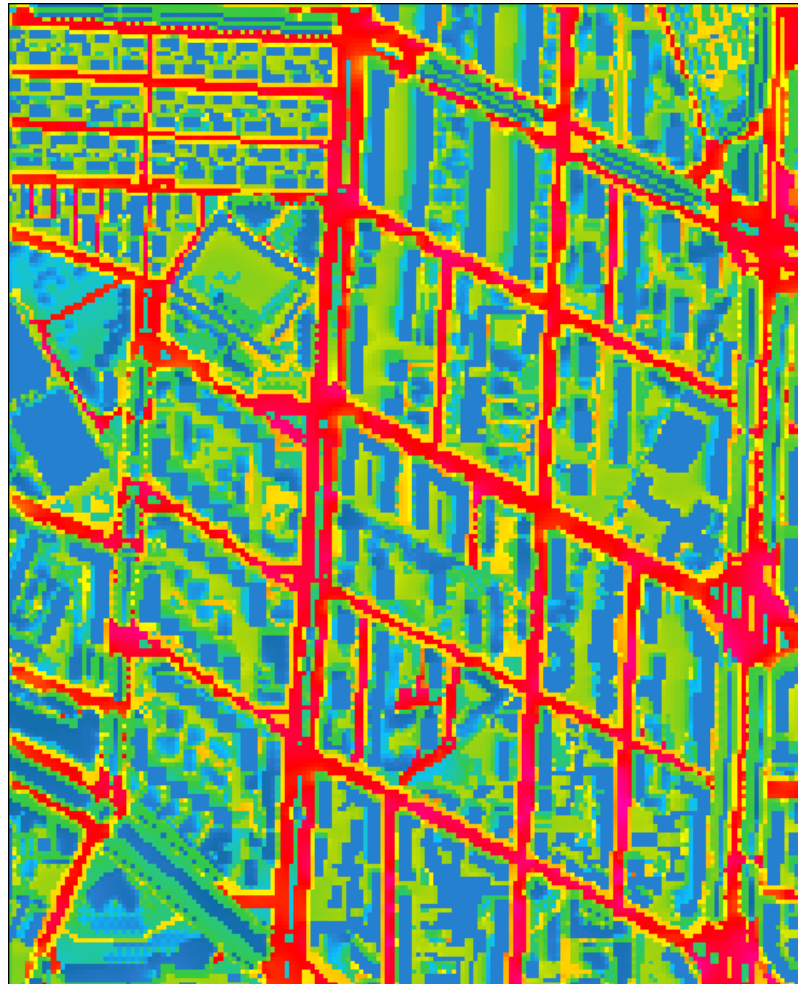
Figure 131. Simulation outputs for surface temperature
on 19/07/2020 at 12:00. (Exported from ENVI-met)



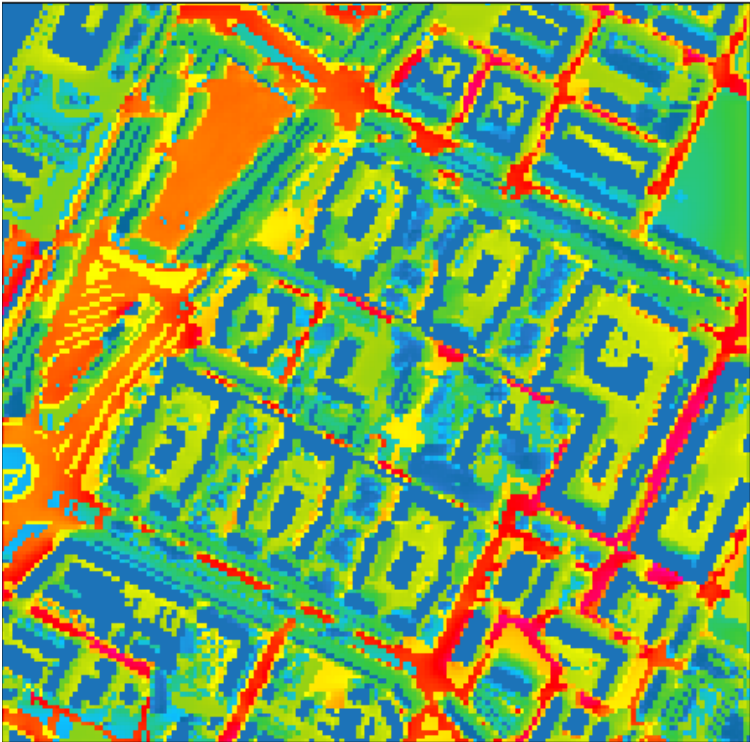
**ex-mercati
generali**



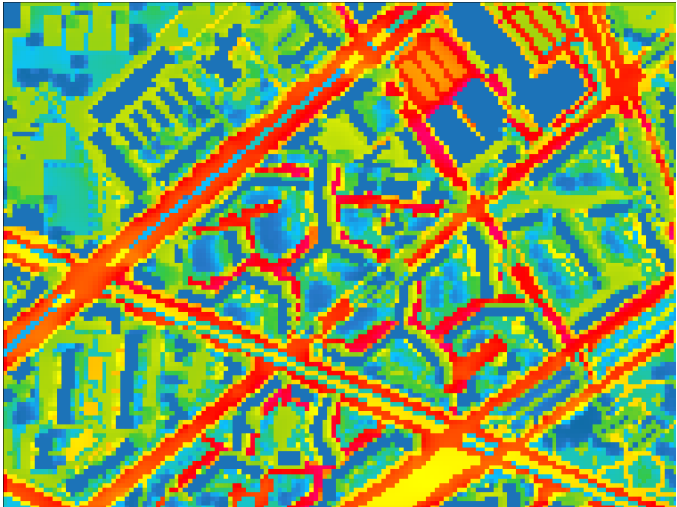
mirafiori sud



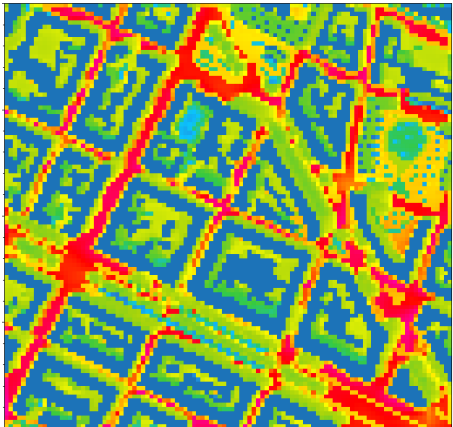
mirafiori nord



lingotto

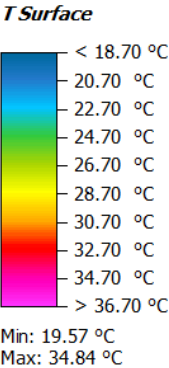


le vallette



san donato

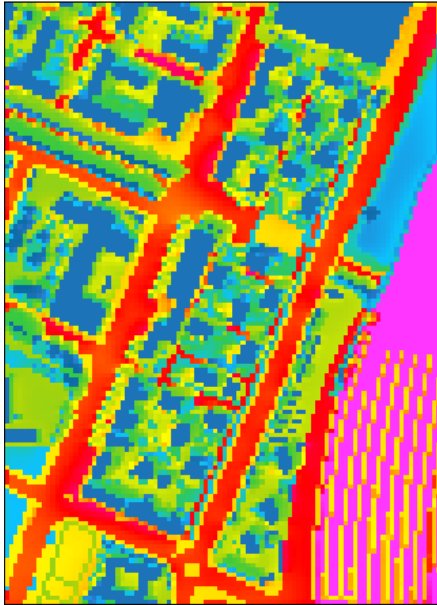
	san donato	vallette	mirafiori nord	mirafiori sud	ex-mercati generali	lingotto
max. at 9h	29.36	29.96	28.42	30.58	32.92	30.84
min. at 9h	17.34	17.34	17.4	16.23	16.36	16.07
max. at 12h	33.48	33.49	33.11	33.52	44.47	34.13
min. at 12h	18.58	18.43	18.38	17.97	18.03	17.98
max. at 15h	34.84	34.18	34.47	33.89	46.61	34.7
min. at 15h	19.57	19.36	19.1	18.88	18.9	18.79
max. at 18h	32.88	31.27	31.54	31.15	38.54	32.91
min. at 18h	19.29	19.26	19.19	18.83	18.99	18.74



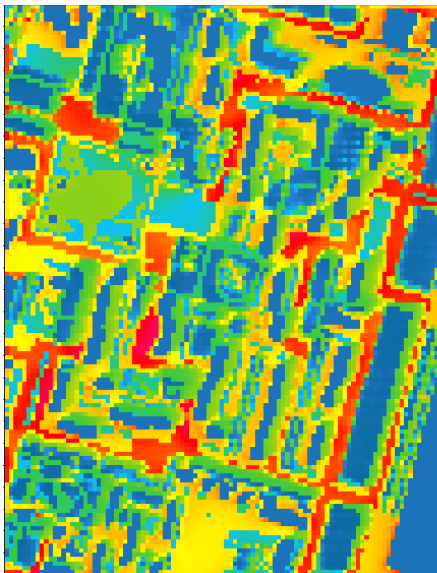
Surface Temperature

on 19/07/2020 at 15:00
position of view plane: 5m (k=0)

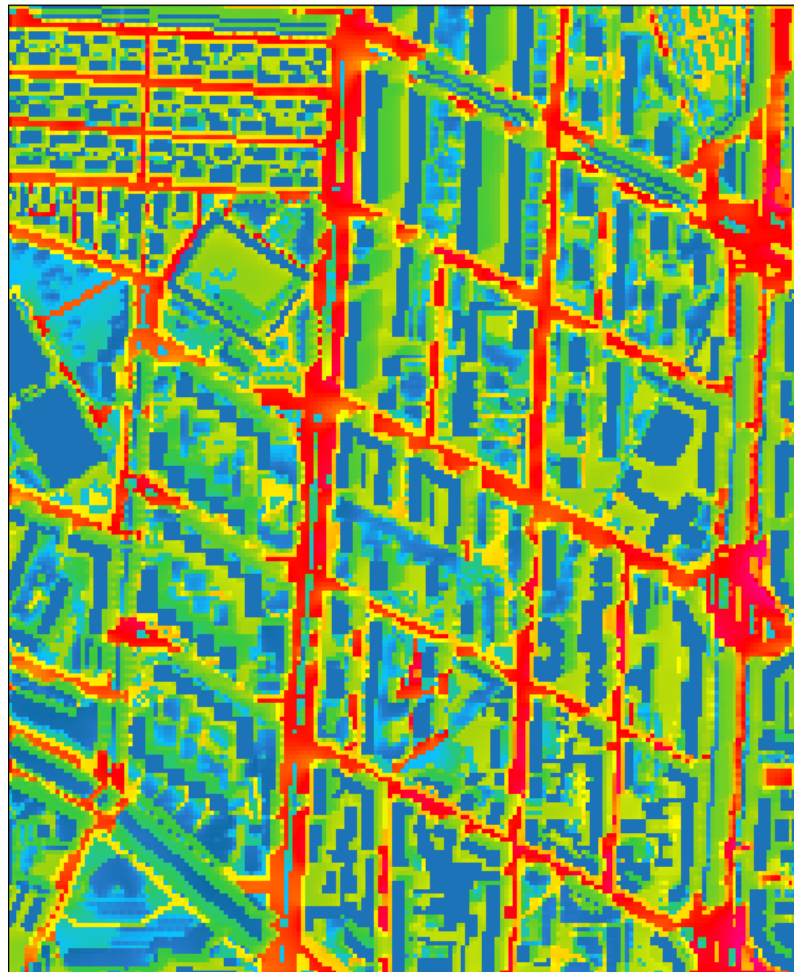
Figure 132. Simulation outputs for surface temperature
on 19/07/2020 at 15:00. (Exported from ENVI-met)



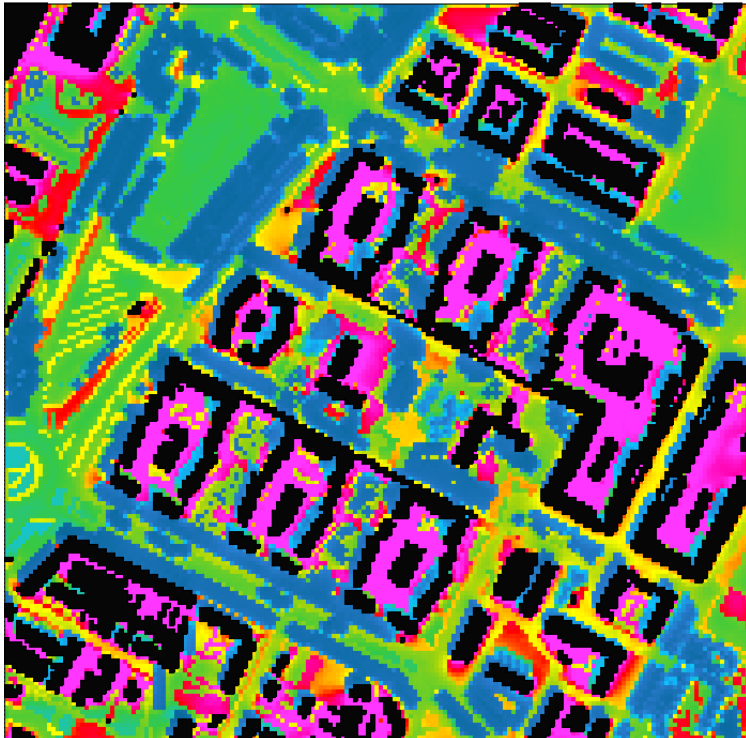
**ex-mercati
generali**



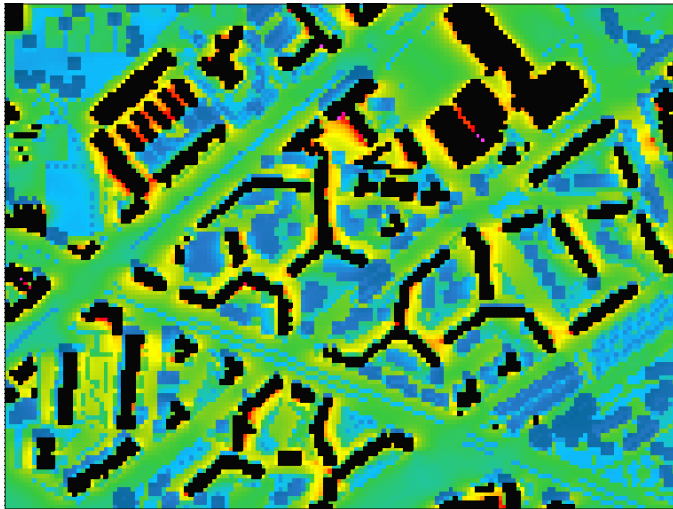
mirafiori sud



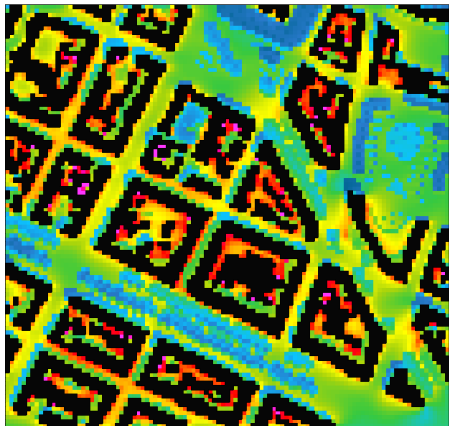
mirafiori nord



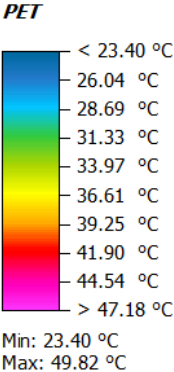
lingotto



le vallette



san donato

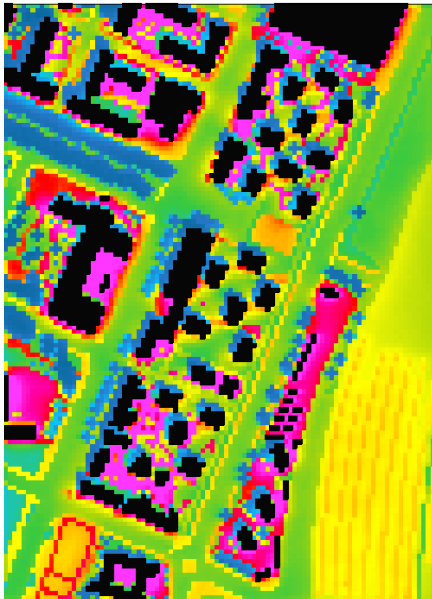


	san donato	vallette	mirafiori nord	mirafiori sud	ex-mercati generali	lingotto
max. at 9h	40.1	38.34	39.95	48.42	57.87	58.24
min. at 9h	18.8	18.4	18.2	16.2	16.6	16.2
max. at 12h	49.82	48.26	48.26	53.58	64.87	68.09
min. at 12h	23.4	22.8	22.8	18.66	18.8	18.69
max. at 15h	52.46	50.24	51.08	56.39	66.33	70.62
min. at 15h	25.68	27.48	23.8	20.29	20.42	20.2
max. at 18h	40.08	39.41	39.95	50.46	54.75	55.88
min. at 18h	21.8	21.4	21.21	20	19.4	19.81

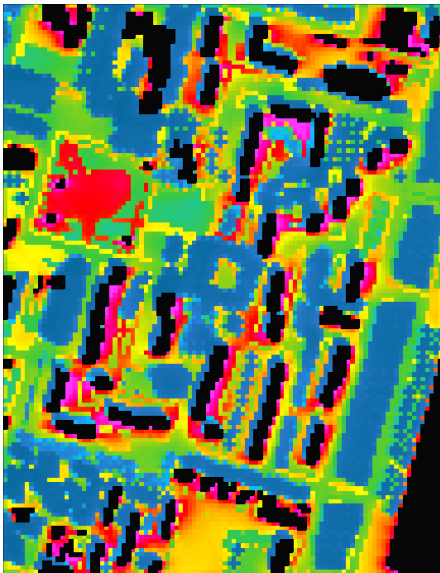
PET

on 19/07/2020 at 12:00
position of view plane: 5m (k=6)

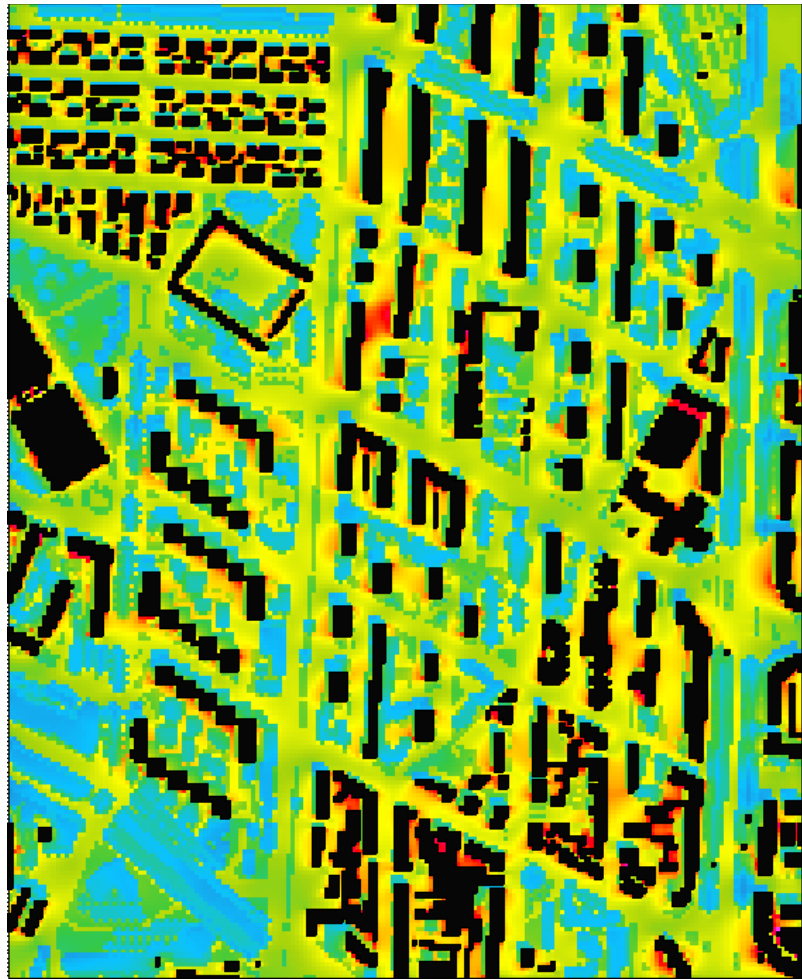
Figure 133. Simulation outputs for PET on 19/07/2020
at 12:00. (Exported from ENVI-met)



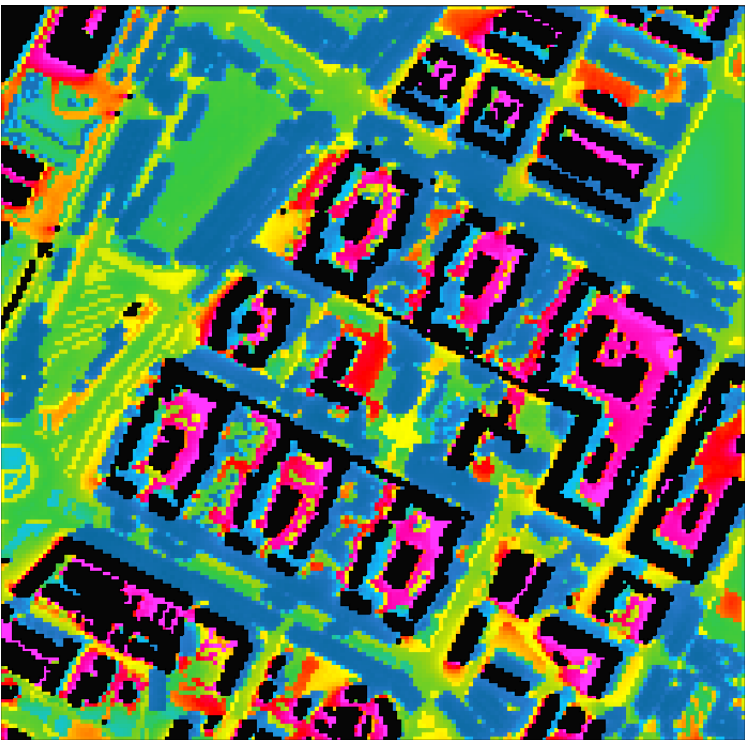
ex-mercati
generali



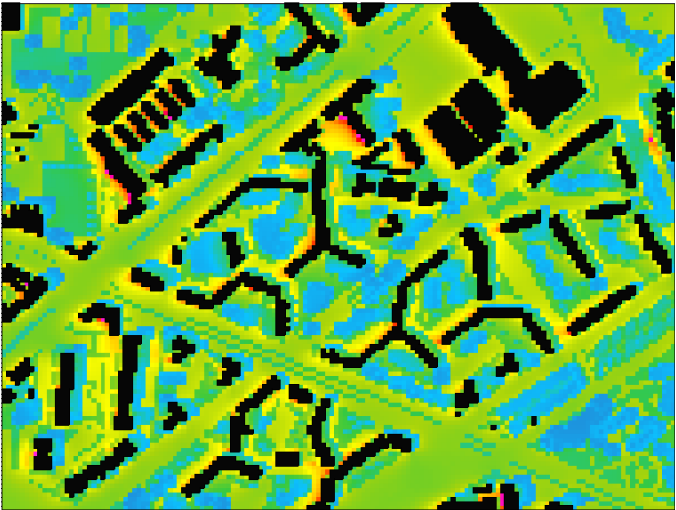
mirafiori sud



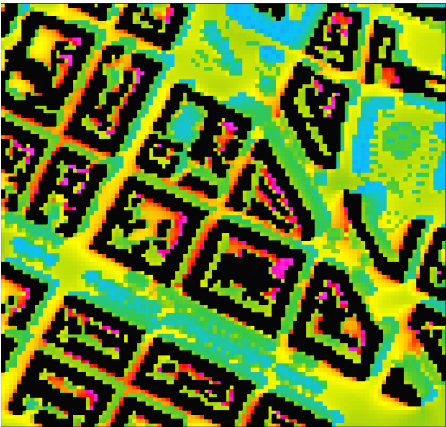
mirafiori nord



lingotto



le vallette



san donato

	san donato	vallette	mirafiori nord	mirafiori sud	ex-mercati generali	lingotto
max. at 9h	40.1	38.34	39.95	48.42	57.87	58.24
min. at 9h	18.8	18.4	18.2	16.2	16.6	16.2
max. at 12h	49.82	48.26	48.26	53.58	64.87	68.09
min. at 12h	23.4	22.8	22.8	18.66	18.8	18.69
max. at 15h	52.46	50.24	51.08	56.39	66.33	70.62
min. at 15h	25.68	27.48	23.8	20.29	20.42	20.2
max. at 18h	40.08	39.41	39.95	50.46	54.75	55.88
min. at 18h	21.8	21.4	21.21	20	19.4	19.81

PET

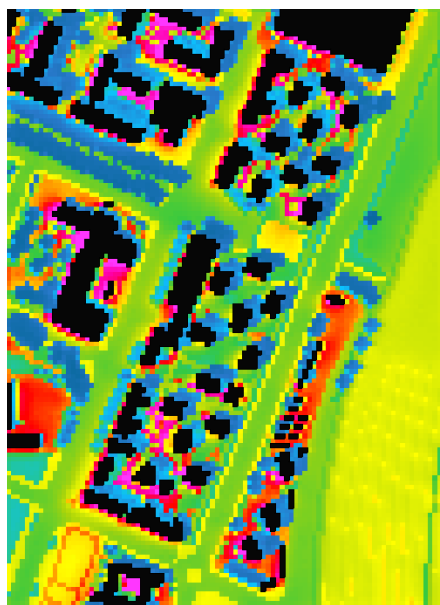
< 20.00 °C
23.50 °C
27.00 °C
30.50 °C
34.00 °C
37.50 °C
41.00 °C
44.50 °C
48.00 °C
> 51.50 °C

Min: 25.68 °C
Max: 52.46 °C

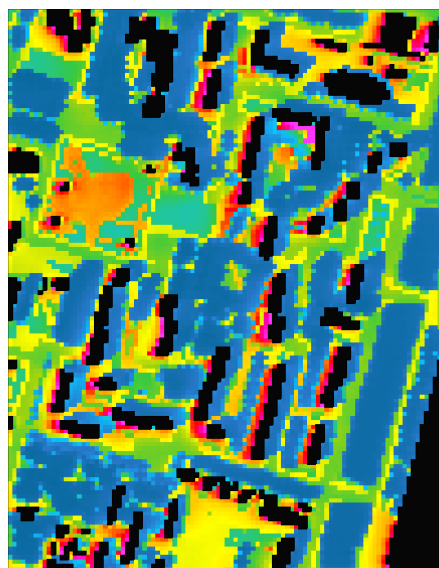
PET

on 19/07/2020 at 15:00
position of view plane: 5m (k=6)

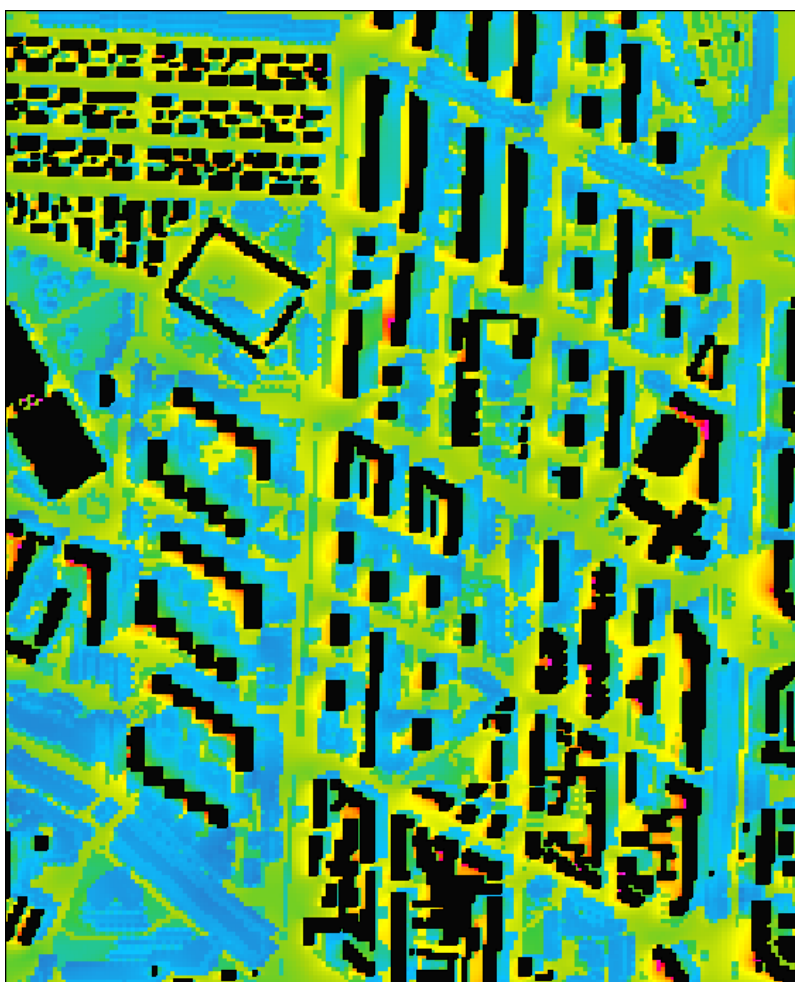
Figure 134. Simulation outputs for PET on 19/07/2020 at 15:00. (Exported from ENVI-met)



ex-mercati
generali



mirafiori sud



mirafiori nord



lingotto

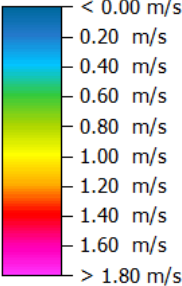


le vallette



san donato

Wind Speed



Min: 0.00 m/s
Max: 1.67 m/s

	san donato	vallette	mirafiori nord	mirafiori sud	ex-mercati generali	lingotto
max. at 9h	1.94	1.83	2.51	1.73	1.61	1.78
min. at 9h	0	0	0	0	0	0
max. at 12h	1.91	1.83	2.45	1.74	1.58	1.68
min. at 12h	0	0	0	0	0	0
max. at 15h	1.84	1.77	2.35	1.68	1.54	1.59
min. at 15h	0	0	0	0.01	0	0
max. at 18h	1.8	1.75	2.31	1.66	1.52	1.56
min. at 18h	0	0	0	0.01	0	0

Wind Speed

on 19/07/2020 at 12:00
position of view plane: 5m (k=6)

Figure 135. Simulation outputs for wind speed on 19/07/2020 at 12:00. (Exported from ENVI-met)



ex-mercati
generali



mirafiori sud



mirafiori nord



lingotto

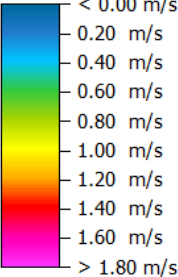


le vallette



san donato

Wind Speed



Min: 0.00 m/s
Max: 1.84 m/s

	san donato	vallette	mirafiori nord	mirafiori sud	ex-mercati generali	lingotto
max. at 9h	1.94	1.83	2.51	1.73	1.61	1.78
min. at 9h	0	0	0	0	0	0
max. at 12h	1.91	1.83	2.45	1.74	1.58	1.68
min. at 12h	0	0	0	0	0	0
max. at 15h	1.84	1.77	2.35	1.68	1.54	1.59
min. at 15h	0	0	0	0.01	0	0
max. at 18h	1.8	1.75	2.31	1.66	1.52	1.56
min. at 18h	0	0	0	0.01	0	0

Wind Speed

on 19/07/2020 at 15:00
position of view plane: 5m (k=6)

Figure 136. Simulation outputs for wind speed on 19/07/2020 at 15:00. (Exported from ENVI-met)



ex-mercati
generali



mirafiori sud



mirafiori nord

5.2

Discussion

5.2.1. Urban structure

When the outputs of the San Donato simulation were examined, the cool conditions within the continuous-regular block became apparent, which could be linked to the self-shading outcome of its density. Although the discontinuous-regular block to the north of it has a remarkable presence of vegetation (both vertical and horizontal) and openings among its borders, the continuous-regular block remains cooler at noon. Furthermore, the southern part of the area seems to hold more thermal stress than the eastern part.

San Donato is the only site that does not show an evidence of temperature that is within the blue (the coolest) zone of the legend, indicating that the overall potential air temperature of the whole site has stayed higher compared to the other sites.

The potential air temperature output of the second case study of Mirafiori Nord illustrates that the gap between linear continuous buildings trap more heat at 15:00, compared to those that have a discontinuous linear urban structure. Similarly, PET outputs of the same case study

demonstrate that an interrupted urban canyon creates more uncomfortable conditions compared to those of a continuous urban canyon, although this difference is not as evident in the results of surface and potential air temperature. It is important to highlight that this consequence is valid when the buildings that are alongside the urban canyon are high, in this case 30-storey. At the northwest end of the Mirafiori Nord modelling area, the densely built area (namely Citta Giardino) only cools off towards south, where it faces the first case study of Mirafiori Nord. The heat is still trapped on the north side due to the compact organization of masses.

Moreover, PET outputs for Lingotto case study indicate that the highest values for all the hours (9:00, 12:00, 15:00 and 18:00) have been recorded within this case study, in comparison to the others. These results are associated with the insufficient density of the block. The PET outputs at 15:00 illustrate that the courtyard is only slightly shaded by the building, confirming the insufficiency of the block density. However, these results are in contradiction with the ones concerning the potential air temperature, as potential air temperature results for the same area illustrates better conditions, not only compared to its PET results, but also when compared to the potential air temperature outputs of the other case studies. Thus, it could be said that the potential air temperature is not dominant in defining the comfort level in this case.

When the interconnections between the wind and urban geometry were examined, it was realized that in several cases, the wind direction has been blocked by one side of a linear building block, creating uncomfortable conditions for the other side of the block. This phenomena is mostly visible in

Mirafiori Nord case study where one can observe the behavior of wind when it flows through an urban canyon that is parallel to the wind direction (providing comfortable conditions) and the contrary behavior when it is not parallel (causing uncomfortable conditions due to insufficient air flow).

5.2.2. Vegetation

The overall results indicate that the impact of vertical vegetation is significant when the trees are in groups or aligned along an axis. (e.g. Corso Regina Margherita in San Donato case study). The urban canyons and streets that are followed by regular and dense placement of trees provided better conditions for potential air temperature (through evapotranspiration), surface temperature (through shading) and PET. On the other hand, the locations where the trees are not in groups (scattered or placed singularly) benefit from the shading effect of the tree locally (which results in local surface temperature improvements), however, significant improvements regarding potential air temperature were not recorded in these configurations.

In particular, the outputs of the Mirafiori Sud case study demonstrate the impact of vegetation on urban microclimate parameters clearly. This case study hosts the lowest values of PET (implying at higher comfort) around the residential areas, which could be linked to the use of vegetation through the public spaces that are surrounded by long and tall residential buildings. These buildings serve as protection from the sun as they provide shading towards the public spaces that they surround. In this case, uncomfortable conditions are concentrated on

the plaza (due to the use of concrete through the whole square) and towards the north of the site where a lack of vegetation and disorganization of building blocks can be observed.

5.2.3. Materials

When considering the case study area of Le Vallette, the outputs illustrate that the air temperature is higher in the inner parts of the site at 12:00, identifying where the thermal mass is collected. Although this area includes an immense amount of vertical greenery, the borders of the buildings have more thermal stress due to the asphalt density. Asphalt, being a low albedo and high emissivity material, absorbs most of the solar radiation that it receives and some of this is converted into heat energy, which causes the asphalt surfaces to feel warm. As a result, higher levels of discomfort are concentrated around the borders of the buildings due to the localized use of asphalt (verified by surface temperature results) and the densely built area towards the north east of the modelling area. It is significant to underline here, that the asphalt ratio in Le Vallette is the same value as the one of the Mirafiori Nord and Mirafiori Sud cases, however, the dense and localized application of this material resulted in warmer conditions. Additionally, according to the results of 15:00, it is possible to observe that the area does not cool off as much as Mirafiori Nord and Mirafiori Sud. The results demonstrate that the area is only cooling off slightly towards the east side.

The case of Ex-Mercati Generali is interesting due to the behaviour of PET value. Despite the presence of the railway and the above-mentioned high potential

air and surface temperature, higher PET values are recorded for the upper and lower parts of Villaggio Olimpico compared to that of the railway zone. This result supports the interpreted outcome indicating that the comfort level is not only depend on the surface temperature and the potential air temperature.

Comparing the outputs of Lingotto and Ex-Mercati Generali, one can simply realize that Ex-Mercati Generali area does not release its thermal stress in the afternoon as much as the area in Lingotto does. The potential air temperature towards the east side of the site in Ex-Mercati Generali reaches the highest value that has been recorded through all the case studies. This is due to the presence of railways in the Ex-Mercati Generali case study area, which are accompanied by pedestrian waiting areas placed in between them, both being low albedo-high emissivity materials. In contrary, more than half of the area in Lingotto (mostly the western part) cools off significantly in the afternoon hours.

5.2.4. Peak points

In addition to the above-mentioned evaluation, the criticalities of each environmental value were analyzed. It has been realized that Mirafiori Sud and Le Vallette have the lowest peak points in most of the cases, whereas Lingotto and Ex-Mercati Generali cases have been recorded to have the highest temperatures.

The maximum and minimum of these variables (potential air temperature, surface temperature, PET) are as follows:

Maximum Potential Air Temperature (°C) at 12:00: Lowest 24.29 (*Mirafiori Sud*), Highest 25.74 (*Ex-Mercati Generali*), Difference: 1.45

Maximum Potential Air Temperature (°C) at 15:00: Lowest 26.4 (*Mirafiori Sud*), Highest 27.12 (*Ex-Mercati Generali*), Difference: 0.72

Maximum Surface Temperature (°C) at 12:00: Lowest 33.11 (*Mirafiori Nord*), Highest 44.47 (*Ex-Mercati Generali*), Difference: 11.36

Maximum Surface Temperature (°C) at 15:00: Lowest 33.89 (*Mirafiori Sud*), Highest 46.61 (*Ex-Mercati Generali*), Difference: 12.72

Maximum PET (°C) at 12:00: Lowest 48.26 (*Le Vallette & Mirafiori Nord*), Highest 68.09 (*Lingotto*), Difference: 19.83

Maximum PET (°C) at 15:00: Lowest 50.24 (*Le Vallette*), Highest 70.62 (*Lingotto*), Difference: 20.38

5.2.5. Behavior of environmental variables for selected points

The following pages provide information on the behavior of PET, surface temperature and potential air temperature on particular points that have been chosen from the case study areas. These points are selected to have the worst conditions of PET in each case study area. The points in the first table have been chosen as the worst conditions in residential public spaces, whereas the points represent the worst conditions for urban canyons for the second (NW-SE orientation) and the third (NE-SW orientation) tables. After the comparison process, it has been noted that the potential air temperature is the

environmental variable that fluctuates the least among different locations in the city, as the graphs for the same hour of the day illustrate similar trends in different neighborhoods. When the PET and PAT trends were analyzed for the urban canyons with different orientations, the NW-SE oriented urban canyons hosted more uncomfortable conditions for both environmental variables, compared to the NE-SW oriented ones.

For both orientations of streets, if trees are present alongside the road, the PET trend shows a significant drop by up to 21°C immediately after the peak point (e.g. NW-SE oriented street in Lingotto, NE-SW oriented street in Mirafiori Sud) and provide comfortable conditions in the afternoon hours.

In the case of Lingotto, it has been realized that the PET value persists around its peak value for 3 to 5 hours in all three selected points. Additionally, PET value for both urban canyon directions show the highest jump in an hour among all case studies with a difference of up to 26°C.

It has been realized that for most of the case studies, the points selected from the urban canyons have lower levels of comfort in means of PET compared to the points picked from residential public spaces. In contrast, surface temperature trends of the residential public space points illustrate lower trends compared to those of the selected points of urban canyons.

Further observations regarding the trends of potential air temperature, surface temperature and PET can be found in the tables (Table 8, Table 7 and Table 8) in the following pages.

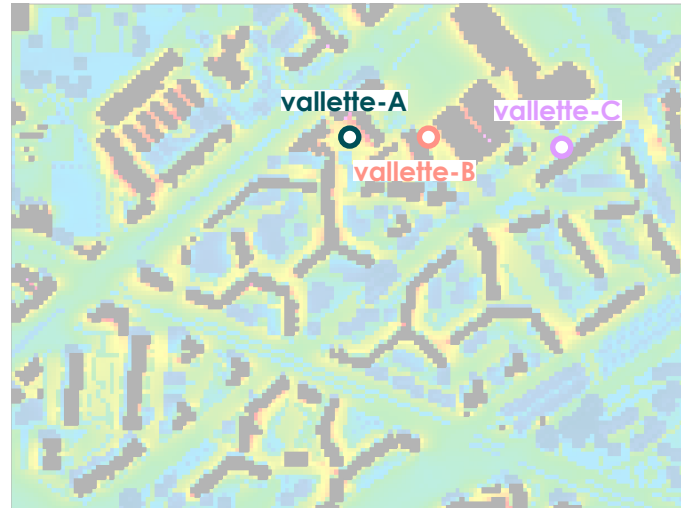
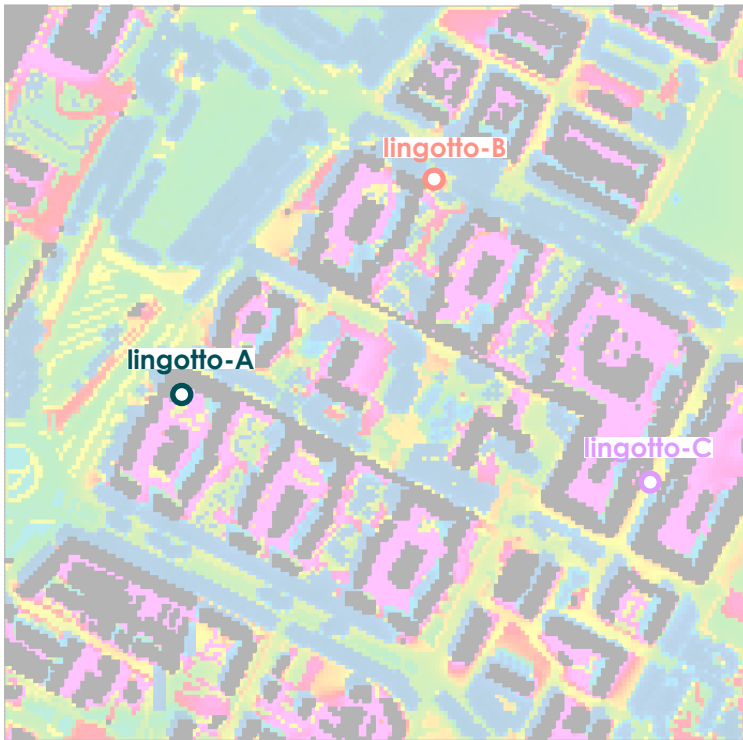
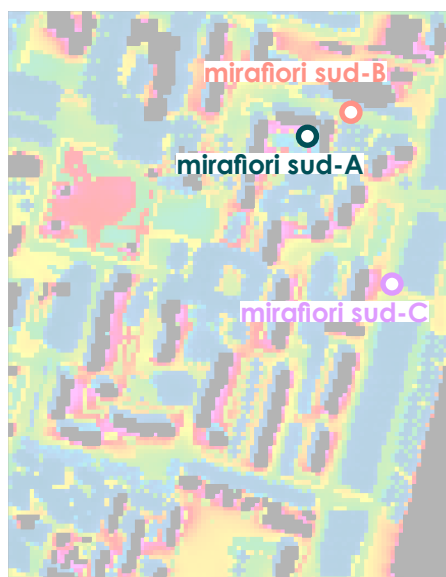
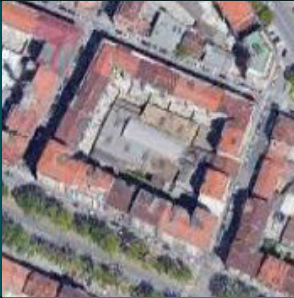

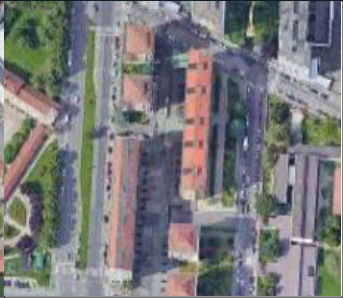
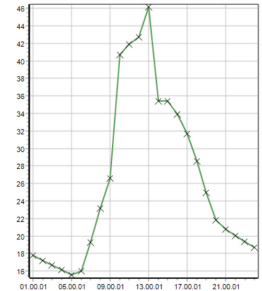
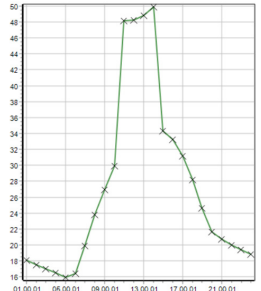
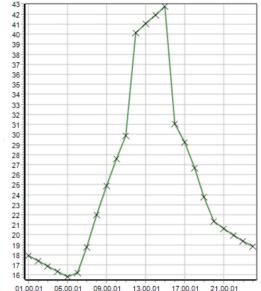
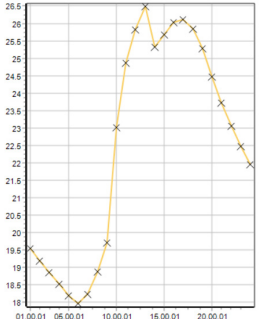
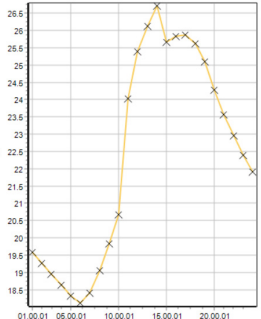
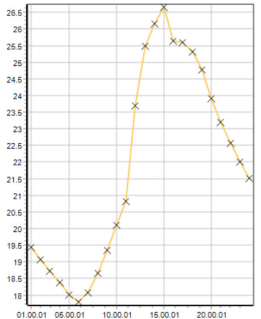
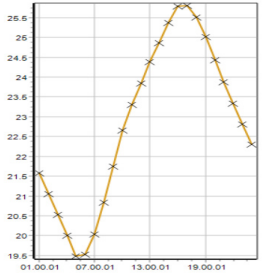
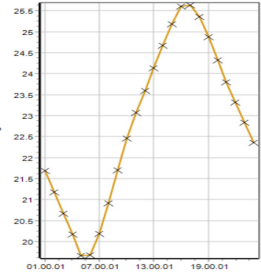
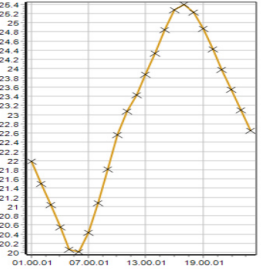


Figure 137. The points with the most unfavorable PET conditions from each case study. (Maps exported from ENVI-met)

- Residential public space (A)
- NW-SE oriented urban canyon (B)
- NE-SW oriented urban canyon (C)



RESIDENTIAL PUBLIC SPACE	san donato	le vallette	mirafiori nord
ortho image of the worst point for PET			
physiological equivalent temperature (PET - °C)	 <p>Major jump of ca. 14°C between 9-10h, peaks at 46°C at 13h, drops by 10°C until 14h</p>	 <p>Major jump of ca. 18°C between 10-11h, peaks at ca. 50°C at 14h, drops by ca. 16°C until 15h</p>	 <p>Major jump of ca. 10°C between 11-12h, peaks at ca. 43°C at 14h, drops by ca. 12°C until 16h</p>
surface temperature (ST - °C)	 <p>Major jump of ca. 4°C between 10-11h, peaks at 28.5°C at 13h, drops by ca. 1.5°C until 14h, rises slightly until 17h and decreases until the end of the day</p>	 <p>Major jump of ca. 3.5°C between 10-11h, peaks at ca. 27°C at 14h, drops by ca. 1°C until 15h, rises slightly until 17h and decreases until the end of the day</p>	 <p>Major jump of ca. 3°C between 11-12h, peaks at ca. 27°C at 15h and decreases until the end of the day</p>
potential air temperature (PAT - °C)	 <p>Lowest values persist around 19.5°C between 5-6h, peak PAT persists around 26°C between 16-17h</p>	 <p>Lowest values persist around 19.5°C between 5-6h, peak PAT persists around 26°C between 16-17h</p>	 <p>Lowest values persist around 20°C between 5-6h, peak PAT at 25.4°C at 17h</p>

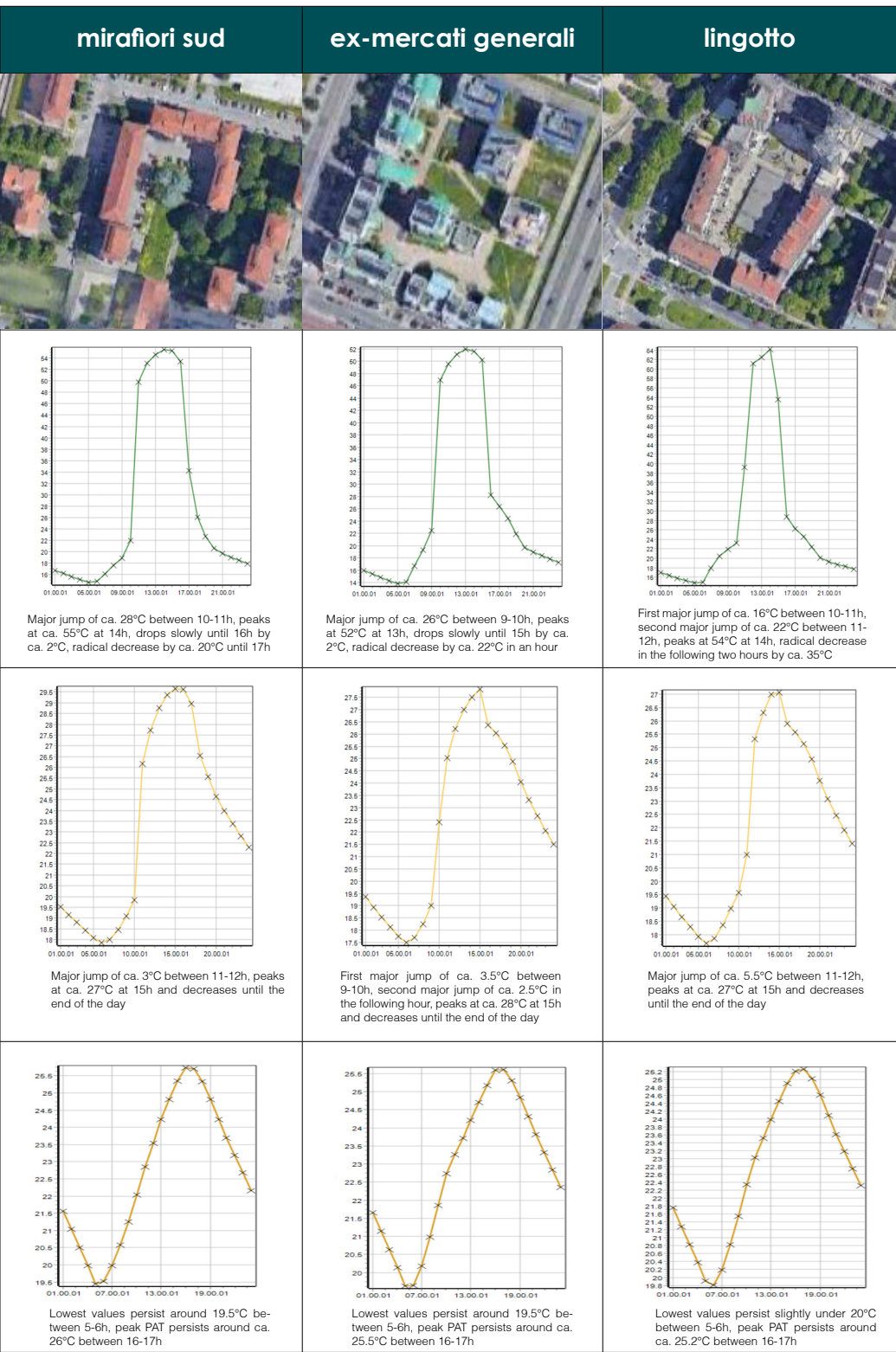


Table 6. Comparison table of PET, PAT and ST on selected points in residential areas. From each case study, the points that have the most unfavorable PET results at 12:00 were selected. (Graphs were exported from ENVI-met, satellite images were exported from Google Earth)

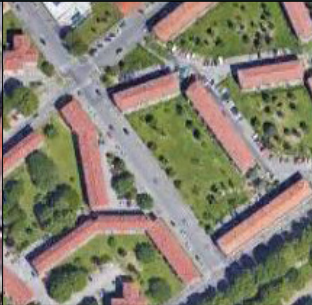
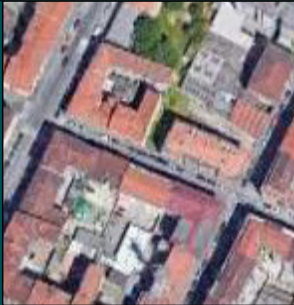
**URBAN CANYONS
(NW-SE)**

san donato

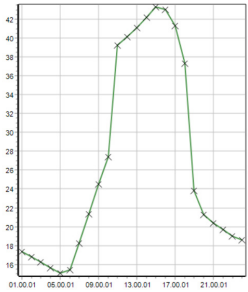
le vallette

mirafiori nord

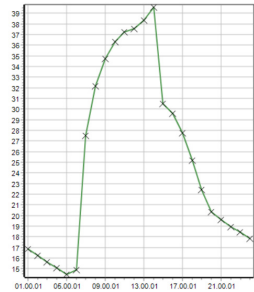
**ortho image of
the worst point
for PET**



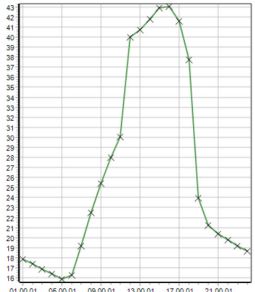
**physiological
equivalent
temperature
(PET - °C)**



Major PET jump of ca. 12°C between 10-11h, peaks at ca. 44°C at 15h, drops by ca. 7°C until 18h, major drop by ca. 13°C between 18-19h

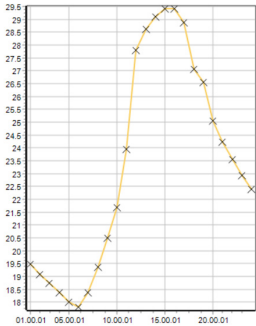


Major PET jump of ca. 12°C between 6-7h, peaks at ca. 40°C at 14h, major drop by ca. 10°C until 15h, decreases for the rest of the day

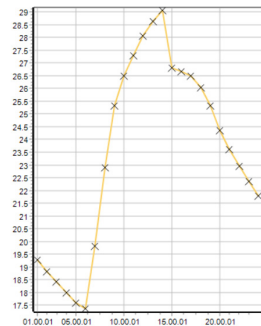


Major PET jump of ca. 10°C between 11-12h, peaks at ca. 43°C at 16h, decreases for the rest of the day with a major drop by ca. 14°C between 18-19h

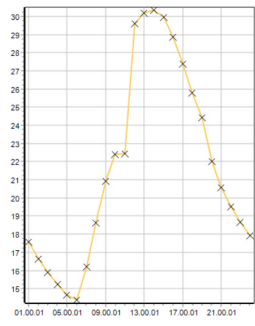
**surface
temperature
(ST - °C)**



Major ST jump of ca. 4°C between 11-12h, peaks at ca. 29.5°C at 15h, decreases for the rest of the day

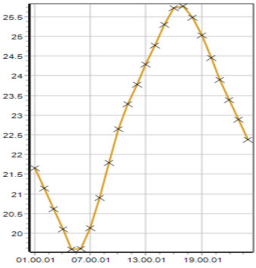


Major ST jumps between 6-7h, 7-8h and 8-9h by ca. 3°C each, peaks at 29°C at 14h, drops by ca. 2.5°C in the following hour, decreases for the rest of the day

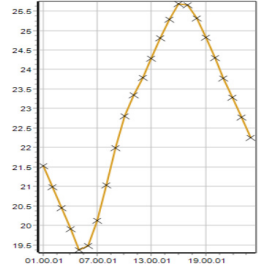


ST rises up until 22.5°C between 6-10h, persists for an hour, major jump of ca 7°C between 10-11h, peaks at ca. 31°C at 14h, drops with a relatively consistent trend for the rest of the day

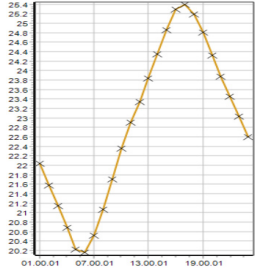
**potential air
temperature
(PAT - °C)**



Lowest values persist around 19.5°C between 5-6h, peak PAT at ca. 26°C at 17h



Lowest values persist around 19-19.5°C between 5-6h, peak PAT at ca. 26°C at 16h



Lowest values persist around 20.2°C between 5-6h, peak PAT at ca. 25.4°C at 17h

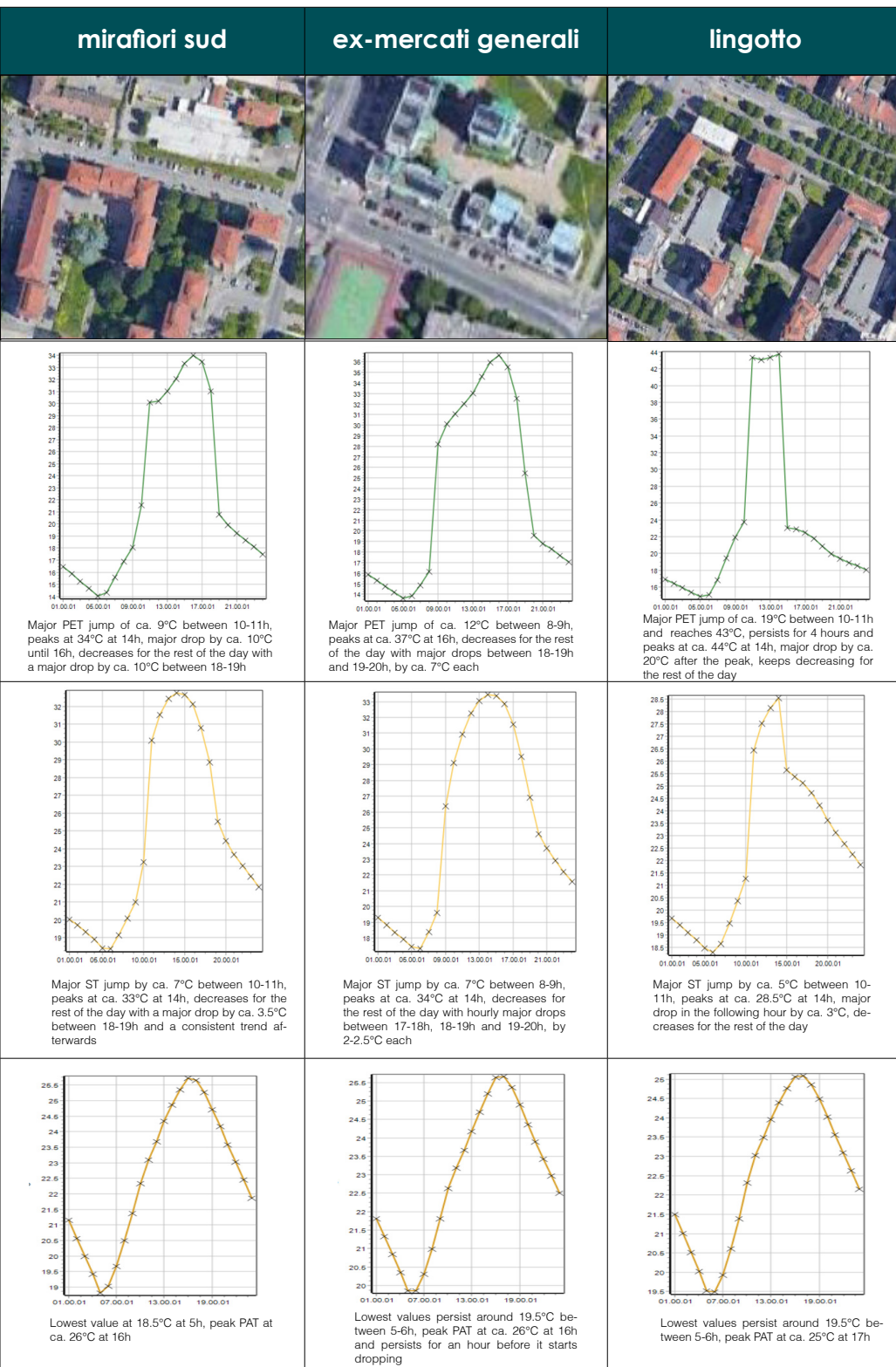


Table 7.

Comparison table of PET, PAT and ST on selected points in NW-SE oriented urban canyons. From each case study, the points that have the most unfavorable PET results at 12:00 were selected. (Graphs were exported from ENVI-met, satellite images were exported from Google Earth)

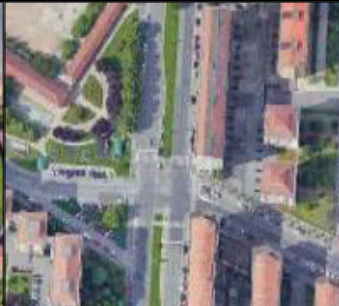
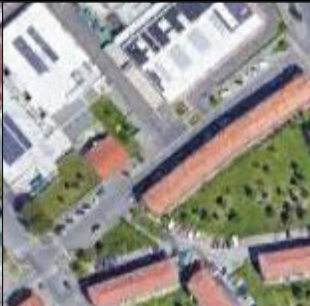
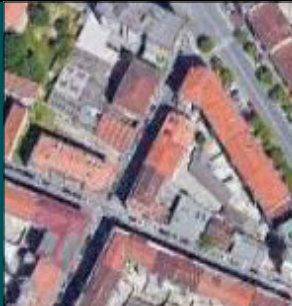
**URBAN CANYONS
(NE-SW)**

san donato

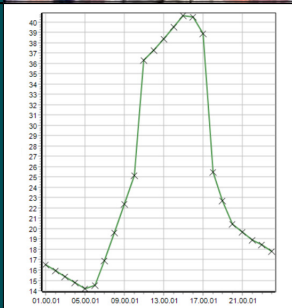
le vallette

mirafiori nord

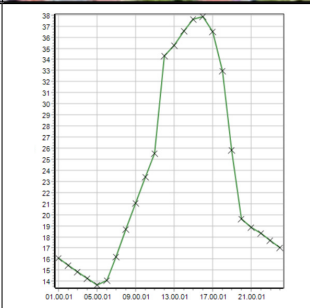
**ortho image of
the worst point
for PET**



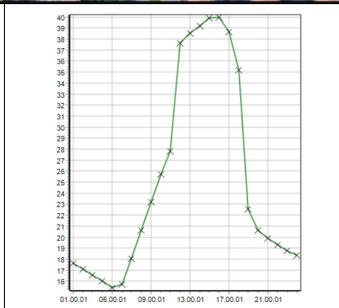
**physiological
equivalent
temperature
(PET - °C)**



Major PET jump of ca. 11°C between 10-11h, peaks at ca. 41°C at 15h and persists until 16h, major drop by ca. 14°C between 17-18h

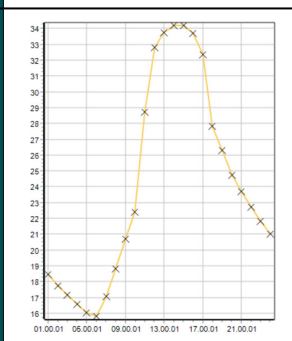


Major PET jump of ca. 9°C between 11-12h, persists between 34-38°C until 16h, peaks at ca. 38°C at 16h, two major drops between 18-19h and 19-20h, by ca. 7°C each

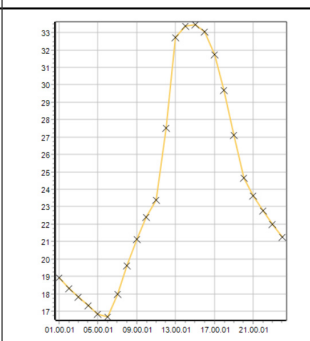


Major PET jump of ca. 10°C between 11-12h, persists above 37°C between 12-17h, peaks at ca. 40°C at 16h, major drops between 18-19h, by ca. 13°C

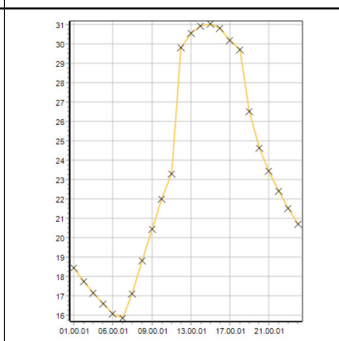
**surface
temperature
(ST - °C)**



Two major ST jumps of ca. 6°C and ca. 4°C between 10-11h and 11-12h, persists above 32°C between 12-17h, peaks at slightly above 34°C at 14h and persists for an hour, major drop by ca. 4.5°C between 17-18h

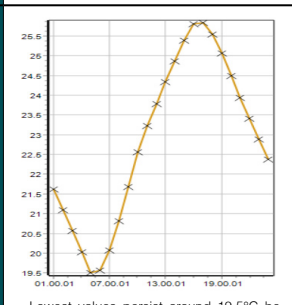


Two major ST jumps of ca. 4°C and ca. 5°C between 11-12h and 12-13h, persists above 32°C between 13-16h, peaks at ca. 33°C at 14h and persists for an hour

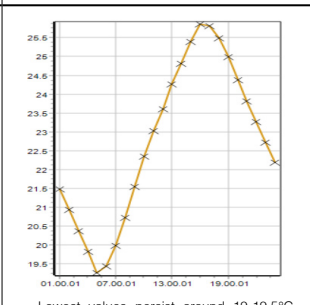


Major ST jump of ca. 6.5°C between 11-12h, persists above 29°C between 12-18h, peaks at ca. 31°C at 15h, major drop by 3°C between 18-19h

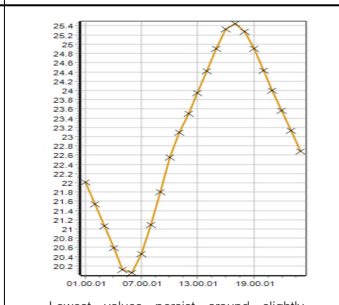
**potential air
temperature
(PAT - °C)**



Lowest values persist around 19.5°C between 5-6h, peak PAT at ca. 26°C at 17h



Lowest values persist around 19.5°C between 5-6h, peak PAT at ca. 26°C at 16h



Lowest values persist around slightly above 20°C between 5-6h, peak PAT at ca. 25.4°C at 17h


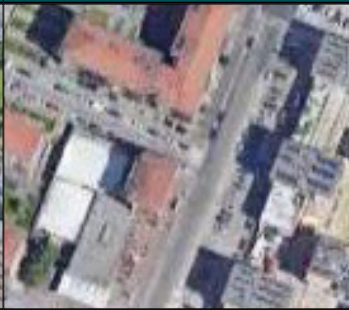

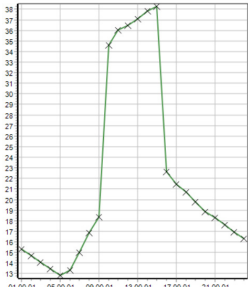
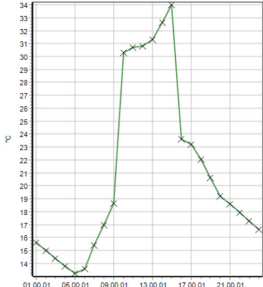
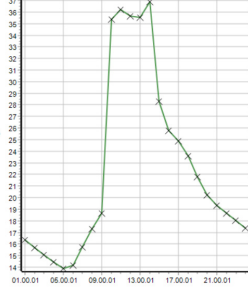
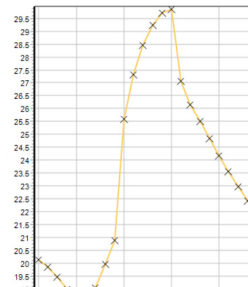
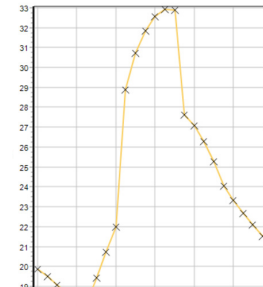
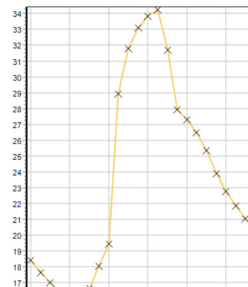
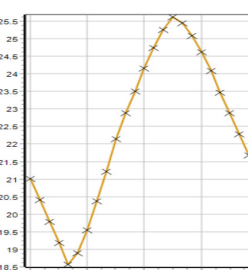
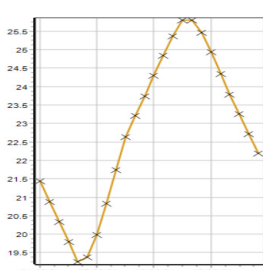
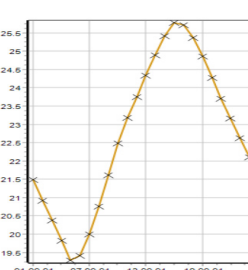
mirafiori sud	ex-mercati generali	lingotto
		
 <p>Major PET jump of ca. 16°C between 9-10h, persists above 34°C between 10-15h, peaks at ca. 38°C at 15h, major drop between 15-16h by ca. 15°C</p>	 <p>Major PET jump of ca. 12°C between 9-10h, persists above 34°C between 10-15h, peaks at ca. 34°C at 15h, major drop between 15-16h by ca. 10.5°C</p>	 <p>Major PET jump of ca. 17°C between 9-10h, persists above 35°C between 10-14h, peaks at ca. 37°C at 14h, major drop between 14-15h by ca. 9°C</p>
 <p>Major ST jump of ca. 5.5°C between 9-10h, persists above 29°C between 12-18h, peaks at ca. 30°C at 15h, major drop by ca. 3°C between 15-16h</p>	 <p>Major ST jump of ca. 7°C between 9-10h, peaks at ca. 33°C at 14h and persists for an hour, major drop by ca. 5.5°C between 15-16h</p>	 <p>Major ST jump of ca. 9.5°C between 9-10h, persists above 31°C between 11-15h, peaks at slightly above 34°C at 14h, major drop by ca. 4°C between 15-16h</p>
 <p>Lowest value at 18.5°C at 5h, peak PAT at ca. 26°C at 16h</p>	 <p>Lowest values persist slightly below 19.5°C between 5-6h, peak PAT at ca. 26°C at 16h and persists for an hour before it starts dropping</p>	 <p>Lowest values persist around 19-19.5°C between 5-6h, peak PAT at ca. 26°C at 16h</p>

Table 8.

Comparison table of PET, PAT and ST on selected points in NE-SW oriented urban canyons. From each case study, the points that have the most unfavorable PET results at 12:00 were selected. (Graphs were exported from ENVI-met, satellite images were exported from Google Earth)



Conclusion

Conclusion

In this thesis, the urban morphology of Turin has been examined in relation to its impact on the local microclimate. This analysis has been performed by relying on a strong scientific background, which is coherent with the conclusions. The outputs do not only prove the impact of building form on the microclimate, but they also illustrate the microclimatic response of the spaces between the buildings.

Through mapping, ten main typologies of urban fabric have been identified in the city. The map made the interconnection between the expansion of the city and its urban fabric evident. It has been confirmed that the urban morphology of the city has been strongly influenced by its industrial growth, leading to rapid urbanization and sudden changes through the urban fabric. Moving from the center to the outskirts, it is possible to see that the compact formations in the city center are transitioning into localized forms as a result of rapid urban decision-making processes of the past.

Moving to a smaller scale, six neighborhoods of Turin have been chosen to analyze the impact of different configurations of urban form

on the microclimate. It has been confirmed that the outcomes of this research are sensitive to geographical location and local climate, as variations could be recorded even within different parts of the city. Temperature variations between the case studies have reached up to 1.45°C for maximum midday potential air temperature, 11.36°C for maximum midday surface temperature and 19.83°C for maximum midday PET.

During the research, it was observed that in Turin, the courtyard formations that have a built density on the south facade of the building block result in more favorable conditions. The courtyard adjustments where the south facade is open to solar radiation lead to lower levels of comfort, due to the intense solar radiation exposure. As for the openings on the borders of the building blocks, it is significant to consider the wind direction to be able to benefit from the air flow. When the wind direction is perpendicular to the orientation of the linear buildings, the built environment acts as a barrier, disrupts cooling paths by slowing down the winds, which results in softer circulation of wind and thus, less favorable conditions within the courtyards in Turin. However, this phenomena could be useful for environments with cooler climatic conditions.

It has been discussed during the earlier stages of the thesis that vegetation provides cooling through its shading effect and evapotranspiration (Kleerekoper, 2016). The results of the research confirm that the horizontal greenery and single tree plantation are not sufficient in isolation to cause a significant positive

impact, as they only result in localized surface temperature improvements. However, when horizontal greenery is supported by trees that are placed in groups or on an axis along the streets, they help in achieving lower potential air temperature and higher levels of comfort. Densely placed trees help stabilizing the temperature, resulting in less day-night surface temperature swings. In addition, the outputs confirm the findings of Koukli and Yiannakou (2021): when the trees are not placed in groups, they are insufficient to form an obstacle against the hot wind flow, which results in heavy thermal loads and uncomfortable conditions.

The courtyards that have a presence of vertical greenery performed better for all environmental variables analyzed. As for the mobility axes, comparing two scenarios where the urban canyon orientations are the same, it was realized that an extra lane of tree in the middle of the road resulted in up to 5°C less day and night surface temperature swing, compared to the one that has two lanes of trees placed on both sides of the road. The scenario where there are three lanes of trees resulted in higher levels of outdoor comfort (measured as PET) by approximately 10°C. As for the surface temperature, materials that have low albedo resulted in less favorable surface temperature, and in some cases, low levels of outdoor comfort due to their lack of ability to reflect the solar radiation.

Comparisons between the urban canyons that have different orientations have been made as well. It has been realized that the NW-SE oriented urban canyons have reached lower levels of comfort compared to the NE-SW oriented ones. Worse conditions of potential air temperature have also been recorded in urban canyons that have NW-SE orientation. This can be linked to the welcoming

behavior of NE-SW oriented urban canyons towards wind, given the prevailing wind direction being northeast.

Within the discussion, the relationship between different microclimatic variables have been analyzed as well. The results demonstrate that the outdoor comfort results are not always in line with the results of potential air temperature and surface temperature. This indicates that the least favorable surface temperature and potential air temperature conditions might not always lead to the worst outdoor comfort conditions. This is due to the fact that the outdoor comfort is dependent on various factors, such as wind, clothing and humidity. Although it is an exceptional case for this research, a comparison between the outdoor comfort outputs of the case studies has demonstrated that the area that is subjected to a low albedo material and high air temperature has performed better in means of outdoor comfort than the area that includes high albedo materials and has lower air temperature.

Possible Adaptation and Mitigation Strategies

All in all, the results highlight the significance of site-specific decision making processes regarding urban planning. As Salat (2011) notes, “there is not a universal answer to the question of optimal texture” as it depends strictly on the climatic and geographical conditions. However, with local studies and analyses, it is possible to estimate possible solutions to improve the microclimatic conditions of a given environment. Through the right use of dense plantation, evaporative cooling, self-shading effect of the buildings and

paying attention to the albedo and the emissivity of materials, it is possible to minimize the negative impact of anthropogenic activities.

To be more specific, it would be useful to list several adaptation and mitigation strategies here, to give an idea about how the results of this thesis could be used as an initial step to start taking action on site. The balance of permeable and impermeable surfaces is remarkable for the management of water cycle as well as cooling. Green roof implementations, for instance, help cooling and humidifying the air by evaporation of retained water from soil and plants, as well as providing thermal insulation for the buildings and thus, lowering the energy consumption and greenhouse gas emissions. Permeable surfaces are useful for rainwater harvesting as well, which helps reducing water consumption and lead to preservation of natural sources.

The lack of water bodies are evident in each case study area. Water bodies provide cooling through evaporation. The cooling potential of wetlands help mitigating urban heat and improve outdoor comfort in urban environments. The scientific community confirms that water-based evaporative technologies achieve cooling as they extract the evaporation latent heat from the air (Santamouris 2019; Seavult et al., 2022). Additionally, the cooling can be provided through convection in the cases where the surface temperature of the water is lower than the ambient temperature (Santamouris, 2019).

One of the main drivers of the greenhouse gas emissions (particularly CO₂) is the use of hard mobility. During the site trip, it has been realized that bicycle lanes are limited or unorganized. Large urban canyons that have a large density of

concrete and asphalt have been noted as well. These urban canyons that have enough space to provide multiple options of mobility could be restructured by limiting hard mobility, promoting better organized bicycle lanes and pedestrianization and introducing soft mobility. During the implementations of soft mobility and pedestrianization, it is important to pay specific attention to using high albedo materials, to avoid overheating of surfaces. Moreover, long axes of plantation serves as a great source to reduce thermal stress, as it has been mentioned in the discussion part that an additional lane of trees in the middle of the street help achieving better conditions.

Limitations

This study has three main limitations. The first one is the fact that the microclimate is strictly dependent on the geographical location and on the specific climate of the location where the assessments are carried out. Therefore, the conclusions that have been reached through this research may not be applicable to other locations throughout the world. The second one is regarding the sensitivity of the research to new urban scale decisions and interventions within the case study areas, as they would change the validity of the outcomes of this research. Different applications of materials would cause variation on the microclimatic conditions of the site and thus, the findings of this thesis. The third limitation is related to the possible variations between the real life measurements and the results that are extracted from ENVI-met software. Although the data from the meteorological station has been used, slight differences could be observed

when the real time data and software outputs are compared. The anomalies regarding high temperatures recorded along the borders of the model are related to this limitation.

Recommendations for further research

The thesis portrays a methodology that is adaptable to further research. The use of the findings of this thesis might be limited to the city under consideration (in this case, Turin) and possibly, the other cities that share the same microclimatic conditions. However, the methodology of this thesis intends to be objective, in the sense that it could be applied to any urban area.

As for the findings regarding Turin, the urban morphology mapping exercise would be a useful input for GIS, as it would be interesting to carry out comparative researches to see the interconnections between the urban form and the other parameters of the city (such as population, quality of living, landuse).

Nevertheless, the approach of studying a city through an analysis of its urban morphology and microclimate creates a useful ground for adaptation and mitigation strategy proposals. Prior studies confirm that the microclimate of an area is strongly connected to the energy demand (Salat, 2011; Santamouris, 2019). The urban elements that have been discussed through this thesis (vegetation, urban canyon, urban fabric etc.) have an important impact on the cooling and heating loads and a well-organized configuration would contribute to optimizing the energy balance of a local system, and therefore the relevant energy consumption costs. Therefore, it would be useful to investigate in detail

how the proposed strategies could be applied locally in detail, to achieve a sustainable future through an approach where adaptation and mitigation strategies are considered complementary.

Bibliography

Ajuntament de Barcelona. (n.d.). *Greenery and Biodiversity Plan for 2012-2020*. Ajuntament de Barcelona. <https://ajuntament.barcelona.cat/ecologiaurbana/en/what-we-do-and-why/green-city-and-biodiversity/green-and-biodiversity-plan>

Ajuntament de Barcelona. (2013). *Barcelona green infrastructure and biodiversity plan 2020*. Medi Ambient i Serveis Urbans - Hàbitat Urbà. Ajuntament de Barcelona.

Allaby, M. (Ed.). (2008). *A Dictionary of Earth Sciences*. Oxford University Press. <https://doi.org/10.1093/acref/9780199211944.001.0001>

American Society of Heating, Refrigerating and Air-Conditioning Engineers. (2021). *Ashrae Standard 55-2020: Thermal Environmental Conditions for Human Occupancy*.

Aria InformAmbiente. (2020, January 28). Comune di Torino. <http://www.comune.torino.it/ambiente/aria/>

Arizona State University Global Institute of Sustainability and Innovation. (n.d.). *North Desert Village Neighborhood Landscaping Experiment | Central Arizona–Phoenix Long-Term Ecological Research*. Global Institute of Sustainability and Innovation; Arizona State University. <https://sustainability-innovation.asu.edu/capltcr/research/long-term-monitoring/north-desert-village-neighborhood-landscaping-experiment/>

Arpa Piemonte. (n.d.). *Dati Ambientali*. Arpa Piemonte. <http://www.arpa.piemonte.it/datiambientali/richiesta-dati-orari-meteorologici>

Arpa Piemonte Dipartimento Rischi Naturali e Ambientali. (2021). Il Clima in Piemonte nel 2021. In *Arpa Piemonte*. https://www.arpa.piemonte.it/rischinaturali/tematismi/clima/rapporti-di-analisi/annuale_pdf/anno_2021.pdf

Arpa Piemonte Dipartimento Rischi Naturali e Ambientali, & Città di Torino. (2020). Analisi di Vulnerabilità Climatica della Città di Torino. In *Città di Torino*. http://www.comune.torino.it/torinosostenibile/documenti/200806_analisi_vulnerabilita_climatica.pdf

Arpa Piemonte, & Città metropolitana di Torino. (2022). Uno Sguardo All'Aria 2021. In *Arpa Piemonte*. Arpa Piemonte. <http://www.arpa.piemonte.it/arpa-comunica/file-notizie/2022/uno-sguardo-allaria-2021-brochure-a4.pdf>

Ayers, J. M., & Huq, S. (2008). The Value of Linking Mitigation and Adaptation: A Case Study of Bangladesh. *Environmental Management*, 43(5), 753–764. <https://doi.org/10.1007/s00267-008-9223-2>

Barosio, M., Eynard, E., Marietta, C., Marra, G., Melis, G., & Tabasso, M. (2016). From urban renewal to urban regeneration: Classification criteria for urban interventions. Turin 1995-2015: Evolution of planning tools and approaches. *Journal of Urban Regeneration and Renewal*, 9(4), 367/380. https://www.researchgate.net/publication/310445787_From_urban_renewal_to_urban_regeneration_Classification_criteria_for_urban_interventions_Turin_1995-2015_Evolution_of_planning_tools_and_approaches

Boeters, R., Donkers, S., Lee, D., Liem, V., Montazeri, S., 6813 van Oostveen, J., Pietrzyk, P., Menenti, M., Gorte, B., & Vebree, E. (2012). *The effect of 3D geometry complexity on simulating radiative, conductive and convective fluxes in an urban canyon*. https://www.researchgate.net/publication/312524500_The_effect_of_3D_geometry_complexity_on_simulating_radiative_conductive_and_convective_fluxes_in_an_urban_canyon

Bruse, M., & Fleer, H. (1998). Simulating surface–plant–air interactions inside urban environments with a three dimensional numerical model. *Environmental Modelling & Software*, 13(3-4), 373–384. [https://doi.org/10.1016/s1364-8152\(98\)00042-5](https://doi.org/10.1016/s1364-8152(98)00042-5)

Butler, A. (2013, April 16). bjarke ingels group chosen to design europa city in france. *Designboom*. <https://www.designboom.com/architecture/big-architects-europacity-france/>

Chen, F. (2014). Urban Morphology and Citizens' Life. *Encyclopedia of Quality of Life and Well-Being Research*, 6850–6855. https://doi.org/10.1007/978-94-007-0753-5_4080

Città di Torino. (2020). Climate resilience plan. In *Comune di Torino*. http://www.comune.torino.it/ambiente/bm~doc/resilienza-climatica_en.pdf

Città di Torino. (2022). Piano Strategico e Piano di Azione sulla Gestione Sostenibile delle Acque in Ambito Urbano (InformAmbiente). In *Torino Vivibile*.

Citta di Torino. https://www.torinovivibile.it/wp-content/uploads/2022/03/Piano-gestione-sostenibile-acque-in-ambito-urbano_CWC.pdf

Città di Torino, Arpa Piemonte, & Azienda Sanitaria Locale. (2019). Raccolta di domande frequenti (FAQ) sul tema della qualità dell'aria. In *Comune di Torino*. Citta di Torino. http://www.comune.torino.it/emergenzaambientale/documenti/2019-20/faq_aria.pdf

Coffel, E. D. (2018). *Extreme heat and its impacts in a changing climate* [PhD Thesis].

Comune di Torino. (n.d.-a). *Circoscrizione 2 - Mirafiori Nord - Storia dei Quartieri*. Comune di Torino. http://www.comune.torino.it/circ2_/storiadeiquartieri/quartieri/mirafiorinord.htm

Comune di Torino. (n.d.-b). *Il verde a Torino – Verde Pubblico*. Comune di Torino. <http://www.comune.torino.it/verdepubblico/il-verde-a-torino/>

Comune di Torino. (n.d.-c). *Urban 2: Area and Interventions*. Comune di Torino. http://www.comune.torino.it/urban2/eng_vers/area.html

Comune di Torino. (2020a, January 28). *Aria InformAmbiente*. Comune Di Torino. <http://www.comune.torino.it/ambiente/aria/>

Comune di Torino. (2020b). Piano Strategico dell'Infrastruttura Verde. In *Comune di Torino*. https://servizi.comune.torino.it/consiglio/prg/documenti1/atti/allegati/202002957_1tc.pdf

Dryden, I. G. C. (Ed.). (1982). Chapter 7 - Electrical heating fundamentals. *The Efficient Use of Energy (Second Edition)*. <https://doi.org/https://doi.org/10.1016/B978-0-408-01250-8.50016-7>

Emmanuel, R. (2005). *An Urban Approach To Climate Sensitive Design*. Taylor & Francis. <https://doi.org/10.4324/9780203414644>

Emmanuel, R. (2021). Urban microclimate in temperate climates: a summary for practitioners. *Buildings and Cities*, 2(1), 402–410. <https://doi.org/10.5334/bc.109>

ENVI-met. (2021). *ENVI-met. A holistic Microclimate Modelling System*. ENVI-Met. <https://envi-met.info/doku.php?id=root:start>

European Commission, & European Environment Agency. (n.d.). *Tropical Nights, 2011-2099*. Climate ADAPT. <https://climate-adapt.eea.europa.eu/metadata/indicators/tropical-nights-2011-2099>

Esch, M. (2015). *Designing the Urban Microclimate. A framework for a design-decision support tool for the dissemination of knowledge on the urban microclimate to the urban design process* [PhD Thesis]. https://www.researchgate.net/publication/307748592_Designing_the_Urban_Microclimate_A_framework_for_a_design-decision_support_tool_for_the_dissemination_of_knowledge_on_the_urban_microclimate_to_the_urban_design_process

European Commission, & European Environment Agency. (2016). *Supporting urban greening and social justice in the city of Barcelona*. Climate-ADAPT. <https://climate-adapt.eea.europa.eu/metadata/case-studies/barcelona-trees-tempering-the-mediterranean-city-climate/>

European Environment Agency. (2016). Urban adaptation to climate change in Europe 2016—Transforming cities in a changing climate. In *European Environment Agency*. <https://www.eea.europa.eu/publications/urban-adaptation-2016>

Fondazione della Comunità di Mirafiori Onlus. (n.d.). *Il quartiere di Mirafiori*. Fondazione Della Comunità di Mirafiori Onlus. <https://fondazionemirafiori.it/mirafiori-sud>

Garzena, D., Acquaotta, F., & Fratianni, S. (2018). Analysis of the long-time climate data series for Turin and assessment of the city's urban heat island. *Weather*, 74(10), 353–359. <https://doi.org/10.1002/wea.3292>

Gauzin-Müller, D., & Favet, N. (2002). *Sustainable architecture and urbanism: concepts, technologies, examples*. Birkhäuser.

Geoportale Comune di Torino. (n.d.). Geoportale Comune di Torino; Comune di Torino. <http://geoportale.comune.torino.it/geocatalogocoto/?sezione=mappa>

Göpfert, C., Wamsler, C., & Lang, W. (2019a). A framework for the joint institutionalization of climate change mitigation and adaptation in city administrations. *Mitigation and Adaptation Strategies for Global Change*, 24(1), 1–21. <https://doi.org/10.1007/s11027-018-9789-9>

Göpfert, C., Wamsler, C., & Lang, W. (2019b). Institutionalizing climate change mitigation and adaptation through city advisory committees: Lessons learned and policy futures. *City and Environment Interactions*, 1. <https://doi.org/10.1016/j.cacint.2019.100004>

Grafakos, S., Viero, G., Reckien, D., Trigg, K., Viguie, V., Sudmant, A., Graves, C., Foley, A., Heidrich, O., Mirailles, J. M., Carter, J., Chang, L. H., Nador, C., Liseri, M., Chelleri, L., Orru, H., Orru, K., Aelenei, R., Bilska, A., & Pfeiffer, B. (2020). Integration of mitigation and adaptation in urban climate change action plans in Europe: A systematic assessment. *Renewable and Sustainable Energy Reviews*, 121. <https://doi.org/10.1016/j.rser.2019.109623>

Höppe, P. (1999). The physiological equivalent temperature - a universal index for the biometeorological assessment of the thermal environment. *International Journal of Biometeorology*, 43(2), 71–75. <https://doi.org/10.1007/s004840050118>

Hotkevica, I. (2013). *Green elements in street canyons: Research by design for heat mitigation and thermal comfort in urban areas*. [MSc Thesis]. <https://edepot.wur.nl/266371>

Hulley, M. E. (2012). The urban heat island effect: causes and potential solutions. *Metropolitan Sustainability*, 79–98. <https://doi.org/10.1533/9780857096463.1.79>

Intergovernmental Panel on Climate Change. (1995). Climate Change 1995: The IPCC Second Assessment Report. In R. T. Watson, M. C. Zinyowera, & R. H. Moss (Eds.), *Harvard Library*. Cambridge University Press. <https://library.harvard.edu/sites/default/files/static/collections/ipcc>

Intergovernmental Panel on Climate Change. (2001). Climate change 2001: Synthesis report. In *IPCC*. Cambridge University Press. <https://www.ipcc.ch/report/ar3/syr/>

Kleerekoper, L. (2016). Urban Climate Design: Improving thermal comfort in Dutch neighbourhoods. *A+BE: Architecture and the Built Environment*, 6. <https://doi.org/10.7480/abe.2016.11>

Kouklis, G.-R., & Yiannakou, A. (2021). The Contribution of Urban Morphology to the Formation of the Microclimate in Compact Urban Cores: A Study in the City Center of Thessaloniki. *Urban Science*, 5(2). <https://doi.org/10.3390/urbansci5020037>

Kuypers, V., Vries, B. d., & Peeters, R. G. J. M. (2008). *Groon voor Klimaat*. https://www.wur.nl/upload_mm/5/8/8/6464c9a7-e6db-4893-ad9c-cd0412364328_GroenvoorKlimaat.pdf

Le Thanh Hoa. (2013). *Measuring urban morphology for adaptation to climate change in Ho Chi Minh City* [PhD Thesis].

Lilley, K. D. (2009). Urban Morphology. *International Encyclopedia of Human Geography*, 66–69. <https://doi.org/10.1016/b978-008044910-4.01093-2>

Lobaccaro, G., De Ridder, K., Acero, J. A., Hooyberghs, H., Lauwaet, D., Maiheu, B., Sharma, R., & Govehovitch, B. (2021). Applications of Models and Tools for Mesoscale and Microscale Thermal Analysis in Mid-Latitude Climate Regions—A Review. *Sustainability*, 13(22). <https://doi.org/10.3390/su132212385>

Locatelli, B. (2011). *Synergies between adaptation and mitigation in a nutshell*. Center for International Forestry Research (CIFOR). <https://doi.org/10.17528/cifor/003619>

Locatelli, B. (2014). *Mitigation-Adaptation Synergies*. <https://www.cifor.org/knowledge/publication/4263/>

Lopez-Cabeza, V. P., Alzate-Gaviria, S., Diz-Mellado, E., Rivera-Gomez, C., & Galan-Marin, C. (2022). Albedo influence on the microclimate and thermal comfort of courtyards under Mediterranean hot summer climate conditions. *Sustainable Cities and Society*, 81. <https://doi.org/https://doi.org/10.1016/j.scs.2022.103872>

Martin, E., & Hine, R. (2008). *A Dictionary of Biology*. Oxford University Press. <https://doi.org/10.1093/acref/9780199204625.001.0001>

Matzarakis, A., Mayer, H., & Iziomon, M. G. (1999). Applications of a universal thermal index: physiological equivalent temperature. *International Journal of Biometeorology*, 43(2), 76–84. <https://doi.org/10.1007/s004840050119>

Middel, A., Häb, K., Brazel, A. J., Martin, C. A., & Guhathakurta, S. (2014). Impact of urban form and design on mid-afternoon microclimate in Phoenix Local Climate Zones. *Landscape and Urban Planning*, 122, 16–28. <https://doi.org/10.1016/j.landurbplan.2013.11.004>

MuseoTorino. (n.d.-a). *Basso San Donato*. MuseoTorino. <https://www.museotorino.it/view/s/ede1dcce876c46c0818790ede2734d5b>

MuseoTorino. (n.d.-b). *Le Vallette*. MuseoTorino. <https://www.museotorino.it/view/s/8e7f1bfe46dd45b8964856ac59b11829>

MuseoTorino. (n.d.-c). *Villaggio Olimpico e Arco*. MuseoTorino. <https://www.museotorino.it/view/s/8e80bedb431e41f98397ac1c89374b16>

MuseoTorino, Comune di Torino, & Direzione Musei. (2012). *MuseoTorino*. MuseoTorino. <https://www.museotorino.it/site/exhibitions/history>

Musikant, S. (2003). Glass. In R. A. Meyer (Ed.), *Encyclopedia of Physical Science and Technology* (3rd ed., pp. 781–806). Academic Press.

Nunez, M., & Oke, T. R. (1977). The Energy Balance of an Urban Canyon. *Journal of Applied Meteorology*, 16(1), 11–19. [https://doi.org/10.1175/1520-0450\(1977\)016<0011:teboau>2.0.co;2](https://doi.org/10.1175/1520-0450(1977)016<0011:teboau>2.0.co;2)

Oke, T. R., Mills, G., Christen, A., Voogt, J. A., & Al, E. (2017). *Urban climates*. Cambridge University Press. Copyright.

Papagiannakis, A., Vitopoulou, A., & Yiannakou, A. (2020). Transit-Oriented Development in the Southern European city of Thessaloniki introducing urban railway: typology and implementation issues. *European Planning Studies*, 29(1), 117–141. <https://doi.org/10.1080/09654313.2020.1724267>

Postaria, R. (2021, May 31). *Superblock (Superilla) Barcelona—a city redefined*. Cities Forum. <https://www.citiesforum.org/news/superblock-superilla-barcelona-a-city-redefined/>

Reckien, D., Salvia, M., Heidrich, O., Church, J. M., Pietrapertosa, F., De Gregorio-Hurtado, S., D'Alonzo, V., Foley, A., Simoes, S. G., Krkoška Lorencová, E., Orru, H., Orru, K., Wejs, A., Flacke, J., Olazabal, M., Geneletti, D., Feliu, E., Vasilie, S., Nador, C., & Krook-Riekkola, A. (2018). How are cities planning to respond to climate change? Assessment of local climate plans from 885 cities in the EU-28. *Journal of Cleaner Production*, 191, 207–219. <https://doi.org/10.1016/j.jclepro.2018.03.220>

Salat, S., Labbe, F., Nowacki, C., & Walker, G. (2011). *Cities and forms : on sustainable urbanism*. CSTB Urban Morphology Laboratory.

Santamouris, M. (2019). Mitigating the Local Climatic Change and Fighting Urban Vulnerability. *Minimizing Energy Consumption, Energy Poverty and Global and Local Climate Change in the Built Environment: Innovating to Zero*, 223–307. <https://doi.org/10.1016/b978-0-12-811417-9.00008-8>

Schipper, E. L. F. (2006). Conceptual History of Adaptation in the UNFCCC Process. *Review of European Community and International Environmental Law*, 15(1), 82–92. <https://doi.org/10.1111/j.1467-9388.2006.00501.x>

Scott, K., Simpson, J., & McPherson, E. G. (1999). Effects of Tree Cover on Parking Lot Microclimate and Vehicle Emissions. *Journal of Arboriculture*, 25(3), 129–142. <https://doi.org/10.48044/jauf.1999.019>

Sevault, A., Vullum-Bruer, F., & Tranås, O. L. (2022). Active PCM-Based Thermal Energy Storage in Buildings. *Reference Module in Earth Systems and Environmental Sciences*, 1, 453–469. <https://doi.org/10.1016/b978-0-12-819723-3.00008-1>

Steidle Architekten. (n.d.). *Villaggio Olimpico Torino 2006*. Steidle Architekten. <https://www.steidle-architekten.de/projekt/villaggio-olimpico-torino-2006/>

Stewart, I. D., & Oke, T. R. (2012). Local Climate Zones for Urban Temperature Studies. *Bulletin of the American Meteorological Society*, 93(12). <https://doi.org/10.1175/bams-d-11-00019.1>

Taha, H. (2004). Heat Islands and Energy. In C. J. Cleveland (Ed.), *Encyclopedia of Energy* (pp. 133–143). Elsevier. <https://doi.org/10.1016/b0-12-176480-x/00394-6>

Taubenböck, H., Debray, H., Qiu, C., Schmitt, M., Wang, Y., & Zhu, X. X. (2020). Seven city types representing morphologic configurations of cities across the globe. *Cities*, 105. <https://doi.org/10.1016/j.cities.2020.102814>

Torino Urban Lab. (2018). TorinoAtlas. In *Urban Lab Torino*. https://urbanlabortorino.it/wp-content/uploads/2020/06/TorinoAtlas_09_ambiente.pdf

Trane, M., Giovanardi, M., Pollo, R., & Martoccia, C. (2021, December). Microclimatic design for micro-urban design. A case study in Granada, Spain. *SMC Magazine*. https://www.researchgate.net/publication/357419598_Microclimatic_design_for_micro-urban_design_A_case_study_in_Granada_Spain

Transsolar KlimaEngineering. (n.d.). *EuropaCity, Paris, France*. Transsolar. <https://transsolar.com/projects/europacity>

UN Habitat. (2011). Global Report on Human Settlements 2011: Cities and Climate Change. In *UN Habitat*. <https://unhabitat.org/global-report-on-human-settlements-2011-cities-and-climate-change>

United Nations. (n.d.). *Goal 11: Sustainable cities and communities*. The Global Goals. <https://www.globalgoals.org/goals/11-sustainable-cities-and-communities/>

United Nations. (2018). *The Sustainable Development Agenda*. United Nations Sustainable Development; United Nations. <https://www.un.org/sustainabledevelopment/development-agenda/>

United Nations. (2021). *Goal 13: Take urgent action to combat climate change and its impacts*. United Nations. <https://www.un.org/sustainabledevelopment/climate-change/>

United Nations. (2022). *Goal 13: Climate Action*. The Global Goals. <https://www.globalgoals.org/goals/13-climate-action/>

United Nations Department of Economic and Social Affairs. (2022). Population Facts. In *United Nations* (p. 1). https://www.un.org/development/desa/pd/sites/www.un.org.development.desa.pd/files/undes_pd_2020_popfacts_urbanization_policies.pdf

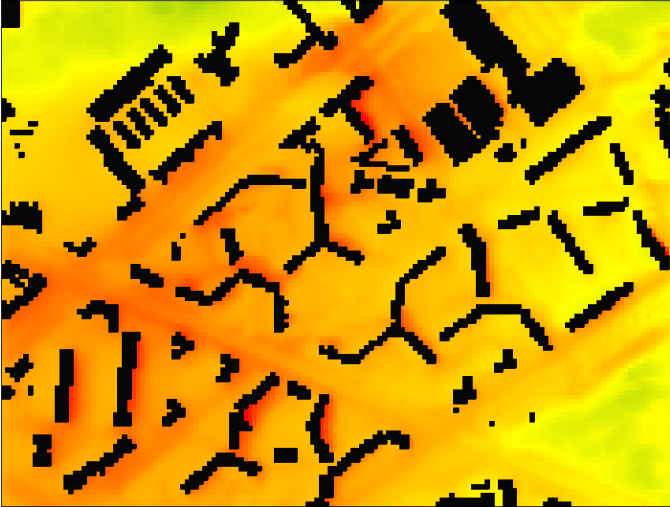
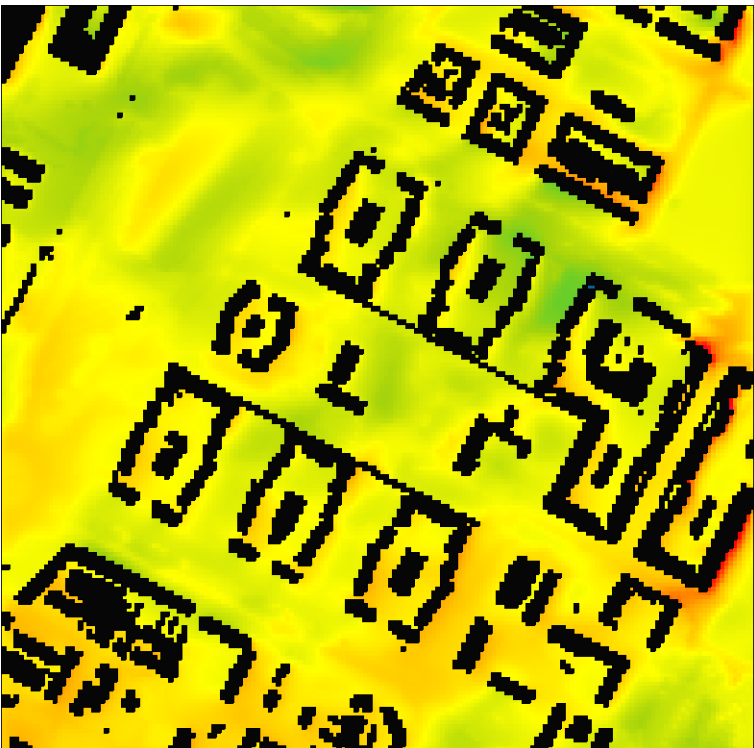
United Nations Development Programme. (2015). *The SDGs in Action*. Sustainable Development Goals. <https://www.undp.org/sustainable-development-goals>

Vinnitskaya, I. (2013, April 15). *BIG Wins Europa City Development in Paris*. ArchDaily. <https://www.archdaily.com/359796/big-design-wins-europe-city-development-in-paris>

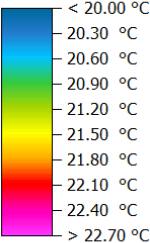
Wong, N. H., & Yu, C. (2005). Study of green areas and urban heat island in a tropical city. *Habitat International*, 29(3), 547–558. <https://doi.org/10.1016/j.habitatint.2004.04.008>

World Bank. (2010). The World Bank Annual Report 2010 : Year in Review. In *Open Knowledge World Bank*. <https://openknowledge.worldbank.org/handle/10986/5906>

Annex



Potential Air Temperature

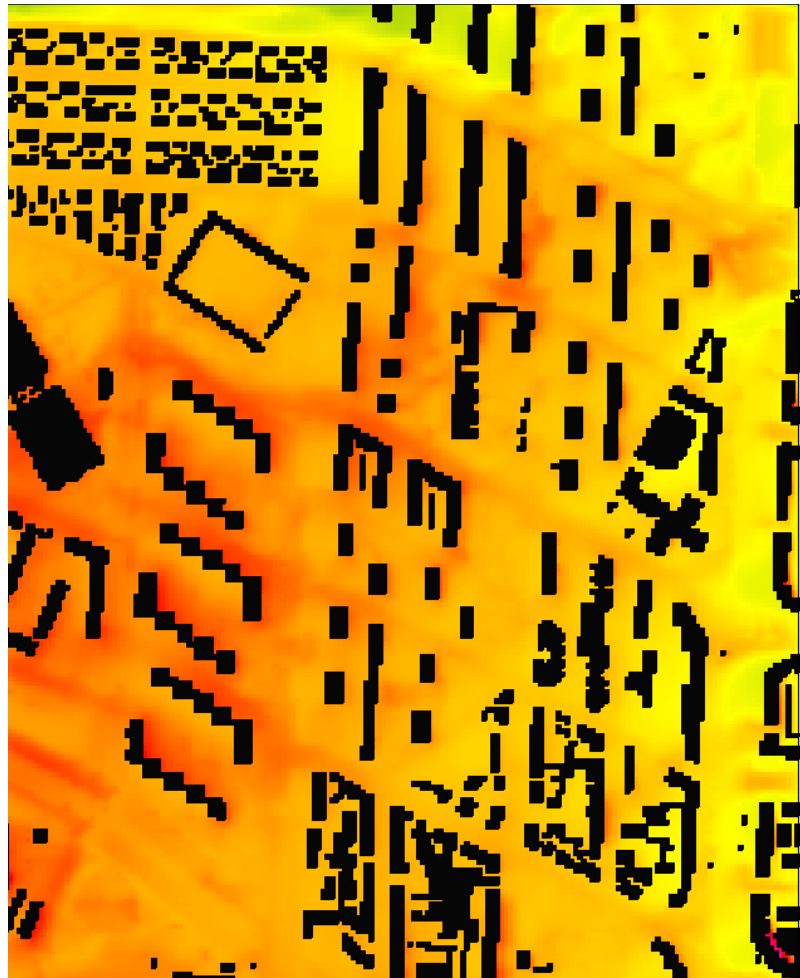
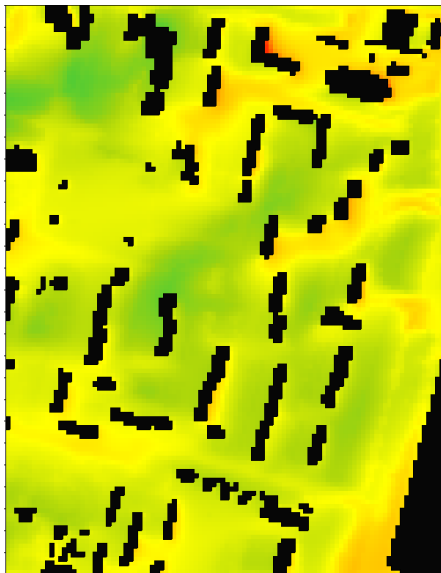
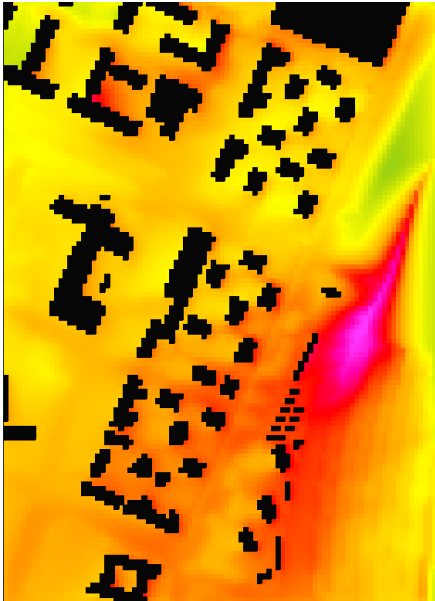


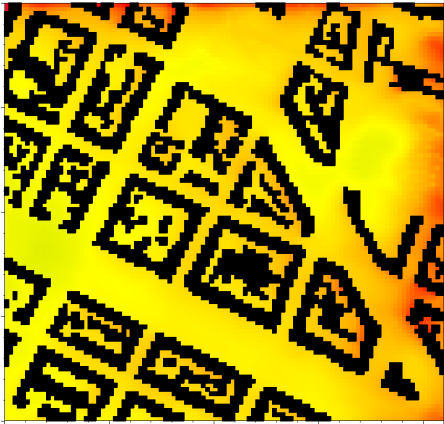
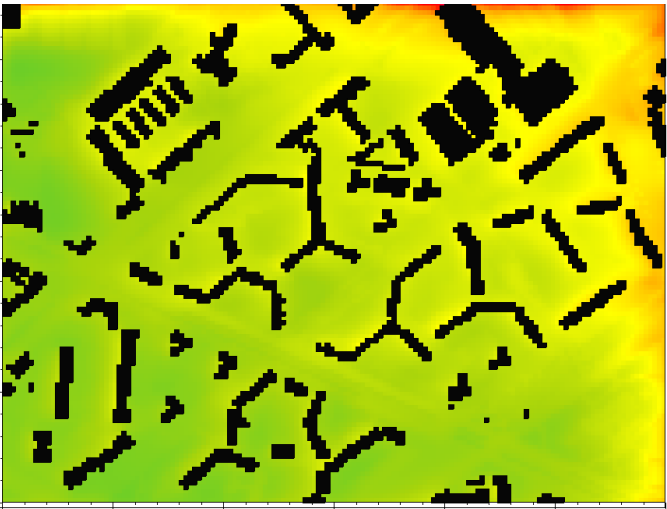
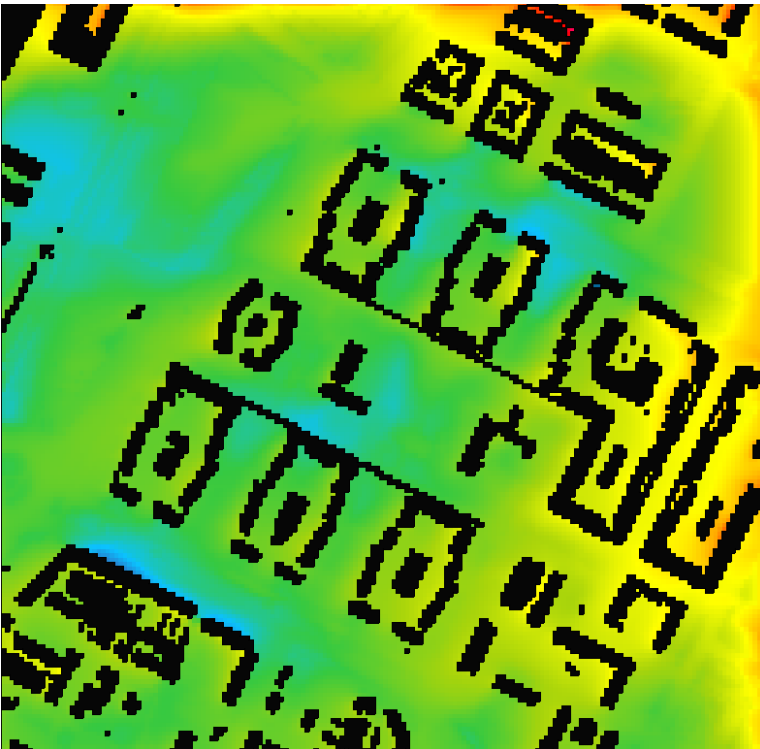
Min: 21.33 °C
Max: 22.22 °C

	san donato	vallette	mirafiori nord	mirafiori sud	ex-mercati generali	lingotto
max. at 9h	22.22	22.15	22.45	22.02	20.42	22.21
min. at 9h	21.33	21.19	21.2	20.98	19.25	19.09
max. at 12h	24.42	24.37	24.43	24.29	25.74	24.41
min. at 12h	23.45	23.22	23.26	22.94	23.19	22.57
max. at 15h	26.51	26.41	26.52	26.4	27.12	26.45
min. at 15h	25.05	24.82	24.65	24.45	24.89	24.28
max. at 18h	25.92	25.92	25.82	25.93	26.46	25.97
min. at 18h	25.32	25.05	24.96	24.65	25.07	24.24

Potential Air Temperature

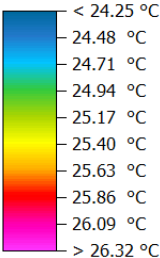
on 19/07/2020 at 09:00
position of view plane: 5m (k=6)





	san donato	vallette	mirafiori nord	mirafiori sud	ex-mercati generali	lingotto
max. at 9h	40.1	38.34	39.95	48.42	57.87	58.24
min. at 9h	18.8	18.4	18.2	16.2	16.6	16.2
max. at 12h	49.82	48.26	48.26	53.58	64.87	68.09
min. at 12h	23.4	22.8	22.8	18.66	18.8	18.69
max. at 15h	52.46	50.24	51.08	56.39	66.33	70.62
min. at 15h	25.68	27.48	23.8	20.29	20.42	20.2
max. at 18h	40.08	39.41	39.95	50.46	54.75	55.88
min. at 18h	21.8	21.4	21.21	20	19.4	19.81

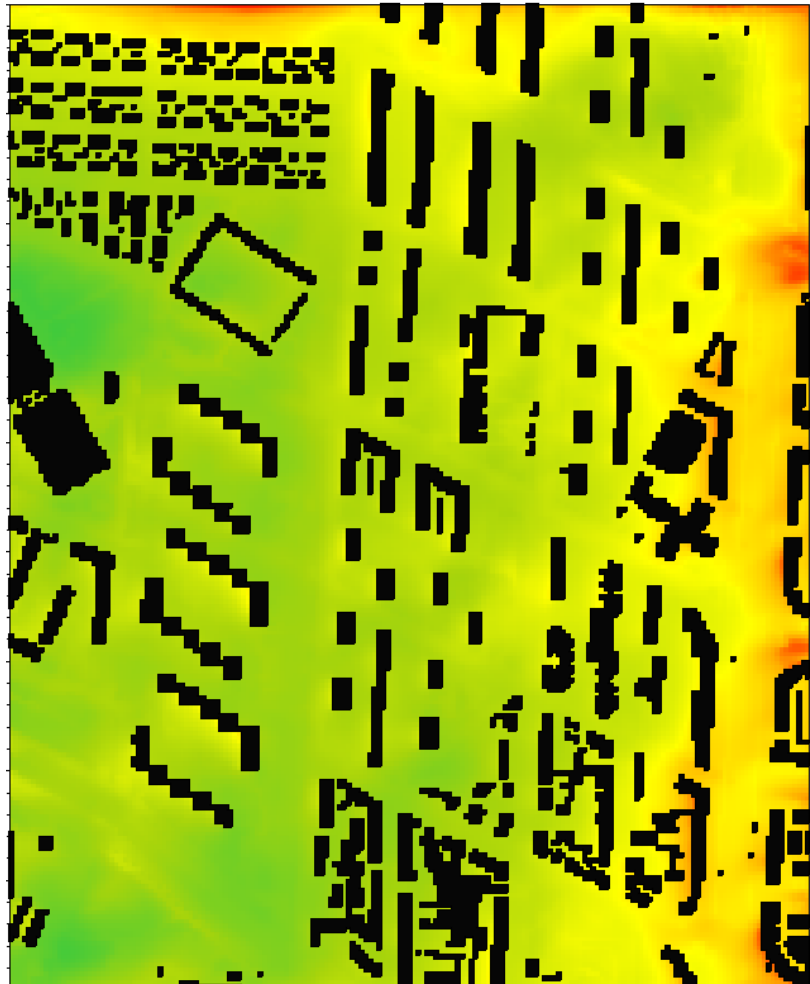
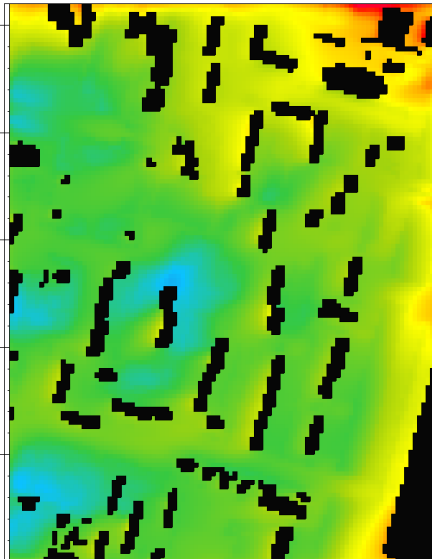
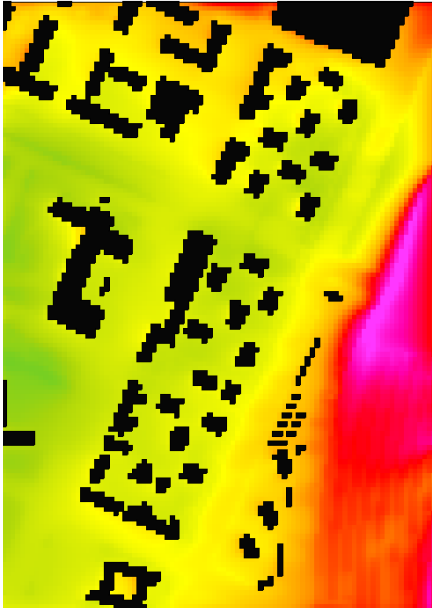
Potential Air Temperature

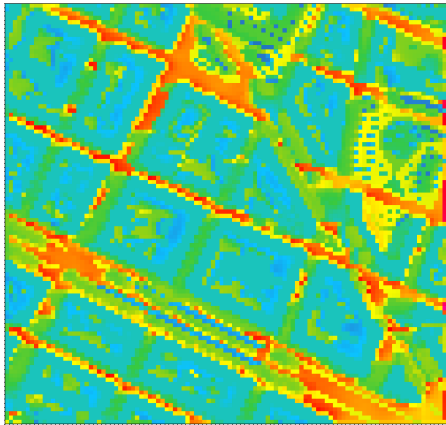
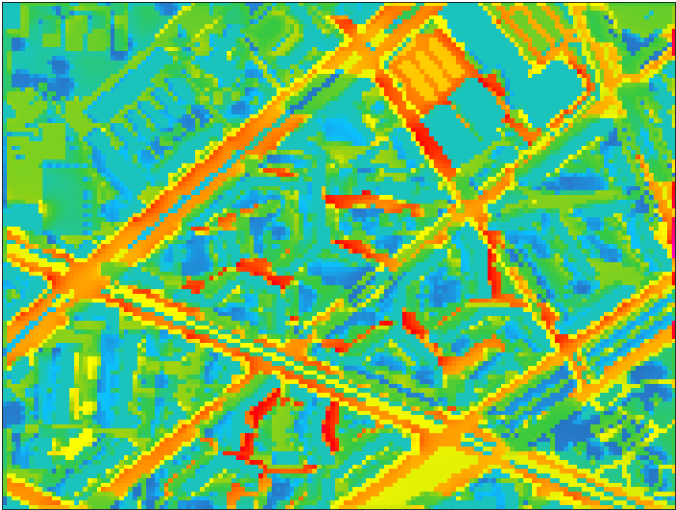
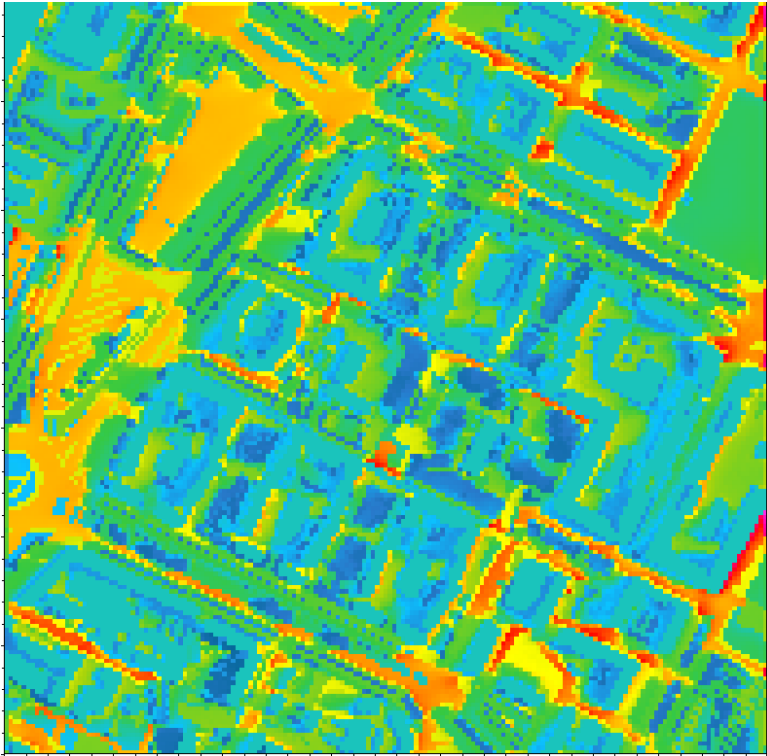


Min: 25.32 °C
Max: 25.92 °C

Potential Air Temperature

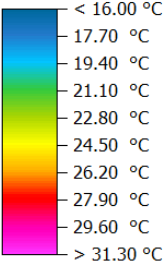
on 19/07/2020 at 18:00
position of view plane: 5m (k=6)





	san donato	vallette	mirafiori nord	mirafiori sud	ex-mercati generali	lingotto
max. at 9h	29.36	29.96	28.42	30.58	32.92	30.84
min. at 9h	17.34	17.34	17.4	16.23	16.36	16.07
max. at 12h	33.48	33.49	33.11	33.52	44.47	34.13
min. at 12h	18.58	18.43	18.38	17.97	18.03	17.98
max. at 15h	34.84	34.18	34.47	33.89	46.61	34.7
min. at 15h	19.57	19.36	19.1	18.88	18.9	18.79
max. at 18h	32.88	31.27	31.54	31.15	38.54	32.91
min. at 18h	19.29	19.26	19.19	18.83	18.99	18.74

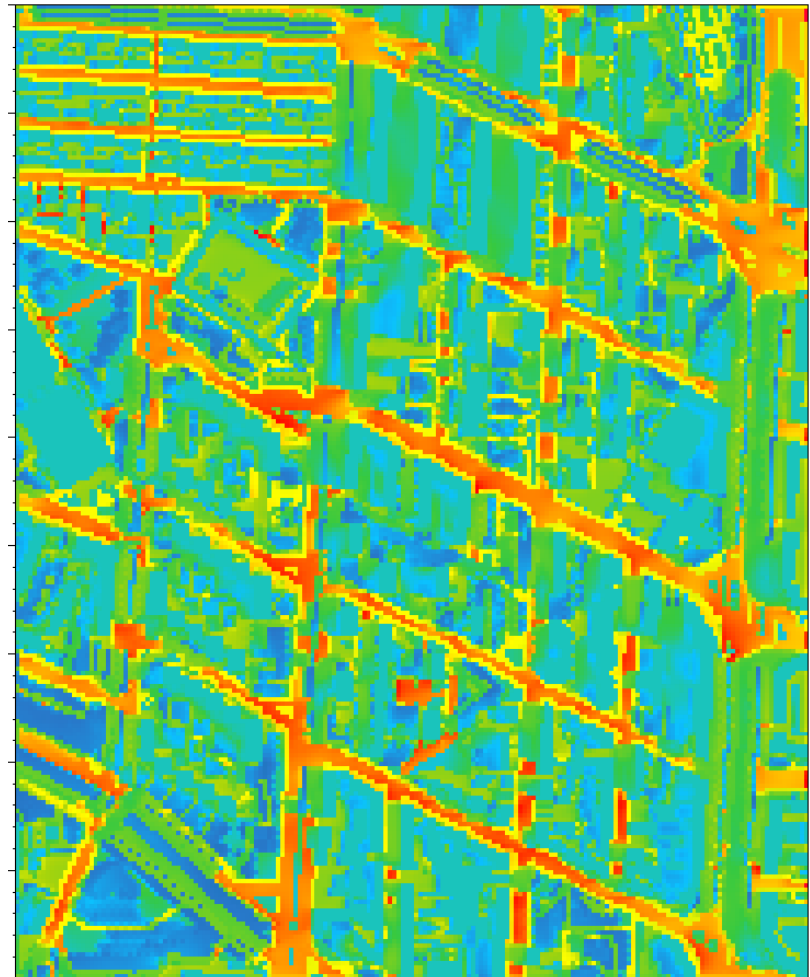
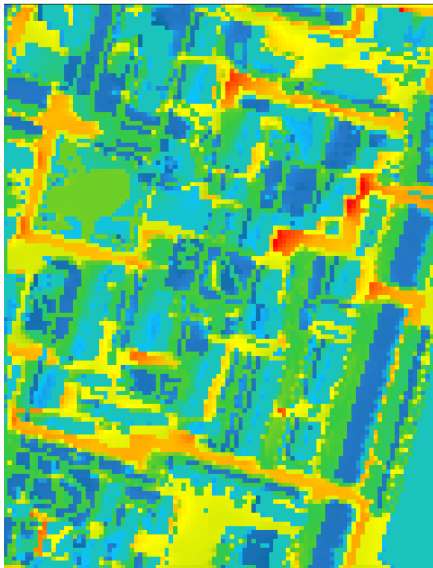
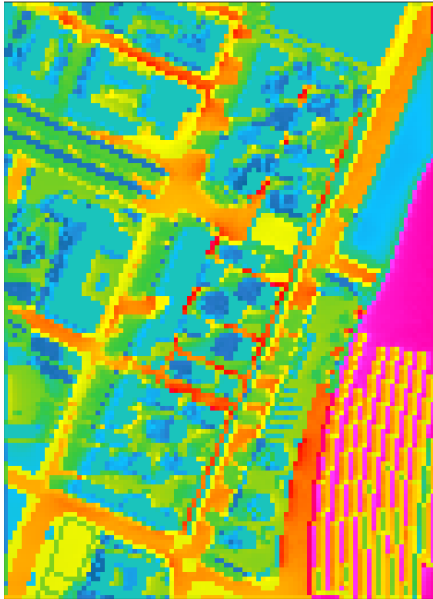
T Surface

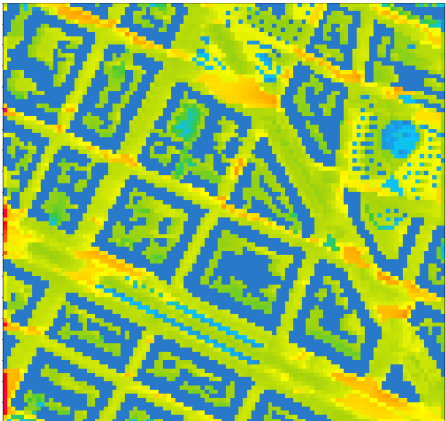
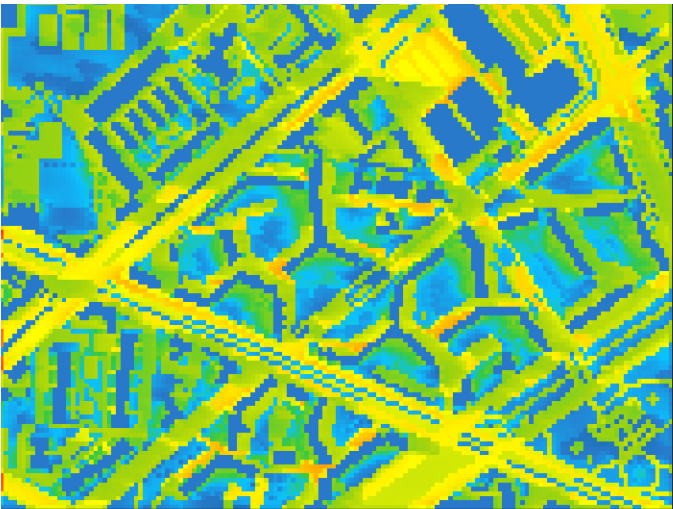
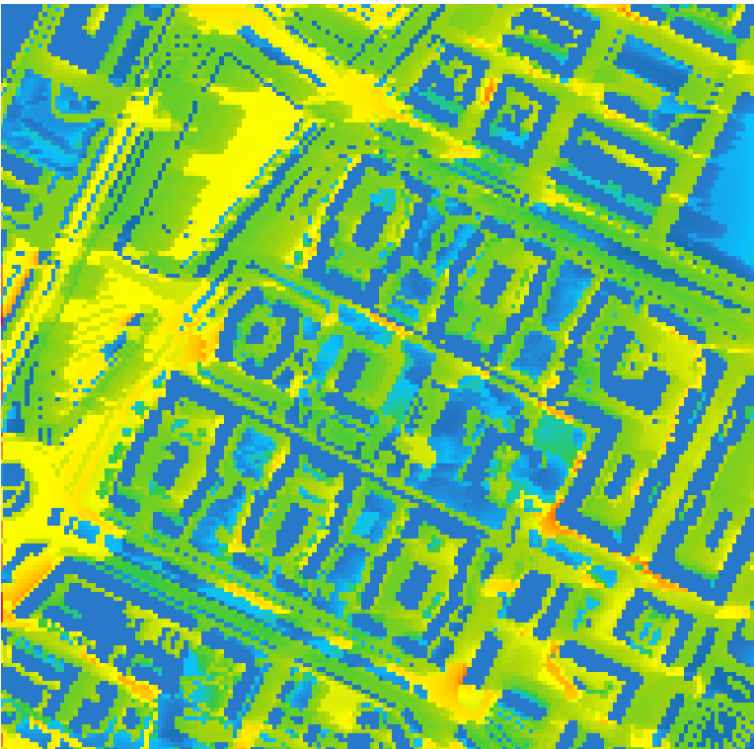


Min: 17.34 °C
Max: 29.36 °C

Surface Temperature

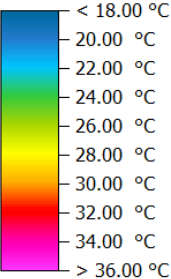
on 19/07/2020 at 09:00
position of view plane: 5m (k=0)





	san donato	vallette	mirafiori nord	mirafiori sud	ex-mercati generali	lingotto
max. at 9h	29.36	29.96	28.42	30.58	32.92	30.84
min. at 9h	17.34	17.34	17.4	16.23	16.36	16.07
max. at 12h	33.48	33.49	33.11	33.52	44.47	34.13
min. at 12h	18.58	18.43	18.38	17.97	18.03	17.98
max. at 15h	34.84	34.18	34.47	33.89	46.61	34.7
min. at 15h	19.57	19.36	19.1	18.88	18.9	18.79
max. at 18h	32.88	31.27	31.54	31.15	38.54	32.91
min. at 18h	19.29	19.26	19.19	18.83	18.99	18.74

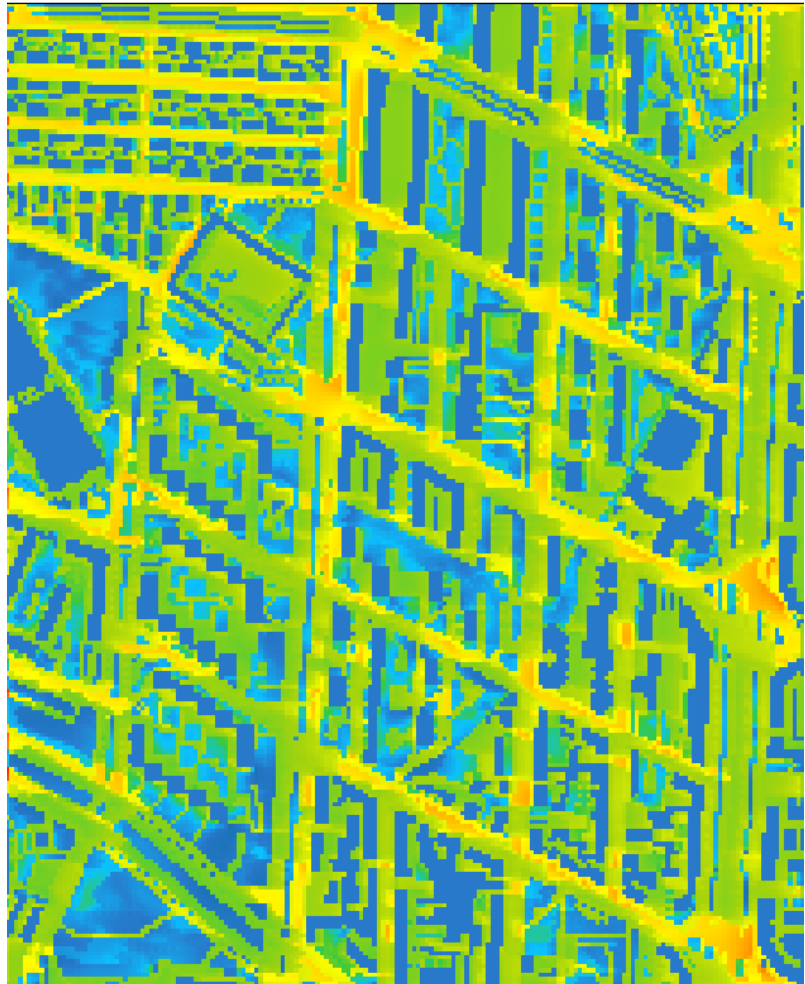
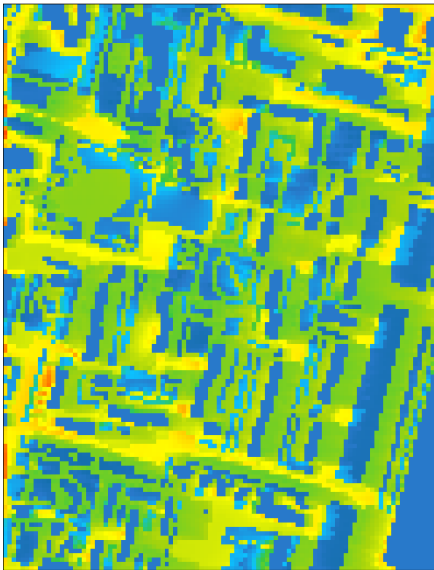
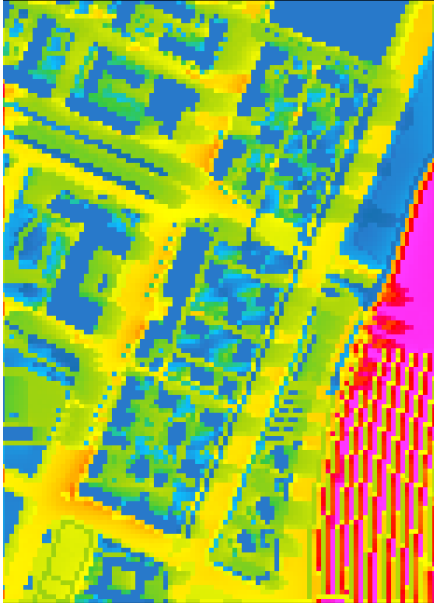
T Surface

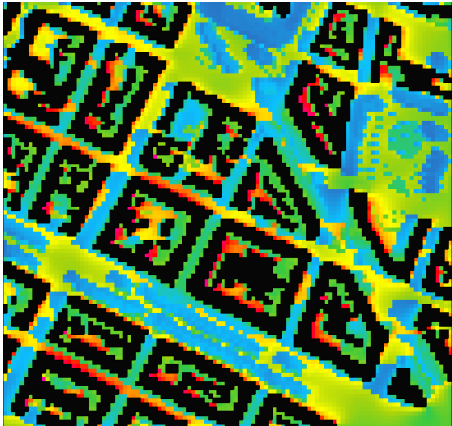
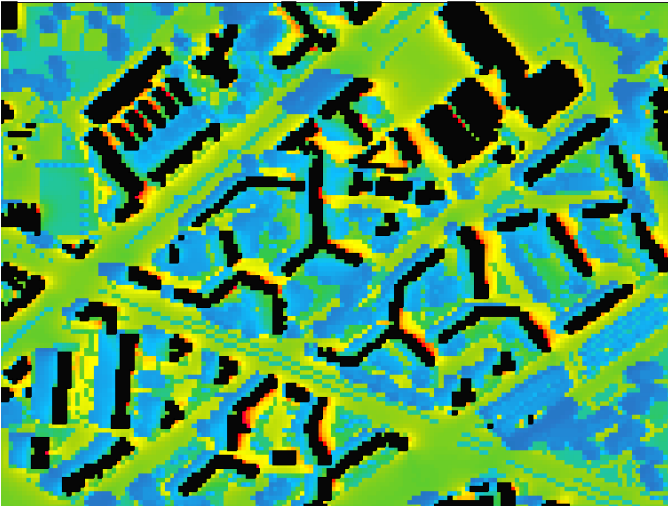
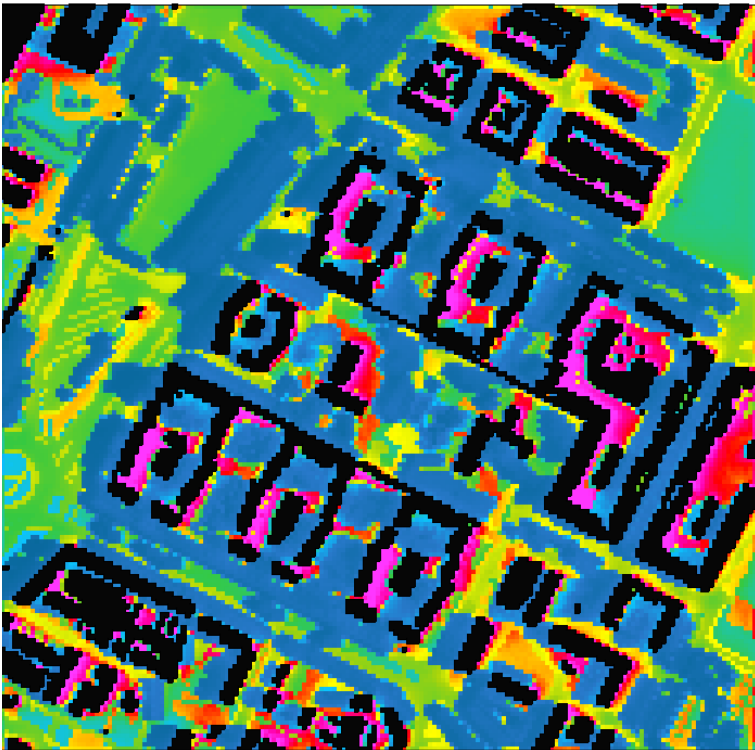


Min: 19.29 °C
Max: 32.88 °C

Surface Temperature

on 19/07/2020 at 18:00
position of view plane: 5m (k=0)





PET

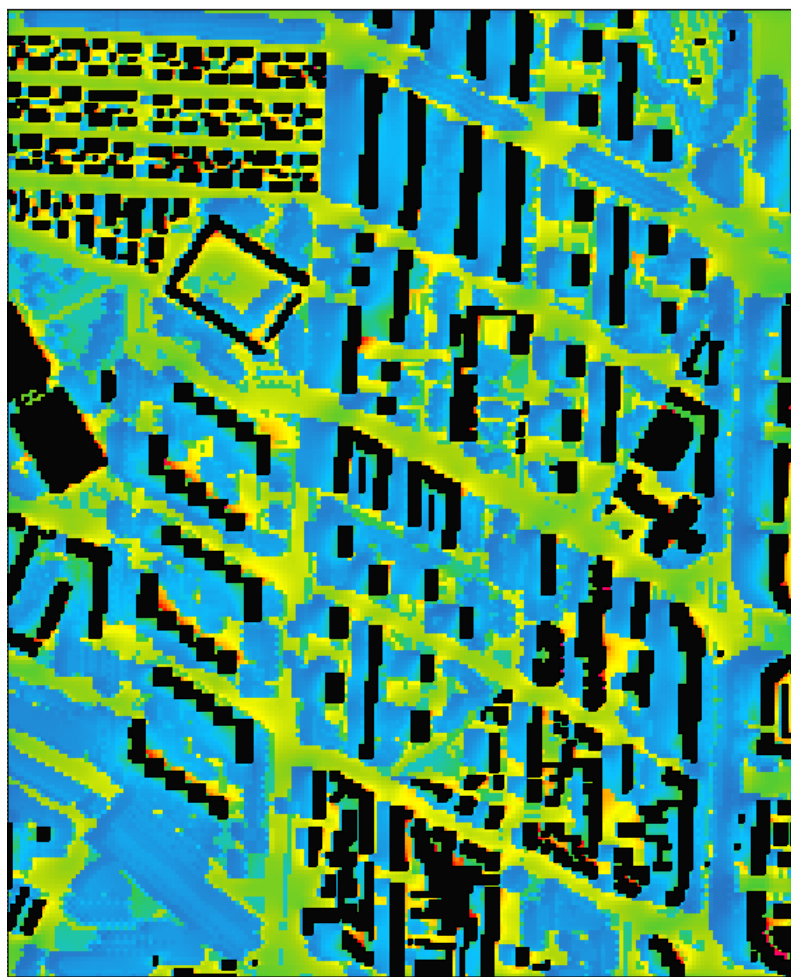
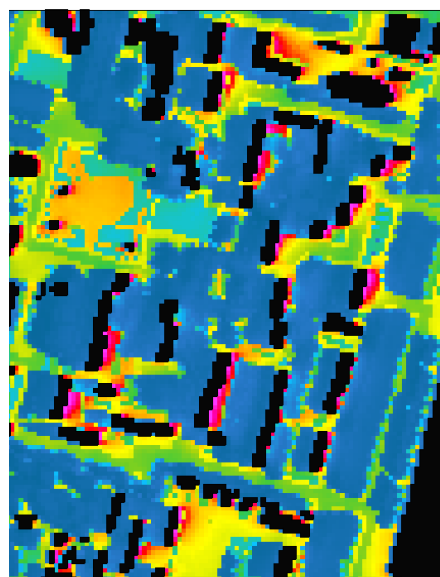
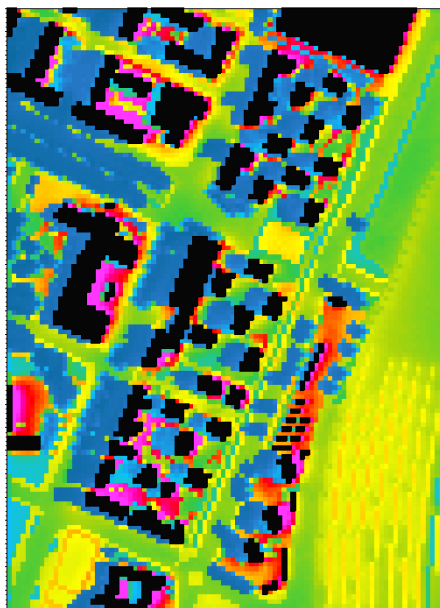
< 16.00 °C
19.00 °C
22.00 °C
25.00 °C
28.00 °C
31.00 °C
34.00 °C
37.00 °C
40.00 °C
> 43.00 °C

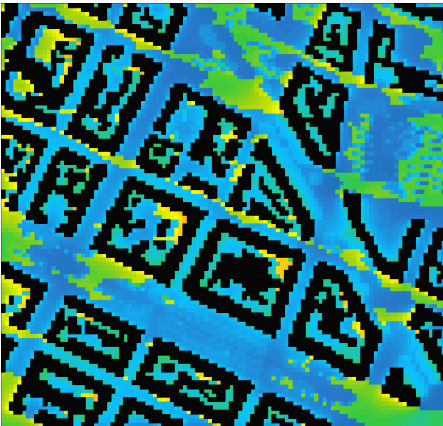
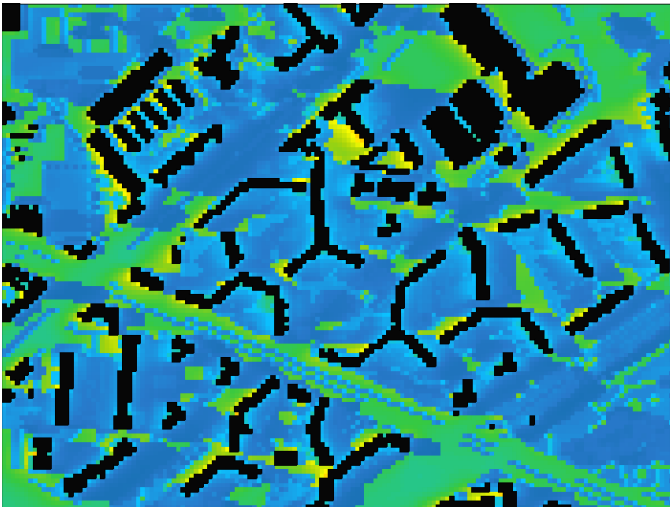
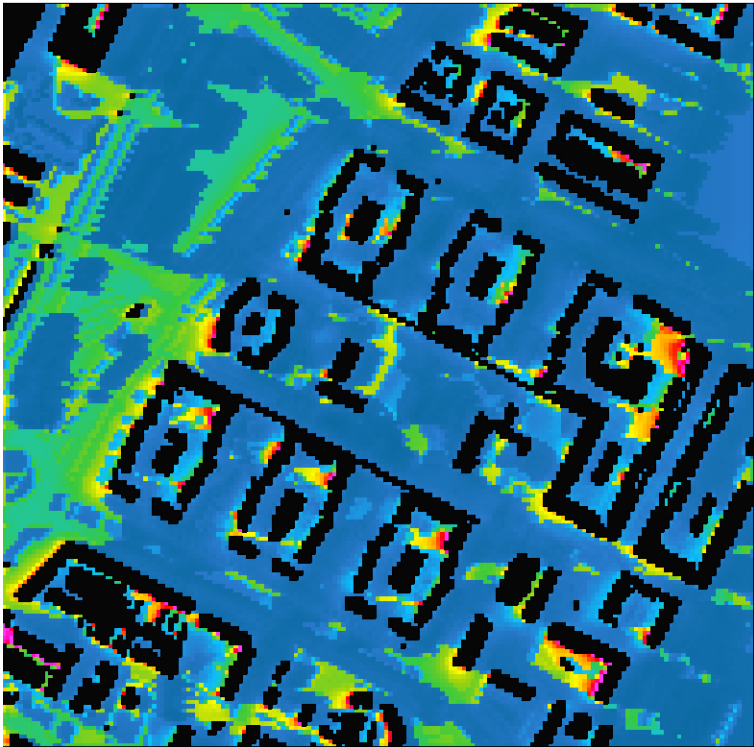
Min: 18.80 °C
Max: 40.10 °C

	san donato	vallette	mirafiori nord	mirafiori sud	ex-mercati generali	lingotto
max. at 9h	40.1	38.34	39.95	48.42	57.87	58.24
min. at 9h	18.8	18.4	18.2	16.2	16.6	16.2
max. at 12h	49.82	48.26	48.26	53.58	64.87	68.09
min. at 12h	23.4	22.8	22.8	18.66	18.8	18.69
max. at 15h	52.46	50.24	51.08	56.39	66.33	70.62
min. at 15h	25.68	27.48	23.8	20.29	20.42	20.2
max. at 18h	40.08	39.41	39.95	50.46	54.75	55.88
min. at 18h	21.8	21.4	21.21	20	19.4	19.81

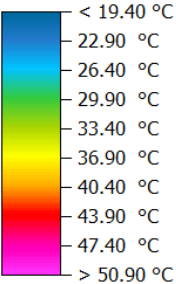
PET

on 19/07/2020 at 09:00
position of view plane: 5m ($k=6$)





PET

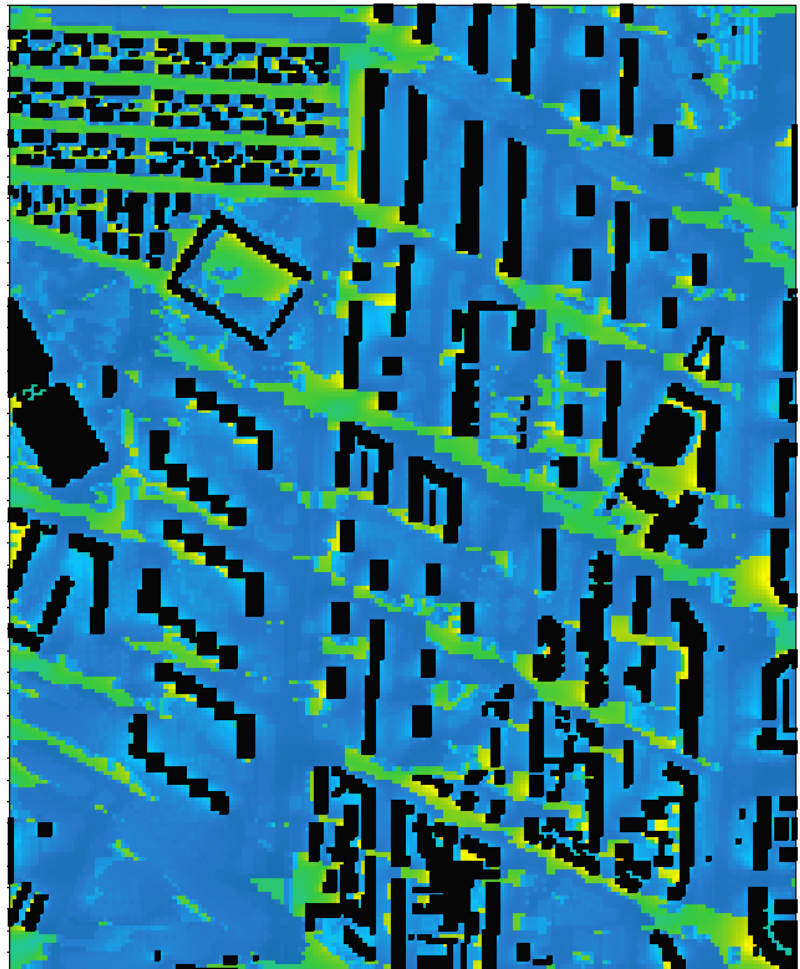
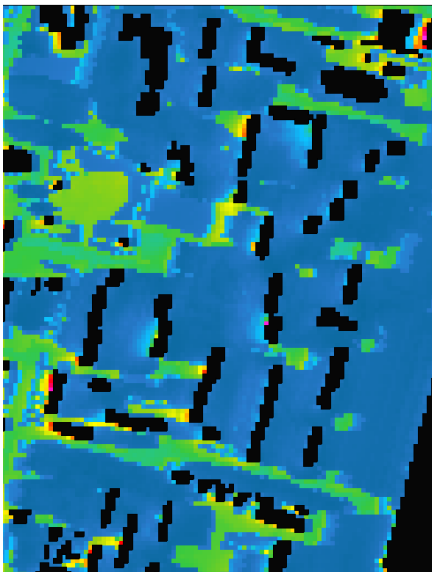
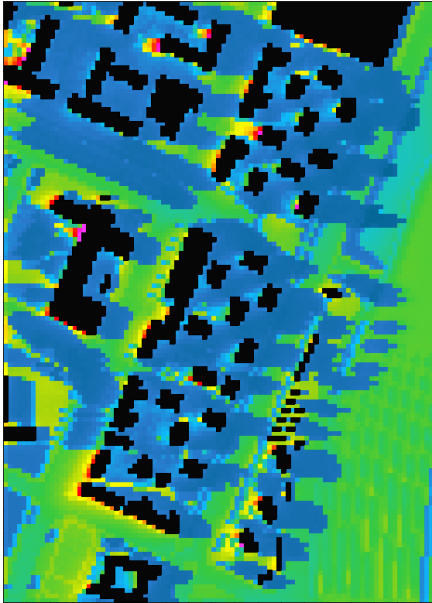


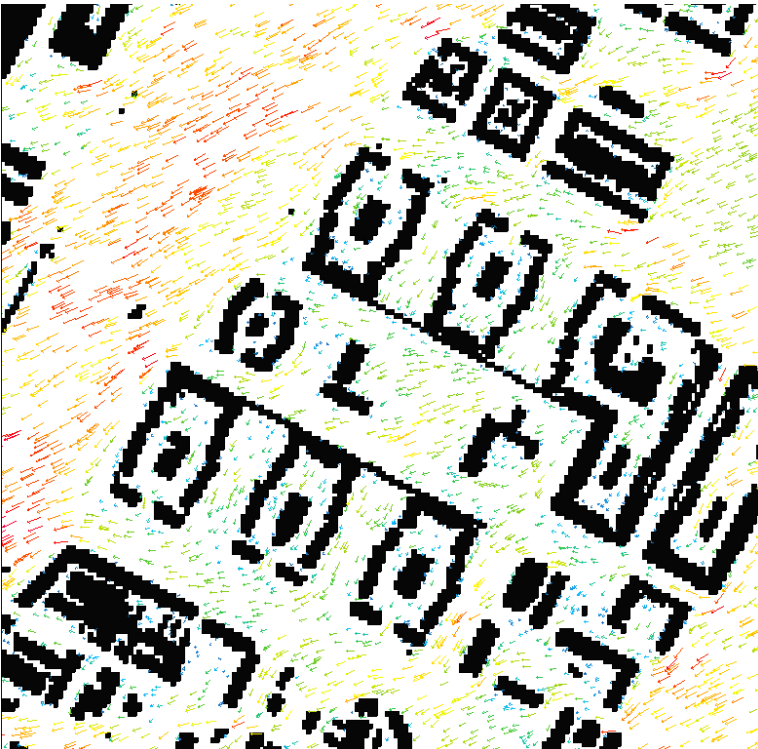
Min: 21.80 °C
Max: 40.08 °C

	san donato	vallette	mirafiori nord	mirafiori sud	ex-mercati generali	lingotto
max. at 9h	40.1	38.34	39.95	48.42	57.87	58.24
min. at 9h	18.8	18.4	18.2	16.2	16.6	16.2
max. at 12h	49.82	48.26	48.26	53.58	64.87	68.09
min. at 12h	23.4	22.8	22.8	18.66	18.8	18.69
max. at 15h	52.46	50.24	51.08	56.39	66.33	70.62
min. at 15h	25.68	27.48	23.8	20.29	20.42	20.2
max. at 18h	40.08	39.41	39.95	50.46	54.75	55.88
min. at 18h	21.8	21.4	21.21	20	19.4	19.81

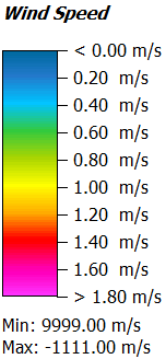
PET

on 19/07/2020 at 18:00
position of view plane: 5m (k=6)





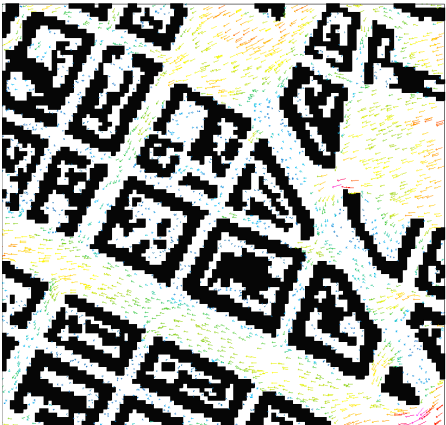
	san donato	vallette	miraffiori nord	miraffiori sud	ex-mercati generali	lingotto
max. at 9h	1.94	1.83	2.51	1.73	1.61	1.78
min. at 9h	0	0	0	0	0	0
max. at 12h	1.91	1.83	2.45	1.74	1.58	1.68
min. at 12h	0	0	0	0	0	0
max. at 15h	1.84	1.77	2.35	1.68	1.54	1.59
min. at 15h	0	0	0	0.01	0	0
max. at 18h	1.8	1.75	2.31	1.66	1.52	1.56
min. at 18h	0	0	0	0.01	0	0



Wind Speed

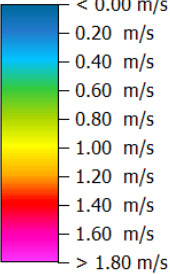
on 19/07/2020 at 09:00
position of view plane: 5m (k=6)





	san donato	vallette	mirafiori nord	mirafiori sud	ex-mercati generali	lingotto
max. at 9h	1.94	1.83	2.51	1.73	1.61	1.78
min. at 9h	0	0	0	0	0	0
max. at 12h	1.91	1.83	2.45	1.74	1.58	1.68
min. at 12h	0	0	0	0	0	0
max. at 15h	1.84	1.77	2.35	1.68	1.54	1.59
min. at 15h	0	0	0	0.01	0	0
max. at 18h	1.8	1.75	2.31	1.66	1.52	1.56
min. at 18h	0	0	0	0.01	0	0

Wind Speed



Min: 0.00 m/s
Max: 1.80 m/s

Wind Speed

on 19/07/2020 at 18:00
position of view plane: 5m (k=6)



STREET

NW-SE oriented, crossing of two urban canyons (both narrow)

STREET

NE-SW oriented, crossing of two urban canyons (narrow/wide)



COURTYARD

discontinuous regular block, presence of vegetation

COURTYARD

continuous irregular block, low density inside the block

COURTYARD

continuous regular block, low amount of breathing spaces, not enough building height in the middle to provide shading

COURTYARD

continuity of surrounding buildings

STREET

main transportation axis (NW-SE oriented), crossing of two streets (main/wide), between the tree axes along the main road

COURTYARD

discontinuous regular block, presence of breathing spaces

COURTYARD

continuous regular block, breathing spaces, not enough density to provide better conditions through shading

Evaluation of the critical points from the case study of San Donato. (PET results at 12:00, exported from ENVI-met)

S1, PET 38.2°C, NW-SE oriented, crossing of two streets (both narrow)

S2, PET 34.6°C, NE-SW oriented, crossing of two streets (narrow/wide)

S3, PET, 31.8°C, main transportation axis (NW-SE oriented), crossing of two streets (main/wide), between the tree axes along the main road

C1, PET 27.6°C, discontinuous regular block, presence of vegetation

C2, PET 33.6°C, discontinuous regular block, breathing spaces

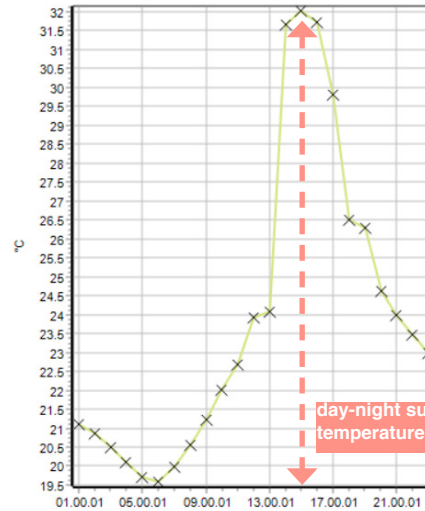
C3, PET 39.9°C, continuous irregular block, low density inside the block

C4, PET 36.9°C, continuous regular block, breathing spaces, not enough density to provide better conditions through shading

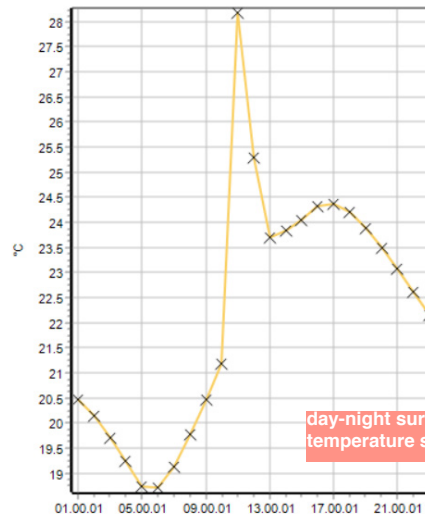
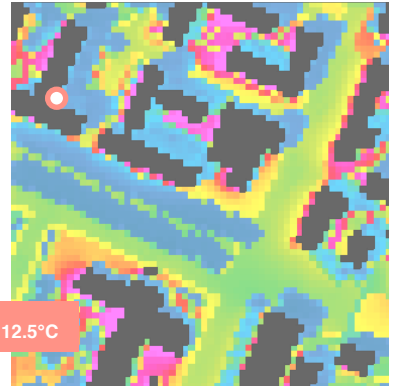
C5, PET 38.6°C, continuous regular block, low amount of breathing spaces, not enough building height in the middle to provide shading

C6, PET 37.1°C, continuous irregular block, heat is concentrated on the areas that do not benefit from the shade of the building borders

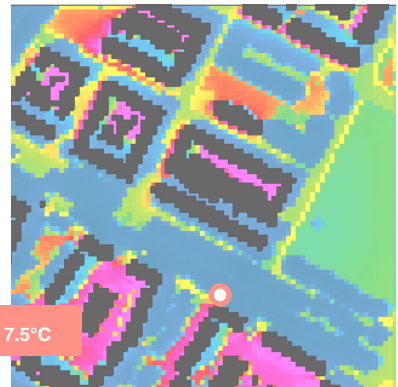
DAY & NIGHT SURFACE TEMPERATURE SWING ON ASPHALT



S12 | 31.6 °C (PET at 15:00)
N-W oriented, trees on both sides of the road



S11 | 20.8 °C (PET at 15:00)
N-W oriented, trees on both sides of the road + extra lane of trees in the middle



STREET
NE-SW oriented, presence of horizontal greenery, lack of trees

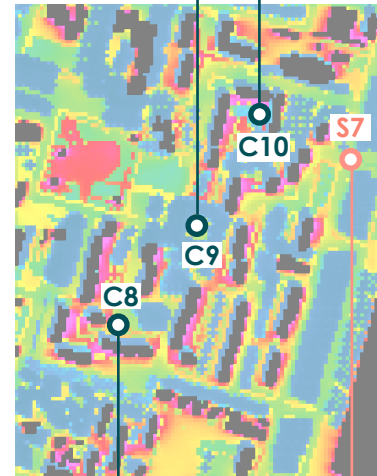


STREET
NE-SW oriented, presence of horizontal greenery and trees

STREET
NW-SE oriented, presence of horizontal greenery, lack of trees

CIRCULATION AREA
faces south, dense application of asphalt along building borders

CIRCULATION AREA
surrounded with greenery



CIRCULATION AREA
open to south

CIRCULATION AREA
sun blocked on the south side

STREET
NE-SW oriented, high presence of vegetation

COURTYARD
sun blocked on the south and north sides, presence of trees

STREET
N-S oriented, low presence of horizontal greenery and trees

STREET
NW-SE oriented, high presence of horizontal greenery and trees



CIRCULATION AREA
continuity of surrounding buildings

CIRCULATION AREA
discontinuity of surrounding buildings

STREET
NW-SE oriented, low presence of horizontal greenery and trees

Critical points from the case studies of Le Vallette (top left), Mirafiori Sud (top right) and Mirafiori Nord (bottom center). (PET results at 15:00, exported from ENVI-met)



C11

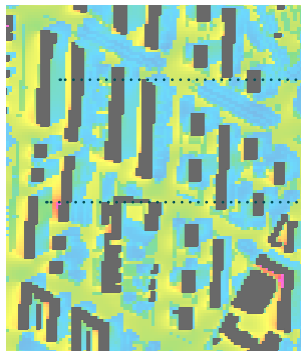
WIND ALIGNED WITH THE BUILDINGS

wind flow orientation is the same as N-S oriented continuous linear canyon

C12

BLOCKED WIND

wind flow from the east blocked by N-S oriented linear building, discontinuous density of buildings



28.5°C

MORE COMFORTABLE

30.9°C

LESS COMFORTABLE



C10

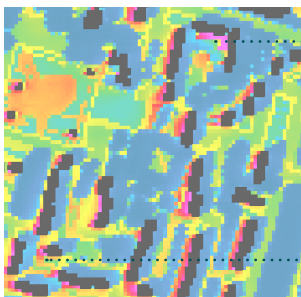
BLOCKED WIND & EXPOSURE TO SUN

wind is blocked by the building on the north, courtyard is not exposed to wind direction and open to solar radiation

C8

BLOCKED WIND

wind flow from the east blocked by N-S oriented linear building

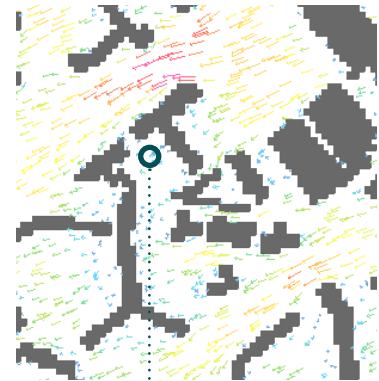


52°C

LESS COMFORTABLE

37.3°C

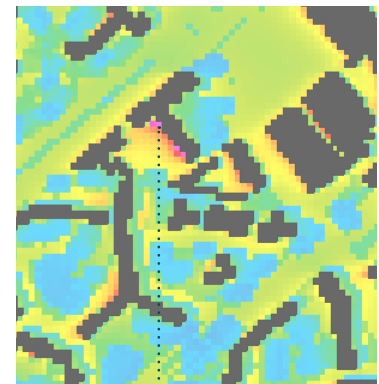
MORE COMFORTABLE



C7

BLOCKED WIND

wind blocked by the building on the east side of the courtyard, high density of concrete, no vegetation, facing south (full exposure to solar radiation)

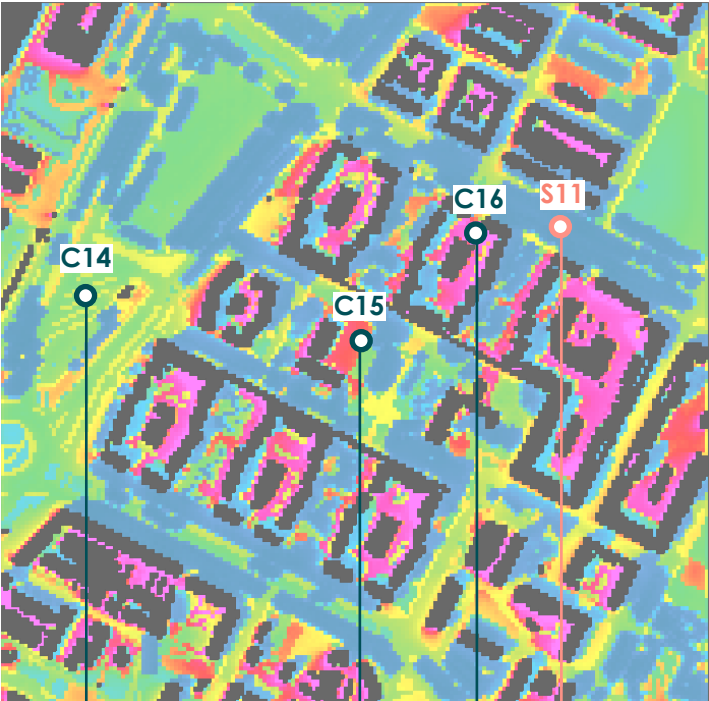


41.1°C

LOW LEVEL OF COMFORT

Evaluation of PET and wind speed results of Mirafiori Nord (top left), Mirafiori Sud (bottom left), (c) Le Vallette (right) case studies at 15:00, zoomed in to a specific portion of the sites. (Exported from ENVI-met)

Critical points from the case studies of Lingotto (left) and Ex-Mercati Generali (right). (PET results at 15:00, exported from ENVI-met)

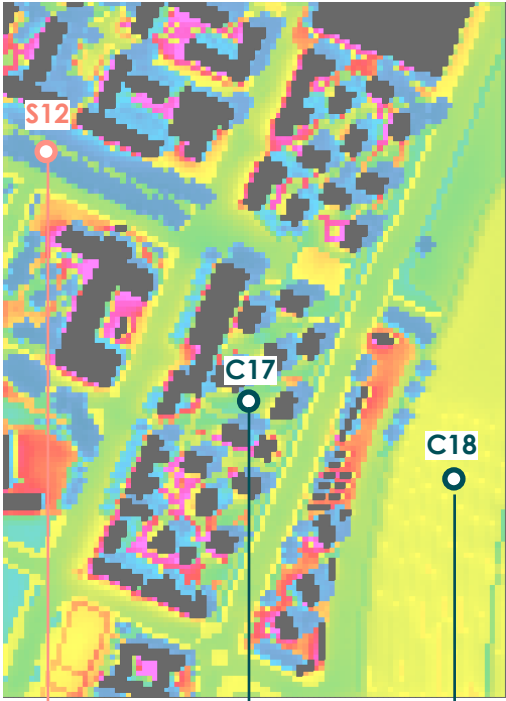


PARKING LOT
composed of asphalt and concrete

STREET
NW-SE oriented,
presence of trees
both on the sides
and in the middle

COURTYARD
concrete pavement,
lack of ventilation gaps

CIRCULATION SPACE
concrete pavement



STREET
NW-SE oriented,
presence of trees
only on the sides

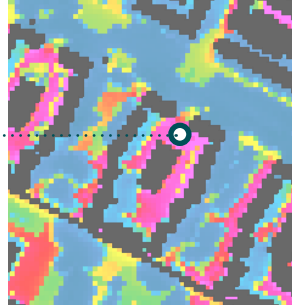
CIRCULATION SPACE
scattered in order,
allows wind circula-
tion

RAILWAY

COURTYARD VS SCATTERED

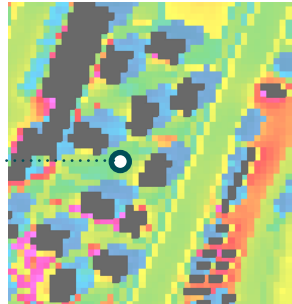
COURTYARD BLOCKING THE WIND C16

despite the opening, the wind does accelerate through the courtyard, which results in uncomfortable conditions



WIND DIRECTION ALIGNED WITH OPENINGS C17

great wind circulation through the openings in the residential public space



WIND DIRECTION & URBAN CANYON ORIENTATION

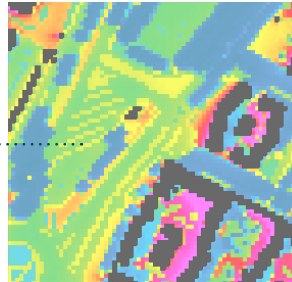
WIND ALIGNED WITH URBAN CANYON C7

a parking lot composed of asphalt and dark concrete, however, placed in the middle of a wide urban canyon which is parallel to the wind direction

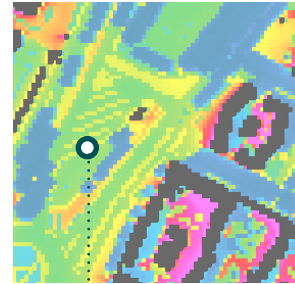


HIGHER LEVELS OF COMFORT COMPARED TO NON-DENSE COURTYARDS C18

better performance compared to C16, although C7 is composed of lower albedo materials

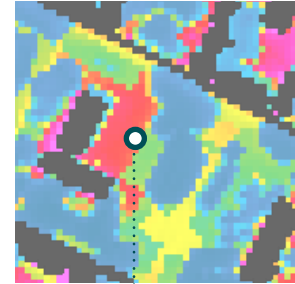


MATERIALS



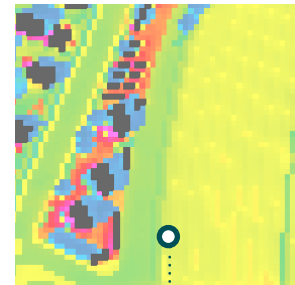
C14 ASPHALT/CONCRETE + WIND

better conditions compared to concrete concentration (C15) rail tracks (C18), due to wind/urban canyon alignment and vegetation presence along the surrounding roads



C15 CONCRETE

localized tree placement does not have a remarkable impact on the area where concrete is densely applied



RAILWAY

higher outdoor comfort compared to C15 (concrete concentration), due to wind circulation